Cristina Isabel Sousa Pires

Biodegradation of Synthetic and Biodegradable Plastics by Leachate Microbiomes

UMinho | 2022

University of Minho
School of Engineering

Cristina Isabel Sousa Pires

Biodegradation of Synthetic and Biodegradable Plastics by Leachate Microbiomes

october de 2022

University of Minho
School of Engineering

Cristina Isabel Sousa Pires

Biodegradation of Synthetic and Biodegradable Plastics by Leachate Microbiomes

Master's Thesis
Master in Biotechnology

Work done under the supervision of
Doctor Andreia Salvador
Doctor Ana Vera Machado

october de 2022

Agradecimentos

Após a chegada ao fim desta etapa, quero agradecer a todas as pessoas que, de alguma forma, contribuíram para que pudesse concluir esta dissertação. A todos, o meu mais sincero e profundo obrigado.

À Doutora Andreia Salvador, minha orientadora, por me ter dado a oportunidade única de trabalhar nesta equipa, por me proporcionar todo o apoio e meios necessários para realizar esta dissertação e por estar sempre pronta a esclarecer todas as minhas dúvidas. Agradeço ainda por toda a paciência e confiança que depositou em mim, assim como pelo conhecimento, e pela exigência e rigor impostos.

À Doutora Ana Vera Machado, minha coorientadora, pela orientação, por toda a ajuda, por todos os ensinamentos que me transmitiu, e pela dedicação que proporcionaram a realização deste trabalho.

A toda a equipa do LBA, por se terem mostrado sempre disponíveis para me auxiliar, pelas discussões científicas, e, em particular, obrigada pelos esclarecimentos e pela companhia ao longo do desenvolvimento desta dissertação.

Declaration of Integrity

I hereby declare having conducted this academic work with integrity. I confirm that I have not used plagiarism or any form of undue use of information or falsification of results along the process leading to its elaboration. I further declare that I have fully acknowledged the Code of Ethical Conduct of the University of Minho.

Resumo

Nos últimos anos, várias estratégias têm sido desenvolvidas para colmatar a acumulação de plásticos no ambiente, como a descoberta de novos microrganismos e enzimas que consigam eficientemente biodegradar plásticos. Neste trabalho, as comunidades microbianas de lixiviado, em aerobiose e anaerobiose em condições termófilas, foram estudadas pela sua capacidade de biodegradar polímeros não-biodegradáveis (PE (polietileno) e PET (politereftalato de etileno)) e biodegradáveis (PCL (policaprolactona e PHB/PBAT (polihidroxibutirato/poli (butileno adipato-co-tereftalato)). Esta biodegradação também foi testada utilizando sedimento marinho como inóculo, em condições aeróbicas, metanogénicas e sulfato-redutores em temperaturas mesófilas.

As experiências com lixiviado demonstraram uma biodegradação completa com PCL em pó, em condições anaeróbicas e aeróbicas (103 ± 18 % e 99 ± 6 %, respetivamente), observando-se, também, uma biodegradação completa para o PCL em filme em condições anaeróbias (100 ± 0,2%), e uma biodegradação de 28 a 100% em condições aeróbias. PHB/PBAT demonstrou uma biodegradação parcial (24 % ± 0,2 %) em anaerobiose. Contudo, não se observou uma produção de metano/consumo de oxigénio significativa para o PE e PET, resultando numa baixa biodegradação. Mesmo assim, um dos ensaios demonstrou uma biodegradação aparente de 5 ± 2%, ao fim de 180 dias.

As comunidades microbianas dos ensaios com PCL demonstraram ser distintas e diversas. *Coprothermobacter* estava presente em grande abundância nos ensaios aeróbios e anaeróbios e poderá ter estado diretamente ligado à biodegradação de PCL. *Methanothermobacter* demonstrou ser o microrganismo metanogénico mais abundante (mais de 55 % abundância relativa), tendo um papel importante na conversão do PCL a metano.

Nos estudos com sedimento marinho, o PCL demonstrou ser biodegradado em condições aeróbias e sulfato-redutoras, mas não em condições metanogénicas. Até ao momento, a comunidade microbiana de sedimento não demonstrou ter capacidade para biodegradar PE e PET

Estes resultados demostram que lixiviado e sedimento marinho são potenciais fontes de microrganismos com a capacidade de biodegradar PCL, sendo necessário mais estudos para isolar e caracterizar estas comunidades microbianas.

Palavras-chaves: Biodegradação, comunidades microbianas, lixiviado, polímeros, sedimento marinho

Abstract

In the last decades, various strategies have been developed to overcome the plastic waste problem, such as using biodegradable polymers, applying treatments that facilitate plastic degradation, and discovering novel microorganisms and enzymes that are capable of biodegrading complex polymers. This work explored leachate microbial communities in aerobic and anaerobic thermophilic conditions for their ability to biodegrade non-biodegradable (PE (polyethylene) and PET (polyethylene terephthalate)) and biodegradable (PCL (polycaprolactone) and PHB/PBAT (polyhydroxy butyrate/polybutylene adipate-co-terephthalate blend)) polymers. Biodegradation was also tested with microbiomes from marine sediment, under aerobic, methanogenic, and sulphate-reducing mesophilic conditions.

With leachate, complete biodegradation of powder PCL was observed both under anaerobic and aerobic conditions (103 ± 18 % and 99 ± 6 %, respectively). PCL films were fully converted to methane (100 ± 0,2%) under anaerobic conditions, and biodegradation under aerobic conditions ranged from 28 to 100 %. The blend PHB/PBAT was partially biodegraded under anaerobic conditions (24 ± 0,2 %). Generally, no significant methane production or oxygen consumption were detected in the assays with PE and PET, indicating no considerable biodegradation. Nevertheless, in one assay PE was apparently converted to methane (5 ± 2 % in 180 days), but further analyses are necessary to confirm this biodegradation.

PCL-degrading microbial communities developed under aerobic and anaerobic assays were diverse and distinct. *Coprothermobacter* sp. was very abundant in aerobic and anaerobic incubations and was potentially involved in PCL biodegradation in both conditions. *Methanothermobacter* sp. was the most abundant methanogen (over 55 % relative abundance), being an important player during PCL conversion to methane.

PCL was also biodegraded by the marine sediment, under aerobic and sulphate-reducing conditions, but not under methanogenic conditions. Thus far, the marine sediment microbiome did not biodegrade PE and PET.

These results show that leachate and marine sediment microbiomes are potentially good sources of microorganisms with the ability to biodegrade PCL, and further attempts should be made to isolate key microorganisms, obtain efficient microbial consortia, facilitate microbial access to the polymers, and stimulate the activity of plastic-degrading microorganisms.

Keywords: Biodegradation, leachate, marine sediment, microbial communities, polymers

Index

Abbreviations and acronyms

AD- alcohol dehydrogenase

ADL- aldehyde dehydrogenase

AFM- atomic force microscopy

AH- alkane hydroxylase

ATR-FTIR- attenuated total- Fourier transform infrared

BHET- bis(2-hydroxyethyl) terephthalate

BMP- biochemical methane potential method

BOD-biochemical oxygen demand

CBM- carbohydrate-binding modules

CEN- European Standardization Committee

CM- β-carboxy muconate

COD- chemical oxygen demand

DCD- 1,6-dihydroxycyclohexa-2,4-diene-dicarboxylate

DES- DNase/Pyrogen-Free water

DGGE- denaturing gradient gel electrophoresis

DMR- direct measurement respirometry

DNA- deoxyribonucleic acid

DSC- differential scanning calorimetry

EG- ethylene glycol

ESEM- environmental scanning electron microscope

GC- gas chromatograph

GPC- Gel permeation chromatography

HPLC- high-performance liquid chromatography

IR- infrared spectroscopy

ISO- International Standardization Organization

MFS- Major Facilitator Superfamily

MHET- mono(2-hydroxyethyl) terephthalic acid

MIR- mid-infrared spectrometry

NDIR- nondispersive infrared sensor

NGS- next-generation sequencing technologies

NIR- Near infrared spectrometry

NMR- nuclear magnetic resonance

PAH- polycyclic aromatic hydrocarbons

PBAT- polybutylene adipate-co-terephthalate

PBM- polyhydroxyalkanoate binding domains

PBS- phosphate-buffered saline

PBS- polybutylene succinate

PCA- protocatechuate

PCDO- 3,4-dioxygenase

PCL- polycaprolactone

PC-polycarbonate

PE- polyethylene

PES- Polyethylene succinate

PET- polyethylene terephthalate

PHA- polyhydroxyalkanoate

PhaC- PHA synthase

PHB- polyhydroxy butyrate

PHMB- polyhexamethyleneguanidine

PHB/PBAT- polyhydroxy butyrate/polybutylene adipate-co-terephthalate blend

PLA- polylactic acid

PP- polypropylene

PS- polystyrene

PUR- polyurethane

PVA- polyvinyl alcohol

PVC- polyvinyl chloride

RNA- ribonucleic acid

SEM- scanning electron microscopy

TCA- tricarboxylic acid

TCD- thermal conductivity detector

TGA- thermogravimetric analysis

TPA- terephthalic acid

TPADO- TPA dioxygenase

TphB- 1,2-dihydroxy-3,5-cyclohexadiene-1,4- dicarboxylate dehydrogenase

VFA- volatile fatty acids

VSS- volatile suspended solids

XRF- X-ray fluorescence spectrometry

1. List of figures

2. List of tables

3. State-of-the-art

In today's society, plastics have a wide range of applications, including in industrial, agricultural, packaging, and domestic markets (Taghavi *et al.*, 2021), due to a variety of functions like high density, strength, flexibility, molecular weight, and high durability (Iram *et al.*, 2019). Plastic waste accumulation has become a serious environmental problem, putting at risk many ecosystems and human health (Kjeldsen *et al.*, 2019; Liao & Chen, 2021). The development of biodegradable plastics to replace synthetic ones and recycling solutions have been contributing to reduce the plastic waste problem (Ahmed *et al.*, 2018). However, the biodegradation of both synthetic and biodegradable plastics still poses as the most environmentally friendly approach to tackle the plastic waste problem (Mohanan *et al.*, 2020). Although several microbes and enzymes can function as biocatalysts for plastics biodegradation, their efficiencies are commonly low (Alshehrei, 2017; Amobonye *et al.*, 2021). Since naturally occurring microbiomes are diverse, they may adapt to these pollutants, increasing the possibility of finding microbes in these contaminated habitats which can biodegrade plastics.

The following sections will provide information on the plastic waste problem and on landfills and marine environments, which are sites with a higher plastic waste accumulation, that might hold microorganisms highly adapted to plastic waste. An overview on non-biodegradable and biodegradable plastics, on the mechanisms of plastic's biodegradation and on the different factors that can affect the efficiency of these processes, will be given. Additionally, the more common techniques used to monitor and evaluate biodegradation will be explained, together with a review on the existing microorganisms, enzymes, and known metabolic pathways involved in plastics biodegradation, as well as thermophilic considerations on plastics biodegradation.

3.1- Plastic waste

Synthetic plastic's large-scale production was initiated in 1950 and has only increased ever since (Iram *et al.*, 2019). Its' production has felt enormous progress over the last 60 years (Iram *et al.*, 2019), and in 2018 global plastic production reached 348 million tons (Ru *et al.*, 2020). However, due to their recalcitrant nature, these plastics have been accumulating both in terrestrial and aquatic ecosystems and in the 1970s the environmental pollution triggered by plastics was first described (Mohanan *et al.*, 2020).

The recycling and waste management of these plastics is extremely insufficient compared with the production and utilization of plastics, putting increasing pressure on the environment (Liao & Chen, 2021). Approximately 80 % of plastic global usage is of synthetic plastics like polyethylene (PE), polypropylene (PP), polyvinyl chloride (PVC), polystyrene (PS), polyurethane (PUR), and polyethylene terephthalate (PET) (Iram *et al.*, 2019). It is estimated a four-fold increase in plastics production by 2050 (Iram *et al.*, 2019), where more than half of those will end up in landfills and enter the ecosphere, like oceans and lakes (Ru *et al.*, 2020). This would lead to the release of 56 million tons of greenhouse gases into the atmosphere, which compromises 13 to 15 % of the carbon budget (Taghavi *et al.*, 2021). The most common type of plastic to be produced is plastic used in packaging, which accounts for 40 % of the plastics produced in Europe, followed by 22 % of consumer and household products and 20 % of construction material (Flury & Narayan, 2021). Additionally, illegal dumping of industrial and domestic waste and poor management of transportation and storage of it leads to constant plastic pollution (Atanasova, Stoitsova, *et al.*, 2021). It is reported that, of the global plastic waste, only 9 % is recycled, 12 % is incinerated and 79 % ends up in landfills or discarded into the environment (Chen *et al.*, 2020; Ru *et al.*, 2020; Taghavi *et al.*, 2021).

Post-industrial wastes are the plastics that are disposed of at the end of the production line, and that never reach the final consumer. These wastes are much more easily recyclable because they are clean, and already sorted in types and sizes. On the contrary, post-consumer plastics wastes are mostly derived from single-used plastics used by consumers and are normally contaminated by other municipal solid wastes and mixed. This makes their recycling much more difficult, time and energy-consuming (Taghavi *et al.*, 2021). Plastic waste management, nowadays, needs the usage of various chemical, mechanical and physical technologies, however, these are not universally efficient and can result in secondary pollution (Chen *et al.*, 2020).

In nature, these plastics can be degraded by photo-, bio-, and thermo-oxidative depolymerization (Mohanan *et al.*, 2020) but they normally result in toxic compounds as well as micro and nano-particles that end up in soil and water systems (Taghavi *et al.*, 2021). It is estimated that these plastics can remain in the environment for up to 1000 years (Taghavi *et al.*, 2021), and disturb the marine animals' endocrine system, causing intestinal blockage, interference with chemical communication in aquatic systems, and a false sensation of satiation due to ingestion (Amobonye *et al.*, 2021). Annually, about 10 to 20 million tons of plastics end up in the ocean, leading to about 1 million seabirds and 100 thousand marine animals

dying each year, where 44 % percent of seabirds, 86 % of turtles, and 43 % of marine mammals suffer from entanglement and ingestion of plastic wastes (Iram *et al.*, 2019; Kaushal *et al.*, 2021).

Human health has also been threatened by these plastics wastes, by ingestion of microplastics that enter the bloodstream and cause serious health problems (Kjeldsen *et al.*, 2019). This ingestion of microplastics also causes inflammation of tissues, alteration of microbiomes, and lipid metabolism, and allows the introduction of environmental contaminants that are toxic to the organism (Shruti & Kutralam-Muniasamy, 2019). Moreover, the unsupervised burning of plastic waste in certain regions can lead to the production of hazardous gases (Kale *et al.*, 2015), like furans, dioxins, heavy metals, and sulphides (Amobonye *et al.*, 2021), that cause lung diseases after inhalation (Amobonye *et al.*, 2021; Kale *et al.*, 2015). About 400 000 to 1 000 000 people die, annually, due to the toxins resulting from the burning of municipal mismanaged waste, in developing countries, and subsequent diseases (Taghavi *et al.*, 2021). These cues an urgent need for innovative recycling and disposal methods.

In the last 4 decades, scientists have shown great concern to overcome the plastic waste problem, exploring treatments that facilitate their degradation and discovering novel microbes that are capable of degrading these plastics (Ahmed *et al.*, 2018; Iram *et al.*, 2019). There has also been a greater focus on developing and producing biodegradable plastics to tackle the biodegradation of synthetic plastics, however, they still pose some risks to the environment without proper management (Ahmed *et al.*, 2018; Folino *et al.*, 2020), and have only been representing 1-2 % of global plastic sales (Pires *et al.*, 2022). So the identification and engineering of plastic-degrading microorganisms and their enzymes provide an opening to enhance plastic recycling and reduce the amount of plastic waste by assimilation of these materials as carbon sources or their biodegradation into value-added compounds (Mohanan *et al.*, 2020).

3.1.1- Landfills

Landfills are disposal sites for various types of municipal solid wastes, that have become attractive for their economic value (El-Fadel & Khoury, 2000). Depending on their size and characteristics, they can also accept commercial solid waste, non-hazardous sludge, and non-hazardous industrial solid waste (Themelis & Ulloa, 2007). They can be designed to be open type, where post-consumer waste of all kinds is deposited on land without an engineering design, or closed type where municipal wastes are buried into a hole with a thick protective layer that minimizes leaching into the soil and water resources (Taghavi *et al.*, 2021). Nowadays, landfills are all regulated and part of waste management disposal plans,

helping decrease the pollution of gasses and toxins to protect human health and the environment (DHEC, 2022).

The most common type of bottom lining of the landfill, although varying slightly from landfill to landfill, is composed of a thick and compacted clay layer, that prevents the leakage of any type of liquid (Cossu & Stegman, 2018; DHEC, 2022). On top of this layer lays a high-density plastic liner, and a thick protective layer, normally of sand, where the trash is added (Cossu & Stegman, 2018; DHEC, 2022). Because leachate easily forms in landfills, due to rainwater infiltration, they need to be equipped with a drainage system that goes on top of the plastic liner. Perforated pipes collect this wastewater into a treatment facility, that can be onsite or in a wastewater treatment plant (Cossu & Stegman, 2018; Osama Ragab, 2019). Besides leachate, landfills also tend to release gasses due to the degradation of some of the materials in them, and those gases (mainly methane and carbon dioxide), if not properly managed, can be released into the atmosphere and contribute to global warming. Therefore, landfills also have a gas collection system, that contains pipes and wells that extract the gas for downstream transformation into power and electricity (Cossu & Stegman, 2018; DHEC, 2022).

The trash itself is added every day, being covered by a dirt layer to minimize odours and pests (Cossu & Stegman, 2018; DHEC, 2022). Once the landfill reaches its maximum capacity, the area is completely covered with another impermeable layer, that gets covered with soil and vegetation, to minimize the entry of water (Osama Ragab, 2019). This layer controls moisture content and minimizes odours, as well as prevents erosion and water infiltration (Osama Ragab, 2019). The degradation of the matter in it continues for several years, and the collection and treatment of gas and liquid effluents continue for a period of up to 30 years, after the closure of the landfill (Themelis & Ulloa, 2007).

Biomass materials like paper, food, wood, and other yard scraps, textile material like leather, cotton, and wood, as well as inorganic material like metals, glass, and gypsum are common wastes found in landfills (Themelis & Ulloa, 2007). Cellulosic material represents the most common solid waste in the generality of landfills, therefore, aerobic and anaerobic microorganisms have an important role in the biodegradation of these wastes (El-Fadel & Khoury, 2000). Normal microbial communities in landfills are composed of bacterial and archaeal populations and anaerobic fungi (Stamps *et al.*, 2016).

Soon after the solid waste is landfilled, the materials suffer aerobic biodegradation due to the abundant presence of oxygen in the matter (El-Fadel & Khoury, 2000; Themelis & Ulloa, 2007), and are oxidized into carbon dioxide, water, and other by-products. (El-Fadel & Khoury, 2000; Themelis & Ulloa, 2007). The carbon dioxide is transformed into nearly the molar equivalent of the oxygen consumed, and

the depletion of oxygen marks the beginning of anaerobic biodegradation. This phase happens throughout the landfill lifespan and is associated with biogas production (El-Fadel & Khoury, 2000; Ruggero *et al.*, 2019). The anaerobic degradative phase starts with the hydrolysis of different compounds into simpler molecules, like proteins, carbohydrates, and lipids, by fermentative bacteria, (El-Fadel & Khoury, 2000; Themelis & Ulloa, 2007) which are then further hydrolysed into its monomers- amino acids, sugar, and high molecular fatty acids, respectively (El-Fadel & Khoury, 2000). This phase leads to a decrease in the pH of the waste, and an increase in the chemical oxygen demand (COD) and the concentration of volatile fatty acids, ammonia, and sulphates (Quecholac-Piña *et al.*, 2020). Afterwards, acid-producing bacteria transform these monomers into organic acids (like propionic acid, ethanol, and butyric acid) (Themelis & Ulloa, 2007) and/or directly ferment them to acetic acid. The fatty acids are oxidized to form some by-products and hydrogen (El-Fadel & Khoury, 2000). At last, methanogenic bacteria use acetic acid to form methane (60-70 %) and carbon dioxide (30-40 %) and transform the carbon dioxide and hydrogen into methane and water (El-Fadel & Khoury, 2000; Ruggero *et al.*, 2019). This methane is then captured to be transformed into a renewable energy source (Themelis & Ulloa, 2007). This anaerobic digestion can happen in a single-phase system or a two-phase system. In Europe, 95 % of landfills work in a single-phase system, where the anaerobic biodegradability happens in a single reactor, while in a two-phase system, the hydrolysis and acidogenesis go down in the first reactor, and the methanogenesis in the second (Ruggero *et al.*, 2019). Factors like temperature, oxygen, moisture content, alkalinity, presence or absence of oxygen, and type of nutrients and inhibitors affect the biodegradation process in landfills (Quecholac-Piña *et al.*, 2020).

While the landfill is still in operation, rainwater tends to infiltrate the waste and drag with it a lot of organic and inorganic compounds as well as heavy metals, producing a complex wastewater called leachate. It is normally a dark-coloured liquid constituted by dissolved organic matter, inorganic compounds (like ions) heavy metals, and xenobiotic organic compounds, releasing a strong smell (Peng, 2017). Because of its toxic, recalcitrant, and complex composition, landfills are obligated to have draining systems that collect this wastewater and take it to nearby facilities that treat it as a non-hazardous material. Conventional procedures for this treatment compromise biological reactors, leachate transfer for treatment with domestic sewage, and chemical and physical methods (Renou *et al.*, 2008). Biological treatments compromise the use of aerobic microorganisms that degrade the organic compounds into carbon dioxide and sludge and anaerobic microorganisms that transform those organic compounds into biogas. These methods are effective in removing organic and nitrogenous matter from leachate (in a high BOD/COD ratio) (Peng, 2017; Renou *et al.*, 2008). Some aerobic treatment processes are aerated

lagoons, conventional activated sludge methods, and sequencing batch reactors, that are based on suspended-growth biomass. There are also a few based on attached-growth systems, that use biofilms or membranes to keep the microorganisms in place (Renou *et al.*, 2008). Leachate transfer is characterized by the transportation of the leachate to a sewage wastewater treatment plant, where it is treated with the rest of the domestic sewage. However, this method posed some problems due to the presence of heavy metals in the leachate, as well as inhibitors, which rendered the process inefficient. Physical and chemical treatments are normally used as a supplement to the treatment line or for the removal of specific pollutants (Renou *et al.*, 2008).

Leachate parameters, like chemical oxygen demand (COD), biochemical oxygen demand (BOD), pH, and others, vary with the age of the landfill (A. Fernandes *et al.*, 2015). In young landfills, the predominant fermentation product present is volatile fatty acids (VFA) because the landfill still contains a lot of biodegradable organic matter, that is biodegraded through rapid anaerobic fermentation (Renou *et al.*, 2008). This phase in the landfill's lifetime is called acidogenic phase, and older landfills tend to be at the methanogenic phase, where these VFA as well as the rest of the biomass is converted to methane, and the older the landfill the lower the COD and BOD concentrations (Peng, 2017).

With regards to plastics in close landfilling, degradation is very limited (Canopoli *et al.*, 2018), because there is no light or oxygen (Taghavi *et al.*, 2021), and the anaerobic biodegradation might not be very effective (Canopoli *et al.*, 2018). However, Canopoli *et al.*, (2020) conducted a study of plastics found in 30 different landfills, reporting on the difference in their physicochemical characteristics, between landfills with more than 10 years, and younger landfills, with less than 10. They showed an increase in degradation of the plastics over time, and that burial in landfills, although not the most efficient solution, can help in plastics degradation. However, it was not clarified if the degradation was due to chemical reactions or biotic factors (Canopoli *et al.*, 2020).

Some studies, that simulate landfill conditions and use microbial isolates from landfills, tested in the laboratory, show promising findings regarding biodegradation. Xochitl *et al.*, (2021) conducted a study to assess the degradation of conventional (High-Density Polyethylene) and oxo-degradable plastics, in reactors mimicking landfill conditions. The study had a duration of three years and it was concluded that the synthetic plastic only showed a slight surface erosion and reduce changes in its mechanical properties (Xochitl *et al.*, 2021). The oxo-degradable plastics, although they showed a higher level of degradation than the conventional plastic, it was still visible in the mixture. They highlighted that these findings were a result of biotic and abiotic factors, even though it was not possible to isolate any microorganisms from

the reactor. In a conclusion, they stated that in real conditions, these results would need a lot more time to be achieved and that therefore, landfilling would not be a good solution for plastic degradation (Xochitl *et al.*, 2021). Kumar *et al.* (2021) conducted a high throughput metagenomic sequencing in the microbial community of a landfill, in India, testing soil, leachate, and compost. They found around 2468 predicted species, and the presence of enzymes/genes associated with the biodegradation of polymers like PE, PET, and PS. This study showed the potential for landfill isolates for plastic biodegradation (Kumar *et al.*, 2021).

Munir *et al.* (2018) studied soil from a landfill in Medan, and found two fungi, *Trichoderma viride* and *Aspergillus nomius*, after incubation with LDPE in powder and in film, for 45 days, at 26℃. The results showed a reduction in the polymer weight of 5,13 % and 6,3 %, respectively, but also a tensile strength decrease in the plastic film (Munir *et al.*, 2018). Park & Kim (2019) also studied a bacterial culture isolated from a landfill site for its potential for PE biodegradation. They found two main microorganisms- *Bacillus sp.* and *Paenibacillus sp.*, that demonstrated a 14,7 % weight loss of the polymer microplastics and a 22,8 % reduction of particle diameter, after 60 days. Further analysis showed degradation compounds in the medium, which confirmed the biodegradation (Park & Kim, 2019). Esmaeili *et al.*, (2013) also studied landfill soil for the comparison of LDPE biodegradation with and without a microbial mixture of *Lysinibacillus xylanilyticus* and *Aspergillus niger.* These microorganisms, also isolated from landfill soil, showed good results for LDPE biodegradation, and the mixture with the two cultures had a higher biodegradation rate than the one without- 7,6 % and 15,8 %, respectively. They also tested UV-treated LDPE and non-UV-treated LDPE, concluding that the carbonyl index was slightly higher for the UV-treated polymer (Esmaeili *et al.*, 2013).

3.1.2- Estuaries

Marine environments are one of the ecosystems on earth that most suffers from plastic pollution (Syranidou *et al.*, 2019). Meso, macro, micro and nano plastics end up in oceans, putting marine life at risk (Gewert *et al.*, 2015). It is estimated 5,25 trillion of these small particles accumulate on the surface of the sea (Oberbeckmann *et al.*, 2016), forming huge masses of floating debris at the centre of the major oceans (A. *et al.*, 2020; Urbanek *et al.*, 2018), or deposit at the bottom of the ocean floors (Urbanek *et al.*, 2018). These polymers end up in the ocean due to poor management of landfills, improper disposal of sewage, improper disposal of waste, that can be carried by streams and rivers, and even littering by ships/boats (A. *et al.*, 2020). Household pollutants enter drainage systems and rivers, reaching seas and

oceans, causing a higher concentration of plastic in coasts and estuaries (Urbanek *et al.*, 2018). These plastics can then be ingested by marine life, and due to their micro and nanoscopic size, they can pass biological barriers, penetrating tissues and accumulating in the organisms (A. *et al.*, 2020).

Microbial communities in marine ecosystems can reach up to millions of microorganisms in a gram of sediment, so floating or sank plastics are susceptible to microbial attack (Urbanek *et al.*, 2018). Microorganisms readily colonize these debris (Oberbeckmann *et al.*, 2016), adapting to these contaminated sites and forming dense biofilms on the polymer surface (A. *et al.*, 2020; Roager & Sonnenschein, 2019). These films start to break down the polymer, reducing its buoyancy and hydrophobicity (A. *et al.*, 2020; Oberbeckmann *et al.*, 2016). In this habitat, the abiotic factors involved that help catalyse some of these reactions are temperature, UV light, pH and salinity, but since temperatures are normally moderate (Gewert *et al.*, 2015), photooxidation is an important factor that produces low molecular weight compounds that are more susceptible to degradation and mechanical forces like wind and waves (A. *et al.*, 2020). However, biodegradation in marine habitats is very slow, as the conditions for microorganisms' growth and action are not near optimal (Gewert *et al.*, 2015). *Bacteria, Archaea, Fungi,* and even microbial eukaryotes have been detected in plastic debris collected from marine environments, or that grew in plastics incubating in marine conditions (Jacquin *et al.*, 2019).

Estuaries are intersections between land and marine ecosystems, and are, therefore, vulnerable to changes and perturbations from natural processes and human activities (Yi *et al.*, 2020). The microbiome of these intersections is an important component that regulates the estuary's activities, having a richer composition than marine habitats (Yi *et al.*, 2020). Because urban estuaries are normally close to plastic-polluting sources, they present a high concentration of microplastic wastes, resulting in a big impact on the ecosystem's microbiome (Baptista Neto *et al.*, 2019). Therefore, estuaries should be studied as a source of potential plastic degraders due to their proximity to plastic-polluting sites.

Some microorganisms like *Rhodococcus ruber* and *Alcanivoras borkumensis* have been reported as important colonizers of plastics in marine ecosystems (A. *et al.*, 2020). *Alphaproteobacteria and Gammaproteobacteria* have been described as primary colonizers of plastic films, while microorganisms from the *Bacteroidetes* family were nominated as secondary colonizers (Delacuvellerie *et al.*, 2019). Recurring groups and families of microorganisms associated with plastic in marine environments are *Erythrobacteraceae, Rhodobacteraceae* and *Flavobacteriaceae* families, as well as some cyanobacteria (Roager & Sonnenschein, 2019). Delacuvellerie *et al.* (2019) conducted a study on microbial communities from plastics found in marine habitats and reported the presence of *Bacteroidetes, Verrucomicrobia,*

Cyanobacteria and *Proteobacteria* in the communities present in the biofilm of the plastics (Delacuvellerie *et al.*, 2019). They also report a 96 % abundance of *Microbulbifer sp.* in the community that was enriched with LDPE, finding also *Alcanivorax borkumensis* and microorganisms from *Rhodobacteraceae* and *Flavobacteriaceae* families (Delacuvellerie *et al.*, 2019). *Zalerion maritimum*, a fungus present in coastal water, was tested for its capacity to degrade PE, showing positive results of 56,7 % ± 2,9 % mass variation, after 14 days of incubation (Paço *et al.*, 2017).

For PET, *Muricauda sp., Thalassospira sp.* (A. *et al.*, 2020) and members of the *Alcanivoraceae* and *Flavobacteriales* family have been identified as capable of degrading it (Roager & Sonnenschein, 2019). *Bacillus cereus* and *Bacillus gottheilii* strains were described as PET degraders, showing a 6,6 % and 3 % weight loss after 40 days (Roager & Sonnenschein, 2019). *Pseudomonas, Alcanivoraz* and *Tenacibaculum* were described as potential PCL degraders, that were isolated from deep-sea sediment (A. *et al.*, 2020). Two *Pseudomonas* strains were isolated from deep seawater (at around 320 m) and were found to be PCL degraders, in incubations at 4℃ (Urbanek *et al.*, 2018). In a study of microorganisms of arctic regions, fungal strains *Clonostachys rosea* and *Trichoderma sp.* were identified as PCL degraders, with a 53 % biodegradation after 30 days (Urbanek *et al.*, 2018).

3.2- Plastics: characteristics and applications

Plastics can be derived from fossil fuels or renewable resources that can be shaped into various forms and objects (Kale *et al.*, 2015) (Table 1).

Conventional plastics are synthetic and semi-synthetic polymers primarily derived from fossil carbon sources like crude oil and natural gas (Gómez & Michel, 2013) and are considered non-biodegradable (Table 1) (M. Fernandes *et al.*, 2020). Their lightweight, stable chemical and physical properties make them extremely durable and fitted for everyday use, and their production is well-established and efficient, which results in their low cost (Mohanan *et al.*, 2020). They are used in industries like pharmaceuticals, food packaging, cosmetics, and beverage, among many others (Taghavi *et al.*, 2021). However, the characteristics that make them so desirable for humans (Chamas *et al.*, 2020), are also the reason why they are the most harmful to the environment- their recalcitrant nature (Ahmed *et al.*, 2018).

Table 1: Types of plastics based on their biodegradability and source of raw material. Adapted from (Havstad, 2020)

		End of Life Option	
		Non-Biodegradable Plastics	Biodegradable Plastics
Resources Basis of the Material	Bio-Based	Bio-Based PE, PET Oxo-Biodegradable	PHA; PLA, starch blends
	Fossil-Based	Conventional PE, PP, PS, PUR, PVC, PET	Aliphatic-aromatic polyesters

Biodegradable plastics have had a major role in controlling the use of these more harmful compounds, being the eco-friendlier alternative, since they need less fossil fuel for their production and introduce fewer greenhouse emissions (Trivedi *et al.*, 2016). According to the definition of the International Standardization Organization (ISO) plastic can be considered biodegradable depending on the changes it suffers in its chemical structure, mechanical strength, and surface properties by the attack of microorganisms (M. Fernandes *et al.*, 2020; Glaser, 2019). However, the European Standardization Committee (CEN) only considers biodegradable plastics the ones that can be converted into microbial metabolic products (M. Fernandes *et al.*, 2020). Nevertheless, they are polymers that can more easily be biodegraded by microorganisms without producing toxic compounds (Alshehrei, 2017). They have been applied in packaging, health, and agriculture industries (Ahmed *et al.*, 2018) although their use in the plastic industry has not been significant enough since they cannot yet entirely substitute conventional plastics (Shen *et al.*, 2020). In 2020, the global production capacity for these plastics was 1,2 Mt/year (Choe *et al.*, 2021). The biodegradability of these safer alternatives still needs to be more studied as they still pose as complex compounds to degrade. Additionally, their use requires yet a proper waste management, garbage control, and community education to not become another danger to the environment (Ahmed *et al.*, 2018; R. Wei & Zimmermann, 2017).

The biodegradation of plastics, either synthetic or biodegradable, by microorganisms or/and enzymes is a good strategy to tackle plastic waste accumulation, that enables the depolymerization of the materials into monomers or their mineralization into carbon dioxide, water, and biomass (Folino *et al.*, 2020; Matjasic *et al.*, 2020; Mohanan *et al.*, 2020). Over the years, the number of publications about plastic biodegradation has been increasing, (Matjasic *et al.*, 2020), however, there is still a need for further research in the optimization of polymer biodegradation, especially for non-biodegradable plastics (Iram *et al.*, 2019).

3.2.1- Non-biodegradable plastics: characteristics and applications

The non-biodegradable fossil-based polymers are derived mainly from non-renewable resources, like petroleum sources, which are highly stable and have a high molecular weight due to long monomers repetitions in their chain. Petroleum-based plastics are extremely bio-inert, with a highly hydrophobic chain, which makes their biodegradation very complicated, but not impossible (Ahmed *et al.*, 2018; Attallah *et al.*, 2021; Iram *et al.*, 2019).

The linkage between monomers determines how biodegradable a certain plastic can be. For example, those with a C-C linkage, like polyethylene (PE), polypropylene (PP), polystyrene (PS), and polyvinyl chloride (PVC) are more recalcitrant than those that contain a C-O hydrolysable backbone, like polyurethane (PUR) and polyethylene terephthalate (PET) (Chen *et al.*, 2020). Because their backbone is made solely out of carbon atoms, the biodegradation of PE, PP, PS, or PVC can be more efficiently done using UV radiation and oxygen, which leads to fragmentation of the chain or its' scission. The resulting smaller fragments are then more susceptible to biodegradation (Mohanan *et al.*, 2020). Most C-C cleavage studies focus on PE, with very few describing PS biodegradation. Polymers like PVC and PP are extremely stable, and the visible biodegradation that they suffer takes months to occur. PET and PUR are linked together by hydrolytic bonds like ester and urethane, respectively, that are more susceptible to biodegradation than C-C bonds (Chen *et al.*, 2020). The presence of these heteroatoms in their chain also gives them improved thermal stability characteristics (Mohanan *et al.*, 2020). Most of the time, it is necessary to make plastics go through pre-treatments to obtain meaningful biodegradation results (Chen *et al.*, 2020).

Synthetic plastics can also be separated into two different classes, thermoplastics and thermosets, depending on their thermal properties (Amobonye *et al.*, 2021). Thermoplastics, like PE, PP, PS, and PVC, do not suffer changes in their chemical composition after reheating, making it possible to remodify them after melting. This property is the main reason for their recalcitrant nature, which makes them flexible and recyclable (Taghavi *et al.*, 2021) but resistant to hydrolytic cleavage (Amobonye *et al.*, 2021). Thermosets, on the contrary, do not recover their original form after reheating because they will cross-link, and bind the molecules in their chain with covalent bonds, making it an irreversible reaction (Amobonye *et al.*, 2021; Kayjhaii & Lindford, 2020). The backbones of these types of plastics are heteroatomic and highly cross-linked, making them more susceptible to hydrolytic cleavage (Amobonye *et al.*, 2021). They are stronger and more brittle than thermoplastics and are most commonly used in

automotive, lighting, and electrical industries (Taghavi *et al.*, 2021). PET and PUR are some examples of thermoset polymers (Amobonye *et al.*, 2021).

Bio-based non-biodegradable plastics are also referred to as oxo-biodegradable, and they fall into this category although they are bio-based, solemnly on the fact that their biodegradation has not been conclusively observed and further research into it is needed (Ahmed *et al.*, 2018; Iram *et al.*, 2019).

In this work, only PE and PET, from synthetic plastic, were studied, so only these two non-biodegradable plastics will be discussed in more detail.

3.2.1.1- Polyethylene (PE)

It is the most broadly produced synthetic plastic (Wilkes & Aristilde, 2017) and is used to produce bags, water bottles, food packaging, films, toys, pipers, and motor oil bottles (Ahmed *et al.*, 2018). It is a very hydrophobic polymer due to the saturation of its chain with ethylene bonds (Figure 1) (Wilkes & Aristilde, 2017).

Pre-treatments like UV irradiation, chemical oxidizing agents, and thermo-oxidation lead to the depolymerization of the long chain and the formation of low molecular weight products, facilitating biodegradation (Ru *et al.*, 2020). PE can have different densities and 3-dimensional and physical structures depending on the manufacturing processes that originate it. There is low molecular weight polyethylene (LMWPE), linear low-density polyethylene (LLDPE), low-density polyethylene (LDPE), and high-density polyethylene (HDPE) (Mohanan *et al.*, 2020). LDPE is more easily biodegraded than HDPE since its' branches arrangement make it easier for microorganisms to access and attack the molecules. It also has a lower molecular mass than HDPE, which also influences the access of enzymes to its chain, making biodegradation easier. Plastic bags made of LDPE are the most common type of plastic garbage found in landfills, accounting for 69,13 % of the waste (Mohanan *et al.*, 2020). HDPE is more commonly used in applications in the construction business (Kaushal *et al.*, 2021) since it has stronger intermolecular forces and higher tensile strength. It also has higher stability due to its bigger density and smaller bond length (Ghatge *et al.*, 2020). PE-degrading microorganisms have been isolated from soil, sea, compost, and active sludge (Mohanan *et al.*, 2020).

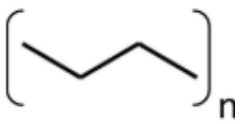

Figure 1: PE monomer's structure. Adapted from Ru, *et al.* (2020) and Danso, *et al.* (2019).

3.2.1.2- Polyethylene terephthalate (PET)

Results from the polymerization of terephthalic acid and ethylene glycol through ester linkages (Figure 2) (Chen *et al.*, 2020; Kaushal *et al.*, 2021). It is a linear polymer whose monomer is bis(2-hydroxyethyl) terephthalate (BHET) (Danso *et al.*, 2019). The most frequent materials that have PET in their structure are carpets, shirts, bags, plastic bottles, food packages, and containers (Ahmed *et al.*, 2018) as well as textile fibres and films (Mohanan *et al.*, 2020). Due to the single-use plastic products it composes, it is one of the main plastic polluters (Kaushal *et al.*, 2021). It is a recalcitrant polymer with high durability, due to the aromatic units composing its' backbone (Table 2), having limited chain mobility (Glaser, 2019). This makes it a very rough and firm polymer (Kaushal *et al.*, 2021), that has a high glass transition temperature (75℃ to 80℃) and above this value, the amorphous regions become more flexible and therefore, more susceptible to microbial attack (Mohanan *et al.*, 2020). PET molecules have a crystalline-like structure, where they are packed together in a non-uniform way, and an amorphous structure with a disordered domain (Ru *et al.*, 2020). Because the polymer chains in the amorphous domains are less densely packed, the surface part of PET containing a high portion of amorphous domains degrades more easily (Ru *et al.*, 2020).

Enzymes that degrade PET can be divided into two types based on what they can degrade: PET surface-modifying enzymes, which degrade only the surface of the polymer, and PET hydrolases, which degrade the inner bulk of PET (at least 10 % weight loss) (Ru *et al.*, 2020). This different capacity to degrade one part of the PET polymer but not its bulk structure is related to the hydrophobic characteristics of the bulk, which make microbial attachment more difficult (Glaser, 2019). With a high temperature of degradation (65°-70℃) the polymer chain in the amorphous PET domain can become mobile enough to allow access to the active site of the PET hydrolases, making the biodegradation process easier and quicker (Glaser, 2019; Ru *et al.*, 2020). However, not many hydrolases can function at these high temperatures, so studies on thermophilic enzymes are needed (Ru *et al.*, 2020).

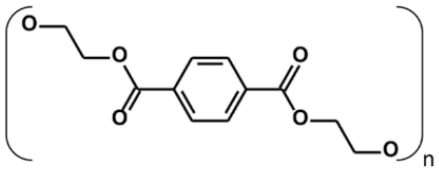

Figure 2: PET monomer's structure. Adapted from Ru, *et al.* (2020) and Danso, *et al.* (2019).

3.2.2- Biodegradable plastics: characteristics and applications

Biodegradable plastics' annual production accounts for about 1 % of the total amount produced per year, having produced around 2,11 million tonnes, in 2019 (Folino *et al.*, 2020). Microorganisms like bacteria and fungi can biodegrade them through enzymatic action, and form products like water, methane, inorganic compounds, and carbon dioxide (Ahmed *et al.*, 2018; Folino *et al.*, 2020).

These polymers are evident replacements for non-biodegradable plastics (Folino *et al.*, 2020) since they can be more easily degraded in the environment and enrichen the soil through their composting, which leads to less effort and costs for removal of plastics from the ecosystems (Iram *et al.*, 2019; Leja & Lewandowicz, 2010). They are also highly accessible and abundant with low toxicity (Pires *et al.*, 2022), which increases the durability and stability of landfills since the amount of waste is diminished (Iram *et al.*, 2019). They are used in different industrial fields since their manufacturing process enables the attribution of different characteristics as needed. Flexibility, strength, memory, and resistance to liquids can be easily changed by altering the processing conditions, resulting in a wider range of applications. The most common applications are in the packaging industry, but they can also be used in agriculture, (Folino *et al.*, 2020), electronics, toys, and medicinal and surgical products (Miri *et al.*, 2022).

Composting turns out to be the principal end-of-life option for most biodegradable plastics, and several standard biodegradability tests are usually performed on plastics, to test their future biodegradability in industrial compost facilities (Flury & Narayan, 2021). However, they also have some limitations, which include high production costs and lower mechanical properties (Emadian *et al.*, 2017; Folino *et al.*, 2020).

Bio-based biodegradable plastics can be made from renewable sources by microorganisms (Bátori *et al.*, 2018), like cellulose, starch, or starch-based polymers, or extracted from proteins, polysaccharides, or lipids (Pires *et al.*, 2022). Therefore, microorganisms' exoenzymes can easily break them down, and quickly take them up and degrade them (Ahmed *et al.*, 2018). A few examples of bio-based polymers are PHA (polyhydroxyalkanoate) and PHB (poly(3-hydroxybutyrate) (Bátori *et al.*, 2018; Pires *et al.*, 2022). In addition, bio-based plastics can arise from bio-derived materials by chemical syntheses, like the case of PLA- poly(lactic acid) and PBS- poly(butylene succinate) (Bátori *et al.*, 2018).

Fossil-based plastics, that have a petrochemical origin, can also be considered biodegradable, like PCL- poly(caprolactone), PBAT- poly (butylene adipate-co-terephthalate), and PVA- poly (vinyl alcohol)

(Bátori *et al.*, 2018). These are considered biodegradable because of their degree of biodegradability (Ahmed *et al.*, 2018). However, they still have a very slow rate of biodegradation (Iram *et al.*, 2019), and can still form microplastics that, although less durable than non-biodegradable ones, can still pose a threat to the environment, (Liao & Chen, 2021). Therefore optimization and further study of these polymer's biodegradability are still needed (Iram *et al.*, 2019; Liao & Chen, 2021).

In this study, the focus on biodegradable plastics will be PCL.

3.2.2.1- Polycaprolactone (PCL)

PCL is a synthetic fossil-based polyester, with high flexibility and non-toxicity (Din *et al.*, 2020) that can be degraded by microorganisms either anaerobically or aerobically (Borghesi *et al.*, 2016; Iram *et al.*, 2019; Trivedi *et al.*, 2016). It is derived from crude oil by chemical synthesis (Sankhla *et al.*, 2020), more specifically derived from caprolactone by polymerization (Havstad, 2020) and it is composed of methylene units and ester groups (Lambert & Wagner, 2017) (Figure 3). There are two mechanisms of production of PCL, one by the polycondensation of a hydroxycarboxylic acid (Thakur *et al.*, 2021) or by ring-opening polymerization of its monomer- ε-caprolactone (Blackwell *et al.*, 2018; Thakur *et al.*, 2021). The ring opening mechanism is the most used in industry, because it produces a polymer with high molecular weight and lower polydispersity (Thakur *et al.*, 2021).

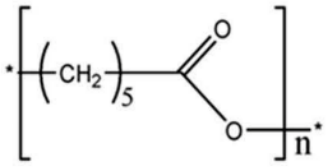

Figure 3: PCL monomer's structure. Retrieved from Din *et al.* (2020).

PCL is a hydrophobic and partially crystalline linear aliphatic polyester with low melting temperature (around 60℃), and relatively low strength (Borghesi *et al.*, 2016; Nevoralová *et al.*, 2020; Tokiwa *et al.*, 2009), low glass transition temperature (around -60℃) that make its' processing easier (Borghesi *et al.*, 2016; Lyu *et al.*, 2019; Tokiwa *et al.*, 2009). It has a great impact on biomedical and tissue applications (Nevoralová *et al.*, 2020), due to its biocompatibility (Blackwell *et al.*, 2018), and is used in blood bags, catheters, packaging material (Iram *et al.*, 2019), sutures, drug delivery systems, tissue engineering, and dentistry (Havstad, 2020). It also has applications in long-term items, like agricultural films, fibres, aquatic weeds, and seedlings containers (Ahmed *et al.*, 2018). Since its melting temperature is below 100℃ it can also be incorporated into a wide range of natural additives for food

packaging (Scaffaro *et al.*, 2019). These applications in the food-packaging and agriculture industry are valuable since PCL is water and oil-resistant, non-toxic, and biodegradable (Nevoralová *et al.*, 2020).

It has compatibility with several other polymers (Nawaz *et al.*, 2015), and as such, it is often used to make blends with bio-based biodegradable plastics such as PLA and PHA (Havstad, 2020), as well as starch (Nevoralová *et al.*, 2020). These blends have been studied to improve some of PCL's properties, like its dyeability, and stress-crack-resistance (Thakur *et al.*, 2021) including its' biodegradability in the environment (Nevoralová *et al.*, 2020).

Its' degradation can greatly vary according to the biodegradation environment (Li *et al.*, 2022; Nevoralová *et al.*, 2020), but, due to the existence of hydrophobic -CH_2 units (Thakur *et al.*, 2021), its' homopolymer degradation is slow (Nevoralová *et al.*, 2020). Even so, biodegradation of PCL polymers has been observed in places like rivers, lakes, sewage sludge, farm soil, paddy soil, creek sediment, roadside sediment, pond sediment, and compost (Nawaz *et al.*, 2015; Nevoralová *et al.*, 2020). Its molecular weight (Nevoralová *et al.*, 2020) and crystallinity play an important part in polymer biodegradation, as they also dictate its properties (Thakur *et al.*, 2021), leading to disperse results between different experiments (Nevoralová *et al.*, 2020).

Due to its low melting temperature, it is thought that composting would be a good method for disposal of PCL waste since in compost the temperature reached is normally around or above 60℃ (Nevoralová *et al.*, 2020; Thakur *et al.*, 2021).

3.3- Mechanisms of polymer biodegradation

Biodegradation is the bio-chemical process executed by microorganisms, that leads to the degradation and assimilation of a certain polymer, with the production of degradation compounds (Alshehrei, 2017). Compared to other end-of-life treatments of plastics, like thermal and hydrothermal degradation techniques, the utilization of microorganisms for plastics degradation does not result in value-added compounds, due to its' low speed. However, the biodegradation of plastics is cheaper than the other methods and doesn't emit toxic gases or hazardous compounds (Taghavi *et al.*, 2021) even contributing to soil fertility, diminishing the accumulation of plastic, and reducing the expenses of waste management (Atanasova, Stoitsova, *et al.*, 2021) making it an eco-friendly alternative (Taghavi *et al.*, 2021).

The biodegradability of a plastic depends on the raw material it is made of, its chemical composition, the structure of the final product, and the environmental conditions necessary for its biodegradation (Havstad, 2020). It was observed that biodegradation in aquatic environments is much less efficient and slower than in soil and compost, mainly due to the lower temperature and lesser microbial activity (Flury & Narayan, 2021). Plastic biodegradation is a complicated process that still lacks an exact definition and measuring techniques, as different studies use different variables' measurements to evaluate the degree of biodegradability of a material. It can be evaluated by weight loss of the plastic, change in its mechanical and physical properties, or the percentage of carbon dioxide emission (Mohanan *et al.*, 2020). It depends on various factors, like the availability of substrate, surface characteristics of the plastics, morphology, or molecular weight (Mohanan *et al.*, 2020). It is normally a surface erosion process since it is difficult for extracellular enzyme to penetrate the polymer, making biodegradation a more superficial process (Kale *et al.*, 2015).

The mechanisms used by microorganisms to degrade the polymers can be various, but the main principle is the breaking down of the complex molecules into their simpler monomers, dimers, or oligomers (Glaser, 2019; Iram *et al.*, 2019). The biodegradation of plastic begins with hydrolysis which can be an enzymatic or non-enzymatic process (Ahmed *et al.*, 2018). Since the resulting polymers are smaller, they can be easily taken up by the cells and used as a nutritional source, either by anaerobic or aerobic mechanisms (Ahmed *et al.*, 2018).

On a general note, the biodegradation step, either in aerobic or anaerobic conditions, can be synthesized into 3 steps, biodeterioration, biofragmentation, and assimilation (Figure 4) (Iram *et al.*, 2019).

Biodeterioration is the initial stage where abiotic and biotic factors affect the superficial degradation of the plastic, by altering the mechanical, physical and chemical properties of the polymer (Figure 4) (Amobonye *et al.*, 2021; Iram *et al.*, 2019; Jaiswal *et al.*, 2020). There is a formation of carbonyl groups that are oxidized into carboxylic acids (Mohanan *et al.*, 2020). These changes can also be enhanced by persistent exposure to environmental factors, like light, temperature, and even chemicals (Amobonye *et al.*, 2021) so some techniques can be implemented to increase the percentage of biodegradation- such as chemical, thermal, photo and biological technologies (Glaser, 2019). For example, in thermal degradation, the polymer suffers an overheating that causes the split of the chemical bonds (Matjasic *et al.*, 2020). For instance, autoclaving is a common type of thermal pre-treatment used in various papers (Matjasic *et al.*, 2020).

This stage helps to break down the material into its' smaller fragments and can be done by environmental conditions, like humidity and weather (Glaser, 2019), as well as by microbial activity (Figure 1) (Iram *et al.*, 2019). Other abiotic factors, like non-ionizing radiation, temperature, wind effects, and atmospheric gases can make this step easier (Glaser, 2019). This stage helps speed up the biodegradation process because the fragmentation and erosion of the surface help accelerate the diffusion of oxygen and microbial enzymes (Folino *et al.*, 2020).

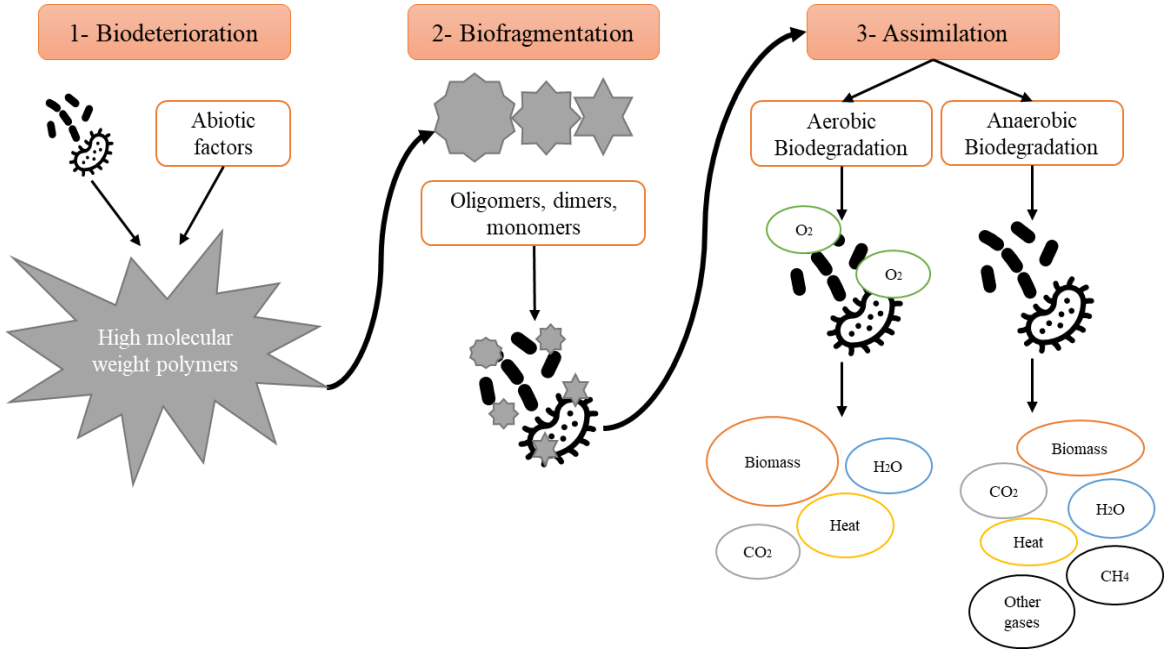

Figure 4: General representation of the main steps of polymer biodegradation under aerobic and anaerobic conditions. Adapted from Iram *et al.* (2019) and Bátori *et al.* (2018).

Biofragmentation is the phase where the microorganisms secrete their enzymes and free radicals, which will break down the polymers to produce their lower molecular weight fragments (Figure 4). It can also be referred to as depolymerization (Glaser, 2019). The biodegradation process starts with the adhesion of microorganisms to the surface of the polymer, followed by colonization (Ahmed *et al.*, 2018). The addition of hydrophilic functional groups enhances the hydrophobicity of the material (Iram *et al.*, 2019; Miri *et al.*, 2022), promoting cell adhesion due to the attraction between the hydrophilic cells and the normally hydrophobic polymer (Wilkes & Aristilde, 2017). This would lead to surface deterioration, which would make the internal colonization of the microorganisms easier (Taghavi *et al.*, 2021). Then, the excreted enzymes start to break down the polymers into their smaller counterparts, like monomers, dimers, or oligomers (Ahmed *et al.*, 2018). These extracellular enzymes attack specific bonds or chemical groups on the polymer chain, however, it is implausible that they diffuse into the polymer, causing only superficial biodegradation, which may lead to cracks and holes (Miri *et al.*, 2022). Amorphous regions,

with greater branching, and chains with a higher number of functional groups are more easily accessible by enzymes, and therefore attacked first, when in comparison with crystalline regions or linear non-reactive fragments (Iram *et al.*, 2019; Kjeldsen *et al.*, 2019).

This adhesion process can include a biofilm formation by the different microorganisms of a microbial community (Ali *et al.*, 2021). Biofilms are composed of functionally and phylogenetically diverse microbial communities that are attached to a surface and are held together to the material by the production and release of exopolysaccharides which act as an adhesive for further colonization (Ghosh *et al.*, 2019; Glaser, 2019). Bacteria are normally the primary colonizers in biofilm formation, which leads to the entrapment of other microorganisms, like fungi (Atanasova, Stoitsova, *et al.*, 2021). This results in a significantly different community of microorganisms compared to the surrounding environment (Atanasova, Stoitsova, *et al.*, 2021). Biofilms help with the chemical and physical degradation of the polymer, and its formation will depend on the structure and composition of the plastic (Jaiswal *et al.*, 2020). As a consequence, a wider spectrum of enzymes are produced, cellular viability is increased due to bigger bioavailability of nutrients, and by-products do not accumulate (Ghosh *et al.*, 2019; Glaser, 2019). In other words, with the attack of different microbial species, included in the biofilm, a better breakdown of the polymer can be observed, since some will be responsible for breaking down into smaller molecules, others will degrade those monomers and excrete the by-products, and others will use those excreted wastes as feed (Shah *et al.*, 2008).

When the molecular size of the polymer molecules reaches 10-50 carbon atoms, the products can be then assimilated by the cells, starting the next phase of biodegradation-assimilation (R. Wei & Zimmermann, 2017) (Figure 4). This assimilation process has yet to be well elaborated, but it is thought that it involves active and passive transport (Amobonye *et al.*, 2021). Some of these receptors in the cell membrane recognize some of these molecules and make their entry possible. The fragments that are not recognized by the cell, have to go through further biotransformation reactions, to produce molecules that can easily diffuse through the cell membrane. (Glaser, 2019; Iram *et al.*, 2019). However, some fragments that are still too big to enter cells end up not being assimilated (Jaiswal *et al.*, 2020). It was observed the facilitated passive transport of a degradative product, in *Pseudomonas sp.* DG17, when in high concentrations, and the energy-dependent active transport when in lower concentrations. It was also noted the role of membrane-bound monooxygenases and porins in the transport of degradative compounds (Amobonye *et al.*, 2021). Nevertheless, the transport of these molecules inside the cell is still

a subject that needs more attention and study, since intracellular enzymes responsible for this transport remain unknown (Miri *et al.*, 2022).

After entering the cell, the fragments take part in diverse metabolic pathways as an energy and carbon source (Ahmed *et al.*, 2018). Metabolic products with carbonyl or hydroxyl functional groups can enter metabolic pathways like β-oxidation or the tricarboxylic acid (TCA) cycle (Miri *et al.*, 2022). During this process, various metabolites are secreted into the extracellular surroundings, like organic acids, aldehydes, and terpenes (Iram *et al.*, 2019), and intracellular metabolites are hydrolysed completely, reaching a stage called mineralization (Iram *et al.*, 2019). The mineralization step can occur either in aerobic or anaerobic conditions (Figure 4) (Iram *et al.*, 2019) and results from the complete degradation of the plastic derivates, inside the cells, into oxidised metabolites (Amobonye *et al.*, 2021). The secondary metabolites formed during this stage can find their way outside of the cell, where they are utilized by other microorganisms (Jaiswal *et al.*, 2020).

When oxygen is present, aerobic biodegradation happens, as it is used as a final electron receptor, and molecules of carbon dioxide and water are produced (Figure 4) (Glaser, 2019; Iram *et al.*, 2019; Leja & Lewandowicz, 2010). On the other hand, when no oxygen takes part in this process, it is called anaerobic biodegradation, and the final products include water, organic acids, and biogas (Figure 4) (Ahmed *et al.*, 2018; Glaser, 2019; Iram *et al.*, 2019). This biogas is a mixture of methane, carbon dioxide, small amounts of nitrogen, ammonium, hydrogen sulphide, and water vapour (Iwańczuk *et al.*, 2015). Methane can be used in other processes as fuel, for example, to produce light and heat, or as a substrate in the manufacturing process of organic acids (Kaushal *et al.*, 2021), so this biogas is considered a renewable energy source (Iwańczuk *et al.*, 2015). Anaerobic microorganisms use other molecules as electron acceptors such as nitrate, iron, manganese, and carbon dioxide, to form these by-products (Ahmed *et al.*, 2018; Iram *et al.*, 2019), and this form of biodegradation is an important process for the attenuation of contaminants in hazardous waste sites (Alshehrei, 2017).

When comparing the two forms of biodegradation, the aerobic process tends to be more efficient, since respiration converts more energy (Glaser, 2019). However, in aerobic biodegradation energy stored as organic matter is released in the form of heat, which requires constant turnover of the biomass for its release, and it cannot be recovered (Bátori *et al.*, 2018). On the contrary, in anaerobic degradation, this energy is largely released as methane, a renewable energy source, that can be used for other processes, but there is less biomass produced due to the lack of oxygen (Bátori *et al.*, 2018). However, this type of biodegradation is predominantly useful for the biodegradation of biodegradable plastics that do not

decompose well (Flury & Narayan, 2021). In the environment, aerobic biodegradation is the type of biodegradation that most often happens, while anaerobic degradation happens in sediments and landfills. In compost and soil, biodegradation is partly aerobic (Alshehrei, 2017).

In the environment, since plastics are not the only source of carbon, their biodegradation is normally very low, and the enrichment of strains that can degrade plastics is also reduced (Taghavi *et al.*, 2021). Nevertheless, at a laboratory scale, optimization of the medium and growth conditions can be accomplished to help in the limiting step of plastic biodegradation- the initial hydrolysis. These, together with genetic engineering to enhance the production of degrading enzymes, allow the improvement of microorganisms' activity and consequently the plastic biodegradation (Atanasova, Stoitsova, *et al.*, 2021).

3.3.1- Factors affecting plastic biodegradation

The efficiency of biodegradation can be affected by several factors, such as the type of microorganism, the pre-treatment, and the polymer characteristics. (Ahmed *et al.*, 2018) (Figure 5).

Microorganisms capable of biodegrading plastics have been isolated from the environment, like soil of a plastic dumpling site, the films of marine water, soils contaminated by crude oil, sewage sludge, landfills, and the gut of a variety of animals (Ru *et al.*, 2020). It was observed better performance in plastic biodegradation by microbial communities rather than by isolated microorganisms (Ali *et al.*, 2021). This can be explained by the cooperation that likely exists between microorganisms degrading polymers, that otherwise would result in a lower biodegradation efficiency due to the limited metabolic capacity of individual microorganisms (Ali *et al.*, 2021; Lear *et al.*, 2021; Taghavi *et al.*, 2021). This way, microorganisms collaborate with each other, and with abiotic factors, like heat and light, to trigger a bigger impact on the plastic's structural integrity (Lear *et al.*, 2021).

Some of the polymer characteristics that influence biodegradation are the surface characteristics of the plastic (hydrophobic or hydrophilic, surface area), their structure (molecular weight, mobility, crystallinity, type of functional group, melting temperature) (Bátori *et al.*, 2018; Folino *et al.*, 2020), the physical form of the polymer (films, powder, pellets or fibres) (Alshehrei, 2017) and the addition of compounds like additives, which influence the final percentage of biodegradation of a polymer (Kale *et al.*, 2015) (Figure 5).

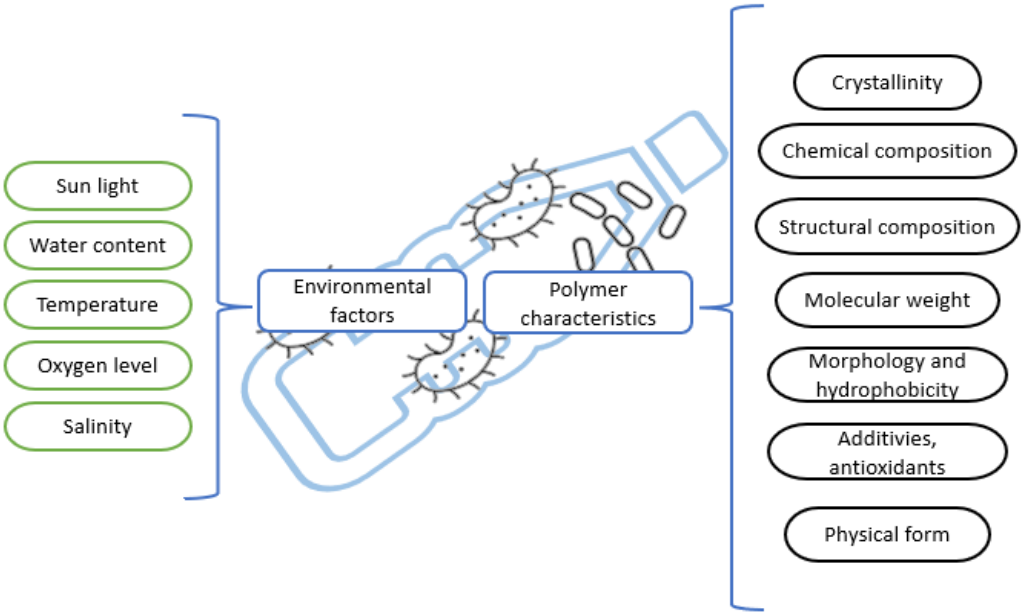

Figure 5: Environmental factors and polymer characteristics that influence polymer biodegradation. Adapted from Ali *et al.,* 2021.

The molecular weight of a polymer defines many of its properties and the lower the molecular weight, the easier it is degraded by enzymes (Ahmed *et al.*, 2018; Iram *et al.*, 2019). A high molecular weight polymer has a lower solubility compared to a low molecular weight plastic, which makes the microbial attack and the consequent assimilation through the microbial membrane of the monomers an unfavourable and harder process (Shah *et al.*, 2008).

Larger surface areas lead to greater biodegradation by enzymes (Iram *et al.*, 2019), since they allow the increase of microbial-colonized areas, resulting in a faster biodegradation rate (Glaser, 2019). The chemical structure of the polymer also directly affects the degree of biodegradation (S. H. Zeng *et al.*, 2016). The addition of hydrophilic compounds or the use of amphiphilic compounds produced in living surfaces can facilitate the colonization and increase the biodegradation of the polymer (Ali *et al.*, 2021; Glaser, 2019; S. H. Zeng *et al.*, 2016). With a higher number of hydrophilic functional groups, cell surface attachment is made easier, since cell surfaces are hydrophilic and are repelled by hydrophobic polymer surfaces (Wilkes & Aristilde, 2017). On the contrary, the presence of additives, antioxidants, and stabilizers in the polymers, used in the manufacturing process, will decrease the biodegradation rate (Kale *et al.*, 2015). Furthermore, linear and powder polymers are more easily biodegraded than cross-linked and branched polymer films (S. H. Zeng *et al.*, 2016). Additionally, polar covalent bonds, like ester or amide bonds, compared to carbon-carbon bonds, also facilitate the biodegradation of plastics (Atanasova, Stoitsova, *et al.*, 2021).

The degree of crystallinity dictates the tightness of the polymer chain and the tighter it is, the harder it is for the microorganisms to attach themselves to the surface of the plastic (Glaser, 2019; Lambert & Wagner, 2017). The degree of flexibility of the chain is higher with more amorphous chains, and therefore, easier for a microbial attack to happen (S. H. Zeng *et al.*, 2016). Additionally, the more crystalline the polymer is, the more water and oxygen are necessary for the biodegradation process to initiate (Ali *et al.*, 2021). The addition of biosurfactants can enhance the process of biodegradation because the addition of these specific functional groups enhances the susceptibility to microorganisms (Iram *et al.*, 2019).

Microorganisms, environmental factors like moisture, pH, temperature (Iram *et al.*, 2019), salinity and the presence or absence of oxygen (Kale *et al.*, 2015) can also affect biodegradability (Figure 5). Sufficient water content is necessary for the basic function and survival of the microorganisms (Iram *et al.*, 2019), and polymeric degradation, in certain cases, can only happen in the presence of some humidity (S. H. Zeng *et al.*, 2016). A lack of water will lead to a decline in cell growth, and therefore, in cell metabolism, and excess moisture can cause anaerobiosis and the packing down of the substrate, making aerobic degradation more difficult (Grima *et al.*, 2000). Additionally, hydrolytic activity increases with the increase in water content (Iram *et al.*, 2019), and more water content can increase hydrolysis by generating more chain scission reactions (Ahmed *et al.*, 2018). pH directly affects the growth of the microorganisms, although the optimum pH will vary from organism to organism (Ahmed *et al.*, 2018). In optimal pH conditions, microbial activity will also be enhanced by humidity (S. H. Zeng *et al.*, 2016), and hydrolytic reactions will be affected by changes in the pH (Iram *et al.*, 2019).

When comes to the effect of temperature, it can have a dual effect on biodegradation (S. H. Zeng *et al.*, 2016), since it has a direct impact on the structure and functionality of the biomolecules and the integrity of cellular structures (Gomes *et al.*, 2016). To a certain threshold, high temperatures can help enhance biodegradation, since they speed up metabolic processes and have a positive effect on microbial growth (S. H. Zeng *et al.*, 2016). However, in higher temperatures, mesophilic enzyme activity will be reduced, but most polymers have a high melting point (ranging from 56℃ to 180℃ (Suzuki *et al.*, 2021)), so at that melting temperature, there's a high chance of mesophilic enzymes being deactivated (Iram *et al.*, 2019).

3.4- Techniques to evaluate and monitor biodegradation

The evaluation of some characteristics, like hydrophobicity, crystallinity, functional groups, mechanical properties, and molecular weight distribution, allows the monitorization of the polymer's biodegradation (Glaser, 2019). It can be performed through visual observation techniques, evaluation of changes in the physical or chemical properties of the polymer, monitoring of final electron acceptor and product formation (CO_2/CH_4 production or O_2 consumption), radiolabelling, and biological tests (Alshehrei, 2017; Glaser, 2019) (Figure 6).

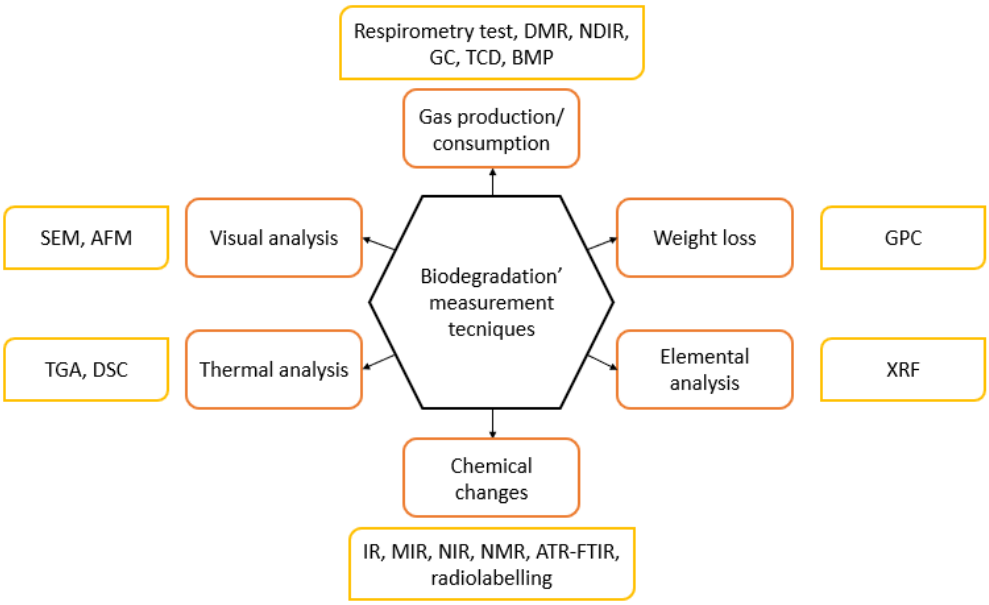

Figure 6: Analytical techniques for monitorization of plastic biodegradation. Adapted from Atanasova, Stoitsova, *et al.*, 2021. DMR- direct measurement respirometry; NDIR- nondispersive infrared sensor; GC- gas chromatograph; TCD- thermal conductivity detector; BMP- biochemical methane potential method; GPC- Gel permeation chromatography; XRF- X-ray fluorescence spectrometry; IR- infrared spectroscopy; MIR- mid-infrared spectrometry; NIR- Near infrared spectrometry; NMR- nuclear magnetic resonance; ATR-FTIR- total reflectance spectroscopy; TGA- thermogravimetric analysis; DSC- differential scanning calorimetry; SEM- scanning electron microscopy and AFM- atomic force microscopy.

It is important to note that for better evaluation of biodegradation, it is recommended the usage of more than one method, as a way to confirm the results and identify possible discrepancies between them (Matjasic *et al.*, 2020; Ruggero *et al.*, 2019). However, even when following standardised tests for the evaluation of plastics' biodegradability, the laboratory conditions do not mimic the environmental ever-changing conditions, and therefore, the results obtained in the laboratory cannot be exactly expected in the natural environment (Choe *et al.*, 2021). Consequently, the biodegradation rate of a certain plastic can either be slower or faster in the natural environment when compared to laboratory experiments (Flury & Narayan, 2021). Additionally, it is also worth noting that there needs to be minimum information about the experiment conditions, so different authors can more easily compare, repeat, or improve their work.

Information like growth medium, temperature, length of the incubations, and the application or not of pre-treatment (Matjasic *et al.*, 2020).

3.4.1- Gel permeation chromatography (GPC)

Gel permeation chromatography (GPC) measures the polymer molecular weight (Ruggero *et al.*, 2019). Measurement of mass loss is a biodegradability index, that takes into account the decrease of the molecular weight, experimental mass loss, or disintegration degree of a sample (Ruggero *et al.*, 2019). GPC gives precise measurements of the molecular weight distribution of a sample (Kayjhaii & Lindford, 2020). As a drawback, it is not very sensitive, since the analysis is done on the bulk polymer, and cannot detect the changes that occur at the surface (Raddadi & Fava, 2019). Additionally, the formation of biofilms on the surface of the polymer can lead to an increase in this weight, even though biodegradation has been observed (Jaiswal *et al.*, 2020). As such, and also due to the possible presence of additives in plastics, weight loss measurements are not a direct proof of biodegradation, especially in cases where the polymer is easily fragmented/disintegrated (Raddadi & Fava, 2019). For the analysis, polymers need to be dissolved in an organic solvent and injected into high-performance liquid chromatography (HPLC) column, with a cross-linked gel that leads to the separation of the molecules according to their size (Kayjhaii & Lindford, 2020). The degree of disintegration takes into account the percentage of particles that are held in those sieves (Ruggero *et al.*, 2019). With this method qualitative data on the long-chain branching of the sample can be obtained, as well as the identification of the composition distribution of it, using the appropriate detection and analysis methods (Al-mutairi & Mousa, 2021).

3.4.2- Thermogravimetric analysis (TGA) and Differential Scanning Calorimetry (DSC)

Thermal analysis, the evaluation of the changes in the response to temperature is an important factor in polymer characterization (Kayjhaii & Lindford, 2020). For this, methods like thermogravimetric analysis (TGA) and differential scanning calorimetry (DSC) are normally used (Al-mutairi & Mousa, 2021). TGA determines the change in mass of a certain polymer when exposed to a controlled temperature (Al-mutairi & Mousa, 2021). It is normally used as a qualitative or comparative technique (Kayjhaii & Lindford, 2020). A decrease in the thermal stability of a polymer, after biodegradation, is an indicator of degradability, when compared to non-biodegraded plastic, but the presence of heat stabilizers in the polymer affects the result (Raddadi & Fava, 2019). DSC determines the different thermal characteristics of the polymer (Raddadi & Fava, 2019), like heat capacities, phase transitions, thermal stability, sample

composition, and purity (Al-mutairi & Mousa, 2021) as well as the glass transition temperature and the decomposition temperature (Kayjhaii & Lindford, 2020) It can be performed by measuring the heat flow through time, with an increase in temperature, or measuring the heat flow at a constant temperature, throughout a determined period (Al-mutairi & Mousa, 2021). Due to biodegradation, the stability of a polymer can decrease, causing the glass temperature to decrease (Raddadi & Fava, 2019).

3.4.3- Spectroscopy

The chemical changes of the polymers can be measured by various techniques. When using spectroscopy, one can assess the biodegradability of a polymer by changes in the plastic's spectrum (Ruggero *et al.*, 2019). It can be measured by infrared spectroscopy (IR), which allows the visualization of the frequency and magnitude of the graph, due to the absorption of the radiation in the wavenumber range of 4000-400 cm^{-1}. The results are shown in graphics where the frequency matches the absorbed IR wavenumbers and is signed in the horizontal axis, while the magnitude consists of the quantity of IR, and corresponds to the peaks of the spectrum (Ruggero *et al.*, 2019). Infrared spectrometry is used to describe a certain sample of organic waste and observe the decomposition of a material. In mid-infrared (MIR) spectrometry, the sample is mixed with KBr and formed into a pellet, and its reflectance measured. Near-infrared (NIR) works in a lower spectral range, and it's used in the characterization of media, and solid bulk material. Measurements are quick and low-cost and can be done directly in the batch, by reflectance (Lesteur *et al.*, 2010). Nuclear magnetic resonance (NMR), is another type of spectroscopy, that provides the sequence of nucleic acids of the material, normally expressed based on C, H, and O (Ruggero *et al.*, 2019).

Fourier-transform infrared spectroscopy (FTIR) allows the observation of the chemical changes in the polymer structure, enabling the detection of functional groups formed during the microbial attack (Raddadi & Fava, 2019). When there is an increase in the number of peaks, compared with the polymer before biodegradation, there is an increase in simple bounds, which corresponds to a breakdown of the more complex polymer, into simpler molecules (Ruggero *et al.*, 2019). When the plastic has a higher quantity of additives, this technique becomes less effective, and biofilms in the polymer must be removed from its surface to not lead to misreadings of the functional groups. The removal of the biofilm will guarantee that the readings correspond to changes in the polymer and not to the cell debris (Raddadi & Fava, 2019).

Radiolabelling is normally used when slowly degradable materials are being studied, in a mixture with other carbon sources (Alshehrei, 2017). With this method, it is easier to distinguish CO_2 emitted by the plastic from the ones exhausted from the medium (Grima *et al.*, 2000). The carbon in the polymer is labelled with radioactive isotopes (^{14}C), and if there is biodegradation, the resulting gases will be constituted by these radioactive isotopes (Raddadi & Fava, 2019). It is a precise method, that does not suffers interference from impurities or additives in the polymer (Shah *et al.*, 2008). However, although non-destructive, its' usage is limited by its' difficult application, expensiveness and the need for qualified laboratories (Grima *et al.*, 2000; Raddadi & Fava, 2019). Additionally, the waste disposal of radioactive waste can also become a problem (Shah *et al.*, 2008).

X-ray fluorescence spectrometry (XRF) analyses the elemental structure of a sample, in a quick non-destructive way (Kayjhaii & Lindford, 2020). Each element can emit a characteristic X-ray line spectrum, and this method takes advantage of that to evaluate the polymer in study. When an X-ray beam is directed at an element, the inner-shell electrons are ejected and substituted by outer electrons that release energy in the form of X-ray radiation- X-ray fluorescence. (Kayjhaii & Lindford, 2020). The resulting electronic configuration is unique to each element, only varying in intensity, which is dependent on the concentration of the element in the sample (Kayjhaii & Lindford, 2020).

3.4.4- Biological tests

The "clear-zone" test is a simple semi-quantitative biological test used for biodegradation evaluation. This compromises the use of an agar plate, where the polymer is dispersed in the agar as fine particles, and after inoculation with organisms the formation of a clear halo is observed, (Alshehrei, 2017; Shah *et al.*, 2008). If the microbes are capable of releasing extracellular enzymes that degrade the polymer, it is decomposed into water-soluble components that form the clear halo in the agar plate (Iram *et al.*, 2019) indicating that the microorganisms are at least able to depolymerize the plastic (Alshehrei, 2017; Shah *et al.*, 2008).

3.4.5- Carbon dioxide production and/or oxygen consumption

Under aerobic conditions, microorganisms use oxygen as the final electron acceptor, producing carbon dioxide, as a result of the oxidation of the carbon source (Y. Zhang *et al.*, 2022). As such, the measurement of CO_2 production or O_2 consumption (respirometry test) are two ways of evaluating plastic biodegradation (Alshehrei, 2017; Shah *et al.*, 2008). These can give direct information on the bio-

conversion of the plastic to its' end products, being one of the most used methods for plastics biodegradation assessment (Alshehrei, 2017). These tests can be performed in closed- bottles, where no aeration occurs, or in dynamic assays, where oxygen flows throughout the test (Lesteur *et al.*, 2010). These aerobic assays have an advantage over anaerobic degradability tests, because they are less time-consuming, and can be used with different types of waste (Lesteur *et al.*, 2010). CO_2 production or O_2 consumption measurements can be performed using equipment like direct measurement respirometry (DMR), which evaluates the quantity of CO_2 in the output gas, by using a non-dispersive infrared sensor (NDIR) or a gas chromatograph (GC) coupled with a thermal conductivity detector (TCD) (Ruggero *et al.*, 2019). Although some carbon from the polymer is assimilated for the formation of new biomass, respirometry tests are precise systems for biodegradation determination (Choe *et al.*, 2021).

3.4.6- Carbon dioxide and/or methane production

Carbon dioxide and methane are the main gases produced by methanogenic cultures, and their quantification by Gas Chromatography (GC), is used to assess a polymer's biodegradation over time (Alshehrei, 2017). In CO_2 or CH_4 measuring, the results may be expressed in the percentage of material biodegraded depending on the levels of transformed carbon dioxide and methane, measured with the biochemical methane potential method (BMP) (Ruggero *et al.*, 2019). These levels will vary according to factors like the content of organic matter, pH, and temperature. Normally, the higher the organic content, the higher the percentage of biogas produced, and in thermophilic conditions, there is a higher methanogenic activity, and therefore, faster breakdown of the organic matter.

In either anaerobic or aerobic biodegradability tests, a blank and a positive control (normally cellulose) are used to compare the results obtained for the polymers in study (Ruggero *et al.*, 2019). The quantity of the gasses produced is corrected by subtraction of the blank assay and compared with a theoretical production, which is based on the amount of carbon of the polymer (Quecholac-Piña *et al.*, 2020). This method is normally and more easily done in smaller closed reactors. In larger reactors, assessment of the biodegradation is usually done by direct analysis of the physical and chemical characteristics of the polymer (Quecholac-Piña *et al.*, 2020).

3.4.7- Scanning Electron Microscopy (SEM)

Visual analysis methods are used as a confirmation of the obtained results since it assesses the surface changes of the tested material. The distribution of the particle size pieces (consistency, roughness

of the surface, holes and cracks, discolouring, defragmentation, erosion, and/or formation of biofilms) (Shah *et al.*, 2008), and other signs of microbial colonization are visualized as an indicator of biodegradability (Alshehrei, 2017; Ruggero *et al.*, 2019). Corrosive degradation can be evaluated through SEM (Scanning Electron Microscopy), which also identifies the biofilms on the polymer's surface (Pires *et al.*, 2022). This method uses a beam of electrons that when in contact with the sample, leads to an image with information about the surface topography and composition of the sample (Al-mutairi & Mousa, 2021). However, samples need to be electrically conducted, to be able to be examined by this method, therefore, polymers need to be covered in a conductive material, normally gold particles, or use another technique, like environmental scanning electron microscope (ESEM) (Kayjhaii & Lindford, 2020). The presence of biofilm in the polymer does not necessarily mean there is biodegradation, as microorganisms can use the polymer surface only as support (Raddadi & Fava, 2019). Atomic force microscopy (AFM) characterizes the crystal surface of the polymer. High-resolution photographs can also be used as a technique to report macroscopy features of biodegradation, like colour changes, size, and roughness (Ruggero *et al.*, 2019). However, these visual changes cannot be interpreted as signs of metabolic biodegradation, only as signs of microbial attack (Alshehrei, 2017; Shah *et al.*, 2008).

3.5- Microorganisms involved in plastics' biodegradation

The fast capacity that microorganisms show to adapt their metabolism to new anthropogenic compounds has made them a valuable asset in the maintenance of different environmental issues (Amobonye *et al.*, 2021). Due to their quicker genetic modifications, and the natural selection of mutants, they have been responsible for preventing the bioaccumulation of many hazardous compounds (Amobonye *et al.*, 2021). Even though human exploitation of nature has created an unprecedented disturbance in the natural balance, microorganisms have become a big focus in science to tackle this problem (Amobonye *et al.*, 2021).

There are already several microorganisms reported to be capable of degrading plastics to a certain degree, due to the presence of polymer degrading mechanisms and enzymes (Kaushal *et al.*, 2021). Over 90 genera of bacteria and fungi with the ability to biodegrade polymers were reported, even if the process was very slow and not very efficient (Alshehrei, 2017). The first plastic film formation through colonization of microorganisms was observed in the 1970s, and since then, the number of biodegradability studies has increased, increasing as well as the number of microorganisms found to be able to degrade plastics (Miri *et al.*, 2022; Taghavi *et al.*, 2021).

Distinct species of bacteria and fungi have been discovered to be able to degrade polymers, with higher relevance for biodegradable polymers. Among them are dominant bacterial species like *Pseudomonas, Comamonas, Clostridium, Butyrivibrio* (Borghesi *et al.*, 2016), *Arthrobacter, Corynebacterium, Bacillus,* and *Micrococcus* (Atanasova, Stoitsova, *et al.*, 2021) and the actinomycetes *Streptomyces, Rhodococcus* and *Actinomadura* (Amobonye *et al.*, 2021). Generally, the most significant places of biomass sources for plastics biodegradation studies are contaminated sites, like landfill and contaminated soil, where the microbial community of the sites is in close contact with plastic waste (Matjasic *et al.*, 2020). This leads to the isolation of competent degrading microorganisms, leading to higher efficiency of degradation (Miri *et al.*, 2022).

In the study of Matjasic *et al.*, (2020), which reviewed 145 biodegradation reports, he found that 21 % of the studies reported the genera of *Pseudomonas* as an effective initiator of plastic biodegradation, followed by 15 % of the studies reporting *Bacillus* and 17 % a mixture of the two genera (Matjasic *et al.*, 2020). Fungi have also played an important role in plastic biodegradation, with studies showing *Aspergillus* genes as the most prominent (Amobonye *et al.*, 2021). Other fungal species with significant impacts on plastic biodegradation are *Fusarium solani, Alternaria solani, Spicaria spp., Geomyces pannorum, Phoma sp.,* and *Penicillium spp.* (Amobonye *et al.*, 2021). Leja & Lewandowicz (2010) also point out genera like *Phanerochaete, Thermomyces, Clodosporium, Candida* and others (Leja & Lewandowicz, 2010). Their hyphae' special capacity to penetrate compounds and their ability to secrete hydrophobins that enhance hyphal attachment has shown to be significant in the initial colonization of a polymer (Amobonye *et al.*, 2021).

Tables A1.1 to A1.6 (Appendix 1) compile most of the bacteria (more than 280) and fungi (more than 100) known as PE degraders. Regarding PET, more than 40 bacteria and 15 fungi are involved in its biodegradation (Tables A1.7 and A1.8, Appendix 1), and the microorganisms degrading PCL are over 50 (Tables A1.9 and A1.10, Appendix 1).

In the following sections, specific information will be given about the microorganisms that are considered PE, PET, and PCL degraders.

3.5.1- Microbiology of PE biodegradation

Various gram-negative and gram-positive bacteria can degrade PE, including genera like *Pseudomonas, Rhodococcus, Streptococcus,* and *Bacillus* among others (Ghatge *et al.*, 2020). For instance, *Phormidium lucidum* and *Oscillatoria subbrevis*, two cyanobacteria, showed a decrease of 30 %

of the initial molecular weight of the polymer after 42 days (Ru *et al.*, 2020). Taghavi *et al.* (2021) report an increase in the percentage of degradation of PE polymer (around 15 wt%) when incubated with a mixed culture of *Pseudomonas sp.* and *Aspergillus niger*, compared to the pure cultures (7.2 wt% and 12.4 wt%, respectively). *Serratia marcescens* was described to be able to biodegrade PE, being observed a 36 % weight loss after 70 days of incubation (Ru *et al.*, 2020). *Pseudomonas sp.* strain AKS2 was observed to form biofilms in the polymer surface and degraded around 5 % of PE in 45 days (Ghatge *et al.*, 2020).

In terms of fungi, genera like *Aspergillus, Fusarium, Penicillium,* and *Phanerochaete* were reported to biodegrade PE (Ghatge *et al.*, 2020). It is thought that fungi are more efficient at degrading PE than bacteria due to their ability to attach to hydrophobic surfaces (Ghatge *et al.*, 2020). A study of biodegradability using soil mixed with sewage sludge, found that fungal strains *Fusarium sp. AF4, Aspergillus terreus,* and *Penicillium sp.* were able to form biofilms on the plastic's surface after 10 months, hinting at some capacity to utilize the polymer as a carbon source. that used soil mixed with sewage sludge (Shah *et al.*, 2008). In another study, *Fusarium sp. FSM-10* and *Aspergillus sp. FSM-3* showed good results, with a weight reduction of 8- 9 % after 60 days of incubation (Ghatge *et al.*, 2020).

It was observed that for PE, the upper molecular weight limit for microbial degradation was around 2000 Da, being considered a very important factor in the biodegradation of this polymer (Ru *et al.*, 2020).

3.5.2- Microbiology of PET biodegradation

The most promising bacterial isolates known to be able to degrade PET, are gram-positive bacteria from the phylum *Actinobacteria*, and the most characterized genera are *Thermobifida* and *Thermomonospora* (Danso *et al.*, 2019).

Ideonella sakaiensis is a bacterium discovered in 2016, in a PET recycling factory, reported for its' capacity to assimilate PET, due to the secretion of a cutinase-like enzyme (Amobonye *et al.*, 2021; W. Zeng *et al.*, 2022). Microorganisms like *Bacillus licheniformis, Bacillus subtilis, Thermobifida fusca,* and *Thermomyces insolens* have also shown promising results in PET biodegradation (R. Wei & Zimmermann, 2017), and will be discussed further in section 3.6.2.

In terms of fungi, species like *Pichia pastoris* and *Yarrovia lipolytica* have been used to study PET biodegradation, especially as expression systems (X. Qi *et al.*, 2022). *Fusarium oxysporum* and *Fusarium*

solani have also been reported to be able to biodegrade PET, although their mechanism has yet to be studied (Taniguchi *et al.*, 2019).

3.5.3- Microbiology of PCL biodegradation

Under laboratory conditions, strains like *Pseudomonas* and *Streptomyces* have shown promising activity relating to PCL biodegradation (Borghesi *et al.*, 2016). A bacteria belonging to the genus *Clostridium* was found to biodegrade PCL under anaerobic conditions (Tokiwa *et al.*, 2009). Another bacteria reported to biodegrade this polymer was *Bacillus pumilus* strain KT102 (Tokiwa *et al.*, 2009)).

In terms of fungi, species from *Aspergillus* and *Fusarium* genera were found to be among the number of microorganisms that can biodegrade PCL (Hosni, 2019). A fungus isolated from soil- *Penicillium oxalicum* strain DSYD05-1 was reported to be able to completely biodegrade high molecular weight PCL only after 10 days. Another fungus, *Aspergillus sp.* Strain ST-01, also isolated from soil, was incubated with PCL for 6 days at 50℃, and results showed it was capable of biodegrading the polymer under aerobic conditions (Hosni, 2019). *Colonostachys roseas* was also reported to efficiently degrade PCL, with a degradation of 52,91 % for the film after 30 days, at 28℃ (Iram *et al.*, 2019). Another *Penicillium* sp. (strain 26-1 (ATCC 36507) has also been reported to degrade PCL. This fungus can assimilate unsaturated aliphatic and alicyclic polyesters, and biodegradation results on PCL showed that it was able to almost completely degrade it in 12 days (Tokiwa *et al.*, 2009). New microorganisms belonging to the *Clostridium* genus were also found to degrade PCL under anaerobic conditions (Hosni, 2019).

3.6- Enzymes and metabolic pathways involved in plastics' biodegradation

Enzymes are biological catalytic proteins that can act in reactions, making the turnover of substrates into products a quicker and more efficient process (Kaushal *et al.*, 2021). The main mechanism of action of the enzymes involved in plastic biodegradation is the hydrolysis/oxidation/hydroxylation of the polymer chain into oligomers and monomers (Mohanan *et al.*, 2020).

It is thought that extracellular enzymes are the first to attack large, high molecular weight polymers (Mohanan *et al.*, 2020), and they act in two different ways. In exo-attacks cleave the chain terminus and result in small oligomers or monomers products, while endo-attacks cleave along the

polymer chain, forming different molecular weight fragments. Normally, products from exo-attacks are small enough to be directly assimilated by the cell, while products from endo-attacks need further degradation to be assimilated (Wilkes & Aristilde, 2017).

Esterases, lipases, depolymerases, and cutinases are members of the hydrolase family, which comprises the majority of the known polymer degrading enzymes (Kaushal *et al.*, 2021). Their binding grooves are often extensive and adaptable to accommodate the binding of the polymer long chain, possessing a flat active site that facilitates the binding of the enzyme to the substrate (Chen *et al.*, 2020). Additionally, because of their small size and low molecular weight, these typically extracellular enzymes can permeate into dense polymer structures (Chen *et al.*, 2020). Oxygenases also play an important role in plastic biodegradation, since they add oxygen molecules to their chains, which leads to the creation of alcohol and proxyl products, that are less recalcitrant and, consequently, easier to biodegrade (Jaiswal *et al.*, 2020). Hydrolases are hydrolytic enzymes that function in the presence of water, (Kaushal *et al.*, 2021) and are considered crucial in plastic biodegradation (Wilkes & Aristilde, 2017). Enzymes adhere to the surface of the plastic by hydrophobic interactions, due to the presence of a hydrophobic cleft near the active site of the enzymes (Kaushal *et al.*, 2021), that increases the access of the polymer to the enzymes, accommodating of the polymer's hydrophobic groups (Kaushal *et al.*, 2021).

Although many enzymes that can degrade polymers have been discovered, there is still a long path to achieve the goal of making polymers biodegradation an efficient and industrial process. One of the first steps to be considered is the need to enhance enzyme activity in plastics, that can be achieve by manipulation of enzymes. This could lead to more stable and resistant enzymes to different environments, and to an easier and more efficient accommodation of the polymers to their active site. Additionally, the fusion of enzymes together could help improve their efficiency and even accommodate more than one plastic at once. The microorganisms isolation processes also needs to be standardised to make results more uniform between experiments (Kaushal *et al.*, 2021). In this section, the enzymes known to be involved in PE, PET and PCL's biodegradation will be discussed. Additionally, information on the known metabolic pathways for the biodegradation of the aforementioned polymers will also be given.

3.6.1- Biodegradation of PE

Contrary to the number of microorganisms that have been found so far to be able to degrade PE, only four types of enzymes have been discovered that can attack the PE chain (Ru *et al.*, 2020).

Laccases are a group of enzymes capable of catalysing the oxidation of different polyaromatic compounds and some non-aromatic substrates and are primarily produced and secreted by lignin-degrading fungi (Kale *et al.*, 2015). PE-degrading *Actinomyces* and ligninolytic white-rot fungus produce these laccases that increase the number of carbonyl groups in PE, lowering its molecular weight (Chen *et al.*, 2020). This activity needs the presence of co-factors like Cu, and the presence of redox catalysts increases the biodegradation observed (Chen *et al.*, 2020). The oxidation of the polymer by *Rhodococcus ruber C208* extracellular laccase was also observed, leading to the generation of carbonyl groups and a decrease in the plastic molecular weight (Ru *et al.*, 2020).

Alkane hydroxylase (AH), was first found in *Pseudomonas sp. E4* (Amobonye *et al.*, 2021), and its system is comprised of 3 components, an electron-generating reductase, an electron-transporting small Fe-binding protein, and a membrane-bound oxygenase (non-haemic iron monooxygenase- alkB) (Chen *et al.*, 2020). Although the metabolic pathway involved in this biodegradation remains unclear, the understanding of these mechanisms has already allowed for recombinant expression of the genes corresponding to three alkane hydroxylase- *alkB, alkB1,* and *alkB2*, in *Escherichia coli* system, with a 30 % loss in polymer molecular weight (Chen *et al.*, 2020). These enzymes are known to metabolize n-alkanes compounds, a characteristic common to the species that can degrade PE (Mohanan *et al.*, 2020).

The pyrolytic hydrocarbons of PE can be degraded through a terminal oxidation process. It starts with the action of an alkaline hydroxylase (AH) that oxidases a terminal methyl group, generating a primary alcohol (Figure 7) (Montazer *et al.*, 2020; Ru *et al.*, 2020). This product then suffers further oxidation by alcohol dehydrogenase (AD) to form an aldehyde that is transformed into fatty acids by aldehyde dehydrogenase (ADL) (Figure 7) (Ru *et al.*, 2020). These fatty acids are joined to CoA by an acetyl-CoA synthase and then converted to acetyl-CoA, L-β-hydroxy acyl-CoA, and trans-2-decenoyl-CoA by β-oxidation (Ru *et al.*, 2020). Acetyl-CoA enters then the tricarboxylic acid cycle to generate succinic acid or acetoacetyl-CoA, which can be converted to PHA. The L-β-hydroxy acyl-CoA can be converted to D-β-hydroxy acyl- CoA by isomerization, being the next step in its conversion to PHA through a PHA synthase (PhaC) (Ru *et al.*, 2020). The last by-product has a more complex end pathway, that ends in its transformation into biosurfactants.

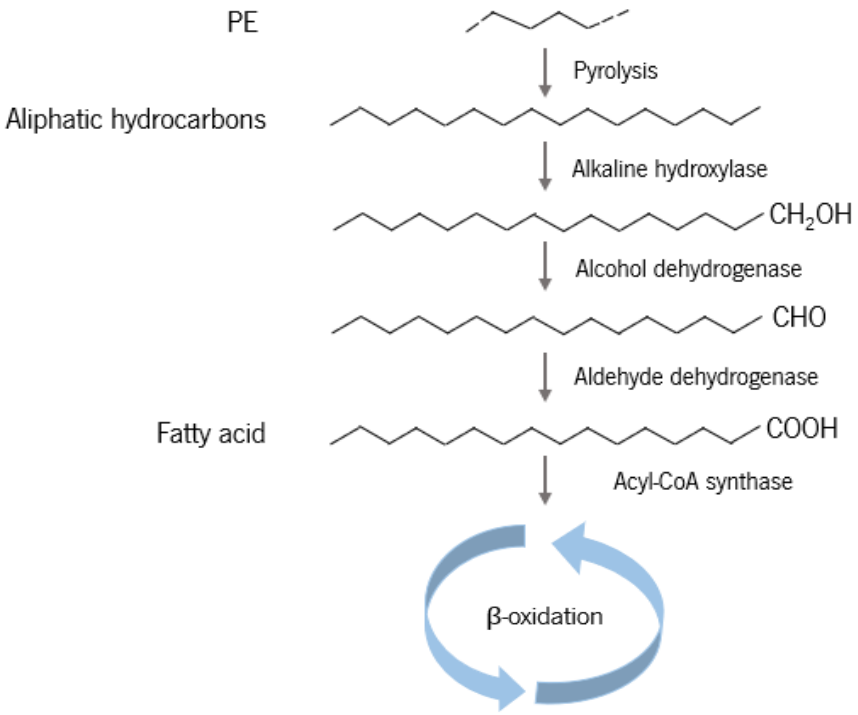

Figure 7: Proposed metabolic pathway for PE biodegradation. Adapted from Ru *et al.* (2020).

On the other hand, pyrolysis in aerobic conditions would cleave PEs' long chain, but also introduce carbonyl and hydroxyl groups into its backbone, improving the bioavailability of pyrolytic hydrocarbons (Ru *et al.*, 2020). This would allow its usage as a carbon source for microbial fermentation, producing PHA by some microorganisms (Ru *et al.*, 2020).

Peroxidases and reductases are also involved in the biodegradation of PE polymers (Amobonye *et al.*, 2021). In specific, manganese peroxidase first screened from lignin-degrading fungi- *Phanerochaete chrysosporium* was shown to be able to decrease the polymer tensile strength and average molecular weight (Kale *et al.*, 2015; Ru *et al.*, 2020).

Regarding reductases, it was concluded that the biodegradation of PE chains begins with the reduction of rubredoxin by the enzyme (that contains this rubredoxin in its constitution). That leads to the formation of electrons that are transported to an oxygenase, which reacts with oxygen to conduct hydrocarbon oligomers oxidation (Chen *et al.*, 2020). This results in products that can then be further oxidized and degraded (Chen *et al.*, 2020).

Santacruz-ju *et al.*, (2021) reported hypothetical pathways for PE biodegradation in aerobic conditions, with three different enzymes, a laccase (Lac), a manganese peroxidase (MnP), and a lignin peroxidase (LiP) (Santacruz-ju *et al.*, 2021). After the initial oxidation, PE fragments become more

hydrophilic, resulting in easier access to enzymes like lipases and esterases, that help with further degradation of the polymer (Jacquin *et al.*, 2019). Manganese peroxidase and lignin peroxidase need H_2O_2 as an electron-accepting co-substrate. With MnP, the H_2O_2 would be cleaved into OH free radicals, that bind to the hydrogen water of the heme group of the enzyme and the Fe^{2+}. After some other reactions, this would lead to the generation of oxymanganese free radicals, and its' oxygen molecule would react with PE once the polymer enters the active site of MnP (Santacruz-ju *et al.*, 2021). This would form the oxoferryl-MnP free radical complex, resulting in the cleavage of PE into several small molecules, like alkanes, ethyl free radicals, and ethanol. Ethanol can then be oxidised into acetic acid, entering the Krebs cycle. The other molecules would enter the catalytic site of the enzyme once more, breaking down and forming an oxymanganese free radical, causing an oxidation reaction. Otherwise, alkane free radicals could be oxidized to dodecanal, which in turn would be oxidised into dodecanoic acid. This compound would react with ethyl free radical, forming tetradecanoic acid, which would react with CoA producing tetradecanoyl-CoA. This molecule would then undergo β-oxidation, forming acetyl-CoA, and entering the Krebs cycle (Santacruz-ju *et al.*, 2021).

The laccase from *Tinea versicolor* has copper ions organized in three Cu centres- Cu_1, Cu_2, and Cu_3. In PE biodegradation, it was hypothesized that the polymer would come in contact with Cu_1, resulting in a released electron that would bind to Cu_2 centres' hydroxyl group, releasing a water molecule. With this, the Cu centres would form an electron flux, regulating the concentration of H_2O_2 in the medium. This would lead to OH free radicals, one of which would bind to Cu_3, forming PE free radicals, and the other generating a water molecule (Santacruz-ju *et al.*, 2021). The free radicals would be then homolytically cleaved, generating alkane free radicals, which would be oxidized by Lac into alcohols, liberating a water molecule. The compounds would be oxidized into aldehydes and then into carboxylic acids, which can enter the Krebs cycle (Santacruz-ju *et al.*, 2021).

The hypothetical path of PE biodegradation by LiP starts with the homolytic N-Fe^{3+} bond cleavage of the iron-porphyrin complex of the enzyme, resulting in the porphyrin π-cation free radical• H_2O_2. This leads to the breakage into two OH free radicals, where one binds to the propionic acids' hydrogen, and the other to Fe^{3+}, releasing a water molecule (Santacruz-ju *et al.*, 2021). Then, this would form an oxyferryl complex, that reacts with PE, generating free radicals and releasing a water molecule. This would form alkane free radicals, being then oxidized into alcohols in the presence of H_2O_2, liberating a water molecule. The alcohols would then be transformed into carboxylic acids, forming the heme iron-superoxo complex free radicals. This would release a water molecule, with the acids entering the Krebs cycle (Santacruz-ju

et al., 2021). Santacruz-ju *et al.* (2021) also report a hypothetical pathway for biodegradation with the three enzymes, highlighting that MnP and LiP have higher efficiency in biodegrading PE since they have bigger active centres, but Lac is important since it provides the H_2O_2 those enzymes need (Santacruz-ju *et al.*, 2021).

In *Rhodococcus rhodochrous*, after the cleavage of the polymer to oligomers with 600 Da, they are transported into the cells by Major Facilitator Superfamily (MFS) carriers or harbouring ATP-binding cassettes. Then β-oxidation transforms these oxidized carboxylic molecules into acetyl CoA or propionyl CoA that is integrated into the normal metabolism of the microorganism (Jacquin *et al.*, 2019). Another metabolic pathway for PE was described, where, in a succession of oxidations, dehydrogenations, and carbon-carbon bond breaking, PE is transformed into acetic acid, which is assimilated into the cells and integrated into the TCA cycle (Wilkes & Aristilde, 2017).

3.6.2- Biodegradation of PET

Carboxylesterases, lipases, esterases, and cutinases can hydrolyse PET, and its enzymatic hydrolysis has been observed to be based on surface erosion mechanisms (Amobonye *et al.*, 2021; X. Qi *et al.*, 2022). However, in studies reported so far, these enzymes have only been able to biodegrade a limited part of PET (Taniguchi *et al.*, 2019) and most PET-hydrolysing enzymes are cutinases (Maurya *et al.*, 2020; Taniguchi *et al.*, 2019).

Cutinases don't have a lid covering their hydrophobic binding site, contrary to lipases, which results in broader binding site, allowing them to bind to a wider range of substrates (Chen *et al.*, 2020; R. Wei & Zimmermann, 2017). Improving these cutinases would be the next step toward higher PET biodegradation, making them more stable and thermotolerant (Chen *et al.*, 2020). One way to improve this enzyme is to fuse them to binding domains, like carbohydrate-binding modules (CBM) or polyhydroxyalkanoate binding domains (PBM) that confer the enzyme a higher affinity by having that hydrophobic binding domain (Mohanan *et al.*, 2020). It was shown that the binding to hydrophobins, increased the depolymerization of PET by 16 times, using a cutinase, however, few cutinases have been discovered that can degrade the inner bulk (by at least 10 %) of this polymer (Mohanan *et al.*, 2020). Because of the limited volume of the esterase binding site, they can only work on the oligomers rather than the entire polymer (Chen *et al.*, 2020).

PETase and MHETase are two well-studied enzymes that can degrade PET to some extent. They were first discovered through the study of *Ideonella sakaiensis,* which was able to grow on waste bottles

and degrade PET into its' terephthalic acid and ethylene glycol monomers (Kaushal *et al.*, 2021). These PET-degrading hydrolases contain disulphide bonds produced by cysteine residues, that confer thermal stability and the specific binding to PET (Danso *et al.*, 2019). The PETase described from this microorganism has a 3-dimensional structure akin to cutinases, but with an additional disulphide bond (Danso *et al.*, 2019). Both enzymes have specific roles in PET biodegradation, with PETase hydrolysing the conversion of the polymer to its oligomers, and MHETase hydrolysing further those oligomers into monomers (Figure 8) (Taniguchi *et al.*, 2019).

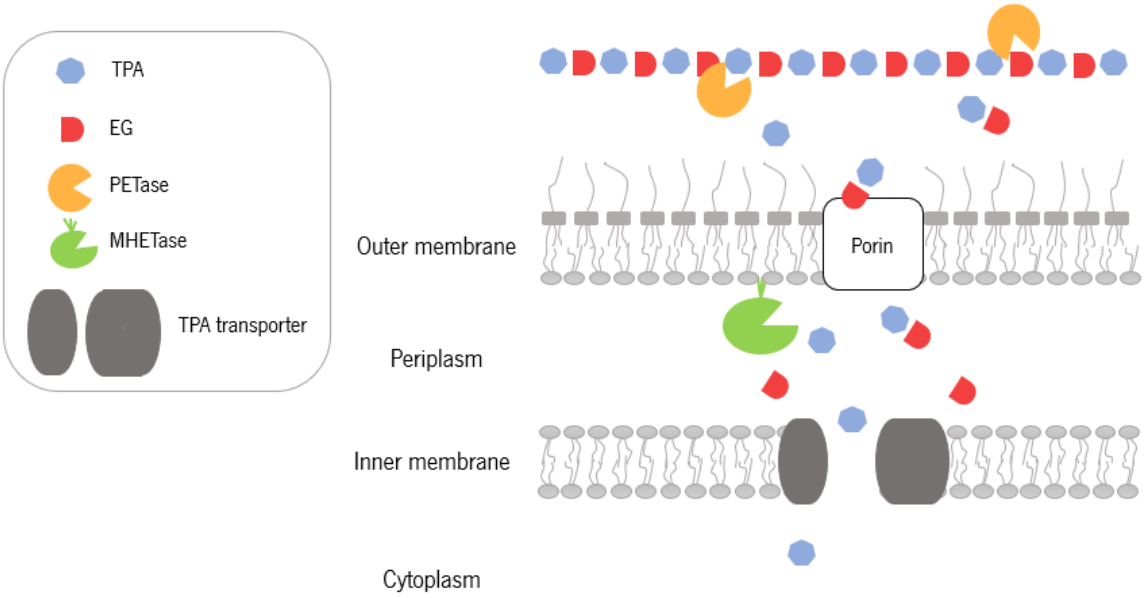

Figure 8: Suggested PET metabolic pathway, by *Ideonella sakaiensis*. TPA- terephthalic acid, EG- ethylene glycol, PETase, and MHETase- two *I. sakaiensis* enzymes. Adapted from Tanigchi *et al.* (2019).

The metabolic pathway for *Ideonella sakaiensis* 201-F6 is well described (Chen *et al.*, 2020). PET biodegradation starts with the cleavage of the polymer ester bond by hydrolases, resulting in incomplete hydrolysis products like MHET (mono(2-hydroxyethyl) terephthalate), and BHET (bis(2-hydroxyethyl) terephthalate). In some microorganisms, MHET is further hydrolysed into TPA (terephthalic acid) and EG (ethylene glycol), and BHET into MHET, TPA, and EG. TPA and EG can be then used by other non-PET-degrading microorganisms, by entering the tricarboxylic acid cycle (TCA cycle) (Figure 9) (X. Qi *et al.*, 2022).

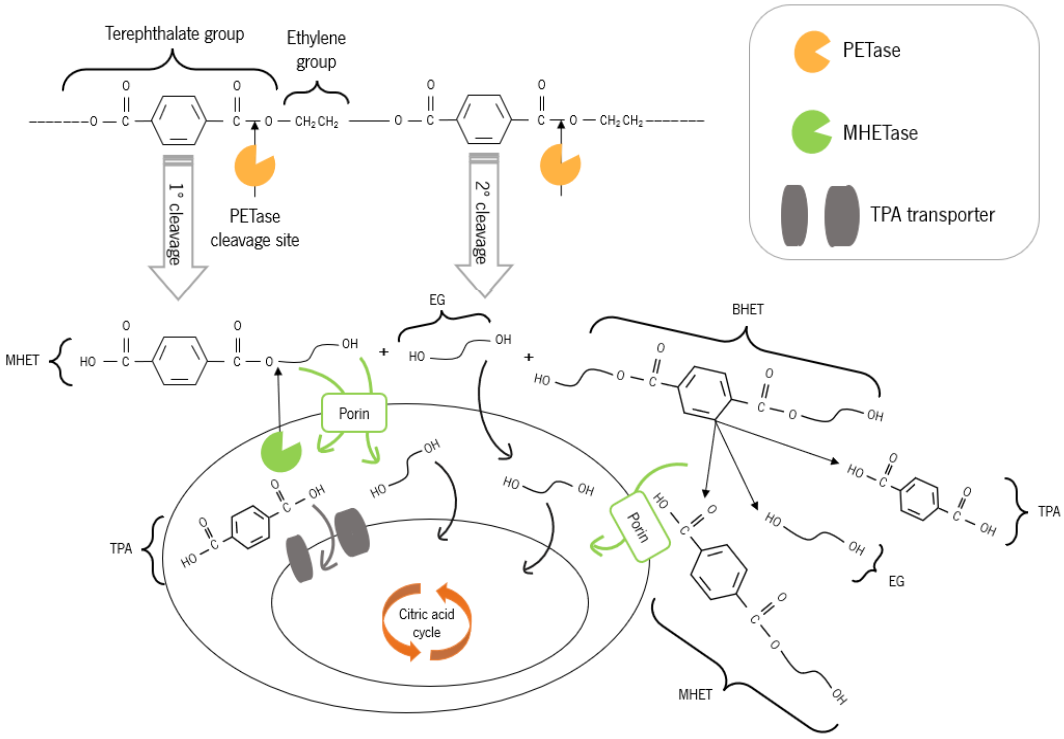

Figure 9: Proposed PET biodegradation pathway. Adapted from Miri *et al.* (2022) and Mohanan *et al.* (2020).

The mechanism of degradation of *Ideonella sakaiensis* 201-F6 starts with the secretion of *Is*PETase, which hydrolyses the ester bonds of PET to produce MHET, and small amounts of BHET and TPA (Chen *et al.*, 2020; Miri *et al.*, 2022; Mohanan *et al.*, 2020). Some fungi were discovered to have this same mechanism, transforming PET into BHET and MHET (Jacquin *et al.*, 2019). Then, these products are taken up by the cell and transformed into TPA by MHETase (Chen *et al.*, 2020; Mohanan *et al.*, 2020). Its crystal structures suggest a broader binding site than other PET-hydrolysing cutinases, making binding to larger PET molecules easier which would result in a higher preference for PET (Chen *et al.*, 2020). Once within the cell and converted to TPA, these products suffer transformation by TPA dioxygenase (TPADO) into DCD (1,6-dihydroxycyclohexa-2,4-diene-dicarboxylate) (Ru *et al.*, 2020). DCD can then be further oxidized by a dehydrogenase- TphB (1,2-dihydroxy-3,5-cyclohexadiene-1,4-dicarboxylate dehydrogenase) and form PCA (protocatechuate). This compound can be degraded by 3,4-dioxygenase (PCDO), 4,5-dioxygenase, and 2,3-dioxygenase onto different cleavage pathways (Ru *et al.*, 2020). In one of those, it is transformed into 4-carboxy-2-hydroxymuconic which is the substrate of a dehydrogenase and forms 2-pyrone-4,6- dicarboxylic acid. This substrate can then enter the TCA cycle, being transformed into oxaloacetate and pyruvate (Figure 9) (Amobonye *et al.*, 2021; Jacquin *et al.*, 2019).

EG, the other by-product of MHET hydrolysis, can be easily degraded by acetogens, to form ethanol and acetaldehyde, which are then converted into acetate via acetyl-CoA (Figure 9) (Ru *et al.*, 2020). It was also reported the metabolism of EG into oxidation products like glycolaldehyde, glyoxal, glycolate, and glyoxylate (Mohanan *et al.*, 2020).

Pseudomonas putida KT2440 was found to not be able to use EG as its sole carbon source, but a laboratory isolated mutant was discovered to be able to grow on it. Comparative genomic analyses between the two strains revealed a regulator (GclR) that had a central role in repressing the glyoxylate carboligase pathway (Ru *et al.*, 2020). As a result of overexpression of the glyoxylate carboligase and glycolate oxidase operons, the wild strain was able to use EG as its sole carbon source for growth (Mohanan *et al.*, 2020; Ru *et al.*, 2020).

Fungal cutinases have also shown the capacity to partly degrade PET, and some examples reside in the phyla *Fusarium* and *Humicola* (Danso *et al.*, 2019). *Thermomyces insolens* cutinase has shown to be a very active fungal hydrolase. It is known that PET's glass transition temperature is above 65℃, and above this temperature, the amorphous parts of its' chain become more flexible, facilitating the enzymatic attack (R. Wei & Zimmermann, 2017). The cutinase from *T. insolens* is thermostable, so in a study conducted at 70℃, for 96h, the PET in film used was almost entirely degraded, showing the high efficiency of this enzyme, even for the crystalline part of the polymer (R. Wei & Zimmermann, 2017). Additionally, an *Actinomycete* cutinase- TfH, from *Thermobifida fusca* was also reported to effectively degrade PET, with a weight loss of up to 50 % of low-crystallinity PET after 3 weeks at 55℃ (Ru *et al.*, 2020).

A large-scale global genome and metagenome database search has been performed for PET hydrolases, and it identified more than 800 potential enzymes in bacterial and archaeal genomes. This suggests the global distribution of these enzymes through marine and terrestrial metagenomes (Danso *et al.*, 2019).

3.6.3- Biodegradation of PCL

PCL biodegradation in nature has been observed to be attributed to extracellular enzymes like depolymerases- esterases, cutinases, and lipases (Lyu *et al.*, 2019; Nawaz *et al.*, 2015). PCL's chemical structure enables biodegradation by microorganisms through the hydrolysis of the ester linkage between the molecules, which leads to chain scission (Borghesi *et al.*, 2016; Nevoralová *et al.*, 2020). This stage includes a non-enzymatic hydrolytic ester cleavage, that results in gradual chain scission. It is

autocatalyzed by the carbon end groups, of the polymer chain (Leja & Lewandowicz, 2010; Woodruff & Hutmacher, 2010). Then, oligomers start to diffuse from the bulk, contributing to a weight loss stage, and the fragmented polymer can start suffering enzymatic erosion or phagocytosis (Leja & Lewandowicz, 2010).

Lipases have been more extensively studied in terms of PCL biodegradation, and three lipases, from different microorganisms (*Rhizopus delemar, Rhizopus arrhizus,* and *Pseudomonas* PS) have been reported as efficient accelerators of the polymer's biodegradation (Stamps *et al.*, 2016). Additionally, esterases and lipases from other microorganisms, like*, Achromobacter sp., Candida cylindracea*, but also *Rhizopus delemar, and Rhizopus arrhizus* were found to degrade polymers like PCL (Ahmed *et al.*, 2018).

A depolymerase from *Streptomyces thermoviolaceus subsp. Thermovio-laceus 76T-2* was discovered to be responsible for the polymer degradation (Emadian *et al.*, 2017). Efficient degradation was observed by a *Rhizopus delemar* lipase, especially because of the polymer's low melting temperature (Ahmed *et al.*, 2018). Other examples include the complete biodegradation of the polymer by a *Pseudomonas* lipase, in just four days (Blackwell *et al.*, 2018; Thakur *et al.*, 2021), and the biodegradation of the polymer by fungal phytopathogens, where their cutinases could have acted as PCL depolymerases (Blackwell *et al.*, 2018). Other studies reported that enzymatic degradation by *Aspergillus favus* and *Penicillium funiculosum* was faster in the polymer's amorphous regions (Tokiwa *et al.*, 2009).

In a recent study, two esterases were fused, using an end-to-end fusion technique to evaluate the biodegradability of PCL (Kaushal *et al.*, 2021). After overexpression in *Pichia pastoris* it was observed that, only after 6 hours of incubation, the degradability rate of the polymer was much higher than with the two enzymes alone (Kaushal *et al.*, 2021). The two principal by-products of the degradation were 6-hydroxyhexanoic acid and a small percentage of ε-caprolactone (Kaushal *et al.*, 2021). Another recent study reported two novel enzymes, a cutinase and a lipase, originated from a bacteria isolated from activated sludge- *Pseudomonas hydrolytica sp*. DSWY01T. Both enzymes biodegraded PCL into monomers and oligomers, with the cutinase reaching 70 % of biodegradation after 3 days, and the lipase 75 % biodegradation after 8 days, preferentially attacking the amorphous region of the polymer (Li *et al.*, 2022). It was also highlighted that the modes of enzymatic attack were different between the two enzymes, in the sense that the degradation by the cutinase was linear throughout the experiment time, while the lipase had a slow stage for the first three days of degradation, followed by a fast stage in the next 4 days. This shows that different enzymes have different degradation rates, due to different degradation modes (Li *et al.*, 2022).

The PCL biodegradation mechanisms reported include two different processes (Thakur *et al.*, 2021; Woodruff & Hutmacher, 2010), through surface erosion pathways, or the degradation of poly(α-hydroxy) esters via bulk degradation, through hydrolytic degradation (Thakur *et al.*, 2021; Woodruff & Hutmacher, 2010). Surface erosion, as the name suggests, implies the degradation of the polymer surface by hydrolytic cleavage. When the rate of water diffusion into the bulk is slower than the rate of hydrolysis of the chain, the degradation of the polymer starts with surface erosion. As a consequence, monomers and oligomers that diffuse into the medium are produced, resulting in a thinning of the polymer, without disturbing the molecular weight of the inner bulk of PCL (Thakur *et al.*, 2021; Woodruff & Hutmacher, 2010). This results in a big weight loss of the polymer, but little decrease in molecular weight. This enzymatic degradation happens more frequently at the end of the chain and in chain folds (Thakur *et al.*, 2021).

In bulk degradation, which happens when water can more rapidly diffuse into the polymer bulk, there is a hydrolytic chain scission that can produce a reduction in the molecular weight of the plastic (Figure 10) (Thakur *et al.*, 2021; Woodruff & Hutmacher, 2010). This hydrolysis reacts randomly in the polymer chain (Thakur *et al.*, 2021), and the monomers and oligomers produced would then slowly diffuse out of the bulk, resulting in gradual erosion of the polymer (Woodruff & Hutmacher, 2010). However, it is observed an increase in crystallinity, since the cleavage will mainly occur in amorphous regions (Thakur *et al.*, 2021). When these by-products do not diffuse quickly enough, they start to accumulate in the bulk and create an acidic environment, since new carboxyl end groups keep accumulating. As a consequence, the internal degradation of the polymer is accelerated, in comparison to surface erosion, producing a polymer with a low molecular weight interior, and a high molecular weight surface (Thakur *et al.*, 2021; Woodruff & Hutmacher, 2010). In higher temperature environments, where PCL is found to biodegrade, it is cleaved by end chain scission, while random chain scission happens at lower temperatures (Thakur *et al.*, 2021).

In a study of biodegradation of PCL in medical applications, it was observed, first, the non-enzymatic hydrolytic cleavage of the ester groups (Figure 10) (Azimi *et al.*, 2014), mainly in amorphous parts of the polymer (Thakur *et al.*, 2021). Then, intracellular degradation would happen, after the crystallinity increases and the molecular weight drops to 3000 (Azimi *et al.*, 2014). This was shown in the degradation by macrophages and giant cells (Azimi *et al.*, 2014; Woodruff & Hutmacher, 2010). Woodruff & Hutmacher (2010) studied the biodegradation of PCL in living organisms and reported that high-molecular-weight polymers pose a much harder plastic to biodegrade than lower molecular weight

ones. This higher molecular weight implied a longer chain length and a bigger number of ester bonds that needed to be cleaved to produce water-soluble monomers and oligomers (Woodruff & Hutmacher, 2010). They reported the case of an *in vivo* experiment in rats, wherein the first two weeks, was only observed a non-enzymatic bulk hydrolysis. After 9 months it was observed an implant fragmentation, since only then was the molecular weight reduced to 5000 g/mol, resulting in a mass loss, that fragmented PCL (Woodruff & Hutmacher, 2010).

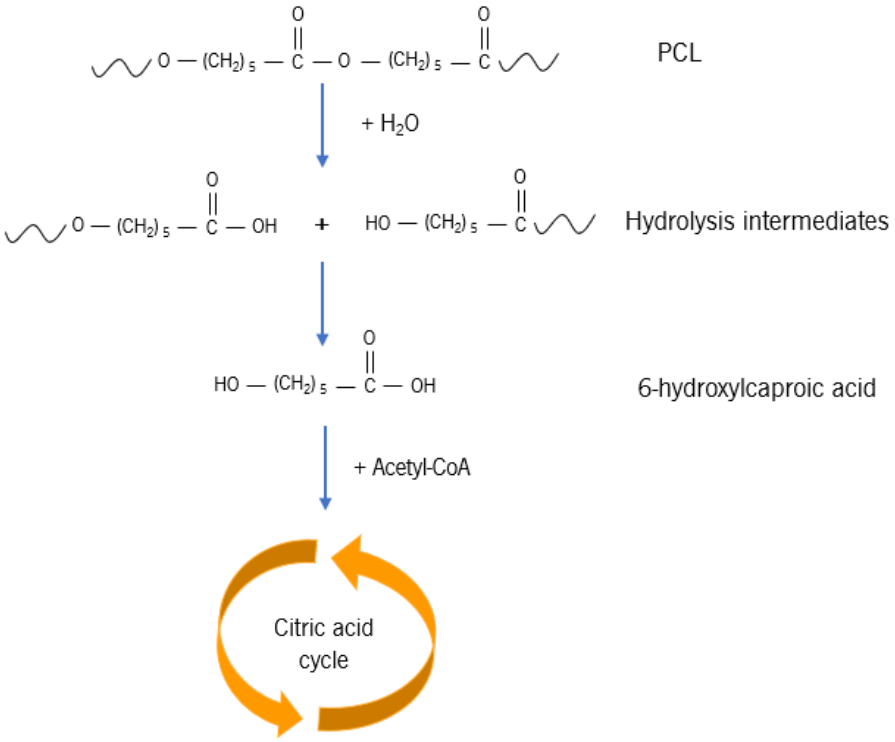

Figure 10: Proposed metabolic pathway for PCL biodegradation. Adapted from Woodruff & Hutmacher (2010).

In another study, with low molecular weight powder, it was observed a rapid degradation and absorption of the polymer, by the organism, only after 13 days. The body's macrophages and giant cells were able to uptake the polymer, and it was degraded in their phagosomes, resulting in a sole by-product- 6-hydroxyl caproic acid (Figure 10). This intermediate is known to enter the citric acid cycle, together with Acetyl-CoA, before being eliminated from the organism (Figure 10) (Woodruff & Hutmacher, 2010). It was observed that the presence of polysaccharides enhances the rate of degradation of PCL by microorganisms (Nevoralová *et al.*, 2020).

3.7- Plastic biodegradation under thermophilic conditions

Thermophilic microorganisms are organisms that are able, not only to endure, but to actively grow in extreme conditions, more specifically, in extreme temperatures (Atanasova, Stoitsova, *et al.*, 2021). Most of the thermophiles are assigned to *Bacteria* and *Archaea* domains, but also to *Eukarya* (Gomes *et al.*, 2016), although they are less appropriate for thermophilic studies since they endure lower temperatures compared to prokaryotes (Atanasova, Stoitsova, *et al.*, 2021). Thermophiles grow in temperatures between 45℃ and 122℃, and depending on the range they can endure, they are divided into different groups (Atanasova, Stoitsova, *et al.*, 2021). Hyperthermophiles have an optimal growth temperature above 80℃, and some typical bacterial genera of hyperthermophiles are *Aquifex, Hydrogenobacter,* and *Thermotoga* (Atanasova, Stoitsova, *et al.*, 2021).

Extreme thermophiles thrive at temperatures between 65℃ and 80℃ and some representative genera are *Thermus* and *Rhodothermus*. With a range of growth between 50℃ to 70℃, they are called obligate thermophiles, although their optimum temperature is between 55℃ and 65℃. Some examples are the *Anoxybacillus, Brevibacilus* and *Geobacillus* genera (Atanasova, Stoitsova, *et al.*, 2021). Finally, there are facultative thermophiles that have an optimum growth temperature between 41℃ and 50℃. Some mesophilic microorganisms can stand temperatures below 41℃, being called thermotolerant because they have, however, a lower optimum temperature (Atanasova, Stoitsova, *et al.*, 2021). The majority of thermophilic fungi stand in the *Zygomycota* and *Ascomycota* phyla (Gomes *et al.*, 2016).

The tolerance to higher temperatures is caused by an adaptation of thermophilic and hyperthermophilic microorganisms' membranes, proteins, and DNA. Proteins are resistant to higher temperatures because of intrinsic characteristics, where their' molecular structure suffers an increase in rigidity and resistance to folding (Gomes *et al.*, 2016). The main mechanism thought to influence this resistance is the "hydrophobic effect" where hydrophobic residues are retained by the molecule, blocking contact with water. This results in a native structure that has a low tendency for unfolding. Additionally, the secondary structure of thermophilic proteins has a propensity to have a higher number of β-sheet and α-helices than mesophilic proteins (Gomes *et al.*, 2016). Furthermore, they can also present shorter proteins and the involvement of heat shock proteins that assist protein folding (Atanasova, Stoitsova, *et al.*, 2021). Their membranes have suffered the incorporation of branched fatty acids, which makes them more stable to those temperatures, and also have an active system for DNA damage repair (Atanasova, Stoitsova, *et al.*, 2021). In terms of differences in their enzymes, these microorganisms have evolved to

produce more rigid enzymes that are resistant to proteolysis and denaturing agents (Atanasova, Stoitsova, *et al.*, 2021).

The advantages of thermophiles in biotechnological processes go from the reduction of contamination by mesophilic microorganisms to diminishing the viscosity of the medium, as well as boosting the bioavailability and solubility of organic compounds and the diffusion of substrates and products, which results in higher reaction rates (Gomes *et al.*, 2016). The use of stable enzymes at higher temperatures results in a longer period of hydrolysis of the backbone of the polymers (Gomes *et al.*, 2016), and therefore, higher enzyme activity in a decreased polymer strength (Atanasova, Stoitsova, *et al.*, 2021).

3.7.1- Thermophilic microbiology of PE biodegradation

Bacteria like *Brevibacillus borstelensis* and *Aneurinibacillus* sp. were observed to reduce PE's molecular weight at 50℃ (Atanasova, Paunova-krasteva, *et al.*, 2021). Specifically, *Brevibacillus borstelensis* strain 707 was isolated from soil and studied for its capacity to degrade LDPE, for 30 days. The study resulted in a reduction in gravimetric weight by 11 % and a weight loss of 30 %. FTIR analysis revealed a reduction in carbonyl groups, indicating bacterial degradation (Arutchelvi *et al.*, 2008; Atanasova, Stoitsova, *et al.*, 2021; Kale *et al.*, 2015). Another study isolated *Bacillus sp.* BCBT21 from composting agricultural residues and observed about a 44 % decrease in the polymer molecular weight, after 30 days of incubation, at 55℃ (Atanasova, Stoitsova, *et al.*, 2021). Skariyachan *et al.* (2017) reported degradation of LDPE and HDPE strips and pellets (by 75 % for LDPE strips, 55 % for LDPE pellets, 60 % for HDPE strips and 43 % for HDPE pellets) in incubation with cow dung as inoculum. The experiment was performed for 120 days at 55℃, and a bacterial consortium composed of *Pseudomonas spp.*, *Stenotrophomonas spp., Bacillus spp.*, and *Paenibacillus spp.*, among others was responsible for that biodegradation (Skariyachan *et al.*, 2017).

3.7.2- Thermophilic microbiology of PET biodegradation

PETs' polymer chain's amorphous sectors become more mobile at temperatures ranging from 65℃ to 75℃. Some microorganisms that can degrade PET belong to the phylum *Actinobacteria*, like the genera *Thermobifida* and *Thermomonospora*, are all thermophilic microorganisms. Species like *Thermobifida alba*, *Thermobifida halotolerans*, *Thermobifida fusca*, and *Thermomonospora curvata* have been specifically studied (Atanasova, Stoitsova, *et al.*, 2021). Specifically, *Thermobifida fusca* was able

to decrease the molecular weight of the polymer by 50 %, after 3 weeks of incubation at 55℃. The recombinant expression of *T. fusca* enzyme was done in *Bacillus subtilis*, it was reported the dominant presence of that enzyme in the medium, and a 97 % degradation of the amorphous part of the polymer after 120h of incubation at 70℃ (Atanasova, Stoitsova, *et al.*, 2021). Additionally, it was also reported the degradation of PET by genetically engineered *Clostridium thermocellum*, at 60℃, with 60 % of degradation after 14 days. The bacterium was engineered to produce a thermophilic cutinase- LCC, resulting in better degradation than other whole-cell-base mesophilic biodegradation of PET (X. Qi *et al.*, 2022; Yan *et al.*, 2021).

3.7.3- Thermophilic microbiology of PCL biodegradation

Several thermophilic species of microorganisms have been reported to be able to degrade PCL. Its melting point is around 60℃, which makes the degradation at these higher temperatures more efficient (Atanasova, Stoitsova, *et al.*, 2021). In one study, 31 isolates of thermophilic polyester degrading actinomycetes were reported to be able to degrade PCL, as well as other plastics like PHB and PES (Polyethylene succinate). Some of the genera discovered were *Actinomadura, Microbispora, Streptomyces, Thermoactinomyces* and *Saccharomonospora* (Tokiwa *et al.*, 2009).

Thermophilic bacteria isolated from compost have been discovered to degrade PCL at 55℃. It was observed that *Streptomyces thermonitrificans* degraded PCL more efficiently when co-cultured with *Bacillus licheniformis* HA1, at 50℃ for 48h, being observed 70 % degradation with compost as a co-substrate. The single culture with *S. thermonitificans* showed a decrease in the molecular weight of the plastic 72h after incubation and 35 % decomposition after 6 days of composting. Nevertheless, when co-cultured with *B. licheniformis*, the degradation reached 70 % after only 48h (Atanasova, Stoitsova, *et al.*, 2021). In another study, complete biodegradation of PCL was observed within 6h of incubation at 45℃ by *Streptomyces thermoviolaceus* subsp. *Thermoviolaceus* 76T-2 (Atanasova, Stoitsova, *et al.*, 2021).

Thermomyces lanuginosus, isolated from compost, was reported as capable of biodegrading PCL, at 50℃ (Hosni, 2019). A thermophilic *Bacillus* sp. TT96, isolated from soil, was reported to have the capacity to form clear zones on PCL agar plates (Tokiwa *et al.*, 2009). Moreover, a thermotolerant *Aspergillus* sp. strain ST-01, also isolated from soil, was reported to degrade PCL after 6 days at 50℃ (Tokiwa *et al.*, 2009).

3.8- Taxonomic identification of microorganisms in complex microbial communities

Microbial communities are usually highly diverse, and knowing which microorganisms have key functions for plastics biodegradation, is still challenging. Nevertheless, microbial ecology methodologies are useful to get further insights into microbial diversity and function, without the need for isolation (Boughner & Singh, 2016; Mishra *et al.*, 2019).

Most microbial ecology methods rely on the analysis of taxonomic markers, such as the 16S rRNA or the 18S rRNA genes, for the identification of the prokaryotic and eukaryotic microorganisms, respectively, that are present in microbial communities (Boughner & Singh, 2016; Phadke *et al.*, 2017). The recent development of next-generation sequencing (NGS) technologies has allowed to rapidly sequence those genes from microbial communities and retrieve both microbial identification and relative abundance of the different species inside the communities (Boughner & Singh, 2016).

Sequencing of the rRNA gene is a very efficient method for metagenomic studies, used for microbial identification (Sogin *et al.*, 2006). rRNA is present in all organisms and has a constant functionality and a dominant concentration in the cells since is it needed for the transduction of new proteins (Boughner & Singh, 2016). It contains conserved regions that are similar in all prokaryotes and eukaryotes, and enable the usage of specific target sites for PCR primers, but also contains 9 variable regions that allow the differentiation between strain identification (Illumina Tecnical Support, 2013; Phadke *et al.*, 2017). The information it contains in those variable regions makes it a biomarker and a phylogenetic marker (Boughner & Singh, 2016).

Most of the NGS technologies used are PCR-dependent, which are based on the amplification of the fragment of interest to increase the signal-to-noise ratio (Phadke *et al.*, 2017). The first step in this methodology is the extraction of the DNA and the isolation from cellular debris (Mishra *et al.*, 2019). This happens through cell disruption, which can be performed through mechanical or chemical methods. Then the cell debris are separated from the genetic material, usually through centrifugation, followed by the separation of proteins from the nucleic acids (Phadke *et al.*, 2017). It is necessary to take the sample origin and characteristics into consideration when performing DNA extraction, as some environments have natural nucleic acid binders or PCR inhibitors (Boughner & Singh, 2016). Then, PCR is performed by using specific primers to amplify the sequence of interest, like the 16S or 18S rRNA genes (Phadke *et al.*, 2017) followed by one of three different approaches.

The first one is microbial community identification through cloning of the fragment into a cloning vector and its insertion in a host for prior sequencing, which can result in clone libraries (Mishra *et al.*, 2019). The second approach for PCR-based methods of DNA/RNA characterization is the separation by electrophoreses right after the PCR, which can be coupled with other techniques that allow more accurate differentiation of the fragments (like denaturing gradient gel electrophoresis- DGGE) (Mishra *et al.*, 2019). The third methodology involves enzymatic digestion and separation by electrophoresis, also coupled with other techniques that give a clear identification of the microorganisms in the sample (Mishra *et al.*, 2019). These techniques are relatively fast and easy to perform, comparing several samples at the same time, and are culture-independent (Phadke *et al.*, 2017).

Sequencing can be done by various methods, with Sanger Sequencing being the most common, but it may also be performed by Illumina MiSeq technology (Boughner & Singh, 2016). The resulting sequences are compared with sequences in databases, like NCBI, using sequence alignment tools like Blast (Mishra *et al.*, 2019). The percentage of similarity between the sequences of interest and the results from the sequence alignment dictates the identity of the microorganisms in the sample. When using Illumina technologies, after the first PCR amplification, the samples undergo another PCR, where specific primers with overhang adapters are used. This enables attachment of Illumina sequencing adaptors and indices (also called barcodes) to the samples in study. Illumina technologies (MiSeq, HiSeq, and NextSeq) are the most commonly used NGS platforms (Phadke *et al.*, 2017).

4. Aims

The aim of this thesis is to test the biodegradability of two synthetic plastics (polyethylene (PE) and polyethylene terephthalate (PET)) and two biodegradable plastics (polycaprolactone (PCL) and polyhydroxy butyrate/polybutylene adipate-co-terephthalate blend (PHB/PBAT)) by natural occurring microbiomes, i.e., leachate and marine sediments. Additionally, the aim is to identify the most active microorganisms during biodegradation.

5. Materials and Methods

Plastic biodegradation assays were performed under aerobic and anaerobic conditions, using leachate or marine sediment as inoculum, and testing different plastics- PE, PET, PCL and PHB/PBAT. The leachate was collected from the municipal landfill (Resulima) in Viana do Castelo and the sediment was collected in an estuary near Esposende.

5.1- Biodegradation with leachate as inoculum

The incubations with leachate as inoculum started with a first biodegradation experiment, under anaerobic thermophilic (55℃) conditions, which was performed to evaluate the biodegradation capacity of the inoculum under those conditions and to estimate the best time points to sample for the characterization of the microbial communities. This first experiment was conducted for about 4 months, testing PE and PET, PCL, and a mixture of PHB/PBAT. Additionally, control assays with volatile fatty acids (VFA- with 1 M of acetate, 1 M of propionate and 0,5 M of butyrate) as the sole carbon and energy source were performed to evaluate the anaerobic activity of the inoculum, and control assays with cellulose were conducted to evaluate the biodegradability activity by the inoculum, on polymeric substances. Blank assays were used as a negative control, containing only growth medium and leachate.

The second biodegradation assays were performed under anaerobic thermophilic (55℃) and aerobic thermophilic (55℃) conditions. In both cases, PE, PET, and PCL in powder and in film were tested. Control assays with cellulose in powder and blank assays were performed. All assays were done in triplicate. The biodegradation in the anaerobic experiments was assessed by following methane production and in the aerobic assays, the oxygen consumption was followed over time. Methane and oxygen were measured by gas chromatography.

The leachate used as inoculum in the first assay was collected at a different time than the one used in the second assays, although collected at the same site.

5.1.1- First anaerobic experiment

The leachate was transported in jerrycans from the Resulima landfill to the laboratory, where it was stored at 4℃ for about three days, until submission to concentration by decantation and consecutive

centrifugations (8000g for 10 minutes) (Figure 11). Before the start of the incubations the concentrated inoculum was stored at 4℃, in a closed glass bottle which was fluxed with a mixture of N_2.

Figure 11: Collected leachate.

After the concentration of the biomass, and to determine the quantity of leachate to use in the incubations, the VSS of the biomass was determined. This determination was done by the standard experimental methods for VSS determination (Appendix 2, section 2.1). It began with the cleaning of 3 muffle filters (Figure 12), which were placed into the muffle (550℃) for about half an hour, and later, 500 µL biomass were added to each filter (Figure 12) using a vacuum system. These were then placed in the oven overnight, at a temperature of 105℃ to evaporate all the water content in the samples (Figure 12). Afterwards, the filters were cooled down at room temperature in the desiccator and weighed. The filters were then placed in the muffle for 2 hours, to remove the organic matter content (Figure 12), and later cooled down and weighed again. The VSS was calculated following Equation 1.

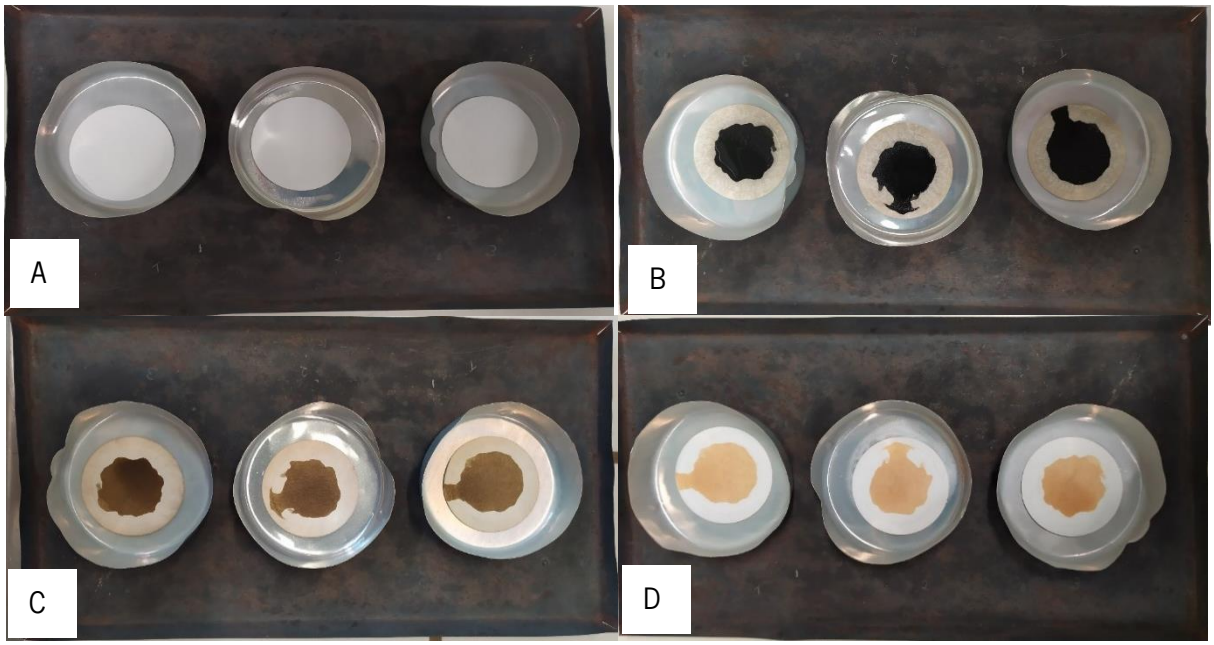

Figure 12: VSS's determination of the leachate inoculum; A) filters after the wash with distilled water; B) filters with the 500µL of biomass; C) filters with the biomass after spending the night at 150℃; D) filters with the biomass after incubation at 550℃.

$$VSS = \frac{(Weight\ after\ the\ stove - Weight\ after\ the\ muffle)}{Sample\ volume} \qquad \text{Equation 1}$$

After having the VSS value, the volume of biomass to be used in the experiment was calculated considering the desired concentration (3 g/L VSS), the volume of the medium in each vial (Vwork), and the resulting value of the VSS (Equation 2).

$$Vbiomass = \frac{3\ (g/L) \times Vwork}{VSS\ (g/L)} \qquad \text{Equation 2}$$

The plastic films (PE, PET, PCL, and PHB/PBAT) used were synthesized in the Polymer Department of University of Minho. Before the preparation of the assay, these were weighed and put aside in eppendorfs, until the start of the incubations. The description of the vials from the first experiment is described in Table A2.1 (Appendix 2).

The anaerobic medium was prepared with KH_2PO_4, Na2HPO$_4$•H2O, trace elements of H^+ and OH^- and resazurin (Appendix 2, section 2.3). After boiling the mixture, it was let to cool down, while it was being refluxed with N_2. Once at room temperature, 5 % of the total volume of the medium of the

bicarbonate and 5 % volume of vitamins and salts solution was added to the erlenmeyer with the anaerobic medium.

Afterwards, 11 mL of medium and 1,5 mL of the inoculum were added to each 25 mL bottle, and these were encapsulated and pressured with a mixture of N_2/CO_2 (80 %:20 %, vol/vol, at $1.7x10^5$ Pa), and depressurized, to clean the airspace of the bottles. They were placed incubating overnight at 55℃. The following day, the bottles were opened, the plastics films inserted, in the vials and these were closed and pressured again. The controls, with just medium and biomass, were only depressurized. After that, 0,1 mL of Na_2S was added to the medium, and the bottles returned to the 55℃ incubator (Figure 13).

Figure 13: Vials used in the first biodegradation experiment. The darker powder on the walls of the vials is the leachate biomass.

For the first few weeks, weekly methane measurements were taken, and after that, measurements were only done once or twice a month.

At the end of the incubation, the bottles were depressurized and opened, and the plastics were taken out. The non-biodegradable films were carefully collected and set aside, and the biodegradable plastics were too fragile and decomposed to be collected, so the medium was passed directly to a falcon tube for centrifugation. After the centrifugation at 10000 rpm for 10 minutes, the supernatant was separated from the pellet and frozen, for later VFA analysis. The pellet was resuspended in 400 μL RNA later, transferred to an eppendorf and stored frozen, for a possible later microbial community analysis.

PE and PET plastic films collected were resuspended in a solution of phosphate-buffered saline (PBS) for about an hour to try and analyse the microbes that were on the surface of the films. The plastic films were then removed from the buffer into a new falcon and cleaned. The PBS solution was centrifuged for another ten minutes, and the pellet was separated from the supernatant and resuspended in RNA

later before freezing. The films were cleaned with distilled water, for about 15 minutes with frequent agitation, and 96 % alcohol for another 15 minutes, before being left to air-dry.

For the VFA's analysis, the supernatant of each sample was let to defreeze, and 2 mL were collected to an eppendorf. These were centrifuged for 10 minutes at 10 000 g, and the supernatant was filtered with nylon filters (13 mm in diameter and 0,22 µm of pore size). Then 160 µL were placed in HPLC tubes, together with 40 µL of crotonic acid, and analysed. The HPLC analysis was performed as described by Salvador *et al.* (2019), with a mobile phase with H_2SO_4 0,005N (0,005 M), a flow rate of 0,6 mL/min and an oven temperature of 60℃.

The PE and PET films collected from the incubation vials were submitted for a FTIR analysis, as well as the original polymers (without biodegradation), for comparative purposes. The analysis was performed using a 4100 Jasco spectrometer in the range of 4500-400 cm^{-1}, with a resolution of 4 cm^{-1} and averaging 16 scans. The PE film was also subjected to a SEM analysis on a NanoSEM FEI Nova 200. First, the samples were coated with a gold/palladium (80/20 wt. %) mixture, before being examined at various magnifications, and an acceleration voltage of 10000kV in second image mode.

5.1.2- Second anaerobic experiment

Leachate collection and preparation were done as described in section 5.1.1, except that the collected leachate was placed in the cold room for about a week, before concentration.

For the second assay, PE, PET, and PCL in film (Figure 14) and in powder (Figure 15) were tested. The films were prepared by hot pressing of pellets, where the thickness was measured using a micrometre, at various points of the films formed, and the average value was calculated. The powders were prepared by mechanical grinding of the pellets (Figure 16), using a sieve that resulted in 1 mm diameter particles. These films and powders were used for the second anaerobic assay and the aerobic assay. Before use, the films were washed with distilled water for 15 minutes, with frequent agitation, and then with alcohol 96 %, for also 15 minutes. They were let to dry overnight before use.

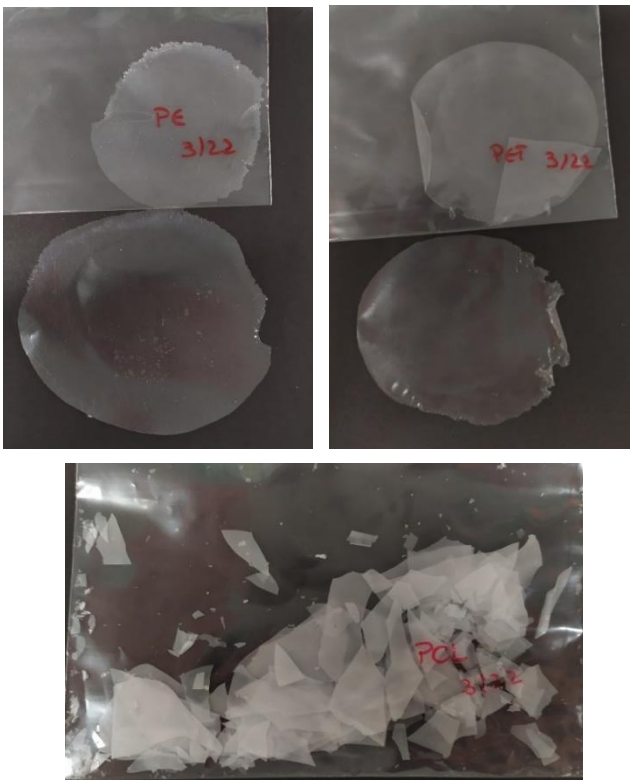

Figure 14: Different polymer films used in the biodegradation experiment. On the left upper corner, is the PE film used, on the right upper corner the PET film, and the lower picture shows the PCL film used.

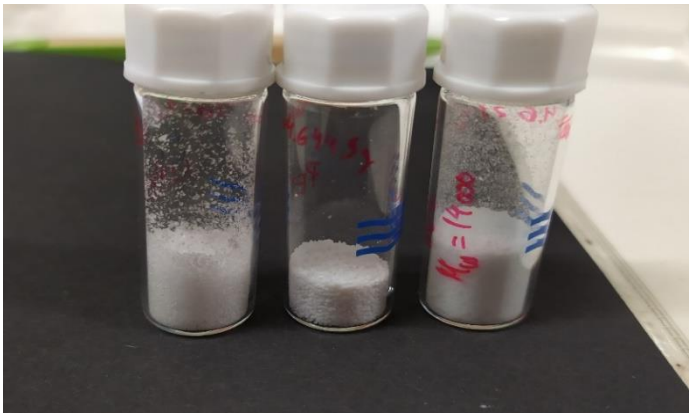

Figure 15: Polymer powders used in the biodegradation experiments. from the right to the left, there is the PE, PET, and PCL powders.

Figure 16: Mechanical grinder used to form the polymer powders used in the experiments.

The anaerobic assay was prepared similarly to the first assay, with minor differences. In terms of vials, 120 ml bottles were used instead of the 25 mL vials, and 62,5 mg of plastics in films and powder were weighed and added to each vial before the anaerobic medium. The amount of plastic in the biodegradation assays was defined with reference to the work performed by Moura *et al.* (2010), and the description of the vials from the second anaerobic experiment is described in Table A2.2 (Appendix 2).

The anaerobic medium was prepared as described in section 5.1.1 (Appendix 2, section 2.3), and 45 mL were dispensed to each bottle (already containing the respective film/powder). These were then encapsulated and pressured with a mixture of N_2/CO_2 (80 %:20 %, vol/vol, at $1.7x10^5$ Pa), and depressurized, to clean the airspace of the bottles.

The vials containing the medium, the bicarbonate solution and the salts solution, were autoclaved for 20 min, at 120℃. After cooling, and in sterile conditions, 0,1 mL of Na_2S were added to the bicarbonate solution, followed by the addition of 5 % volume of that solution to each vial. Then, 5 % volume of salts and vitamins solution was also added to every bottle. Lastly, 1,5 mL of biomass were added (Figure 17), (with exception of incubations with PE and PET in film which were inoculated with only 0,7 mL, due to experimental limitations) and the vials were placed in the incubator at 55℃. Weekly methane measurements were taken using Gas Chromatography.

Figure 17: Anaerobic vials with PE, PET, PCL, and cellulose in powder and film, and blank assay.

At the end of the incubations, samples were taken for further microbial community analysis and VFA's analysis as described in section 5.1.1, except that the pellet resulting from the centrifugation was resuspended in 350 µL of phosphate-buffered saline (PBS) solution, instead of RNA later. The sampling for VFA analysis during the incubations was done by sampling 1,6 mL with a syringe and needle, centrifuged at 10000 g for 10 minutes, and the supernatant was filtered.

5.1.3- Aerobic experiment

For the aerobic experiment, the protocol followed was the same described in section 5.1.1. The leachate used was the same used in the second anaerobic experiment, although separate concentrations and VSS determinations were done. The inoculum, after concentration, was frequently aerated by opening the glass shot to maintain oxygenation. The description of the vials of this incubation is present in Table A2.3 (Appendix 2).

The growth medium used was basal medium composed of 40 mL/L of solution A (28,25 g/l of KH_2PO_4, 146,08 g/L of K_2HPO_4), 30 mL/L of solution B (3,36 g/L of $CaCl_2 \bullet 2H_2O$, 28,64 g/L of NH_4Cl) and 30 mL/L of solution C (3,06 g/L of $MgSO_4 \bullet 7H_2O$, 0,7 g/L of $FeSO_4$ and 0,4 g/L of $ZnSO_4$) (Moura *et al.*, 2010). A volume of 49 mL of medium was added to each 120 mL bottle, as well as 1,5 mL of biomass. The bottles were encapsulated, and oxygen measurements were taken, using the Gas Chromatograph. The vials were then placed incubating at 55℃ (Figure 18), and oxygen measurements were taken twice a week. When the O_2 levels were becoming low, the headspace was washed and new air injections were made, using a syringe, in a non-sterile environment.

Figure 18: Aerobic assay vials, with PE, PET, PCL, and cellulose in film and powder, and the three blank assays.

At the end of the incubations, samples were taken and preserved for further microbial community analysis and VFA quantification as described in section 5.1.2.

5.1.4- Measurement of methane production and oxygen consumption by Gas Chromatography

The methane production and oxygen consumption of the samples was done using a MolSieve column (MS 13X, 80/100 mesh) connected to a thermal conductivity detector Bruker Scion 456 chromatograph (Bruker, Billerica, MA) (Figure 19). The carrier gas used was argon (30 ml, min⩾1) and the injector and detector temperatures were set at 100℃ and 130℃, respectively (Salvador *et al.*, 2019). For the methane analysis, the column temperature was set at 70℃, while for oxygen measures, the temperature was set at 35℃. After injection of the samples in the Gas Chromatography, the area of the corresponding methane or oxygen peaks was taken and transformed into mmol or mM of methane/oxygen in each bottle. Then, using the average of the triplicates, and taking into consideration the value of the blank, it was possible to determine the percentage of biodegradation that happened until that point.

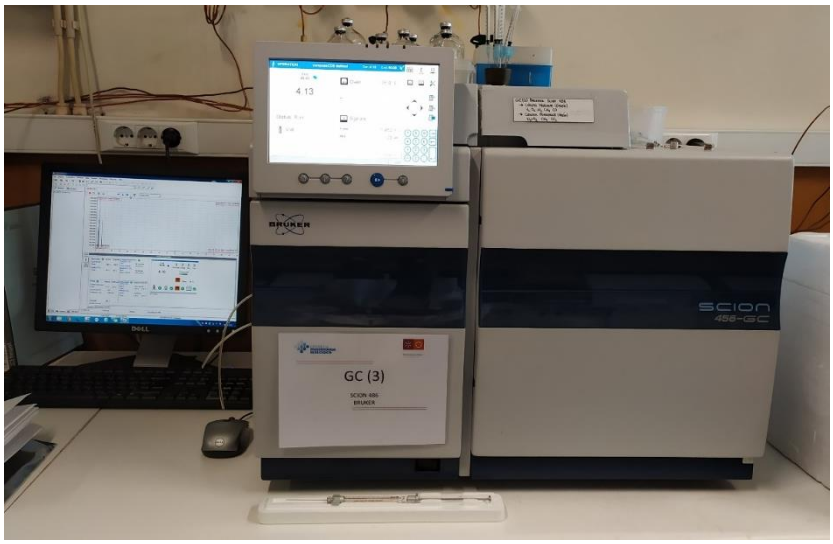

Figure 19: Gas Chromatographer used in methane and oxygen measurements.

The transformation of the value of the area of each peak to the concentration of methane was determined by calculating the mmol of methane in the syringe with sample, recurring to the average value of the peaks of the standard gas (with 40 % methane) and the mmol of methane in the syringe with standard gas (0,0083 mmol CH_4) (Equation 3). Then, with the volume of headspace in each bottle it is possible to calculate the mmol of methane in the bottle (Equation 4).

$$mmol\ of\ CH_4\ in\ the\ syringe\ with\ sample = \frac{Value\ of\ the\ area\ of\ the\ peak \times mmol\ CH_4\ in\ the\ syringe\ with\ standard\ gas}{Average\ of\ standard\ gas}$$

Equation 3

$$mmol\ of\ CH_4\ in\ the\ bottle = \frac{Volume\ of\ headspace \times mmol\ of\ CH_4 in\ the\ serynge}{Sampled\ volume\ in\ the\ serynge\ (0{,}5\ mL)}$$

Equation 4

The determination of oxygen in the bottles is a similar procedure to the determination of methane but knowing that the air sample used as standard gas has 21 % of oxygen. Then, following Equation 3, and 4, it is possible to determine the oxygen in the vials. The addition of more oxygen to the vials was also taken into consideration in the calculations of the oxygen consumed.

With the biodegradability results and the theoretical methane production, it was possible to predict the percentage of polymer that was biodegraded for the duration of the incubations. First, using

the chemical formula of each plastic and the total conversion into carbon dioxide and methane (Appendix 2, Table A2.4), it is possible to dictate the number of moles of methane produced. For example, knowing that PE formula is C_2H_4, its total conversion into those compounds will be $\boldsymbol{2C_2H_4 + 2H_2O \rightarrow CO_2 + 3CH_4}$. This means that for each PE molecule 1,5 moles of CH_4 are produced. Then, taking into consideration the mass of polymer used in the assays (15,6 or 62,5 mg) and the molar mass of the plastic, it is possible to determine the number of moles of plastic in the bottle. Using the moles of CH_4 per molecule of plastic, and the number of moles of the plastic in the bottle, the theoretical methane can be determined (Appendix 2, Table A2.5).

With the theoretical value of methane produced, and the results obtained in the experiment, it is possible to determine the percentage of degradation, using Equation 5.

$$Biodegradation\ (\%) = \frac{(real\ value - blank\ value) \times 100}{theoretical\ value} \qquad \text{Equation 5}$$

The same calculations were made for oxygen consumption, using the conversion of the reaction of each polymer with oxygen, producing carbon dioxide and water (Appendix 2, Table A2.6). This will lead to the theoretical oxygen consumption needed to degrade the polymers completely (Appendix 2, Table A2.7). Then, using Equation 6, the percentage of degradation of each polymer is calculated.

5.1.5- Microbial community analysis

The frozen biomass samples were left to defreeze at room temperature, and DNA extraction was done using the *FastDNA® SPIN Kit for Soil* (MP Biomedicals, Solon, OH). The methodology followed was the one recommended by the kit, with some small alterations. After using the *FastPrep® System* for 40 seconds, the samples were put in ice for 30 seconds (to help with cell lysis) and homogenized in the system two more times. Additionally, after the following centrifugation and saving the catch tube with the eluted DNA, a new volume of DES was added to the SPIN filter, in a new catch tube, and placed into the thermoblock once again, to guarantee that the majority of the extracted DNA is eluted.

Following this extraction, the samples were measured in the Nanodrop equipment, to quantify the DNA (Phadke *et al.*, 2017). The DNA samples were stored in the fridge overnight, until the PCR. The PCR was performed on the extracted DNA sample, using 24 µL of premix (with 5 µL of buffer, 0,5 µL of primer forward F-U968 and 0,5 µL of primer reverse R-1401 (Table 2), 0,5 µL of Taq polymerase and

18,5 µL of PCR water) and 1 µL of DNA sample. After the PCR, a gel electrophoresis (1 % agarose (w/v) stained with safe green (NZYtech, Portugal)) was run to evaluate the results.

Table 2: Primers used in the microbial community analysis, its' correspondent sequence, and the source where they were first used

Primers	Sequence	Reference
F-U968	5'-CGC CCG GGG CGC GCC CCG GGC GGG GCG GGG GCA CGG GGG GAA CGC GAA GAA CCT TAC-3	(Nübel *et al.*, 1996)
R-1401	5'-CGG TGT GTA CAA GAC CC-3'	(Nübel *et al.*, 1996),
515F	5'-GTGCCAGCMGCCGCGGTAA-3'	(Caporaso *et al.*, 2011).
806R	5'-GGACTACHVGGGTWTCTAAT-3'	(Caporaso *et al.*, 2011).
EUK1391F	5'-GTACACACCGCCCGTC-3'	(Stoeck *et al.*, 2010)
EUKBR	5'-TGATCCTTCTGCAGGTTCACCTAC3'	(Stoeck *et al.*, 2010)

Before sending the samples for sequencing, the DNA was precipitated with ethanol. The extracted DNA was placed in a new eppendorf, adding a third of the DNA extracted volume of 3M of Sodium Acetate (pH 5,2). With soft flicks to the eppendorf, the mixture was homogenized, and 2,5 times the total volume of DNA of 100 % ethanol was added to the mixture. After homogenization, the samples were left overnight at -20℃. The samples were centrifuged for 20 minutes at 4℃, at maximum speed, and the supernatant was discarded. The pellet was then washed with 70 % cold ethanol, with enough volume to cover the DNA sample (around 100 µL), and homogenized. Afterwards, the samples were centrifuged at 4℃ for 5 minutes, and the ethanol was carefully removed from the eppendorf. Finally, the samples were left to air-dry with the lid open and kept in the fridge until being sent for sequencing.

Prokaryotic and eukaryotic community analysis was performed, following the protocol described by Salvador *et al.* (2019) (Supplementary material, pages 19-20), with the difference in the primers used in the first amplification, that were 515F and 806R for prokaryotic community amplification and EUK1391F and EUKBR for the eukaryotic community (Table 2). The sequencing results were filtered by removing the identified microorganisms which had a relative abundance lower than 0,01 % and that did not suffer a 10-fold increase compared to the inoculum. Finally, because prokaryotes have a variable copy number of the 16S gene in their genome (Louca *et al.*, 2018), normalization was performed, taking into consideration the number of copies for each prokaryote. This enabled the determination of a more realistic value of the percentage of the microorganisms in the sample.

5.2- Biodegradation with marine sediment

The marine sediment was collected from an estuary in Esposende (kept at 4℃ until use) and used as inoculum in both aerobic and anaerobic assays performed at mesophilic temperatures. The anaerobic assays were performed under methanogenic and sulphate-reducing conditions. The plastics PE, PET and PCL were added in powder, and the salinity of the surrounding water was measured by using a Consort™ C3010 (Fisher Scientific, USA). First, the sediment was incubated at 37℃, in saline conditions, to assure the total consumption of possible subtracts that may have been present in the sample. The inoculum used in the aerobic assay was incubated under aerobic conditions (in an erlenmeyer with a cotton cap, to allow oxygen flow) and with 20 g/L of NaCl, while the anaerobic assays were incubated under anaerobic conditions (in a closed shot with an atmosphere of N_2/CO_2 (80 %:20 %, vol/vol, at $1.7x10^5$ Pa)) and 10 g/L of NaCl. The difference in the salinity in aerobic and anaerobic assays is justified by the fact that methanogenic microorganisms cannot stand high concentrations of salt in the medium (Riffat & Krongthamchat, 2006; S. Wang *et al.*, 2017). After two nights of this incubation at 37℃, the biodegradability assays were prepared. First, VSS determination was performed according to section 5.1.1, and the powders were weighed and placed in the corresponding vial.

The basal medium for the aerobic experiment was prepared as described in section 5.1.3, with the addition of 20 g/L of NaCl. Then, 45,6 mL of medium were dispensed in 120 mL bottles, followed by 4,4 g of sediment. The bottles were encapsulated and pressurised with atmospheric air. Oxygen was measured with GC, and the bottles were incubated at 30℃ with agitation at 150 rpms.

For the anaerobic experiments, the same anaerobic medium used in section 5.1.2 was prepared, with the supplement of 10g/L of NaCl. Then, 45 mL of anaerobic medium was dispensed in 120 mL vials, together with 4,54 g of sediment. The bottles were closed and supplemented with 1mM of Na_2S and pressurized with a mixture of N_2/CO_2 (80 %:20 %, vol/vol, at $1.7x10^5$ Pa). Additionally, the sulphate-reducing assays were supplemented with 20 mM of sodium sulphate. Besides the occasional methane production measurements, sulphide measures using the KIT LCK 653 were performed, to evaluate the sulphate consumption by the biomass. For that, about 0,1 mL of medium was collected from the vials with a syringe and needle and immediately immersed in a solution of 20 g/L of zinc acetate and 2 ml/L of acetic acid. Then the protocol described in the kit was followed. Anaerobic experiments were performed at 37℃ and 105 rpm.

6. Results and discussion

Different results could be obtained in the different assays regarding the biodegradability of the plastics. Insights on PCL biodegradation by leachate and sediment microbiomes could be obtained, as PCL could be degraded in almost all the tested conditions (Figures 23, 24 and 30 and Tables 4, 5, 7 and 8). The blend of PHB/PBAT was also degraded by the leachate (Figure 20 and Table 7), however, in the majority of the incubations with PET and PE, no biodegradation occurred, as evaluated by the methane produced (in the methanogenic experiment) or the oxygen consumed (in the aerobic experiment). The exception was the first anaerobic experiment with PE in film, in which the methane production determined in the assay was higher than the one in the control assay (without PE) (about 5% after 180 days). However, no differences in the chemical structure of PE and PET films were detected, after analysis by FTIR (Figure 21) and no evidence was shown in the SEM analysis performed on the PE film after incubation (Figure 22). The incubations done with sediment showed promising results for the biodegradation of PCL under aerobic and sulphate-reducing conditions, while under anaerobic conditions biodegradation was happening at a slower rate (Figure 30 and Table 7 and 8). These differences between experiments were due to the different origin/microbial composition of the inoculum and to the incubation conditions that favoured the development of different microorganisms. For instance, under aerobic conditions the growth of aerobic microorganisms was favoured, under methanogenic conditions, anaerobic bacteria and methanogens became dominant, and under sulphate-reducing conditions, sulphate-reducing bacteria were in advantage over other bacteria. This divergence in the microbial composition in the different incubations was clear in the assays with PCL, in which the taxonomic identification of the microorganisms was assessed (section 6.1.4). Indeed, *Archaea* were highly abundant in the methanogenic experiment (23 %), while in the aerobic experiment their abundance was drastically reduced (0,07 %). Details on the consumption of oxygen, production of methane or sulphide during the incubation of the plastics in different conditions, and on the microbial communities developed during the assays with PCL will be given in the following subsections.

6.1- Experiments with leachate as inoculum

6.1.1- First anaerobic experiment- biodegradability results

Around 50 mL of inoculum leachate were obtained after concentration resulting in 7,67 ± 0,411 g VSS/L. To perform 20 assays (Table A2.1), 1,5 mL of inoculum were added to each vial, resulting in a final VSS concentration in the incubations of 0,92 g VSS/L (Table A3.1, Appendix 3). This value is lower than the reference value to perform biodegradability tests under methanogenic conditions which are 3 g/L of VSS(Coates, Coughlan, *et al.*, 1996; Colleran *et al.* 1992).

The curves of methane production during the incubation are shown in Figure 20. The methane produced in the control assay, which contains no polymer, is due to the consumption of residual substrates present in the leachate inoculated. Since there is no other carbon or energy source added in the assays containing plastics, the difference in the methane produced in the plastic-containing assays and in the control assay, corresponds to the consumption of the polymers by the microorganisms. The percentages of biodegradation of the carbon sources in this experiment, i.e., PE, PET, PCL, PHB/PBAT, and cellulose are presented in Table 3.

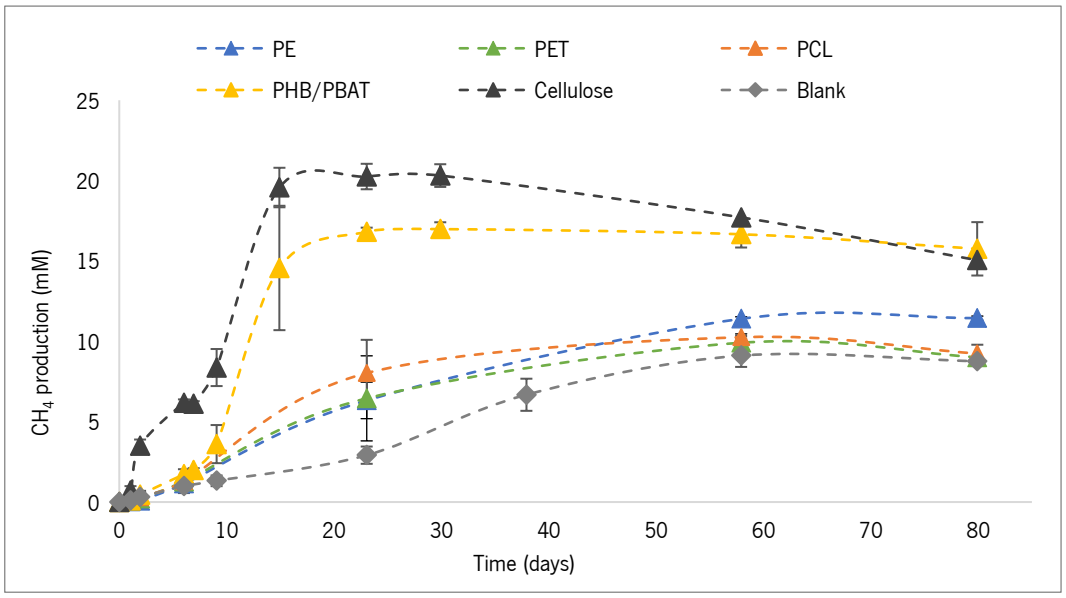

Figure 20: Methane production curves from the first anaerobic incubation, for 80 days of incubation. Average values of methane production for the assays with PE, PET, PCL, the blend of PHB/PBAT, cellulose, and blank assay, and respective standard deviation.

Table 3: Values of theoretical methane production expected, of the methane produced without the contribution of the blank assay, in the first anaerobic experiment, and percentage of biodegradation of the triplicates of each polymer/compound studied, and respective standard deviation

Polymer/carbon and energy source	Theoretical CH_4 (mmol) expected from complete biodegradation of the added carbon source	CH_4 produced (without the contribution of the methane measured in the blank assay) (mmol)	Biodegradation (%)
PE	0,823	0,029	2,22 ± 1,91
PET	0,401	0,010	2,49 ± 1,40
PCL	0,536	0,014	11,65 ± 12,71
PHB/PBAT	0,439	0,098	23,77 ± 0,22
Cellulose	0,284	0,140	51,02 ± 1,51

It is possible to observe a higher methane production, and therefore, a higher percentage of biodegradation for the biodegradable compounds, which are the cellulose, and the blend PHB/PBAT, where the microbial degradative activity happens mostly in the first 20 to 30 days of incubation (Figure 20). Although PCL is also a biodegradable plastic, surprisingly, its percentage of biodegradation was negligible and so were the percentages of biodegradation obtained for the synthetic plastics PE and PET. These incubations were extended until 180 days (Figure A3.1, Appendix 3), but still methane production did not increase considerably, except for the PE assays, that presented a methane production at the 180th day corresponding to 5,1 ± 1,89 % biodegradation (data not shown). These results suggest that neither the synthetic plastics PE and PET nor the biodegradable plastic PCL could be efficiently biodegraded by the inoculum sludge. Nevertheless, this inoculum showed high activity towards cellulose and PHB/PBAT.

Maximum methane production from cellulose was achieved in the first 20 days of incubation, showing almost no lag phase preceding methane production (Figure 20). This means that the microbial community needed very few days to adapt to the new substrate and start to biodegrade it (Massardier-Nageotte *et al.*, 2006). After that peak, the curve of cumulative methane production started to decrease. This was most likely due to loss of pressure because of the frequent headspace sampling, which is particularly relevant because of the small headspace volume (12,5 mL). Yagi *et al.* (2009) reported similar results of gas production for their sample with cellulose in powder while using anaerobic sludge as inoculum at 55℃. They observed a quick increase in gas production in the first 20 days, followed by a prolonged phase of constant gas production (Yagi *et al.*, 2009). Because of this behaviour of methane production, a high percentage of biodegradation was expected, and similar results have been reported. Wataru (2015) described the biodegradation of cellulose by landfill leachate at 35℃ of 32,4 % after 90 days of incubation (Wataru, 2015). It is worth noting, however, that these percentages of biodegradation,

originate from approximations of direct transformation of the polymer/compound into CO_2 and CH_4 (Appendix 2, section 2.6), which in reality does not happen since part of the carbon is used in other metabolisms, like new biomass formation (Choe *et al.*, 2021).

The blend of PHB/PBAT had a similar behaviour to cellulose, i.e., a quick increase of methane production that reached a peak around the 18th day of incubation. However, there was an initial lag phase slightly longer (Figure 20) which may indicate a higher period of adaptation of the microbial community to redirect their metabolism for the blend's biodegradation (Massardier-Nageotte *et al.*, 2006), or to adapt to the growth conditions imposed (Yagi *et al.*, 2009). In terms of percentage of biodegradation, the results obtained for this blend was 23,77 ± 0,22 %, but the complete theoretical biodegradation of PHB alone is around 53,2 %. Since this polymer is easier to attack than PBAT (Tabasi & Ajji, 2015), the biodegradation observed is most likely due to PHB and not PBAT. However, to confirm this theory, additional analysis would have to be performed, to identify the nature of the polymer that was left to biodegrade. Tabasi & Ajji (2015) studied biodegradation in compost of PHB/PBAT blend and concluded that there existed a selectivity of biodegradation for the more biodegradable polymer in the blend, in that case, of PHB in comparison with PBAT (Tabasi & Ajji, 2015). The blending of the two components improved the biodegradability results of PBAT in film (R. Qi *et al.*, 2021; Tabasi & Ajji, 2015). Liao & Chen (2021) reported a 6,8 % weight loss for PBAT film in soil, after 6 months, and García-depraect *et al.* (2022) observed no significant biodegradation for the tested PBAT in aerobic and anaerobic aqueous conditions.

PCL is considered a biodegradable plastic (Borghesi *et al.*, 2016; Iram *et al.*, 2019; Trivedi *et al.*, 2016), with a few biodegradation studies that reported good biodegradability results (Borghesi *et al.*, 2016; Cho *et al.*, 2011; Hosni, 2019; Ishigaki *et al.*, 2004; Mandic *et al.*, 2019; Nakasaki *et al.*, 2006; Nawaz *et al.*, 2015; Yagi *et al.*, 2013, 2014), therefore, the results here obtained were not expected. The assays with PCL showed a similar behaviour to the experiments with the non-biodegradable plastics-PE and PET (Figure 20 and Table 3). It showed a slightly higher methane production in the first 60 days, with a constant production from then on (Figure 20). This pattern matches the methane production of the non-biodegradable plastics, where the production went on for about 60 days of incubation, with a slight increase until the 150th day (Figure A3.1, Appendix 3). It is difficult to understand why this conversion of PCL to methane was so low, especially taking into consideration that in the second anaerobic experiment and aerobic experiment, performed also with leachate, PCL showed high biodegradation results (103,34 ± 18,06% for PCL in powder 100,53 ± 0,23% for PCL in film in the anaerobic experiment, 98,53 ± 6,37 % for PCL in powder and 67,58 ± 33,79 % for PCL in film for the aerobic experiment)

(Figure 23 and 24). Some factors that could have influenced this result are the microbial communities of the leachate that did not have the metabolic machinery to degrade the polymer, or even that, due to the low VSS value, there were not enough microorganisms for significant biodegradation. Nevertheless, biodegradation happens when the right conditions for the microorganism's activity are met (Choe *et al.*, 2021), which may imply that some condition in the PCL bottles was inhibiting the action of the microorganisms. Additionally, it has been reported that chemical factors heavily influence the initial stages of PCL biodegradation (Ishigaki *et al.*, 2004), which could mean that there may have been some chemical compound in the medium that influenced this step. Furthermore, anaerobic biodegradation of PCL has shown highly varying results throughout the literature (Federle *et al.*, 2002), so different results between experiments can be expected. For that reason, although many studies present good results for PCL biodegradation, there are still some that report low biodegradation percentages. In a study with leachate at 38°C, under anaerobic conditions and landfill simulation, it was reported no significant mineralization of the powdered PCL tested (Federle *et al.*, 2002). They reported poor biodegradation results, only with some degradation after the 200th day of incubation (Federle *et al.*, 2002). One explanation given for these results is the very slow acclimatization of the microbial community to the PCL, and that they may have preferred to consume the municipal solid waste in the sample than the polymer (Federle *et al.*, 2002). This reasoning could also be applied in the present work, where the microbial community could have needed more time to change their metabolism to biodegrade the polymer, and in the meantime, the microorganisms that survived the conditions applied preferred to feed on the substrate that existed in the leachate than PCL. Another explanation given in the mentioned article, for this slow biodegradation, was that PCL undergoes slow hydrolysis (Federle *et al.*, 2002). However, this last reasoning is refuted by the results obtained in the second anaerobic experiment, because PCL was rapidly and efficiently degraded by the microorganisms, demonstrating a short lag phase (Figure 23). Nevertheless, since the inoculum used in this first assay was different from the one used for the second experiments, it could imply that older leachate (used in the second experiment) may present more suitable microorganisms that can degrade polymers, explaining this big difference in the results obtained.

For PE and PET, in the literature, in a study with leachate at 35°C, PET samples showed a cumulative gas production similar to the blank of the experiment, resulting in no biodegradation (Wataru, 2015). Another study with anaerobic sludge at 55°C also reported no biogas release for the unmodified PET film (Hermanová *et al.*, 2015). Studies conducted in landfill conditions with PE show very poor biodegradation results, where only partial degradation processes were observed (Xochitl *et al.*, 2021). The same was noted with anaerobic sludge (Iwańczuk *et al.*, 2015). It was hypothesized that higher

oxygen levels in landfill conditions could be a driver for PE fragmentation, having, therefore, an impact on its biodegradation (Quecholac-Piña *et al.*, 2020; Xochitl *et al.*, 2021). If that was the case for the experiments of this work, better biodegradation of PE in the aerobic experiment would have been observed (Figure 24), which was not the case. When calculating the percentages of biodegradation, PE and PET showed similar low results, since the methane production was almost identical to the production detected in the blank assay (Figure 20 and Table 3). However, the final biodegradation of PE, after 180 days reached 5,1 ± 1,89 % (data not shown). PCL had a slightly higher percentage of biodegradation (Table 3), but also a very high standard deviation. This happened because there was a replica with a much higher methane production, while in the other two almost no methane was produced. Other studies performed at mesophilic temperatures showed no PCL mass loss and no significant biogas production from the experiment (Massardier-Nageotte *et al.*, 2006). Xochitl *et al.* (2021) showed that PCL biodegradation at 55℃ can vary greatly, from no biodegradation to very high biodegradation percentages (80 % of biodegradation in 50 days) (Xochitl *et al.*, 2021).

No VFAs were detected at the end of the incubations with PE, PET, PCL, PHB/PBAT and cellulose. In the incubation performed with the VFA mixture as the sole carbon and energy source only residual amounts of acetate could be detected by HPLC (about 1% of the acetate present in the beginning of the incubation) (data not shown). This shows that the inoculum presents both fatty acid degrading activity and methanogenic activity.

6.1.1.4- Polymer analysis of films before and after biodegradation

Comparison of FTIR analysis on PE and PET films collected from the vials after 180 days of incubation, and the same polymers without incubation, did not show any changes in the chemical structure of the films, more specifically, in the functional groups of the polymers (Figure 21). However, that does not mean that cleavage of the molecules/biodegradation did not occur since the analysis was performed in some areas of the film and not the complete film. To verify that no change in the functional groups occurred, additional analysis, like molecular mass analysis, would be needed (Al-mutairi & Mousa, 2021; Ruggero *et al.*, 2019). The differences observed in the transmittance between curves can be explained by the higher saturation of the film, which is due to the film being thicker. Therefore, those differences only tell that the second replica of PE and the first replica of the PET in film are thicker films.

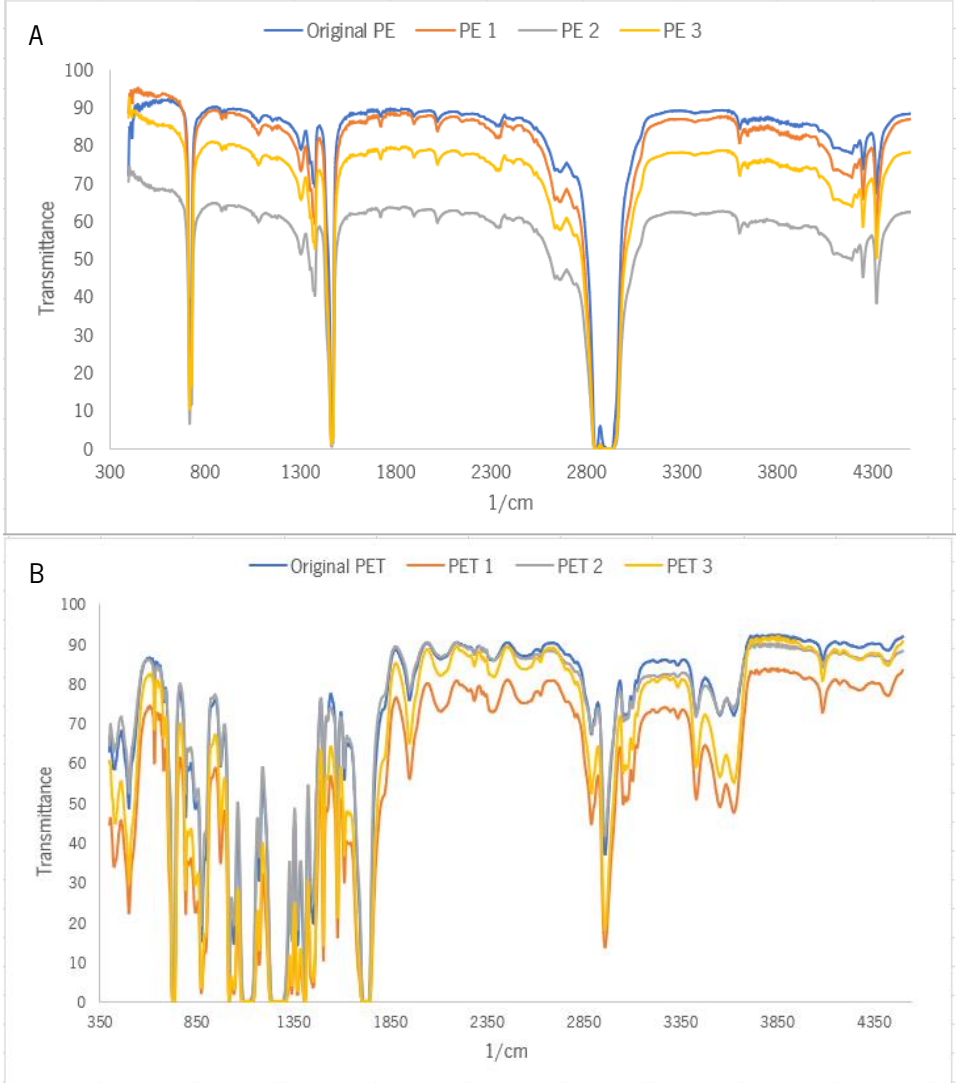

Figure 21: FTIR analysis of the PE and PET in film from the first anaerobic experiment that were not subjected to biodegradation, and the triplicates that suffered biodegradation; A) FTIR spectrum of the original PE film, and the triplicates of the biodegradability tests; B) FTIR spectrum of the original PET in film and the triplicates of the biodegradability test.

For PE, the peak at around 1469 cm^{-1} is a common peak of all PE films, which is due to the -CH_2 bending vibration of the polymer chain (Hou *et al.*, 2022). Other common peaks of PE compounds are shown in Table A3.2 (Appendix 3). For PET films, if degradation was observed, peaks at 2958 cm^{-1}, 1713 cm^{-1}, 1089 cm^{-1}, 888 cm^{-1}, 730 cm^{-1} and 710 cm^{-1} would suffer alterations, being indicative of the formation of ester, carboxyl or alcohol bonds (Roberts *et al.*, 2022).

SEM analysis was only performed in the PE in film since in PE incubations methane production was higher than in the control assay, with a biodegradation percentage of 5,13 % ± 1,89 % at the end of the 180 days (data not shown). This analysis was performed on the replica that showed better results (7,0% of biodegradation based on methane production), and on the original PE film that was not submitted to microbial incubation (Figure 22 and Appendix 3- Figure A3.2).

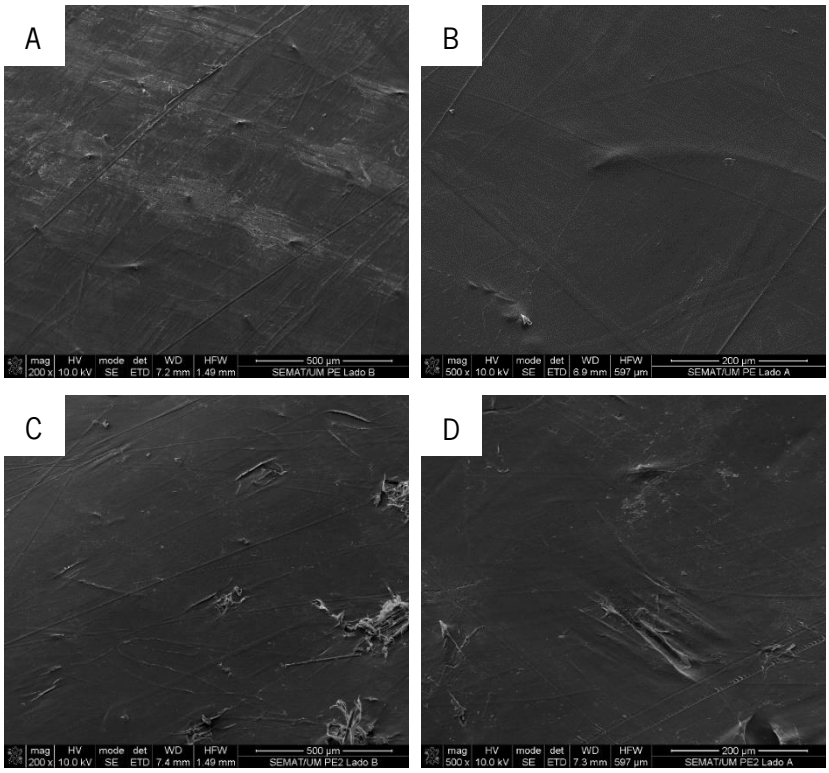

Figure 22: SEM images of the PE original film (A and B) and the tested film (C and D), after 180 days of incubation; A) side A of the original film in 200x magnification; B) side B of the original film with 500x magnification; C) side A of the film used in the biodegradability tests, with 200x magnification; D) side B of the film used in the biodegradability test, with 500x magnification.

The original film presents a clear and smooth surface (Figure 22, A and B), with some minor imperfections most likely due to the extrusion process. The tested film, which was subjected to biodegradation, does not appear to have any characteristic topography of microbial colonization on either side of the film (Figure 22 C and D). If considerable biodegradation had occurred, some holes, pits or other types of erosion would be visible (Ghatge *et al.*, 2020). This does not seem to be the case with the tested film since the irregularities observed should most likely be related to the formation of the film. Nevertheless, it is also worth noting that the analysis of the film was done to a specific point, meaning that there could be other parts of the film that have clearer evidence of a microbial attack. Additionally, this technique is not the most sensitive for film topography changes, so other techniques would be necessary to verify if any surface alteration was provoked by microbial attack. Techniques like AFM (atomic force microscopy) and measure of contact angle, that are more susceptible to topography changes in the polymer surface (Al-mutairi & Mousa, 2021), like rugosity and even chemical structure (De Campos *et al.*, 2012; Kotova *et al.*, 2021).

6.1.2- Second anaerobic experiment- biodegradability results

The second anaerobic experiment was performed with a leachate inoculum containing 45,60 ± 0,43 g VSS/L (Table A3.3, Appendix 3), which corresponds to a VSS concentration in the vials of 1,4 g/L (with exception of the assays with PE and PET in film which were performed with 0,65 VSS/L).

The average values of the thickness of the polymer films used show similar results for PE and PET, i.e., 0,064 ± 0,026 mm and 0,081 ± 0,022 mm, respectively. On the other hand, PCL film were thicker, presenting 0,241 ± 0,051 mm. This was because thinner PCL films were harder to manipulate during the incubation preparation.

The results show that PCL (in film and in powder) and cellulose were completely converted to methane under thermophilic conditions (Figure 23). On the other hand, incubations with PE and PET showed similar methane production to the blank assay (Figure 23), indicating that these polymers were not converted to methane under the conditions tested (Appendix 3, Figure A3.3).

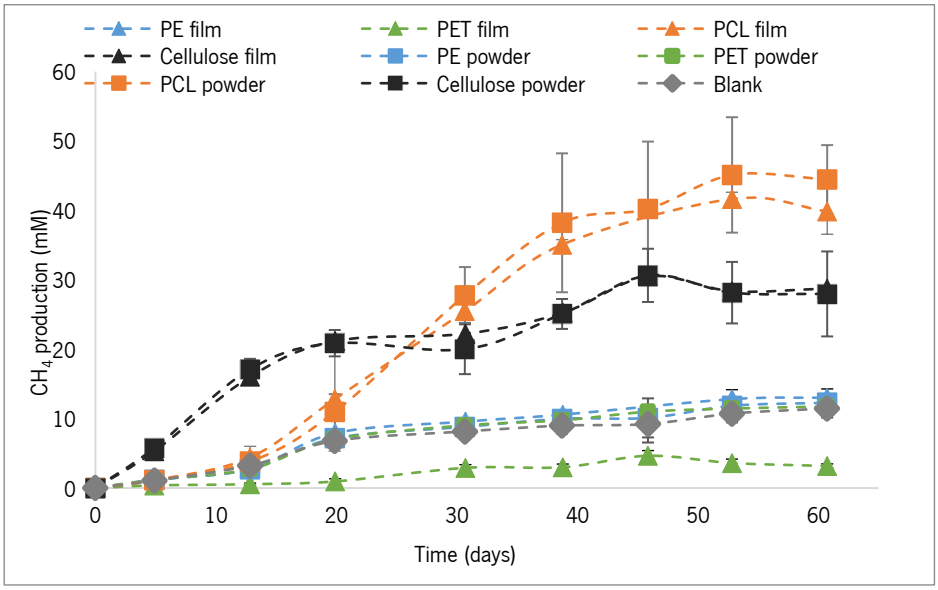

Figure 23: Methane production curves from the second anaerobic experiment with polymers in film and in powder, for 60 days of incubation. Average values of methane production for the assays with PE, PET, PCL, cellulose, and blank and respective standard deviation; PCL film replicas are demonstrated in separate, and cellulose in film only has one replica.

These results were completely different from the ones obtained in the first experiment, in which PCL was almost not degraded. One factor that might have contributed to this difference was the sterilization of the polymers at 120°C, for 20 minutes, which is a thermal pre-treatment (Matjasic *et al.*, 2020). With this in mind and taking into consideration that PCL's melting transition temperature is 60°C (Borghesi *et al.*, 2016), these better results for PCL biodegradation could be due to this pre-treatment applied. Nevertheless, a lag phase of around 13 days was observed, showing the need for microbial

adaptation to the new substrate (Massardier-Nageotte *et al.*, 2006). After the lag phase, the biodegradation proceeded, and all the PCL was converted to methane in 39 days (after 52 days from the beginning of the incubation) (Figure 23 and Table 4).

Table 4: Values of theoretical methane production expected, of the methane produced without the contribution of the blank assay in the second anaerobic experiment, and percentage of biodegradation of the triplicates of each polymer/compound studied, and respective standard deviation. The values for the PE and PET in film samples are not considered correct (*) since the volume of biomass is lower than the one in the blank. ND- not detected

Polymer/carbon and energy source	Theoretical CH_4 (mmol) expected from complete biodegradation of the added carbon source	CH_4 produced (without the contribution of the methane measured in the blank assay) (mmol)	Biodegradation (%)
PE powder	3,60	0,072	1,57 ± 1,52
PE film (*)	3,43	0,100	2,68 ± 1,92
PET powder	1,74	0,030	2,32 ± 2,86
PET film (*)	1,63	-0,534	ND
PCL powder	2,23	1,957	103,34 ± 18,06
PCL film	2,10	2,075	100,53 ± 0,23
Cellulose powder	1,24	1,289	94,56 ± 17,25
Cellulose film	1,201	1,279	100

Studies with thermophilic sludge, at 55 °C, showed no lag phase preceding methane production but PCL in film was not completely degraded (less than 60% of biodegradation in 49 days of incubation) (Šmejkalová *et al.*, 2016). This inexistence of lag phase could be due to the composition of the microbial community used or even to the concentration of the biomass, i.e., there being more microorganisms and/or more active for the hydrolysis of the polymer. They further highlighted that since biological hydrolysis is the limiting step of biogas production, different susceptibilities to hydrolysis of the polymers will lead to different anaerobic degradation profiles (Šmejkalová *et al.*, 2016). This could explain the big difference between the first anaerobic experiment to the second, meaning that the film used in the first experiment was less susceptible to hydrolysis (maybe because of not suffering pre-treatment) which resulted in poorer results of biodegradation. A study on the biodegradation of PCL in powder in thermophilic conditions with an inoculum from an anaerobic waste treatment facility (Jin *et al.*, 2022) reported an initial lag phase of 11 days, followed by a quick increase in methane production for 10 days, and a plateau phase after the 28th day (Jin *et al.*, 2022). The slight differences in methane production from the mentioned study to this work could be related to the difference in the powder size and quantity of powder used, as they reported a significant difference in the speed of degradation of the pellet PCL

tested, stating that this difference in times of biodegradation could be connected to the size of the polymer (Jin *et al.*, 2022).

In terms of percentage of biodegradation Jin *et al.* (2022) also observed similar biodegradation results for the tested powder to the ones obtained in this study (Jin *et al.*, 2022). They reported biodegradation of PCL in powder of 92,3 % under thermophilic conditions, also stating an almost complete degradation after 60 days (Jin *et al.*, 2022). Additionally, Yagi *et al.* (2013) reported an 80 % biodegradation of PCL in powder in thermophilic conditions after 60 days, using anaerobic sludge as inoculum (Yagi *et al.*, 2013). For PCL in film, Šmejkalová *et al.* (2016) reported only 60 % biodegradation after 150 days (with anaerobic sludge) but mention that PCL is reported as practically biodegraded in thermophilic anaerobic incubations (Šmejkalová *et al.*, 2016). Xochitl *et al.* (2021) described an 80 % biodegradation in 50 days at 55℃ but in the same work, also describes insignificant biodegradation values, stating that these variations happen without a visible pattern for temperature or incubation duration (Xochitl *et al.*, 2021). Although no significant differences were observed for the biodegradation related to methane production for the assays with PCL in film and in powder, in theory, it would be expected higher biodegradation for the powder, because it has a higher surface area which leads to higher availability of the polymer to the microorganisms (Choe *et al.*, 2021; Lesteur *et al.*, 2010).

Cellulose was a good control substrate since it was easily degraded by the leachate microbiome. The majority of cellulose was converted in the first 20 days of incubation (Figure 23), something also verified in the first experiment (Figure 22), although with a different behaviour after that point. While in the first anaerobic experiment the methane production becomes constant (Figure 22), in the second experiment, methane increases until the 55th day of incubation. This was observed in the assays with cellulose in film and in powder (Figure 23). In terms of the percentage of biodegradation, cellulose in film was completely degraded, while cellulose in powder reached 94,56 ± 17,25 % biodegradation (Table 4). Yagi *et al.* (2009) reported an 80 % biodegradation of cellulose in powder in just 14 days, with biodegradation of 93 % at the end of the 80 days of incubation, using anaerobic sludge as inoculum (Yagi *et al.*, 2009).

Regarding PE and PET in film, although their comparison to the blank is not so accurate, since these assays were performed with less inoculum leachate, there are not many differences between the methane production in the blank and in PE and PET incubations, suggesting that conversion of the polymers to methane was negligible. Indeed, no significant biodegradation was expected in short-term incubations, due to the recalcitrant nature of these polymers (Hermanová *et al.*, 2015; Wataru, 2015).

For the powders, the methane production was also very similar to the blank, which means that the activity measured is most likely from the residual nutrients in the leachate, and not from the biodegradation of the polymer. Selke *et al.* (2015) tested the biodegradation of PE and PET in film under simulated thermophilic (50℃) anaerobic landfill conditions, with anaerobic sludge, and also observed no difference between the biogas production of the films in comparison to the blank (Selke *et al.*, 2015). They performed this incubation for 500 days, and even at the end of the incubation, biogas production did not show a significant difference between the blank (Selke *et al.*, 2015).

The percentage of biodegradation calculated also points out to the conclusion that no methanogenic biodegradation occurred since biodegradation percentages were 1,57 ± 1,52% for PE in powder, and 2,32 ± 2,86 % for PET in powder (Table 4). A study with anaerobic sludges from the sewage plant, showed no biodegradation for the low-density polyethylene, justifying their results with the fact that polyolefins need activation by the introduction of hydroxyl groups, to suffer biodegradation by the microorganisms (Iwańczuk *et al.*, 2015). Despite the poor results obtained and so far cited from the literature, some studies report good biodegradation of low molecular weight polyethylene, but the trend for those studies seems to be the use of specific microorganisms or microbial consortia that are efficient PE degraders (Nowak *et al.*, 2011; R. Qi *et al.*, 2021; Skariyachan *et al.*, 2017). For PET, studies with sludge in anaerobic thermophilic conditions also did not show biodegradation of the polymer with no modifications (Hermanová *et al.*, 2015; Selke *et al.*, 2015), which shows how difficult it is for PET to be degraded, without additional changes to its structure.

Something that was observed and that could have influenced the biodegradation of these non-biodegradable polymers, is the floating of the polymer films (Appendix 3, Figure A3.4) and powder, which could potentially result in less surface area available. Especially regarding PE, the powder would more easily stick to the walls of the vials, away from the medium, and therefore less available for the microorganisms (Šmejkalová *et al.*, 2016). One way to solve this issue would be the continuous agitation of the bottles. Additionally, another issue was observed in the PET bottles, as normally, all anaerobic growth mediums had a darker characteristic colour no matter the time of incubation. However, PET bottles had an almost translucid anaerobic medium, which was observed only in these vials (Appendix 3, Figure A3.5), although it is not known why or even if it had an impact on biodegradability. Nevertheless, it was not expected high biodegradation for PET, since in the literature, with leachate (at 35℃) no biodegradation was observed (Wataru, 2015).

By comparing the two different anaerobic experiments, it is interesting to see that the thermal pre-treatment applied to the second experiment (and probably allied to a more efficient microbial community regarding PCL biodegradation) seemed to have a big impact on PCL's biodegradation, but no effect on the biodegradability of the non-biodegradable plastic, especially considering LDPE's melting temperature is below 120℃ (around 105-116℃) (Suzuki *et al.*, 2021).

No VFA's were detected, at the end of the experiment, meaning that in some incubations, like the ones with PE and PET, no VFAs were produced, or if they were (for instance in the assays with PCL and cellulose), they were completely consumed, and therefore not detected. No polymer characterization was performed on the films of these assays as neither PE nor PET in film showed significant results to make the characterization worthwhile, and PCL films were completely biodegraded.

6.1.3- Aerobic experiment- biodegradability results

The aerobic experiment was prepared with a concentrated leachate with 30,20 ± 0,33 g VSS/L, resulting in assays with 1,5 mL of leachate and 0,92 g/L of VSS (Appendix 3, Table A3.4).

The oxygen consumption of the assays (Figure 24) showed an almost complete biodegradation of PCL in powder (98,53 ± 6,37 %) and for one of the replicas of PCL in film (100%), followed by cellulose (70,88 ± 10,09 %) and the remaining PCL replicas, with more than 65% biodegradation (Table 5). Similarly, to the anaerobic experiments, the non-biodegradable polymers, PE, and PET had an oxygen consumption similar to the blank assay (Figure 24), showing that the oxygen consumed was not a result of the biodegradation of the polymer. To preserve the microbial communities of the biodegradability assays for later taxonomic identification, PCL and cellulose assays were sampled around the 50th day of incubation. The remaining experiments were left incubating, however, no significant differences in the methane production and the values of the percentage of biodegradation after the 56th day (Figure 24 and Appendix 3-Figure A3.6).

The calculation of the biodegradation percentages was performed considering 56 days of incubation (Table 5).

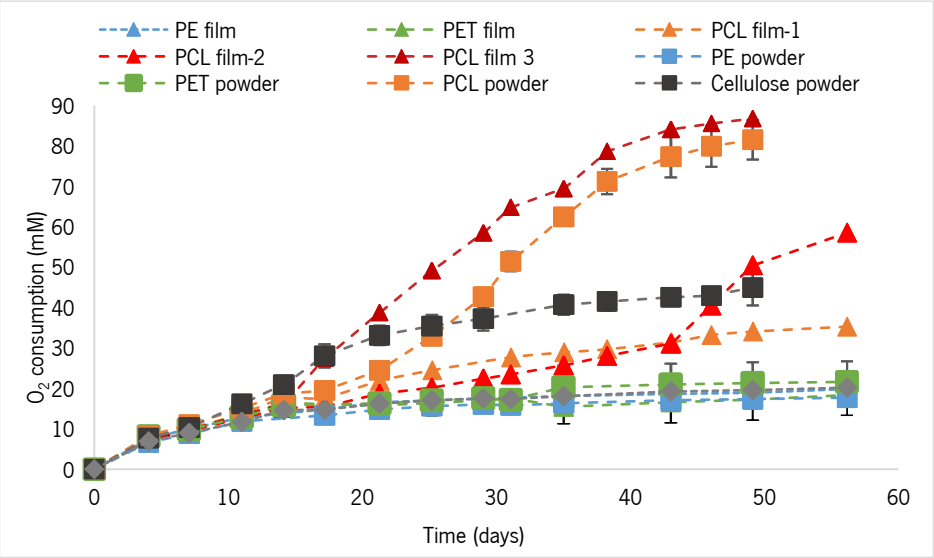

Figure 24: Oxygen consumption curves from the aerobic experiment with films and powder for 56 days of incubation. Average values of methane production of the assay with PE, PET PCL, cellulose, and blank and respective standard deviation; the replicas for PCL are presented separately.

Table 5: Theoretical oxygen consumption expected, of the measured oxygen consumption without the contribution of the blank assays and the consequent percentage of biodegradation and standard deviation. ND_ not detected

Polymer/carbon and energy source	Theoretical O_2 (mmol) expected from complete biodegradation of the added carbon source	O_2 consumed (without the contribution of the oxygen measured in the blank assay) (mmol)	Biodegradation (%)
PE powder	7,21	-0,20	ND
PE film	6,87	-0,05	ND
PET powder	3,49	0,07	1,95 ± 8,25
PET film	3,31	-0,16	ND
PCL powder	4,37	4,30	98,53 ± 6,37
PCL film	4,20	2,00	67,58 ± 33,79
Cellulose	2,49	1,76	70,88 ± 10,09

A considerable difference between the three tested replicas for PCL in film was observed (Figure 24), which is why it was decided to present the triplicates separately, rather than the average value. It was observed that the third replica (PCL 3f) showed a much quicker oxygen consumption before the 20th day of incubation, while the other two replicas kept consuming oxygen at a much slower rate. Only after 40 days, they started to consume more oxygen (Figure 24), probably corresponding to the beginning of the polymer biodegradation. After the 70th day of incubation, it was possible to observe a higher oxygen consumption (Appendix 3, Figure A3.6), which may indicate that only after 70 days these microorganisms started to actively produce the machinery to aerobically biodegrade PCL (García-depraect *et al.*, 2022).

Although this big difference between the three replicas was not expected, it is a normal phenomenon to have different results from experiments performed under the same conditions (Choe *et al.*, 2021). When comparing the third replica to the literature, Massardier-Nageotte *et al.* (2006) also observed similar results for PCL, but in a much shorter period. They observed a lag phase of only one day, with a quick increase in BOD until the 18th day, followed by a stationary phase until the end of the incubation (28th day). However, they performed incubations at 30℃, with a non-specified inoculum (Massardier-Nageotte *et al.*, 2006). On the other hand, García-depraect *et al.* (2022) reported similar results for the biogas production curve of PCL biodegradation with activated sludge, with a lag phase lasting 11-13 days, followed by a quick biogas production. The PCL tested was in powder form and at 25℃ (García-depraect *et al.*, 2022). For PCL in powder, the oxygen consumption only seemed to have differentiated from the blank after the 25th day of incubation, which was later compared to the results with the film (Figure 24). In simulated compost conditions, the results for PCL also showed a similar curve and percentage of biodegradation. They reported a 30-day lag phase, followed by an almost linear growth of the biodegradation curve (Pradhan *et al.*, 2010). In a study with soil, and soil + leachate, PCL carbon dioxide emission was observed to be below the blank used in both experiments, but it was detected that the addition of the leachate to the soil promoted surface changes while inhibiting the evolution of the carbon dioxide (Campos *et al.*, 2011).

In terms of the percentage of biodegradation (Table 5), PCL in powder reached almost a complete degradation (98,53 ± 6,37%), while the average value of the film was around 67,58 ± 33,79%. This result and high standard deviation is explained by the difference in biodegradation of the three replicas, clearly seen in the oxygen consumption graph (Figure 24 and Appendix 3, Table A3.5) Nevoralová *et al.* (2020) described a quick complete biodegradation of the PCL tested, under thermophilic (58℃) composting conditions after 60 days, referring that at that temperature, the crystalline parts of the polymer are an easier target for microbial enzymes, because PCL melting temperature is around 60℃ (Nevoralová *et al.*, 2020). In another experiment simulating aerobic composting conditions, PCL in powder reached 60 % biodegradation after 180 days, showing a slow evolution (Pradhan *et al.*, 2010), similar to the first replica of the PCL in film tested in this work. Additionally, low values of PCL biodegradation have also been reported, where Massardier-Nageotte *et al.* (2006) reported 34,8 % biodegradation for PCL in film, after 28 days at 30℃, showing how diverse these results can be. Comparing results with the second anaerobic experiments, PCL in powder was biodegraded similarly in aerobic conditions for a similar time of incubation, while PCL in film did not. However, if only the third replica is considered, then aerobic degradation of PCL presents slightly better results than the anaerobic one.

For cellulose, after the first few days of incubation, a higher consumption than the blank was observed showing a constant oxygen consumption from then on (Figure 24). Selke *et al.* (2015) also reported a very similar behaviour of carbon dioxide production with the sample with cellulose, in simulated aerobic compost conditions, with anaerobic sludge at 58°C. They demonstrated an almost linear increase in gas production throughout the incubation time but show a bigger difference between the sample and the blank (Selke *et al.*, 2015). Castro-aguirre *et al.* (2017) conducted a study in simulated composting conditions at 58°C and reported varying results of cumulative carbon with cellulose. They performed the same biodegradation tests at different times and demonstrated that, in the same incubation conditions, biodegradation can vary greatly (Castro-aguirre *et al.*, 2017). They stated that similar cumulative gas of two different samples resulted in different percentages of mineralization due to the blank, which also behaved differently throughout the experiment (Castro-aguirre *et al.*, 2017). In a study with compost at 58°C, the biodegradation curve shown for cellulose makes it seem that the results obtain in the present work are only the exponential phase of oxygen consumption, and that a stationary phase would soon be observed since the stationary phase observed in the study started after the 60th day of incubation (Weng *et al.*, 2011). Regarding the percentage of biodegradation, around 70 % of the compound was degraded (Table 5), which was less than for PCL in powder, and almost the same for the average value of the PCL in film. However, given the time of incubation, it can be considered a good result, since Selke *et al.* (2015) also reported 50 % mineralization of the cellulose tested in simulated aerobic compost conditions, at 58°C, after 50 days and about 70 % only after 140 days (Selke *et al.*, 2015).

In terms of non-biodegradable polymers, incubations with both PE and PET in film had a lower oxygen consumption than the blank (Figure 24), which implies that no biodegradation occurred, as the oxygen consumed was a consequence of the consumption of residual substrates in the leachate. A study under simulated compost conditions, at 58°C, showed a lower carbon dioxide evolution of PE and PET in film in comparison to the blank, concluding that non-biodegradable films in industrial aerobic composting processes would be unaffected (Selke *et al.*, 2015). Furthermore, they also tested films that were subjected to UV treatment to lower their molecular weight, stating that CO_2 production was also not different from the blank. This means that even a molecular weight reduction would not make aerobic biodegradation under composting conditions more efficient (Selke *et al.*, 2015). Castro-aguirre *et al.* (2017) conducted a study in simulated compost conditions at 58°C and observed different behaviours of cumulative carbon dioxide, from PE in film. With the same conditions, but with incubations starting at different times, PE showed low mineralization values, and even some negative ones, that were explained to be related to less availability of the carbon in the film to the microorganisms (Castro-aguirre *et al.*,

2017). For the powders, on the 56th day, PET showed a slightly higher value of oxygen consumption than the blank, while PE consumption was lower (Figure 24). Castro-aguirre *et al.* (2017) also report a negative value of mineralization for the PE in powder tested in simulating composting (58°C) conditions, stating that this could be due to a physical barrier of the film, which limits the availability of carbon to the microorganisms (Castro-aguirre *et al.*, 2017). As a consequence of these oxygen consumption values, most of these non-biodegradable polymers showed no results of biodegradation. Selke *et al.* (2015) reported low mineralization percentages for the PE in film and in powder tested, in simulated composting conditions, with anaerobic sludge at 58°C (Selke *et al.*, 2015). In the case in study, an issue observed that could have influenced the biodegradation was the floating of the films and powder (Appendix 3, Figure A3.7), which together with the lower availability of the carbon in the polymer, makes the plastic less available to the microorganisms (Castro-aguirre *et al.*, 2017; Šmejkalová *et al.*, 2016). Many studies focussing on the biodegradation of non-biodegradable plastic highlight the importance of longer periods of incubation, that allow the adaptation of the microorganisms to the substances (Massardier-Nageotte *et al.*, 2006). Studies that occurred for more than 6 months showed better results in polymer changes and isolation of microorganisms (Matjasic *et al.*, 2020), proving that longer incubations in these conditions may help the ability of these microorganisms for biodegrading plastics.

Because new oxygen injections were not made in the first week of incubation, some bottles started to present anaerobic activity, due to the low concentration of dissolved oxygen. Therefore, on the second measurement made to evaluate the oxygen consumed, it was possible to observe methane peaks, that hinted at that activity. Additionally, the bottles with higher methane concentration started to present a darker colour of the growth medium, compared to the other bottles, which was characteristic of the anaerobic incubations (Appendix 3, Figure A3.8). Although this production of methane decreased throughout the incubation time, some assays, like the ones with PCL (in film and in powder) and cellulose (Figure 25) still produced some quantity in the first few days of incubation.

The third replica of PCL, besides having the highest oxygen consumption, was also the replica with more methane production, which seemed to have reached its peak around the 40th day of incubation (Figure 25). The second replica showed an increasing methane production until the 35th day, after which methane stopped being detected by the GC. The first replica showed very few points of detection of methane, where the concentration increased from the first to the second measure, and then again from the third to the fourth (Figure 25). PCL's powder triplicates had very different concentrations detected, with higher production in the second replica (PCL 2) (Figure 25). This activity, like before, was first

observed due to a darkening of the medium, which diminished to a lighter colour throughout the incubation, and the consecutive oxygen injections. With cellulose, the methane production seemed to accompany the oxygen consumption (Figure 25), which allows the assumption that there was simultaneous degradation of the compound by aerobic and anaerobic activities. Nevertheless, the oxygen consumed was in higher concentrations than the methane produced, which means that aerobic degradation was predominant. In terms of the standard deviation of the methane curve, although the three replicas had similar behaviour for methane production the curves were in different concentration ranges, which explains the higher standard deviation.

Although the methane production in this experiment was unexpected, it is not an uncommon phenomenon. At the beginning of the incubation, oxygen was quickly consumed by the microorganisms resulting in a low concentration of dissolved oxygen in the medium, and anaerobic microorganisms have already been reported to survive such micro-aerophilic conditions (Wagner, 2017), even though oxygen was toxic for them (M. T. Kato *et al.*, 1993; Pedizzi *et al.*, 2016). It was reported that some *archaea*, described as strictly anaerobic, could endure small oxygen concentrations for short periods (Wagner, 2017), withstanding periods of up to 48 hours in those conditions, without dying (M. T. Kato *et al.*, 1993). Additionally, the resulting products of the degradation of cellulose, H_2, CO_2 and acetate, are used as substrates by the anaerobic microorganisms to produce the methane detected. This, together with being at the bottom of the biofilm where oxygen is even less available (M. T. Kato *et al.*, 1993), enables them to grow and produce methane (Wagner, 2017). Moreover, there is also the possibility of existing some facultative bacteria, that under these lower oxygen concentrations, resolve to anaerobic activity to survive (M. T. Kato *et al.*, 1993).

No VFAs were detected in the aerobic assays.

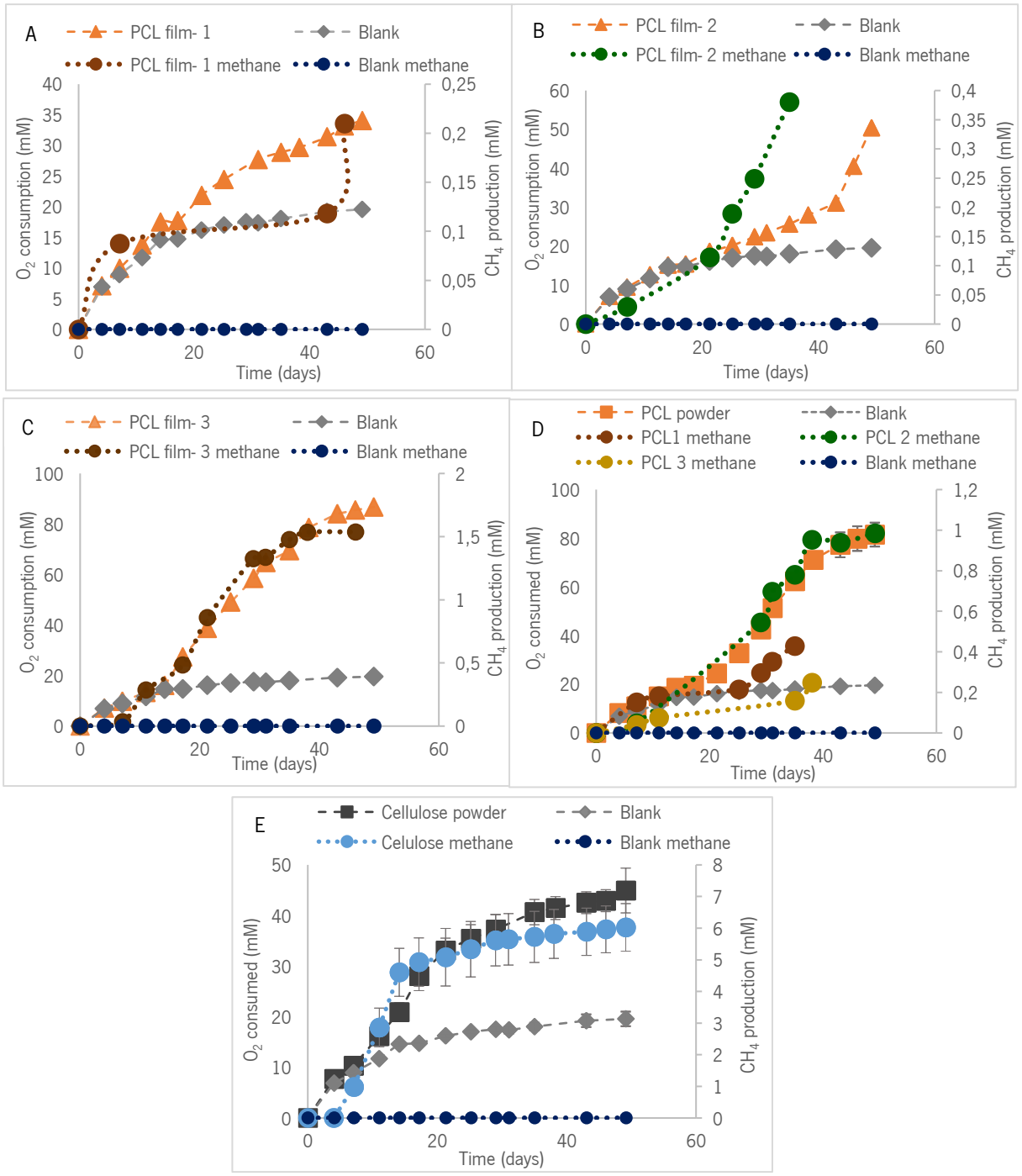

Figure 25: Values of oxygen consumption and methane production of the replicas with PCL in film, PCL in powder, cellulose and blank assays from the aerobic experiment, in an incubation time of 56 days: A) Replica number 1 of PCL in film, with the respective methane production; B) Replica number 2 of PCL in film, and respective methane production; C) Replica number 3 of PCL in film, and the respective methane production; D) Average value of PCL in powder and blank oxygen consumption, triplicates of PCL in powder and blank methane production E) Average value of cellulose and blank oxygen consumption and methane production.

6.1.4- Taxonomic analysis of the microbial communities degrading PCL under aerobic and anaerobic conditions

The concentration of the DNA isolated from the samples collected from the aerobic and anaerobic experiments with PCL, as well as from the inoculum leachate are presented in Table 6. Almost no DNA could be eluted in the first elution, but high concentrations of DNA were quantified in the second elution. The DNA collected in the first and second elutions were merged, before the precipitation step.

Table 6: DNA quantity of the samples extracted for sequencing (ng/µL), from the first and second elution with DES water. ND- Not detected. Samples tested were two of the triplicates of PCL in powder assays of the aerobic experiment, and two from the secondary anaerobic experiment, as well as the leachate inoculum

Sample	First elution DNA (ng/µL)	Second elution DNA (ng/µL)
Aerobic PCL 2 powder	ND	140,6
Aerobic PCL 3 powder	40,5	207,2
Anaerobic PCL 1 powder	ND	175,9
Anaerobic PCL 3 powder	ND	236,4
Leachate Inoculum	ND	103,7

The extracted DNA was submitted to PCR amplification to verify if it was amplifiable prior to sending it for Illumina sequencing. All DNA samples were amplified with primers targeting the bacterial 16S rRNA gene (Figure 26), indicating the presence of bacteria. The negative control, having no band, confirms that the PCR went well, and no impurities were present in the reagents and materials used.

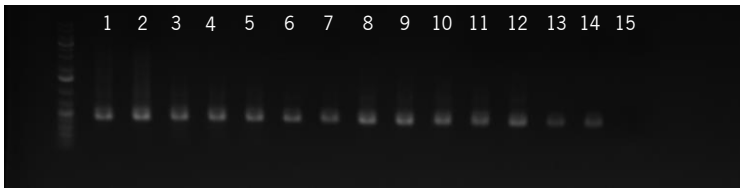

Figure 26: Electrophoresis gel that resulted from the PCR analysis of the studied samples. From left to right, there's the DNA ladder, 1-aerobic PCL 2p, 2-aerobic PCL 3p, 3-anaerobic PCL 1p, 4-anaerobic PCL 3p, 5-inoculum, 6-sample unrelated to this work, 7-sample unrelated to this work 2, 8-aerobic PCL 1p with dilution 1:10, 9- aerobic PCL 2p with dilution 1:10, 10-anaerobic PCL 1p with dilution 1:10, 11-anaerobic PCL 3p with dilution 1:10, 12- inoculum with dilution 1:10, 13- sample unrelated to this work with dilution 1:10, 14- sample unrelated to this work with dilution 1:10, 15- negative control.

The sequencing results showed significant differences between the different samples (Appendix 4, Figure A4.1, A4.2 and A4.3 and Table A4.1 and A4.2), with the anaerobic community having the greatest number of *Archaea* microorganisms (23 %) in comparison to the other samples (aerobic- 0,07 % *Archaea*, inoculum-0,2 % *Archaea*), with 76 % being *Bacteria* and 0,5 % sequences that did not match

any other sequence in the database used. The inoculum presented a high abundance of *Bacteria* (99 %) and the aerobic sample showed some surprising results, as 61 % of the sequences did not significantly match any other sequence in the database used. This high percentage is thought to be small fragments of the microorganism's genome, but that did not code for any identifying sequence or even parts of the genome of eukaryotic microorganisms in the sample. The rest of the aerobic microbial community was assigned to *Bacteria* (39 %). However, after the data analysis was performed, the percentage of these sequences that did have a match in the database was not considered in the calculations. The relative abundances of the microorganisms identified in the PCL incubation performed under aerobic conditions are shown in Figure 27.

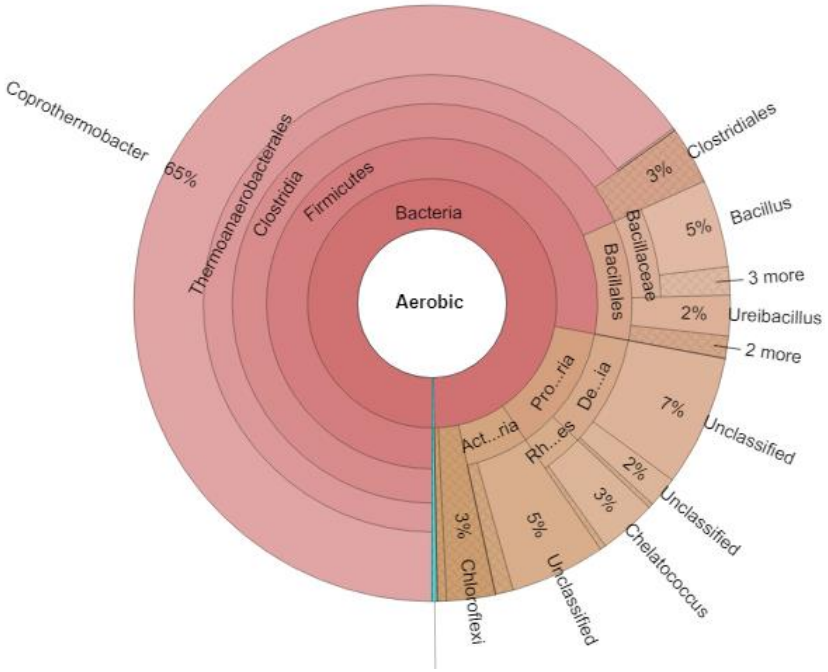

Figure 27: Relative abundance of the microorganisms given by the 16S amplicon sequencing of the PCL incubation performed under aerobic conditions, represented by a krona plot, after removing the contribution of the sequences that received no annotation. Bacteria account for 99,7 % of the community, and Archaea (in blue) account for only 0,3 % of the community.

In the aerobic community, it is possible to observe a predominance of microorganisms from the Bacteria domain. The two most abundant bacteria- *Coprothermobacter* and *Bacillus*, were described as PCL biodegrades in the literature (Atanasova, Stoitsova, *et al.*, 2021; Jin *et al.*, 2022; Tokiwa *et al.*, 2009). In terms of fungi, all the fungi described were not reported in any PCL biodegradation study but were described as being able to biodegrade other polymers, like PU (for *Exophiala* degrader (Liu *et al.*, 2021; Magnin *et al.*, 2020)), PHB and PVC (for *Penicillium expansum* (Gowda & Shivakumar, 2015; Pardo-Rodríguez & Zorro-Mateus, 2021; Urbanek *et al.*, 2022), polycarbonate (PC) and

polyhexamethyleneguanidine (PHMB) (for *Geotrichum candidum* (Srikanth *et al.*, 2022; Swiontek *et al.*, 2019) and PBS (for *Mucor recemosus* (Hosni, 2019)).

The most predominant prokaryote in this sample is *Coprothermobacter sp.*, with a 65 % relative abundance. This is a gram-negative, rod-shaped, thermophilic bacteria, that is reportedly found in strictly anaerobic conditions. It is known due to its proteolytic properties, being an effective degrader in anaerobic thermophilic digesters. It also has acidogenic functions and has been found to be one of the most predominant bacteria in petroleum reservoirs, hinting at a capacity to degrade hydrocarbons (Jin *et al.*, 2022). It was stated that it forms a syntropy association with methanogenic bacteria (Liczbiński *et al.*, 2022), like species from the *Methanothermobacter* genus, that was also found to exist in this sample. This *Archaea* is a strictly thermophilic hydrogenotrophic methanogen (Kato *et al.*, 2008), and was found with an abundance of 72 %, in the 0,3 % of *Archaea* organisms in this aerobic sample. Various studies have reported the syntrophic association of these two bacteria (Jin *et al.*, 2022; Sasaki *et al.*, 2011), however, they were observed only in anaerobic thermophilic conditions. This arises the question of how these anaerobic bacteria survived for so long in aerobic conditions, especially the methanogen *Methanothermobacter*. Some explanations could be in the reasons already described in section 6.1.3, that the initial low concentrations of oxygen could allow the survival of some microorganisms that are nominated strictly anaerobic, but that have been observed to survive to low concentrations of oxygen for some periods (M. T. Kato *et al.*, 1993; Wagner, 2017). However, it is curious that these microorganisms managed to survive for almost three months in an environment with intermittent additions of oxygen, especially after the first 20 days, when the oxygen concentration in the bottles became higher and more stable. Even if they were protected in the biofilm formed, they would have been in contact with some significant dissolved oxygen concentration, in the last days of incubation. Still, they have been reported to be involved in PCL degradation, but under anaerobic conditions (Jin *et al.*, 2022).

In addition to *Coprothermobacter,* a *Bacillus* sp. (with 5 % relative abundance), and some microorganisms belonging to the *Deltaproteobacteria* Class (with 7 % of relative abundance) were the most abundant taxonomic groups. *Bacillus* strains have been frequently reported as PCL degraders. *Bacillus pumilus* strain KT102 in mesophilic conditions (Tokiwa *et al.*, 2009), and in thermophilic conditions (Atanasova, Stoitsova, *et al.*, 2021; Tokiwa *et al.*, 2009) are some of the examples reported as PCL degraders. Tiago et al (2004) conducted a study of mesophilic and thermophilic (50℃) degradation of PCL, using sewage sludge as inoculum, and reported a thermophilic degradation of the polymer of only *Bacillus* genus microorganisms (Tiago *et al.*, 2004).

Due to the high percentage of unidentified sequences in the 16S rRNA gene sequencing in the aerobic assay, 18S rRNA amplicon sequencing was also performed, and microorganisms from different kingdoms could be identified (because the primer pair utilized targeting the 18S rRNA can amplify also some 16S rRNA sequences). Various microorganisms assigned to *Bacteria* (83 % of the matches in the sequencing) were identified, as well as *Eukaryota* (0,03 %) and *Fungi* (0,7 %). Additionally, some matches were observed for the *Plantae* kingdom (3 %), which are most likely seeds or organic waste that were present in the leachate since it sits in open pools at the landfill site. One match for a nematode was observed (*Panagrolaimus* sp.). Sequences that did not significantly match any other sequence in the database were still present in about 13 %. Aerobic PCL degrading cultures were observed at the microscope and besides the pool of unrecognisable microorganisms, some structures very similar to nematode eggs were observed (data not shown).

From this 18S sequencing, only the hits assigned to eukaryotes and fungi were explored. In terms of fungi, the results are shown in Figure 28 and for the *Eukaryota*, in (Appendix 4, Figure A4.4). The most abundant fungi belong to the *Ascomycota* phylum (77 % of the total fungi community), followed by the *Mucor* genus (21 %), and the *Basidiomycota* phylum (2%).

Inside the *Ascomycota* phylum, *Exophiala sp.* is the most abundant (41 %), followed by *Penicillium expansum* (17 %) and *Geotrichum sp.* (7 %). Other known fungi that belong to this phylum are *Penicillium* species, *Aspergillus* and *Pichia* (Figure 28). *Exophiala* compromises a genus of black yeast and has been isolated from the environment, animal tissues, plants, arsenic mine soil and deep-sea sediment. Some are even human pathogens. *Exophiala sp.* in specific has been described as capable of degrading benzene, toluene and xylenes (C. Zhang *et al.*, 2019). The action of this fungus on PCL biodegradation did not appear documented yet, however, it is considered a PU (a non-biodegradable polymer) degrader (Liu *et al.*, 2021; Magnin *et al.*, 2020). *Penicillium expansum* is more commonly known as blue-rot fungus that attacks postharvest fruit with lesions (Luciano-rosario *et al.*, 2020). It was not found a direct impact on PCL biodegradation for this species, however, it is known that this genus is highly correlated to the biodegradation of polymers, especially biodegradable polymers, including PCL (Antipova *et al.*, 2018). This species in particular has been documented to degrade PHB (Gowda & Shivakumar, 2015; Urbanek *et al.*, 2022), and grow on a medium with PVC (Pardo-Rodríguez & Zorro-Mateus, 2021).

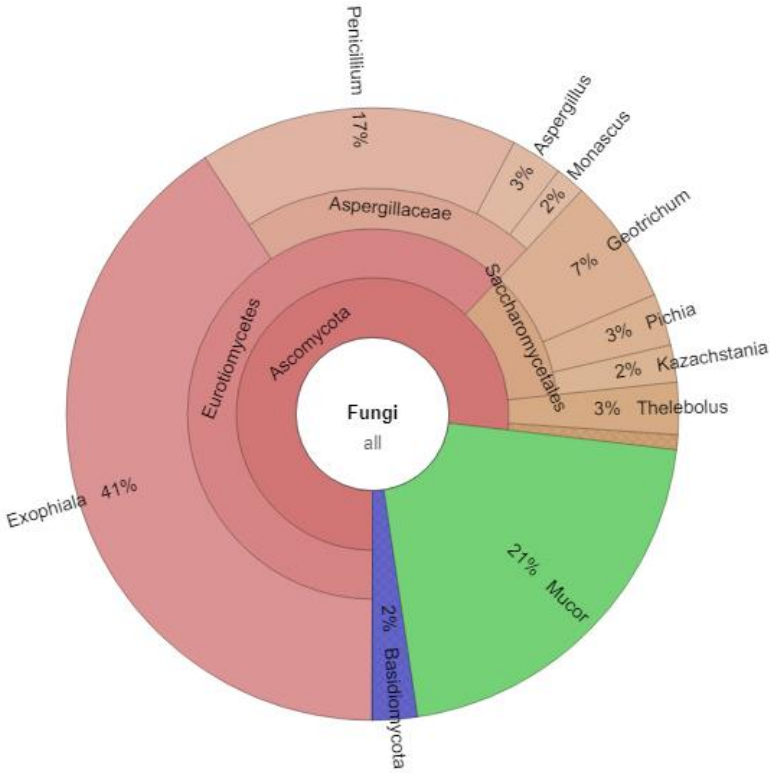

Figure 28: Relative abundance of the microorganisms assigned to *Fungi* given by the 18S amplicon sequencing of the PCL incubation performed under aerobic conditions, represented by a krona plot.

Geotrichum candidum is also a postharvest rot fungus of fruits and vegetables, but can also colonize human skin (Keene *et al.*, 2019). No data was found in the literature that hinted at its action on PCL biodegradation, however, it was described as having some degrading properties for other plastics, like polycarbonate (PC) (Srikanth *et al.*, 2022) and polyhexamethyleneguanidine (PHMB) (Swiontek *et al.*, 2019). In terms of *Mucor* microorganisms, the most abundant is *Mucor recemosus* (18 %). It's also a fungus commonly observed in rotten food (Botha & Botes, 2014), and it can infect immunocompromised people (Myoken *et al.*, 2002). Again, no evidence in the literature was found that showed its ability to biodegrade PCL, however, some studies report degradation for other polymers, like PVC (Pardo-Rodríguez & Zorro-Mateus, 2021), PBS (polybutylene succinate) (Hosni, 2019) and even crude petroleum by-products (Adedotun & Oluyode, 2005).

The identified *Eukaryota* in the sample had very little relative abundance (0,03 %). Only four matches occurred, *Cholamonas cyrtodiopsidis* with 47 % abundance, *Colpodella* sp. with 13 %, *Anurofeca* sp. with 20 % and a microorganism that was not possible to classify at the genus and species taxonomy, but that belongs to the *Eimeriidae* family (with 20 % abundance) (Appendix 4, Figure A4.4).

For the anaerobic sample and the inoculum, only 16S amplicon sequencing was performed. The krona plot from the sequencing of the anaerobic sample is shown in Figure 29.

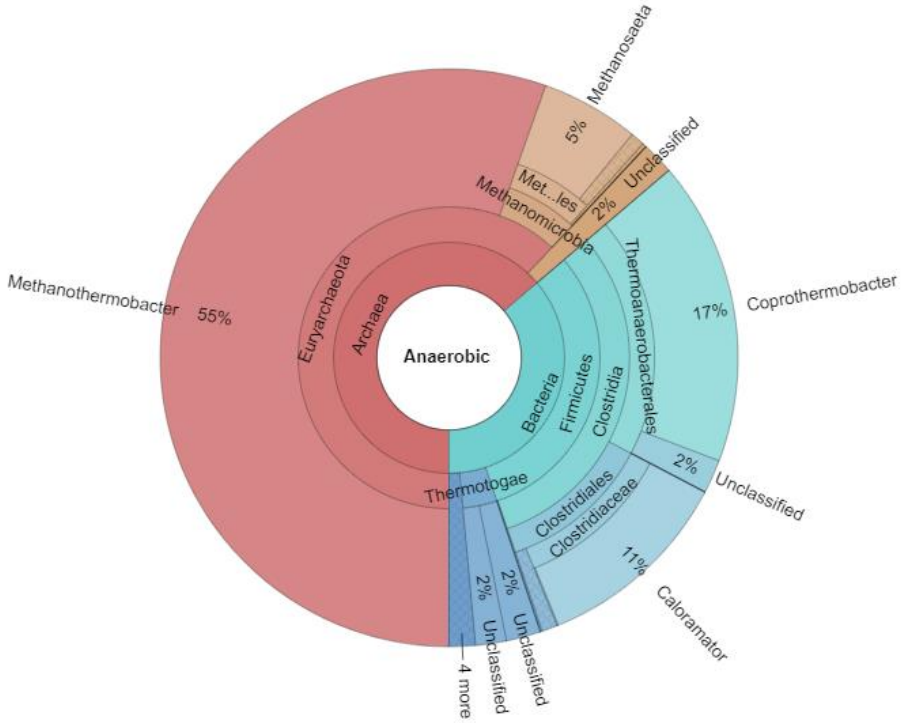

Figure 29: Relative abundance of the microorganisms given by the 16S amplicon sequencing of the PCL incubation performed under anaerobic conditions, represented by a krona plot, after removing the contribution of the sequences that received no annotation. Bacteria (in blue) account for 34 % of the community, and Archaea (in reddish) account for only 64 % of the community.

In the anaerobic assays, *Archaea* are the predominant domain of the community, although methanogenesis results from sequential metabolic reactions between fermentative *Bacteria* and methanogenic *Archaea* (S. Kato *et al.*, 2008). In this domain, all the microorganisms with a higher relative abundance (*Methanosaeta, Coprothermobacter* and *Methanothermobacter*) were reported in PCL biodegradation studies, except for *Caloramator* which was only described as participating in the biodegradation of plant biomass (Ahlert *et al.*, 2016; Hatmaker *et al.*, 2019).

The predominant microorganism in the anaerobic sample was *Methanothermobacter* sp., a methanogenic prokaryote that has an abundance of 55 % in the sample. As stated previously, this microorganism is a thermophilic hydrogenotrophic methanogen, that is highly studied in thermophilic anaerobic digesters. Hydrogen is its' primary energy source (S. Kato *et al.*, 2008) that it uses for methane production (Liczbiński *et al.*, 2022).

Methanosaeta sp. accounts for about 5 % of the prokaryotes in the anaerobic sample. This *archaea* is also a methanogen with acetoclastic activity and CO_2-reducing methanogenesis (Carr *et al.*, 2017). However, in the literature, it appears both in studies conducted in thermophilic and mesophilic conditions and even in different environments. One study reported its presence in deep-sea marine sediment collected from Antarctica (Carr *et al.*, 2017), another in a treatment system for wastewater with a high organic load from coffee processing (Suárez *et al.*, 2018) and another in a microbial community of a petroleum reservoir (Kobayashi *et al.*, 2012). Because it only has acetoclastic and CO_2-reducing activity, it is not reported as a PCL biodegrader, however, it has been reported in a PCL biodegradation study, in mesophilic conditions (Yagi *et al.*, 2014).

In the Bacteria domain, *Coprothermobacter* sp. is the most abundant (17 %), followed by *Caloramator sp*. (11 %).

Coprothermobacter sp. was also found in the aerobic sample, and the literature reports its presence in anaerobic digesters, in thermophilic conditions, like sewage sludge, slaughterhouse waste, and cattle manure treatment facilities, among others (Liczbiński *et al.*, 2022). It was reported an increase of hydrolysis in the digesters with this bacterium because it is known that it promotes an association with methanogens, by producing hydrogen (Liczbiński *et al.*, 2022) and simplifying interspecies hydrogen transfer (Jin *et al.*, 2022). This molecule is used by methanogens, like *Methanothermobacter,* as an energy source (Liczbiński *et al.*, 2022). This association between *Methanothermobacter* and *Coprothermobacter* has been reported before (Sasaki *et al.*, 2011) where it was stated an increase in methane production, in cell number, a decrease in protein content (which is *Coprothermobacter* main substrate) and lower concentration of hydrogen (meaning the *Methanothermobacter* consumed it for methane production) in the co-culture with both microorganisms than in the mono-culture with *Coprothermobacter* (Sasaki *et al.*, 2011). This association was also observed in a study of the biodegradation of bioplastics, where one of the polymers studied was PCL (Jin *et al.*, 2022). It was stated that *Coprothermobacter* had an involvement in the fermentation and hydrolysis of PCL, in thermophilic conditions, and that its abundance and efficiency were highly correlated with the presence of *Methanothermobacter* (Jin *et al.*, 2022). This association hints at the fact that not all the most abundant microorganisms reported have a direct influence on PCL's biodegradation. Some can only be consuming the by-product of the ones that attack PCL, which seems to be the case of *Methanothermobacter* regarding *Coprothermobacter*.

Caloramator is a genus of rod-shaped, strictly anaerobic thermophilic bacteria, that have been isolated from different thermal biotopes, and even methanogenic sludge (Hatmaker *et al.*, 2019). In the literature, this microorganism does not appear to be related to PCL biodegradation, only to the degradation of plant biomass (Ahlert *et al.*, 2016; Hatmaker *et al.*, 2019).

At last, the results from the sequencing of the microbial community of the inoculum are shown in (Appendix 4, Figure A4.5). The results show that from the 72 % of *Bacteria*, *Bacillus sp*. is the most predominant (27 %), followed by a microorganism in the *Actinobacteria* genus (19 %), another in the *Thermotogae* genus (12 %) and finally another in the *Thermoanaerobacterales* (10 %). *Bacillus* is a genus commonly found in landfills, especially in soil (Szulc *et al.*, 2022), and *Actinobacteria* are a phylum of gram-negative bacteria, that are present in aquatic and terrestrial environments. They produce some mycelium, like fungi, and can reproduce by sporulation. Most microorganisms in this phylum are aerobic and mesophilic, but there are some exceptions in terms of anaerobic and thermophilic microorganisms (Barka *et al.*, 2016). In terms of their presence in landfills, studies have been conducted and found a higher abundance of the phylum in soil than in the leachate (Szulc *et al.*, 2022), existing in the leachate, nevertheless (Remmas *et al.*, 2017). *Thermotogae* phylum compromises anaerobic thermophilic and mesophilic bacteria, which are gram-negative (Bhandari & Gupta, 2014), and are found in leachate, thriving in more thermophilic conditions (Zhao *et al.*, 2021). *Thermoanaerobacterales* genus belongs to the *Clostridia class*. The *Clostridia* class compromises anaerobic and aerotolerant microorganisms, present in landfill soil (Gu *et al.*, 2022) and leachate (Burrell *et al.*, 2004).

In terms of *Archaea*, the taxonomic information retrieved from the samples was not enough to classify the prokaryotes more than their domain. They still, however, account for a considerable abundance in the sample. This percentage shows that, when in anaerobic conditions, the microbial community from the leachate, tends to increase in the number of *Archaea* prokaryotes, and when in aerobic conditions, this abundance decreases significantly.

From the data analysis performed, there were microorganisms which were not detected in the inoculum but were identified with very high abundances in the aerobic and anaerobic assays. For the aerobic sample, these microorganisms included *Coprothermobacter sp.* (with a relative abundance of 65 %), *Chlatococcus sp.* (with a relative abundance of 3,12 %) and organisms from the *Deltaproteobacteria class* (with a relative abundance of 7,12 %). In the anaerobic sample, the microorganisms were *Methanothermobacter sp.* (with a very high relative abundance of 55,43%),

Methanosaeta sp. (with a relative abundance of 5,50 %), *Caloramator sp.* (with a relative abundance of 11,13 %) and *Coprothermobacter sp.* (with a relative abundance of 17,04 %).

6.2- Experiments with marine sediment

VSS determination with marine sediment was done separately for the aerobic experiment and for the two anaerobic incubations. In the aerobic incubation, 4,40 ± 0,0001 g (Appendix 5, Table A5.1,) of sediment was dispersed, and for the anaerobic experiments 4,45 g ± 0,0001 g, were placed in each vial (Appendix 5, Table A5.2) to get a VSS concentration of 3 g VSS/L.

The results for oxygen consumption, and methane and sulphide production are shown in Figure 30.

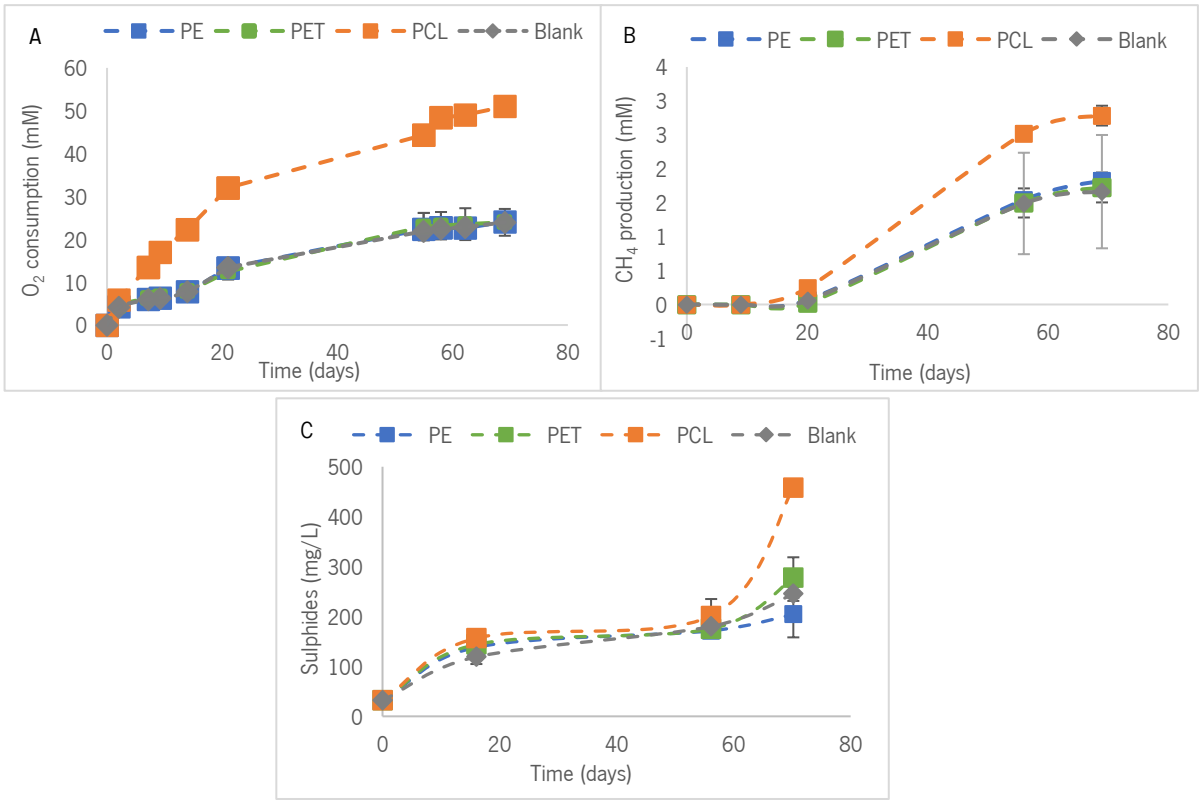

Figure 30: Curves from the experiments with marine sediment as inoculum, for 70 days of incubation; A) Average value of oxygen consumption (mM) of the samples with PE, PET, PCL and blank of the aerobic experiment; B) Average values of methane production (mM) of the samples with PE, PET, PCL and blank from the anaerobic methanogenic experiment; C) Average values of sulphide production (mg/L) of the samples with PE, PET, PCL and blank of the anaerobic sulphuric experiment.

No methane production was observed for the sulphate-reducing experiment. Biodegradation in these conditions works similarly to anaerobic methanogenic biodegradability, but sulphate works as the electron acceptor, producing hydrogen sulphide, carbon dioxide and water as final products (Eubeler,

2010). The last value of oxygen consumption and methane production observed were used to calculate the percentage of biodegradation of the plastics in the aerobic (Table 7) and anaerobic methanogenic assays (Table 8), respectively.

Table 7: Theoretical oxygen consumption expected, measured oxygen without the contribution of the blank assay, and percentage of biodegradation of the tested plastics- PE, PET and PCL for the aerobic experiment with marine sediment

Polymer/carbon and energy source	Theoretical O_2 (mmol) expected from complete biodegradation of the added carbon source	O_2 consumed (without the contribution of the oxygen measured in the blank assay) (mmol)	Biodegradation (%)
PE powder	6,69	0,09	1,33 ± 0,37
PET powder	3,26	0,08	2,87 ± 5,79
PCL Powder	4,11	1,98	48,09 ± 2,75

In the aerobic assay, results show that PCL had an oxygen consumption lower than the blank until the 20th day of incubation, which may indicate that microorganisms were still adapting their organism to the new substrate. After that, until the 60th day, oxygen consumption was the same as the blank, and only after that point did the production start to be higher (Figure 30), indicating that only after that point, real biodegradation of the polymer started to occur. With PE and PET, until the 70th day of incubation, oxygen consumption was the same as the blank assay (Figure 30). As shown by the oxygen consumption profile, PCL shows a high percentage of biodegradation (Table 7), raising some good prospects for the biodegradation of biodegradable plastics in estuary environments. In the literature, different biodegradation percentages are present for PCL in marine environments. This is mostly because tests are performed in different environments, from artificial seawater to coastal sediment (in laboratory and sea) and static river sediment, which varies greatly in their microbial community. Even coastal sediments from different seas present a varying microbial community (G. X. Wang *et al.*, 2021). G. X. Wang *et al.* (2021) reported a 32 % weight loss of PCL in seawater after 52 weeks, while at the same time verifying a 14 % weight loss in static river water, and 12 % in laboratory static water (G. X. Wang *et al.*, 2021). Narancic *et al.* (2018) tested the biodegradation of PCL under an aerobic marine environment and anaerobic aquatic digestion. In the aerobic experiment, they observed about 40 % biodegradation of PCL after 56 days (Narancic *et al.*, 2018), showing higher biodegradation in less time than the one presented in this work, but allowing to conclude that PCL shows good biodegradation results in marine environments (Narancic *et al.*, 2018; Suzuki *et al.*, 2021).

The anaerobic results with marine sediment were not as satisfactory as the ones observed for the aerobic experiment. PCL's lag phase lasted until the 20th day of incubation, with a high production of methane after, that lasted until the 55th (Figure 30). PE and PET showed no differences in methane production compared to the blank, indicating that this production was due to the consumption of the possible substrates in the sediment, and not the polymer's biodegradation. In terms of percentages of biodegradation, this mimics methane production, showing very low percentages for the three polymers (Table 8), especially compared to the results of the aerobic experiment. Even PCL, which seemed to present better methane production, only shows around 4 % of biodegradation. One hypothesis that could explain these results, especially because of the long lag phase compared to the aerobic experiment, was that estuary microbial communities do not have many methanogenic microorganisms, since estuary zones are more in contact with air, and only occasionally are submerged under water. Additionally, since methanogens do not seem to thrive well under salinity conditions (Riffat & Krongthamchat, 2006; S. Wang *et al.*, 2017), maybe the salt concentration in the medium may be inhibiting the microorganism's activity. Nevertheless, the behaviour could change with extended incubation times. In the literature, it appears that poor anaerobic biodegradation of polymers with marine microbial communities is frequent. Narancic *et al.* (2018) observed only 2,1 % of biodegradation of PCL in anaerobic aquatic digestion, after 56 days (Narancic *et al.*, 2018).

Table 8: Theoretical methane production expected, measured methane production without the contribution of the blank, and percentage of biodegradation for the assays with PE, PET and PCL, from the methanogenic experiments with marine sediment

Polymer/carbon and energy source	Theoretical CH_4 (mmol) expected from complete biodegradation of the added carbon source	CH_4 produced (without the contribution of the oxygen measured in the blank assay) (mmol)	Biodegradation (%)
PE powder	3,35	0,011	0,34 ± 0,04
PET powder	1,63	0,004	0,26 ± 0,77
PCL powder	2,06	0,078	3,81 ± 0,40

For the sulphide production, on the 18th day of incubation, all the polymers seemed to have started to produce more sulphide than the blank, but on the last measure, only PCL showed a higher sulphide concentration than the blank (Figure 30). This means that the microorganisms needed about 58 days to adapt their metabolism for the degradation of the polymer, as only after that did the sulphide production increase drastically. Apparently, no big differences can be observed for the production of sulphide in the PE and PET assays, until the 70th of incubation, and PCL shows a difference of

212,67 mg/L of sulphate reduction compared to the blank, indicating PCL biodegradation under sulphate-reducing conditions. The sulphide production means that sulphates are being used as final electron acceptors in the biodegradation chain, indicating biodegradation of the plastics, particularly PCL. Sulphate reducing microorganisms have been reported to be efficient in the biodegradation of petroleum hydrocarbons (Coates, Anderson, *et al.*, 1996; Machel, 2001; Y. Wei *et al.*, 2018), like n-alkanes and polycyclic aromatic hydrocarbons (PAHs) (Alexandre, 2015; K. Zhang *et al.*, 2019). Zhang *et al.* (2019) observed the fastest biodegradation of n-alkanes and PAHs in sulphate-reducing conditions, reporting a half-life of 49,51 and 58,74 days, respectively. Although no reports were found on the sulphate-reducing biodegradation of PCL, this ability of sulphate-reducing bacteria to biodegrade petroleum hydrocarbons hints at the ability to biodegrade this polymer. Additionally, it has been reported that some methanogens can be outcompeted by sulphate-reducing bacteria when competitive substrates are used and that in tidal-flat sediment, where methanogenic activity only occurs after sulphate depletion (Mckew *et al.*, 2013). This explains why methanogenic activity was not observed in the experiments described. However, Mckew *et al.* (2013) reported the coexistence of methanogenic and sulphate-reducing activity in the intertidal sediments, which may mean that methane production can still be observed in the current experiment further ahead.

6.3- Final remarks

As a final note, with this work, it was possible to conclude that marine sediment has presented promising results for aerobic mesophilic and sulphate-reducing biodegradation, while anaerobic biodegradation did not present good results so far. Reports of polymer biodegradation on methanogenic conditions with marine sediment also do not show good results (Narancic *et al.*, 2018), and literature on the biodegradation in sulphate-reducing conditions is scarce.

In terms of the biodegradation of the polymers, according to the current knowledge, PE seems to have a better percentage of biodegradation when in contact with specific microbial consortiums, or single microorganisms (R. Qi *et al.*, 2021; Ru *et al.*, 2020; Skariyachan *et al.*, 2017), like *Pseudomonas* and *Bacillus* (Matjasic *et al.*, 2020). Pre-treatments like UV-radiation, chemical oxidizing agents, and thermo-oxidation, seem to have a big impact on polymer biodegradation (Ru *et al.*, 2020), and thermophilic conditions also seemed to result in higher biodegradation for PE (Skariyachan *et al.*, 2017). However, most studies under simulated conditions with naturally occurring microbial consortiums do not seem to result in high biodegradation rates for these non-biodegradable polymers (Hermanová *et al.*,

2015; Wataru, 2015). This was observed in the current work, where neither of the tested experiments showed biodegradation rates higher than 5 %. This indicates that the collected leachate under thermophilic anaerobic and aerobic conditions is not an appropriate biomass source for PE biodegradation, with the same being observed with marine sediment. However, long periods of incubation in these natural conditions seem to benefit biodegradation (Matjasic *et al.*, 2020). The same was observed for PET, where no significant biodegradation was observed for the incubations performed. In the literature, higher biodegradation percentages have been observed when in contact with specific microorganisms (Amobonye *et al.*, 2021; Danso *et al.*, 2019; W. Zeng *et al.*, 2022), and with higher incubations temperatures (Atanasova, Stoitsova, *et al.*, 2021; W. Zeng *et al.*, 2022).

PCL biodegradation is extremely influenced by temperature, due to the polymer melting temperature (60℃), and composting conditions seem to be the most efficient for its degradation (Nevoralová *et al.*, 2020), reaching values of 70% only after 48 hours (Atanasova, Stoitsova, *et al.*, 2021). Thermophilic anaerobic conditions also seem to benefit the polymer biodegradation (Šmejkalová *et al.*, 2016), with high results also observed in aerobic conditions (Massardier-Nageotte *et al.*, 2006; Nevoralová *et al.*, 2020). Nevertheless, results seem to vary greatly between different experiments, and even experiments with the same conditions (Massardier-Nageotte *et al.*, 2006; Xochitl *et al.*, 2021). This work showed that leachate as inoculum in thermophilic anaerobic and aerobic conditions appears to be adequate for biodegradation studies with PCL.

7. Conclusions and future perspectives

Leachate and marine sediment have the potential to biodegrade PCL. In this work, it was shown that PCL can be biodegraded in anaerobic and aerobic thermophilic conditions, in about 50 days, by a leachate inoculum, but also by a marine sediment in aerobic and sulphate-reducing conditions. However, the more recalcitrant polymer, PE, and PET, apparently were not biodegraded, although in the first anaerobic experiment with leachate, methane production seems to indicate that some biodegradation happened. Further tests would be needed to take that conclusion with certainty. Taxonomic analysis of the PCL samples from the aerobic and anaerobic assays showed that *Coprothermobacter* and *Methanothermobacter* had a higher impact on PCL, in both assays. They were previously described as syntrophic microorganisms that collaborated with each other, with the ability to biodegrade PCL.

As future perspectives, more and longer assays need to be performed to better evaluate the biodegradation of the polymers, especially when it comes to non-biodegradable plastics. First, the period of incubation should be prolonged, adding some agitation to the vials, to allow the mixing of the films/powders to the medium. Then, it would be interesting to test different pre-treatment (like UV-treatment, thermos-oxidation) and additives to the polymers, and even different temperature conditions during incubation. Additionally, it would be necessary to better evaluate the biodegradation by studying the films' topography, using other techniques like AFM or measure of contact angle. At last, a more extensive study of the microbial community, especially to understand their interaction with polymers, and the enzymes and metabolic pathways that may be involved in biodegradation. For this, metagenomics and other omics studies could be used to understand the expression of genes during biodegradation of plastics.

8. References

A., G. K., K., A., M., H., K., S., & G., D. (2020). Review on plastic wastes in marine environment – Biodegradation and biotechnological solutions. *Marine Pollution Bulletin*, *150*(May 2019), 110733. https://doi.org/10.1016/j.marpolbul.2019.110733

Adedotun, A. A., & Oluyode, T.-F.-. (2005). Biodegradation of crude petroleum and petroleum products by fungi isolated from two oil seeds (melon and soybean). *Journal of Environmental Biology*, *26*(1), 37–42.

Ahlert, S., Zimmermann, R., Ebling, J., & König, H. (2016). Analysis of propionate-degrading consortia from agricultural biogas plants. *MicrobiologyOpen*, *5*(6), 1027–1037. https://doi.org/10.1002/mbo3.386

Ahmed, T., Shahid, M., Azeem, F., Rasul, I., Shah, A. A., Noman, M., Hameed, A., Manzoor, N., Manzoor, I., & Muhammad, S. (2018). Biodegradation of plastics: current scenario and future prospects for environmental safety. In *Environmental Science and Pollution Research* (Vol. 25, Issue 8, pp. 7287–7298). Springer Verlag. https://doi.org/10.1007/s11356-018-1234-9

Al-mutairi, N. H., & Mousa, Z. O. (2021). Some Methodes for Measurements of Polymer Degradation : A Review. *Journal of University of Babylon for Engineering Sciences*, *29*(2), 99–114.

Alexandre, C. I. N. (2015). *Biodegradation treatment of petrochemical wastewaters*. Universidade de Lisboa.

Ali, S. S., Elsamahy, T., Al-Tohamy, R., Zhu, D., Mahmoud, Y. A. G., Koutra, E., Metwally, M. A., Kornaros, M., & Sun, J. (2021). Plastic wastes biodegradation: Mechanisms, challenges and future prospects. *Science of the Total Environment*, *780*, 146590. https://doi.org/10.1016/j.scitotenv.2021.146590

Alshehrei, F. (2017). Biodegradation of Synthetic and Natural Plastic by Microorganisms. *Journal of Applied & Environmental Microbiology*, *5*(1), 8–19. https://doi.org/10.12691/jaem-5-1-2

Amobonye, A., Bhagwat, P., Singh, S., & Pillai, S. (2021). Plastic biodegradation: Frontline microbes and their enzymes. *Science of the Total Environment*, *759*, 143536. https://doi.org/10.1016/j.scitotenv.2020.143536

Antipova, T. V, Zhelifona, V. P., Zaitsev, K. V., Nedorezova, P. M., Aladyshev, A. M., Klyamkina, A. N., Kostyuk, S. V., Danilogorskaya, A. A., & Kozlovsky, A. G. (2018). Biodegradation of Poly-ε-caprolactones and Poly-l-lactides by Fungi. *Journal of Polymers and the Environment*, *26*(12), 4350–4359. https://doi.org/10.1007/s10924-018-1307-3

Arutchelvi, J., Sudhakar, M., Arkatkar, A., Doble, M., Bhaduri, S., & Uppara, P. V. (2008). Biodegradation of polyethylene and polypropylene. *Indian Journal of Biotechnology*, *7*(1), 9–22.

Atanasova, N., Paunova-krasteva, T., Stoitsova, S., Kambourova, M., Shapagin, A., Matveev, V., Provotorova, E., Elcheninov, A., Sokolov, T., & Bonch-osmolovskaya, E. (2021). Plastic Degradation by Extremophilic Microbial Communities Isolated from Bulgaria and Russia. *Ecologia Balkanica*, *13*(2), 211–222.

Atanasova, N., Stoitsova, S., Paunova-krasteva, T., & Kambourova, M. (2021). Plastic degradation by extremophilic bacteria. *International Journal of Molecular Sciences*, *22*(11).

https://doi.org/10.3390/ijms22115610

Attallah, O. A., Mojicevic, M., Garcia, E. L., Azeem, M., Chen, Y., Asmawi, S., & Fournet, M. B. (2021). Macro and Micro Routes to High Performance Bioplastics : Bioplastic Biodegradability and Mechanical and Barrier Properties. *Polymer Testing*. https://doi.org/https://doi.org/10.3390/polym13132155

Azimi, B., Nourpanah, P., Rabiee, M., & Arbab, S. (2014). Poly (ε-caprolactone) fiber: An overview. *Journal of Engineered Fibers and Fabrics*, *9*(3), 74–90. https://doi.org/10.1177/155892501400900309

Baptista Neto, J. A., Gaylarde, C., Beech, I., Bastos, A. C., da Silva Quaresma, V., & de Carvalho, D. G. (2019). Microplastics and attached microorganisms in sediments of the Vitória bay estuarine system in SE Brazil. *Ocean and Coastal Management*, *169*(September 2018), 247–253. https://doi.org/10.1016/j.ocecoaman.2018.12.030

Barka, E. A., Vatsa, P., Sanchez, L., Gaveau-Vaillant, N., Jacquard, C., Meier-Kolthoff, J. P., Klenk, H.-P., Clément, C., Ouhdouch, Y., & van Wezel, G. P. (2016). Taxonomy, Physiology, and Natural Products of *Actinobacteria*. *Microbiology and Molecular Biology Reviews*, *80*(4). https://doi.org/10.1128/mmbr.00044-16

Bátori, V., Åkesson, D., Zamani, A., Taherzadeh, M. J., & Sárvári Horváth, I. (2018). Anaerobic degradation of bioplastics: A review. *Waste Management*, *80*, 406–413. https://doi.org/10.1016/j.wasman.2018.09.040

Bhandari, V., & Gupta, R. S. (2014). The Phylum *Thermotogae*. In *The Prokaryotes: Other Major Lineages of Bacteria and The Archaea* (pp. 1–1028). https://doi.org/10.1007/978-3-642-38954-2

Blackwell, C. J., Haernvall, K., Guebitz, G. M., Groombridge, M., Gonzales, D., & Khosravi, E. (2018). Enzymatic degradation of star poly(ε-caprolactone) with different central units. *Polymers*, *10*(11), 1–15. https://doi.org/10.3390/polym10111266

Borghesi, D. C., Molina, M. F., Guerra, M. A., & Campos, M. G. N. (2016). Biodegradation study of a novel poly-caprolactone-coffee husk composite film. *Materials Research*, *19*(4), 752–758. https://doi.org/10.1590/1980-5373-MR-2015-0586

Botha, A., & Botes, A. (2014). *Mucor*. In *Encyclopedia of Food Microbiology* (Vol. 2, pp. 834–840). https://doi.org/10.1016/B978-0-12-384730-0.00228-7

Boughner, L. A., & Singh, P. (2016). Microbial Ecology: Where are we now? *Postdoc Journal*, *4*(11), 3–17. https://doi.org/10.14304/surya.jpr.v4n11.2

Burrell, P. C., O'Sullivan, C., Song, H., Clarke, W. P., & Blackall, L. L. (2004). Identification, Detection, and Spatial Resolution of *Clostridium* Populations Responsible for Cellulose Degradation in a Methanogenic Landfill Leachate Bioreactor. *Applied and Environmental Microbiology*, *70*(4), 2414–2419. https://doi.org/10.1128/AEM.70.4.2414-2419.2004

Campos, A. De, Marconato, J. C., & Martins-franchetti, S. M. (2011). Biodegradation of Blend Films PVA / PVC , PVA / PCL in Soil and Soil with Landfill Leachate. *Brazilian Archives of Biology and Technology*, *54*(December), 1367–1378. https://doi.org/https://doi.org/10.1590/S1516-89132011000600024

Canopoli, L., Coulon, F., & Wagland, S. T. (2020). Degradation of excavated polyethylene and polypropylene waste from landfill. *Science of the Total Environment*, *698*.

https://doi.org/10.1016/j.scitotenv.2019.134125

Canopoli, L., Fidalgo, B., Coulon, F., & Wagland, S. T. (2018). Physico-chemical properties of excavated plastic from landfill mining and current recycling routes. *Waste Management*, *76*, 55–67. https://doi.org/10.1016/j.wasman.2018.03.043

Caporaso, J. G., Lauber, C. L., Walters, W. A., Berg-Lyons, D., Lozupone, C. A., Turnbaugh, P. J., Fierer, N., & Knight, R. (2011). Global patterns of 16S rRNA diversity at a depth of millions of sequences per sample. *Proceedings of the National Academy of Sciences of the United States of America*, *108*(1), 4516–4522. https://doi.org/10.1073/pnas.1000080107

Carr, S. A., Schubotz, F., Dunbar, R. B., Mills, C. T., Dias, R., Summons, R. E., & Mandernack, K. W. (2017). Acetoclastic *Methanosaeta* are dominant methanogens in organic-rich Antarctic marine sediments. *Nature Publishing Group*, *12*(2), 330–342. https://doi.org/10.1038/ismej.2017.150

Castro-aguirre, E., Auras, R., Selke, S., Rubino, M., & Marsh, T. (2017). Insights on the aerobic biodegradation of polymers by analysis of evolved carbon dioxide in simulated composting conditions. *Polymer Degradation and Stability*, *137*, 251–271. https://doi.org/10.1016/j.polymdegradstab.2017.01.017

Chamas, A., Moon, H., Zheng, J., Qiu, Y., Tabassum, T., Jang, J. H., Abu-Omar, M., Scott, S. L., & Suh, S. (2020). Degradation Rates of Plastics in the Environment. *ACS Sustainable Chemistry and Engineering*, *8*(9), 3494–3511. https://doi.org/10.1021/acssuschemeng.9b06635

Chen, C. C., Dai, L., Ma, L., & Guo, R. T. (2020). Enzymatic degradation of plant biomass and synthetic polymers. *Nature Reviews Chemistry*, *4*(3), 114–126. https://doi.org/10.1038/s41570-020-0163-6

Cho, H. S., Moon, H. S., Kim, M., Nam, K., & Kim, J. Y. (2011). Biodegradability and biodegradation rate of poly(caprolactone)-starch blend and poly(butylene succinate) biodegradable polymer under aerobic and anaerobic environment. *Waste Management*, *31*(3), 475–480. https://doi.org/10.1016/j.wasman.2010.10.029

Choe, S., Kim, Y., Won, Y., & Myung, J. (2021). Bridging Three Gaps in Biodegradable Plastics : Misconceptions and Truths About Biodegradation. *Green and Sustainable Chemistry*, *9*(May), 1–8. https://doi.org/10.3389/fchem.2021.671750

Coates, J. D., Anderson, R. T., Woodward, J. C., Phillips, E. J. P., & Lovley, D. R. (1996). Anaerobic hydrocarbon degradation in petroleum-contaminated harbor sediments under sulfate-reducing and artificially imposed iron-reducing conditions. *Environmental Science and Technology*, *30*(9), 2784–2789. https://doi.org/10.1021/es9600441

Coates, J. D., Coughlan, M. F., & Colleran, E. (1996). Simple method for the measurement of the hydrogenotrophic methanogenic activity of anaerobic sludges. *Journal of Microbiological Methods*, *26*(3), 237–246. https://doi.org/10.1016/0167-7012(96)00915-3

Colleran, E., Concannon F., Golden T., Geoghegan F., Crumlish B., Killilea E., Henry M., Coates J.; (1992) Use of Methanogenic Activity Tests to Characterize Anaerobic Sludges, Screen for Anaerobic Biodegradability and Determine Toxicity Thresholds against Individual Anaerobic Trophic Groups and Species. *Water Science Technology*. 25 (7): 31–40. https://doi.org/10.2166/wst.1992.0136

Cossu, R., & Stegman, R. (2018). Physical Landfill Barriers: Principals and Engineering. In *Solid Waste Landfilling* (pp. 271–287). Elsevier Inc. https://doi.org/10.1016/b978-0-12-407721-8.00015-2

Danso, D., Chow, J., & Streit, W. R. (2019). Plastics : Environmental and Biotechnological Perspectives on Microbial Degradation. *Applied and Environmental Microbiology*, *July*, 1–14. https://doi.org/. https://doi .org/10.1128/AEM.01095-19

De Campos, A., Marconato, J. C., & Martins-Franchetti, S. M. (2012). The influence of soil and landfill leachate microorganisms in the degradation of PVC/PCL films cast from DMF. *Polimeros*, *22*(3), 220–227. https://doi.org/10.1590/S0104-14282012005000029

Delacuvellerie, A., Cyriaque, V., Gobert, S., Benali, S., & Wattiez, R. (2019). The plastisphere in marine ecosystem hosts potential specific microbial degraders including *Alcanivorax borkumensis* as a key player for the low-density polyethylene degradation. *Journal of Hazardous Materials*, *380*, 120899. https://doi.org/10.1016/j.jhazmat.2019.120899

DHEC-South Carolina Department of Health and Environmental Control. How Landfills Work. Retrieved from https://scdhec.gov/environment/land-and-waste-landfills/how-landfills-work. Visited in 21/06/2022

Din, M. I., Ghaffar, T., Najeeb, J., Hussain, Z., Khalid, R., & Zahid, H. (2020). Potential perspectives of biodegradable plastics for food packaging application-review of properties and recent developments. *Food Additives and Contaminants - Part A*, *37*(4), 665–680. https://doi.org/10.1080/19440049.2020.1718219

El-Fadel, M., & Khoury, R. (2000). Modeling settlement in MSW landfills: A critical review. *Critical Reviews in Environmental Science and Technology*, *30*(3), 327–361. https://doi.org/10.1080/10643380091184200

Emadian, S. M., Onay, T. T., & Demirel, B. (2017). Biodegradation of bioplastics in natural environments. *Waste Management*, *59*, 526–536. https://doi.org/10.1016/j.wasman.2016.10.006

Esmaeili, A., Pourbabaee, A. A., Alikhani, H. A., Shabani, F., & Esmaeili, E. (2013). Biodegradation of Low-Density Polyethylene (LDPE) by Mixed Culture of *Lysinibacillus xylanilyticus* and *Aspergillus niger* in Soil. *PLoS ONE*, *8*(9). https://doi.org/10.1371/journal.pone.0071720

Eubeler, V. von J. (2010). Biodegradation of Synthetic Polymers in the Aquatic Environment. In *The Chemical Company* (Issue April). Universitat Bremen.

Federle, T. W., Barlaz, M. A., Pettigrew, C. A., Kerr, K. M., Kemper, J. J., Nuck, B. A., & Schechtman, L. A. (2002). Anaerobic biodegradation of aliphatic polyesters: Poly(3-hydroxybutyrate-co-3-hydroxyoctanoate) and poly(ε-caprolactone). *Biomacromolecules*, *3*(4), 813–822. https://doi.org/10.1021/bm025520w

Fernandes, A., Pacheco, M. J., Ciríaco, L., & Lopes, A. (2015). Review on the electrochemical processes for the treatment of sanitary landfill leachates: Present and future. *Applied Catalysis B: Environmental*, *176–177*, 183–200. https://doi.org/10.1016/j.apcatb.2015.03.052

Fernandes, M., Salvador, A., Alves, M. M., & Vicente, A. A. (2020). Factors affecting polyhydroxyalkanoates biodegradation in soil. *Polymer Degradation and Stability*, *182*, 109408. https://doi.org/10.1016/j.polymdegradstab.2020.109408

Flury, M., & Narayan, R. (2021). Biodegradable plastic as an integral part of the solution to plastic waste pollution of the environment. *Green and Sustainable Chemistry*, *30*, 100490. https://doi.org/10.1016/j.cogsc.2021.100490

Folino, A., Karageorgiou, A., Calabrò, P. S., & Komilis, D. (2020). Biodegradation of wasted

bioplastics in natural and industrial environments: A review. *Sustainability (Switzerland)*, *12*(15), 1–37. https://doi.org/10.3390/su12156030

García-depraect, O., Lebrero, R., Rodriguez-vega, S., Bordel, S., Tim, B., Santos-beneit, F., Martínez-mendoza, L. J., & Arag, R. (2022). Biodegradation of bioplastics under aerobic and anaerobic aqueous conditions : Kinetics , carbon fate and particle size effect. *Bioresources and Bioprocessing*, *344*. https://doi.org/10.1016/j.biortech.2021.126265

Gewert, B., Plassmann, M. M., & Macleod, M. (2015). Pathways for degradation of plastic polymers floating in the marine environment. *Environmental Science and Processes and Impacts*, *17*, 1513–1521. https://doi.org/10.1039/c5em00207a

Ghatge, S., Yang, Y., Ahn, J. H., & Hur, H. G. (2020). Biodegradation of polyethylene : a brief review. *Applied Biological Chemistry*, *63*(27). https://doi.org/10.1186/s13765-020-00511-3

Ghosh, S., Qureshi, A., & Purohit, H. J. (2019). Microbial degradation of plastics: Biofilms and degradation pathways. *Contaminants in Agriculture and Environment: Health Risks and Remediation*, *June*, 184–199. https://doi.org/10.26832/aesa-2019-cae-0153-014

Glaser, J. A. (2019). Biological Degradation of Polymers in the Environment. In *Plastics in the Environment* (1st ed., Vol. 32, Issue May 13th, pp. 137–144). IntechOpen. https://doi.org/DOI: 10.5772/intechopen.85124

Gomes, E., Souza, A. R. de, Orjuela, G. L., Silva, R. da, Oliveira, T. B. de, & Rodrigues, A. (2016). Applications and Benefits of Thermophilic Microorganisms and ther Enzymes for Industrial Biotecnology. *Springer International Publishing Switzerland*, *21*, 59–96. https://doi.org/10.1007/978-3-319-27951-0

Gómez, E. F., & Michel, F. C. (2013). Biodegradability of conventional and bio-based plastics and natural fiber composites during composting, anaerobic digestion and long-term soil incubation. *Polymer Degradation and Stability*, *98*(12), 2583–2591. https://doi.org/10.1016/j.polymdegradstab.2013.09.018

Gowda, V., & Shivakumar, U. S. S. (2015). Poly (-b-hydroxybutyrate) (PHB) depolymerase PHAZ Pen from *Penicillium expansum* : purification , characterization and kinetic studies. *3 Biotech*, *5*, 901–909. https://doi.org/10.1007/s13205-015-0287-4

Grima, S., Bellon-Maurel, V., Feuilloley, P., & Silvestre, F. (2000). Aerobic biodegradation of polymers in solid-state conditions: A review of environmental and physicochemical parameter settings in laboratory simulations. *Journal of Polymers and the Environment*, *8*(4), 183–195. https://doi.org/10.1023/A:1015297727244

Gu, Z., Feng, K., Li, Y., & Li, Q. (2022). Microbial characteristics of the leachate contaminated soil of an informal landfill site. *Chemosphere*, *287*(P2), 132155. https://doi.org/10.1016/j.chemosphere.2021.132155

Hatmaker, E. A., Kingeman, D. M., Martin, R. K., Guss, A. M., & Elkins, J. G. (2019). Complete Genome Sequence of Caloramator sp. Strain E03, a Novel Ethanologenic, Thermophilic, Obligated Anaerobic Bacterium. *Microbiology Resource Annoucements*, *8*(32), 16–18. https://doi.org/https://doi.org/10.1128/MRA.00708-19

Havstad, M. R. (2020). Biodegradable Plastics. In *Plastic Waste and Recycling* (Vol. 68, Issue 9, pp. 97–129). https://doi.org/https://doi.org/10.1016/B978-0-12-817880-5.00005-0

Hermanová, S., Smejkalov, P., Merna, J., & Zarevúcka, M. (2015). Biodegradation of waste PET based copolyesters in thermophilic anaerobic sludge. *Polymer Degradation and Stability*, *111*, 176–184. https://doi.org/10.1016/j.polymdegradstab.2014.11.007

Hosni, A. S. Al. (2019). *Biodegradation of Polycaprolactone Bioplastic in comparison with other Bioplastics and its impact on Biota.* The University of Manchester.

Hou, L., Xi, J., Liu, J., Wang, P., Xu, T., Liu, T., Qu, W., & Lin, Y. B. (2022). Biodegradability of polyethylene mulching film by two *Pseudomonas* bacteria and their potential degradation mechanism. *Chemosphere*, *286*(P3), 131758. https://doi.org/10.1016/j.chemosphere.2021.131758

Illumina Tecnical Support. (2013). 16S Metagenomic Sequencing Library. *Illumina.Com*, *B*, 1–28. http://support.illumina.com/content/dam/illumina-support/documents/documentation/chemistry_documentation/16s/16s-metagenomic-library-prep-guide-15044223-b.pdf

Iram, D., Riaz, R. a, & Iqbal, R. K. (2019). Usage of Potential Micro-organisms for Degradation of Plastics. *Open Journal of Environmental Biology*, *4*, 007–015. https://doi.org/10.17352/ojeb.000010

Ishigaki, T., Sugano, W., Nakanishi, A., Tateda, M., Ike, M., & Fujita, M. (2004). The degradability of biodegradable plastics in aerobic and anaerobic waste landfill model reactors. *Chemosphere*, *54*(3), 225–233. https://doi.org/10.1016/S0045-6535(03)00750-1

Iwańczuk, A., Kozłowski, M., Łukaszewicz, M., & Jabłoński, S. (2015). Anaerobic Biodegradation of Polymer Composites Filled with Natural Fibers. *Journal of Polymers and the Environment*, *23*(2), 277–282. https://doi.org/10.1007/s10924-014-0690-7

Jacquin, J., Cheng, J., Odobel, C., Pandin, C., Conan, P., Pujo-Pay, M., Barbe, V., Meistertzheim, A. L., & Ghiglione, J. F. (2019). Microbial ecotoxicology of marine plastic debris: A review on colonization and biodegradation by the "plastisphere." *Frontiers in Microbiology*, *10*(APR), 1–16. https://doi.org/10.3389/fmicb.2019.00865

Jaiswal, S., Sharma, B., & Shukla, P. (2020). Integrated approaches in microbial degradation of plastics. *Environmental Technology and Innovation*, *17*, 100567. https://doi.org/10.1016/j.eti.2019.100567

Jin, Y., Cai, F., Song, C., Liu, G., & Chen, C. (2022). Degradation of biodegradable plastics by anaerobic digestion: Morphological, micro-structural changes and microbial community dynamics. *Science of the Total Environment*, *834*(April), 155167. https://doi.org/10.1016/j.scitotenv.2022.155167

Kale, S. K., Deshmukh, A. G., Dudhare, M. S., & Patil, V. B. (2015). Microbial degradation of plastic: a review. *Journal of Biochemical Technology*, *6*(2), 952–961.

Kato, M. T., Field, J. A., & Lettinga, G. (1993). High tolerance of methanogens in granular sludge to oxygen. *Biotechnology and Bioengineering*, *42*(11), 1360–1366. https://doi.org/10.1002/bit.260421113

Kato, S., Kosaka, T., & Watanabe, K. (2008). Comparative transcriptome analysis of responses of *Methanothermobacter thermautotrophicus* to different environmental stimuli. *Environmental Microbiology*, *10*(4), 893–905. https://doi.org/10.1111/j.1462-2920.2007.01508.x

Kaushal, J., Khatri, M., & Arya, S. K. (2021). Recent insight into enzymatic degradation of

plastics prevalent in the environment : A mini - review. *Cleaner Engineering and Technology*, *2*, 100083. https://doi.org/10.1016/j.clet.2021.100083

Kayjhaii, M., & Lindford, M. R. (2020). Characterization of polymeric materials and their degradation products. *International Journal of New Chemistry*, *8*(2), 142–148. https://doi.org/10.22034/IJNC.2020.139035.1135

Keene, S., Sarao, M. S., Mcdonald, P. J., & Veltman, J. (2019). Cutaneous geotrichosis due to *Geotrichum candidum* in a burn patient. *Microbiology Society*, *1*. https://doi.org/10.1099/acmi.0.000001

Kjeldsen, A., Price, M., Lilley, C., Guzniczak, E., & Archer, I. (2019). A Review of Standards for Biodegradable Plastics. In *Industrial Biotechnology Innovation Centre*.

Kobayashi, H., Endo, K., Sakata, S., Mayumi, D., Kawaguchi, H., Ikarashi, M., Miyagawa, Y., Maeda, H., & Sato, K. (2012). Phylogenetic diversity of microbial communities associated with the crude-oil , large-insoluble-particle and formation-water components of the reservoir fluid from a non-flooded high-temperature petroleum reservoir. *Journal of Bioscience and Bioengineering*, *113*(2), 204–210. https://doi.org/10.1016/j.jbiosc.2011.09.015

Kotova, I. B., Taktarova, Y. V, Tsavkelova, E. A., Egorova, M. A., Bubnov, I. A., & Malakhova, D. V. (2021). Microbial Degradation of Plastics and Approaches to Make It More Efficient. *90*(6), 671–701. https://doi.org/10.1134/S0026261721060084

Kumar, R., Pandit, P., Kumar, D., Patel, Z., Pandya, L., Kumar, M., Joshi, C., & Joshi, M. (2021). Landfill microbiome harbour plastic degrading genes : A metagenomic study of solid waste dumping site of Gujarat, India. *Science of the Total Environment*, *779*(336), 146184. https://doi.org/10.1016/j.scitotenv.2021.146184

Lambert, S., & Wagner, M. (2017). Environmental performance of bio-based and biodegradable plastics: The road ahead. *Chemical Society Reviews*, *46*(22), 6855–6871. https://doi.org/10.1039/c7cs00149e

Lear, G., Kingsbury, J. M., Franchini, S., Gambarini, V., Maday, S. D. M., Wallbank, J. A., Weaver, L., & Pantos, O. (2021). Plastics and the microbiome: impacts and solutions. *Environmental Microbiomes*, *16*(1), 1–19. https://doi.org/10.1186/s40793-020-00371-w

Leja, K., & Lewandowicz, G. (2010). Polymer Biodegradation and Biodegradable Polymers – a Review. *Polish Journal of Environmental Studies*, *19*(2), 255–266.

Lesteur, M., Bellon-maurel, V., Gonzalez, C., Latrille, E., Roger, J. M., Junqua, G., & Steyer, J. P. (2010). Alternative methods for determining anaerobic biodegradability : A review. *Process Biochemistry*, *45*(4), 431–440. https://doi.org/10.1016/j.procbio.2009.11.018

Li, L., Lin, X., Bao, J., Xia, H., & Li, F. (2022). Two Extracellular Poly(ε-caprolactone)-Degrading Enzymes From P*seudomonas hydrolytica sp.* DSWY01T: Purification, Characterization, and Gene Analysis. *Frontiers in Bioengineering and Biotechnology*, *10*(March), 1–9. https://doi.org/10.3389/fbioe.2022.835847

Liao, J., & Chen, Q. (2021). Biodegradable plastics in the air and soil environment : Low degradation rate and high microplastics formation. *Journal of Hazardous Materials*, *418*(March), 126329. https://doi.org/10.1016/j.jhazmat.2021.126329

Liczbiński, P., Borowski, S., & Nowak, A. (2022). Isolation and Use of *Coprothermobacter spp.*

to Improve Anaerobic Thermophilic Digestion of Grass. *Molecules*, *27*(14). https://doi.org/10.3390/molecules27144338

Liu, J., He, J., Xue, R., Xu, B., Qian, X., Xin, F., Blank, L. M., Zhou, J., Wei, R., Dong, W., & Jiang, M. (2021). Biodegradation and up-cycling of polyurethanes : Progress, challenges, and prospects. *Biotechnology Advances*, *48*(December 2020), 107730. https://doi.org/10.1016/j.biotechadv.2021.107730

Louca, S., Doebeli, M., & Parfrey, L. W. (2018). Correcting for 16S rRNA gene copy numbers in microbiome surveys remains an unsolved problem. *Microbiome*, *6*(1), 1–12. https://doi.org/10.1186/s40168-018-0420-9

Luciano-rosario, D., Keller, N. P., & Ii, W. M. J. (2020). *Penicillium expansum* : biology, omics, and management tools for a global postharvest pathogen causing blue mould of pome fruit. *Molecular Plant Pathology*, *21*, 1391–1404. https://doi.org/10.1111/mpp.12990

Lyu, J. S., Lee, J. S., & Han, J. (2019). Development of a biodegradable polycaprolactone film incorporated with an antimicrobial agent via an extrusion process. *Scientific Reports*, *9*(1), 1–11. https://doi.org/10.1038/s41598-019-56757-5

Machel, H. G. (2001). Bacterial and thermochemical sulfate reduction in diagenetic settings - old and new insights. *Sedimentary Geology*, *140*(1–2), 143–175. https://doi.org/10.1016/S0037-0738(00)00176-7

Magnin, A., Pollet, E., Phalip, V., & Avérous, L. (2020). Evaluation of biological degradation of polyurethanes. *Biotechnology Advances*, *39*(August 2019), 107457. https://doi.org/10.1016/j.biotechadv.2019.107457

Mandic, M., Spasic, J., Ponjavic, M., Nikolic, M. S., Cosovic, V. R., Connor, K. E. O., Nikodinovic-runic, J., Djokic, L., & Jeremic, S. (2019). Biodegradation of poly (ε -caprolactone) (PCL) and medium chain length polyhydroxyalkanoate (mcl-PHA) using whole cells and cell free protein preparations of *Pseudomonas* and *Streptomyces* strains grown on waste cooking oil. *Polymer Degradation and Stability*, *162*, 160–168. https://doi.org/10.1016/j.polymdegradstab.2019.02.012

Massardier-Nageotte, V., Pestre, C., Cruard-Pradet, T., & Bayard, R. (2006). Aerobic and anaerobic biodegradability of polymer films and physico-chemical characterization. *Polymer Degradation and Stability*, *91*(3), 620–627. https://doi.org/10.1016/j.polymdegradstab.2005.02.029

Matjasic, T., Simcic, T., Medvescek, N., Bajt, O., Dreo, T., & Mori, N. (2020). Critical evaluation of biodegradation studies on synthetic plastics through a systematic literature review. *Science of the Total Environment*, *752*, 16. https://doi.org/10.1016/j.scitotenv.2020.141959

Maurya, A., Bhattacharya, A., & Khare, S. K. (2020). Enzymatic Remediation of Polyethylene Terephthalate (PET)–Based Polymers for Effective Management of Plastic Wastes: An Overview. *Frontiers in Bioengineering and Biotechnology*, *8*(November), 1–13. https://doi.org/10.3389/fbioe.2020.602325

Mckew, B. A., Dumbrell, A. J., Taylor, J. D., Mcgenity, T. J., & Underwood, G. J. C. (2013). Differences between aerobic and anaerobic degradation of microphytobenthic biofilm-derived organic matter within intertidal sediments. *FEMS Microbiology Ecology*, *84*(3), 495–509. https://doi.org/10.1111/1574-6941.12077

Miri, S., Saini, R., Mohammadreza, S. M., Pulicharla, R., Brar, S. K., & Magdouli, S. (2022). Biodegradation of microplastics : Better late than never. *Chemosphere*, *286*(P1), 131670.

https://doi.org/10.1016/j.chemosphere.2021.131670

Mishra, B., Varjani, S., Iragavarapu, G. P., Ngo, H. H., Guo, W., & Vishal, B. (2019). Microbial Fingerprinting of Potential Biodegrading Organisms. *Current Pollution Reports*, *5*(4), 181–197. https://doi.org/10.1007/s40726-019-00116-5

Mohanan, N., Montazer, Z., Sharma, P. K., & Levin, D. B. (2020). Microbial and Enzymatic Degradation of Synthetic Plastics. *Frontiers in Microbiology*, *11*(November). https://doi.org/10.3389/fmicb.2020.580709

Montazer, Z., Najafi, M. B. H., & Levin, D. B. (2020). Challenges with verifying microbial degradation of polyethylene. *Polymers*, *12*(1), 1–24. https://doi.org/10.3390/polym12010123

Moura, L., Machado, A. V., Duarte, F. M., & Nogueira, R. (2010). Biodegradability Assessment of Aliphatic Polyesters-Based Belnds Using Standard Mehtods. *Journal of Applied Polymer Science*, *119*(5), 2658–2667. https://doi.org/10.1002/app

Munir, E., Harefa, R. S. M., Priyani, N., & Suryanto, D. (2018). Plastic degrading fungi *Trichoderma viride* and *Aspergillus nomius* isolated from local landfill soil in Medan. *IOP Conference Series: Earth and Environmental Science*, *126*(1), 6–13. https://doi.org/10.1088/1755-1315/126/1/012145

Myoken, Y., Sugata, T., & Mikami, Y. (2002). Infection Due to Non-Aspergillus Fungi in Immunocompromised Patients Receiving Itraconazole. *Correspodence*, *35*(4), 494–495. https://doi.org/https://doi.org/10.1086/341495

Nakasaki, K., Matsuura, H., Tanaka, H., & Sakai, T. (2006). Synergy of two thermophiles enables decomposition of poly-ε- caprolactone under composting conditions. *FEMS Microbiology Ecology*, *58*(3), 373–383. https://doi.org/10.1111/j.1574-6941.2006.00189.x

Narancic, T., Verstichel, S., Reddy Chaganti, S., Morales-Gamez, L., Kenny, S. T., De Wilde, B., Babu Padamati, R., & O'Connor, K. E. (2018). Biodegradable Plastic Blends Create New Possibilities for End-of-Life Management of Plastics but They Are Not a Panacea for Plastic Pollution. *Environmental Science and Technology*, *52*(18), 10441–10452. https://doi.org/10.1021/acs.est.8b02963

Nawaz, A., Hasan, F., & Shah, A. A. (2015). Degradation of poly(ε-caprolactone) (PCL) by a newly isolated *Brevundimonas sp*. strain MRL-AN1 from soil. *FEMS Microbiology Letters*, *362*(1), 1–7. https://doi.org/10.1093/femsle/fnu004

Nevoralová, M., Koutný, M., Ujčić, A., Starý, Z., Šerá, J., Vlková, H., Šlouf, M., Fortelný, I., & Kruliš, Z. (2020). Structure Characterization and Biodegradation Rate of Poly(ε-caprolactone)/Starch Blends. *Frontiers in Materials*, *7*(June), 1–14. https://doi.org/10.3389/fmats.2020.00141

Nowak, B., Pajak, J., Drozd-Bratkowicz, M., & Rymarz, G. (2011). Microorganisms participating in the biodegradation of modified polyethylene films in different soils under laboratory conditions. *International Biodeterioration and Biodegradation*, *65*(6), 757–767. https://doi.org/10.1016/j.ibiod.2011.04.007

Nübel, U., Engelen, B., Felsre, A., Snaidr, J., Wieshuber, A., Amann, R. I., Ludwig, W., & Backhaus, H. (1996). Sequence heterogeneities of genes encoding 16S rRNAs in *Paenibacillus polymyxa* detected by temperature gradient gel electrophoresis. *Journal of Bacteriology*, *178*(19), 5636–5643. https://doi.org/10.1128/jb.178.19.5636-5643.1996

Oberbeckmann, S., Osborn, A. M., & Duhaime, M. B. (2016). Microbes on a bottle: Substrate,

season and geography influence community composition of microbes colonizing marine plastic debris. *PLoS ONE*, *11*(8), 1–24. https://doi.org/10.1371/journal.pone.0159289

Osama Ragab. (2019). Solid Waste Management and Design of a Sanitary Landfill for Sohar Area. *International Journal of Engineering Research And*, *V8*(11). https://doi.org/10.17577/ijertv8is110142

Paço, A., Duarte, K., da Costa, J. P., Santos, P. S. M., Pereira, R., Pereira, M. E., Freitas, A. C., Duarte, A. C., & Rocha-Santos, T. A. P. (2017). Biodegradation of polyethylene microplastics by the marine fungus *Zalerion maritimum*. *Science of the Total Environment*, *586*, 10–15. https://doi.org/10.1016/j.scitotenv.2017.02.017

Pardo-Rodríguez, M. L., & Zorro-Mateus, P. J. P. (2021). Biodegradation of polyvinyl chloride by *Mucor sp*. and *Penicillium sp*. isolated from soil. *Revista de Investigación, Desarrollo e Innovación*, *11*(2), 387–400. https://doi.org/10.19053/20278306.v11.n2.2021.12763

Park, S. Y., & Kim, C. G. (2019). Biodegradation of micro-polyethylene particles by bacterial colonization of a mixed microbial consortium isolated from a landfill site. *Chemosphere*, *222*, 527–533. https://doi.org/10.1016/j.chemosphere.2019.01.159

Pedizzi, C., Regueiro, L., Rodriguez-Verde, I., Lema, J. M., & Carballa, M. (2016). Effect of oxygen on the microbial activities of thermophilic anaerobic biomass. *Bioresource Technology*, *211*, 765–768. https://doi.org/10.1016/j.biortech.2016.03.085

Peng, Y. (2017). Perspectives on technology for landfill leachate treatment. *Arabian Journal of Chemistry*, *10*, S2567–S2574. https://doi.org/10.1016/j.arabjc.2013.09.031

Phadke, S., Salvador, A. F., Alves, J. I., Bretschger, O., Alves, M. M., & Pereira, M. A. (2017). Harnessing the power of PCR molecular fingerprinting methods and next generation sequencing for understanding structure and function in microbial communities. In *Methods in Molecular Biology* (Vol. 1620, pp. 225–249). Scopus. https://doi.org/10.1007/978-1-4939-7060-5

Pires, J. R. A., Souza, V. G. L., Fuciños, P., Pastrana, L., & Fernando, A. L. (2022). Methodologies to Assess the Biodegradability of Bio-Based Polymers — Current Knowledge and Existing Gaps. *Polymers*, *14*(1359), 1–24. https://doi.org/https://doi.org/10.3390/ polym14071359

Pradhan, R., Reddy, M., Diebel, W., Erickson, L., Misra, M., & Mohanty, A. (2010). Comparative compostability and biodegradation studies of various components of green composites and their blends in simulated aerobic composting bioreactor. *International Journal of Plastics Technology*, *14*(1). https://doi.org/10.1007/s12588-010-0009-z

Qi, R., Jones, D. L., Liu, Q., Liu, Q., Li, Z., & Yan, C. (2021). Field test on the biodegradation of poly(butylene adipate-co-terephthalate) based mulch films in soil. *Polymer Testing*, *93*, 107009. https://doi.org/10.1016/j.polymertesting.2020.107009

Qi, X., Yan, W., Cao, Z., Ding, M., & Yuan, Y. (2022). Current advances in the biodegradation and bioconversion of polyethylene terephthalate. *Microorganisms*, *10*(1), 1–25. https://doi.org/10.3390/microorganisms10010039

Quecholac-Piña, X., Hernández-Berriel, M. D. C., Mañón-Salas, M. D. C., Espinosa-Valdemar, R. M., & Vázquez-Morillas, A. (2020). Degradation of plastics under anaerobic conditions: A short review. *Polymers*, *12*(1), 1–18. https://doi.org/10.3390/polym12010109

Raddadi, N., & Fava, F. (2019). Biodegradation of oil-based plastics in the environment: Existing

knowledge and needs of research and innovation. *Science of the Total Environment*, *679*, 148–158. https://doi.org/10.1016/j.scitotenv.2019.04.419

Remmas, N., Roukouni, C., & Ntougias, S. (2017). Bacterial community structure and prevalence of *Pusillimonas*-like bacteria in aged landfill leachate. *Environmental Science and Pollution Research*, *24*(7), 6757–6769. https://doi.org/10.1007/s11356-017-8416-8

Renou, S., Givaudan, J. G., Poulain, S., Dirassouyan, F., & Moulin, P. (2008). Landfill leachate treatment : Review and opportunity. *Journal of Hazardous Materials*, *150*, 468–493. https://doi.org/10.1016/j.jhazmat.2007.09.077

Riffat, R., & Krongthamchat, K. (2006). Specific methanogenic activity of halophilic and mixed cultures in saline wastewater. *International Journal of Environmental Science and Technology*, *2*(4), 291–299. https://doi.org/10.1007/BF03325889

Roager, L., & Sonnenschein, E. C. (2019). Bacterial Candidates for Colonization and Degradation of Marine Plastic Debris. *Environmental Science and Technology*, *53*(20), 11636–11643. https://doi.org/10.1021/acs.est.9b02212

Roberts, C., Edwards, S., Vague, M., León-Zayas, R., Scheffer, H., Chan, G., Swartz, N. A., & Mellies, J. L. (2022). Environmental Consortium Containing *Pseudomonas* and *Bacillus* Species Synergistically Degrades Polyethylene Terephtalate Plastic. *Applied and Environmental Science*, *5*(6).

Ru, J., Huo, Y., & Yang, Y. (2020). Microbial Degradation and Valorization of Plastic Wastes. *Frontiers in Microbiology*, *11*(April), 1–20. https://doi.org/10.3389/fmicb.2020.00442

Ruggero, F., Gori, R., & Lubello, C. (2019). Methodologies to assess biodegradation of bioplastics during aerobic composting and anaerobic digestion : A review. *Waste Management and Research*, *37*(10), 959–975. https://doi.org/10.1177/0734242X19854127

Salvador, A. F., Cavaleiro, A. J., Paulo, A. M. S., Silva, S. A., Guedes, A. P., Pereira, M. A., Stams, A. J. M., Sousa, D. Z., & Alves, M. M. (2019). Inhibition Studies with 2-Bromoethanesulfonate Reveal a Novel Syntrophic Relationship in Anaerobic Oleate Degradation. *Applied and Environmental Microbiology*, *85*(2). https://doi.org/10.1128/AEM.01733-18

Sankhla, I. S., Sharma, G., & Tak, A. (2020). Fungal degradation of bioplastics: An overview. In *New and Future Developments in Microbial Biotechnology and Bioengineering* (Issue August, pp. 35–47). Elsevier B.V. https://doi.org/10.1016/b978-0-12-821007-9.00004-8

Santacruz-ju, E., Buendia-Corona, R. E., & Ramírez, E. (2021). Fungal enzymes for the degradation of polyethylene : Molecular docking simulation and biodegradation pathway proposal. *Journal of Hazardous Materials*, *411*(October 2020). https://doi.org/10.1016/j.jhazmat.2021.125118

Sasaki, K., Morita, M., Sasaki, D., Nagaoka, J., Matsumoto, N., Ohmura, N., & Shinozaki, H. (2011). Syntrophic degradation of proteinaceous materials by the thermophilic strains *Coprothermobacter proteolyticus* and *Methanothermobacter thermautotrophicus*. *Journal of Bioscience and Bioengineering*, *112*(5), 469–472. https://doi.org/10.1016/j.jbiosc.2011.07.003

Scaffaro, R., Maio, A., Sutera, F., Gulino, E. ortunato, & Morreale, M. (2019). Degradation and recycling of films based on biodegradable polymers: A short review. *Polymers*, *11*(4). https://doi.org/10.3390/polym11040651

Selke, S., Auras, R., Nguyen, T. A., Aguirre, E. C., Cheruvathur, R., & Liu, Y. (2015). Evaluation of Biodegradation-Promoting Additives for Plastics. *Environmental Science and Technology*, *49*, 3769–

3777. https://doi.org/10.1021/es504258u

Shah, A. A., Hasan, F., Hameed, A., & Ahmed, S. (2008). Biological degradation of plastics: A comprehensive review. *Biotechnology Advances*, *26*(3), 246–265. https://doi.org/10.1016/j.biotechadv.2007.12.005

Shen, M., Song, B., Zeng, G., Zhang, Y., Huang, W., Wen, X., & Tang, W. (2020). Are biodegradable plastics a promising solution to solve the global plastic pollution? *Environmental Pollution*, *263*, 7. https://doi.org/10.1016/j.envpol.2020.114469

Shruti, V. C., & Kutralam-Muniasamy, G. (2019). Bioplastics: Missing link in the era of Microplastics. *Science of the Total Environment*, *697*, 134139. https://doi.org/10.1016/j.scitotenv.2019.134139

Skariyachan, S., Setlur, A. S., Naik, S. Y., Naik, A. A., Usharani, M., & Vasist, K. S. (2017). Enhanced biodegradation of low and high-density polyethylene by novel bacterial consortia formulated from plastic-contaminated cow dung under thermophilic conditions. *Environmental Science and Pollution Research*, *24*(9), 8443–8457. https://doi.org/10.1007/s11356-017-8537-0

Šmejkalová, P., Kužníková, V., Merna, J., & Hermanová, S. (2016). Anaerobic digestion of aliphatic polyesters. *Water Science and Tecnology*, *73*(10), 2386–2393. https://doi.org/10.2166/wst.2016.088

Sogin, M. L., Morrison, H. G., Huber, J. A., Welch, D. M., Huse, S. M., Neal, P. R., Arrieta, J. M., & Herndl, G. J. (2006). Microbial diversity in the deep sea and the underexplored "rare biosphere." *The National Academy of Science of the USA*, *28*(4), TAHP1. https://doi.org/10.4278/ajhp.28.4.tahp

Srikanth, M., Sandeep, T. S. R. S., Sucharitha, K., & Godi, S. (2022). Biodegradation of plastic polymers by fungi : a brief review. *Bioresources and Bioprocessing*, *9*(42). https://doi.org/10.1186/s40643-022-00532-4

Stamps, B. W., Lyles, C. N., Suflita, J. M., Masoner, J. R., Cozzarelli, I. M., Kolpin, D. W., & Stevenson, B. S. (2016). Municipal Solid Waste Landfills Harbor Distinct Microbiomes. *Frontiers in Microbiology*, *7*(April). https://doi.org/10.3389/fmicb.2016.00534

Stams, A. J. M., Van Dijk, J. B., Dijkema, C., & Plugge, C. M. (1993). Growth of syntrophic propionate-oxidizing bacteria with fumarate in the absence of methanogenic bacteria. *Applied and Environmental Microbiology*, *59*(4), 1114–1119. https://doi.org/10.1128/aem.59.4.1114-1119.1993

Stoeck, T., Bass, D., Nebel, M., Christen, R., Jones, M. D. M., Breiner, H. W., & Richards, T. A. (2010). Multiple marker parallel tag environmental DNA sequencing reveals a highly complex eukaryotic community in marine anoxic water. *Molecular Ecology*, *19*(SUPPL. 1), 21–31. https://doi.org/10.1111/j.1365-294X.2009.04480.x

Suárez, W. A. B., Vantini, J. da S., Duda, R. M., Giachetto, P. F., Cintra, L. C., Ferro, M. I. T., & Oliveira, R. A. de. (2018). Predominance of syntrophic bacteria , *Methanosaeta* and *Methanoculleus* in a two-stage up- flow anaerobic sludge blanket reactor treating coffee processing wastewater at high organic loading rate. *Bioresource Technology*, *268*(May), 158–168. https://doi.org/10.1016/j.biortech.2018.06.091

Suzuki, M., Tachibana, Y., & Kasuya, K. (2021). Biodegradability of poly (3-hydroxyalkanoate) and poly (ε - caprolactone) via biological carbon cycles in marine environments. *Polymer Journal*, *53*, 47–66. https://doi.org/10.1038/s41428-020-00396-5

Swiontek, M., Maciej, B., Aleksandra, W., But, B., & Chylińska, M. (2019). Antifungal Activity of Polyhexamethyleneguanidine Derivatives Introduced into Biodegradable Polymers. *Journal of Polymers and the Environment*, *27*(8), 1760–1769. https://doi.org/10.1007/s10924-019-01472-5

Syranidou, E., Karkanorachaki, K., Amorotti, F., Avgeropoulos, A., Kolvenbach, B., Zhou, N. Y., Fava, F., Corvini, P. F. X., & Kalogerakis, N. (2019). Biodegradation of mixture of plastic films by tailored marine consortia. *Journal of Hazardous Materials*, *375*(January), 33–42. https://doi.org/10.1016/j.jhazmat.2019.04.078

Szulc, J., Okrasa, M., Nowak, A., Nizioł, J., Ruman, T., & Kuberski, S. (2022). Assessment of Physicochemical, Microbiological and Toxicological Hazards at an Illegal Landfill in Central Poland. *International Journal of Environmental Research and Public Health*, *19*(8). https://doi.org/10.3390/ijerph19084826

Tabasi, R. Y., & Ajji, A. (2015). Selective degradation of biodegradable blends in simulated laboratory composting. *Polymer Degradation and Stability*, *120*, 435–442. https://doi.org/10.1016/j.polymdegradstab.2015.07.020

Taghavi, N., Udugama, I. A., Zhuang, W. Q., & Baroutian, S. (2021). Challenges in biodegradation of non-degradable thermoplastic waste: From environmental impact to operational readiness. *Biotechnology Advances*, *49*(October 2020), 107731. https://doi.org/10.1016/j.biotechadv.2021.107731

Taniguchi, I., Yoshida, S., Hiraga, K., Miyamoto, K., Kimura, Y., & Oda, K. (2019). Biodegradation of PET: Current Status and Application Aspects. *ACS Catalysis*, *9*(5), 4089–4105. https://doi.org/10.1021/acscatal.8b05171

Thakur, M., Majid, I., Hussain, S., & Nanda, V. (2021). Poly(ε-caprolactone): A potential polymer for biodegradable food packaging applications. *Packaging Technology and Science*, *34*(8), 449–461. https://doi.org/10.1002/pts.2572

Themelis, N. J., & Ulloa, P. A. (2007). Methane generation in landfills. *Renewable Energy*, *32*(7), 1243–1257. https://doi.org/10.1016/j.renene.2006.04.020

Tiago, I., Teixeira, I., Silva, S., Chung, P., Veríssimo, A., & Manaia, C. M. (2004). Metabolic and genetic diversity of mesophilic and thermophilic bacteria isolated from composted municipal sludge on poly-ε-caprolactones. *Current Microbiology*, *49*(6), 407–414. https://doi.org/10.1007/s00284-004-4353-0

Tokiwa, Y., Calabia, B. P., Ugwu, C. U., & Aiba, S. (2009). Biodegradability of plastics. *International Journal of Molecular Sciences*, *10*(9), 3722–3742. https://doi.org/10.3390/ijms10093722

Trivedi, P., Hasan, A., Akhtar, S., Siddiqui, M. H., Sayeed, U., Kalim, M., & Khan, A. (2016). Role of microbes in degradation of synthetic plastics and manufacture of bioplastics. *Journal of Chemical and Pharmaceutical Research*, *8*(3), 211–216. www.jocpr.com

Urbanek, A. K., Arroyo, M., Mata, I. De, & Mirończuk, A. M. (2022). Identification of novel extracellular putative chitinase and hydrolase from *Geomyces sp .* B10I with the biodegradation activity towards polyesters. *AMB Express*, *12*(12). https://doi.org/10.1186/s13568-022-01352-7

Urbanek, A. K., Rymowicz, W., & Mirończuk, A. M. (2018). Degradation of plastics and plastic-degrading bacteria in cold marine habitats. *Applied Microbiology and Biotechnology*, *102*(18), 7669–

7678. https://doi.org/10.1007/s00253-018-9195-y

Wagner, D. (2017). Effect of varying soil water potentials on methanogenesis in aerated marshland soils. *Scientific Reports*, *7*(1), 1–9. https://doi.org/10.1038/s41598-017-14980-y

Wang, G. X., Huang, D., Ji, J. H., Völker, C., & Wurm, F. R. (2021). Seawater-Degradable Polymers—Fighting the Marine Plastic Pollution. *Advanced Science*, *8*(1), 1–26. https://doi.org/10.1002/advs.202001121

Wang, S., Hou, X., & Su, H. (2017). Exploration of the relationship between biogas production and microbial community under high salinity conditions. *Scientific Reports*, *7*(1), 1–10. https://doi.org/10.1038/s41598-017-01298-y

Wataru, S. (2015). Effect of a Biodegradation Promoting Additive on Polyethylene Terephthalate in Anaerobic Digestion. Michigan State University.

Wei, R., & Zimmermann, W. (2017). Microbial enzymes for the recycling of recalcitrant petroleum-based plastics: how far are we? *Microbial Biotechnology*, *10*(6), 1308–1322. https://doi.org/10.1111/1751-7915.12710

Wei, Y., Thomson, N. R., Aravena, R., Marchesi, M., Barker, J. F., Madsen, E. L., Kolhatkar, R., Buscheck, T., Hunkeler, D., & DeRito, C. M. (2018). Infiltration of Sulfate to Enhance Sulfate-Reducing Biodegradation of Petroleum Hydrocarbons. *Groundwater Monitoring and Remediation*, *38*(4), 73–87. https://doi.org/10.1111/gwmr.12298

Weng, Y. X., Wang, X. L., & Wang, Y. Z. (2011). Biodegradation behavior of PHAs with different chemical structures under controlled composting conditions. *Polymer Testing*, *30*(4), 372–380. https://doi.org/10.1016/j.polymertesting.2011.02.001

Wilkes, R. A., & Aristilde, L. (2017). Degradation and metabolism of synthetic plastics and associated products by *Pseudomonas sp.*: capabilities and challenges. *Journal of Applied Microbiology*, *123*(3), 582–593. https://doi.org/10.1111/jam.13472

Woodruff, M. A., & Hutmacher, D. W. (2010). The return of a forgotten polymer — Polycaprolactone in the 21st century. *Progress in Polymer Science*, *35*, 1217–1256. https://doi.org/10.1016/j.progpolymsci.2010.04.002

Xochitl, Q. P., Del Consuelo, H. B. M., Del Consuelo, M. S. M., María, E. V. R., & Alethia, V. M. (2021). Degradation of plastics in simulated landfill conditions. *Polymers*, *13*(7), 1–13. https://doi.org/10.3390/polym13071014

Yagi, H., Ninomiya, F., Funabashi, M., & Kunioka, M. (2009). Anaerobic Biodegradation Tests of Poly (lactic acid) under Mesophilic and Thermophilic Conditions Using a New Evaluation System for Methane Fermentation in Anaerobic Sludge. *International Journal of Molecular Sciences*, *10*, 3824–3835. https://doi.org/10.3390/ijms10093824

Yagi, H., Ninomiya, F., Funabashi, M., & Kunioka, M. (2013). Thermophilic anaerobic biodegradation test and analysis of eubacteria involved in anaerobic biodegradation of four specified biodegradable polyesters. *Polymer Degradation and Stability*, *98*(6), 1182–1187. https://doi.org/10.1016/j.polymdegradstab.2013.03.010

Yagi, H., Ninomiya, F., Funabashi, M., & Kunioka, M. (2014). Mesophilic anaerobic biodegradation test and analysis of eubacteria and archaea involved in anaerobic biodegradation of four specified biodegradable polyesters. *Polymer Degradation and Stability*, *110*, 278–283.

https://doi.org/10.1016/j.polymdegradstab.2014.08.031

Yan, F., Wei, R., Cui, Q., Bornscheuer, U. T., & Liu, Y. J. (2021). Thermophilic whole-cell degradation of polyethylene terephthalate using engineered Clostridium thermocellum. *Microbial Biotechnology*, *14*(2), 374–385. https://doi.org/10.1111/1751-7915.13580

Yi, J., Lo, L. S. H., & Cheng, J. (2020). Dynamics of Microbial Community Structure and Ecological Functions in Estuarine Intertidal Sediments. *Frontiers in Marine Science*, *7*(October), 1–15. https://doi.org/10.3389/fmars.2020.585970

Zeng, S. H., Duan, P. P., Shen, M. X., Xue, Y. J., & Wang, Z. Y. (2016). Preparation and degradation mechanisms of biodegradable polymer: A review. *IOP Conference Series: Materials Science and Engineering*, *137*(1). https://doi.org/10.1088/1757-899X/137/1/012003

Zeng, W., Li, X., Yang, Y., Min, J., Huang, J. W., Liu, W., Niu, D., Yang, X., Han, X., Zhang, L., Dai, L., Chen, C. C., & Guo, R. T. (2022). Substrate-Binding Mode of a Thermophilic PET Hydrolase and Engineering the Enzyme to Enhance the Hydrolytic Efficacy. *ACS Catalysis*, *12*(5), 3033–3040. https://doi.org/10.1021/acscatal.1c05800

Zhang, C., Sirijovski, N., Adler, L., & Ferrari, B. C. (2019). *Exophiala macquariensis sp* . nov . , a cold adapted black yeast species recovered from a hydrocarbon contaminated sub-Antarctic soil. *Fungal Biology*, *123*(2), 151–158. https://doi.org/10.1016/j.funbio.2018.11.011

Zhang, K., Hu, Z., Zeng, F., Yang, X., Wang, J., Jing, R., Zhang, H., Li, Y., & Zhang, Z. (2019). Biodegradation of petroleum hydrocarbons and changes in microbial community structure in sediment under nitrate-, ferric-, sulfate-reducing and methanogenic conditions. *Journal of Environmental Management*, *249*(August), 109425. https://doi.org/10.1016/j.jenvman.2019.109425

Zhang, Y., Pedersen, J. N., Eser, B. E., & Guo, Z. (2022). Biodegradation of polyethylene and polystyrene: From microbial deterioration to enzyme discovery. *Biotechnology Advances*, *60*(May), 107991. https://doi.org/10.1016/j.biotechadv.2022.107991

Zhao, R., Liu, J., Feng, J., Li, X., & Li, B. (2021). Microbial community composition and metabolic functions in landfill leachate from different landfills of China. *Science of the Total Environment*, *767*, 144861. https://doi.org/10.1016/j.scitotenv.2020.144861

Appendices

Appendix 1- Microorganisms known to biodegrade PE, PET, and PCL

Table A1.1: Bacteria reported as PE biodegraders, and information on the isolation source, possible enzymes involved in the biodegradation and the biodegradation conditions

Isolated source	*Bacterium*	Enzymes	Biodegradation conditions	References
-	*Achromobacter denitrificans*	-	-	(Amobonye *et al.*, 2021)
-	*Achromobacter xylosoxidans*	-	-	(Ahmed *et al.*, 2018; Jacquim *et al.*, 2019)
-	*Acinetobacter baumannii*	-	-	(Amobonye *et al.*, 2021; Jacquim *et al.*, 2019)
Municipal landfill	*Acinetobacter baumannii*	-	Incubation time- 30 days, 37℃, no pre-treatment, biomass production	(Montazer *et al.*, 2020)
Municipal landfill	*Acinetobacter bumannii*	-	Biomass production after 30 days	(Zhang *et al.*, 2022)
-	*Acinetobacter haemolyticus*	Alkane hydroxylases	-	(Mohanan *et al.*, 2020)
Contaminated site	*Acinetobacter johnsonii*	-	-	(Matjasic *et al.*, 2020)
-	*Acinetobacter pittii*	Alkane hydroxylases	-	(Mohanan *et al.*, 2020)
-	*Acinetobacter pittii IRN19*	-	-	(Mohanan *et al.*, 2020)
-	*Actinobacter spp*	-	-	(Alshehrei, 2017)
-	*Aneurinibacillus* sp.	-	Molecular weight reduction at 50℃	(Atanasova, Paunova-krasteva, *et al.*, 2021)
Dumped soil area	*Arthobacter defluvii*	-	Incubation time- 1 month, PE bags, weight loss- 20 %-30 %	(Montazer *et al.*, 2020)
Dumpsites	*Arthrobacter sp. GMB5*	-	Incubation time- 30 days, reduction of 12–15 % in plastic weight	(Ali *et al.*, 2021)
Contaminated site	*Arthrobacter spp.*	-	-	(Matjasic *et al.*, 2020)
-	*Arthrobacter viscosus*	-	-	(Nowak et al., 2011)
-	*Bacillus amyloliquefaciens*	-	-	(Amobonye *et al.*, 2021; Jacquim *et al.*, 2019; Nowak et al., 2011)
Dumped soil area	*Bacillus amyloliquefaciens*	-	Incubation time- 1 month, PE bags, weight loss 20 %-30 %	(Montazer *et al.*, 2020)
Solid waste dumped	*Bacillus amyloliquefaciens*	-	Incubation time- 60 days, LDPE, degradation 11 %-16 %	(Montazer *et al.*, 2020)

Table A1.1 (continued)

Isolated source	*Bacterium*	Enzymes	Biodegradation conditions	References
-	*Bacillus amyloliquefaciens*	-	Incubation time 60 days, 11 % weight loss	(Taghavi *et al.*, 2021)
Contaminated site	*Bacillus aquimaris*	-	-	(Matjasic *et al.*, 2020)
Contaminated site	*Bacillus boroniphilus*	-	-	(Matjasic *et al.*, 2020)
-	*Bacillus borstelensis*	-	20 % weight reduction	(Ali *et al.*, 2021)
-	*Bacillus cereus*	-	-	(Amobonye *et al.*, 2021; Nowak et al., 2011)
-	*Bacillus cereus*	-	36 % weight reduction	(Ali *et al.*, 2021)
-	*Bacillus cereus*	-	Incubation time 40 days, 1,6 % weight loss	(Taghavi *et al.*, 2021)
-	*Bacillus cereus*	-	-	(Amobonye *et al.*, 2021; Matjasic *et al.*, 2020)
Soil	*Bacillus cereus*	-	7 %-10 % mineralization after 90 days	(Zhang *et al.*, 2022)
-	*Bacillus cereus VASB1/TS*	-	-	(Matjasic *et al.*, 2020)
-	*Bacillus circulans*	-	Incubation time 45 days, 2,33 % weight loss	(Taghavi *et al.*, 2021)
Contaminated site	*Bacillus drentensis*	-	-	(Matjasic *et al.*, 2020)
Contaminated site	*Bacillus firmu*	-	-	(Matjasic *et al.*, 2020)
-	*Bacillus gottheilii*	-	Incubation time 40 days, 6,2 % weight loss	(Taghavi *et al.*, 2021)
Contaminated site	*Bacillus idriensis*	-	-	(Matjasic *et al.*, 2020)
-	*Bacillus licheniformis, Lysinibacillus fusiformis*	-	2,97 % weight loss after 1 month	(Zhang *et al.*, 2022)
Contaminated site	*Bacillus luciferensis*	-	-	(Matjasic *et al.*, 2020)
Contaminated site	*Bacillus marisflav*	-	-	(Matjasic *et al.*, 2020)
Contaminated site	*Bacillus megaterium*	-	-	(Matjasic *et al.*, 2020)
Soil	*Bacillus megaterium*	-	7 %-10 % mineralization after 90 days	(Zhang *et al.*, 2022)
Soil	*Bacillus megaterium, Bacillus subtilis, Bacillus cereus (MIX together)*	-	Incubation time- 90 days, 45℃, photo-degraded oxobiodegradable PE, 7 %-10 % mineralization	(Montazer *et al.*, 2020)

Table A1.1 (continued)

Isolated source	*Bacterium*	Enzymes	Biodegradation conditions	References
-	*Bacillus mixture*	-	Incubation time 90 days	(Taghavi *et al.*, 2021)
Contaminated site	*Bacillus muralis*	-	-	(Matjasic *et al.*, 2020)
-	*Bacillus mycoides*	-	-	(Jacquim *et al.*, 2019; Nowak et al., 2011)
-	*Bacillus mycoides*	-	Incubation time 60 days, 10,5-11,3 % weight loss	(Taghavi *et al.*, 2021)
Contaminated site	*Bacillus mycoides*	-	-	(Matjasic *et al.*, 2020)
-	*Bacillus pumilus*	-	-	(Nowak et al., 2011)
Pelagic water	*Bacillus pumilus*	-	Incubation time- 1 month, PE bags, weight loss- 1,5 %-1,75 %	(Montazer *et al.*, 2020)
-	*Bacillus pumilus*	-	Incubation time 30 days, 1,5 % weight loss	(Taghavi *et al.*, 2021)
Contaminated site	*Bacillus pumilus*	-	-	(Matjasic *et al.*, 2020)
-	*Bacillus pumilus M27*	-	-	(Jacquim *et al.*, 2019)
Pelagic water	*Bacillus pumilus M27 Bacillus subtilis H1584*	-	Incubation time- 30 days, PE bags, 1,5 %-1,75 % weight loss	(Montazer *et al.*, 2020)
Contaminated site	*Bacillus simplex*	-	-	(Matjasic *et al.*, 2020)
Contaminated site	*Bacillus sp*	-	-	(Matjasic *et al.*, 2020)
Waste coal, a forest and an extinct volcano crater	*Bacillus sp.*	-	Incubation time- 225 days, modified PE, reduction of mechanical properties- 98 %, no weight loss	(Montazer *et al.*, 2020)
-	*Bacillus sp.*	-	-	(Amobonye *et al.*, 2021; Matjasic *et al.*, 2020; Zhang *et al.*, 2022)
Composting agricultural residues	*Bacillus sp.* BCBT21	-	Molecular weight decrease of 44 %, after 30 days at 55℃	
Gut of waxworm	*Bacillus sp. YP1*	-	Incubation time- 60 days	(Ru *et al.*, 2020)
-	*Bacillus sp. YP1*	-	Incubation time 28 days, 10,7 % weight loss	(Taghavi *et al.*, 2021)
-	*Bacillus sp. YP1*	-	-	(Mohanan *et al.*, 2020)
-	*Bacillus sphaericus*	-	-	(Jacquim *et al.*, 2019)
-	*Bacillus sphaericus*	-	Incubation time 365 days, 3,5-10 % weight loss	(Taghavi *et al.*, 2021)

Table A1.1 (continued)

Isolated source	*Bacterium*	Enzymes	Biodegradation conditions	References
Shallow water ocean	*Bacillus sphericus*	-	Incubation time- 1 year, HDPE and LDPE, untreated (biodegradation 3,5 %-10 %) and heat treated (9 %- 10 %)	(Montazer *et al.*, 2020)
Soil	*Bacillus subtilis*	-	7 %-10 % mineralization after 90 days	(Zhang *et al.*, 2022)
Pelagic water	*Bacillus subtilis*	-	Incubation time- 1 month, PE bags, weight loss of 1,5 %-1,75 %	(Montazer *et al.*, 2020)
-	*Bacillus subtilis*	-	Incubation time- 30 days, biosurfactants, unpretreated, 9,26 % weight loss	(Montazer *et al.*, 2020)
Dumped soil area	*Bacillus subtilis*	-	Incubation time- 1 month, PE bags, weight loss- 20 %-30 %	(Montazer *et al.*, 2020)
-	*Bacillus subtilis*	-	Incubation time 30 days, 9,26 % weight loss	(Taghavi *et al.*, 2021)
-	*Bacillus subtilis*	-	Incubation time 60 days, 17,7-23,1 % weight loss	(Taghavi *et al.*, 2021)
-	*Bacillus subtilis*	-	Incubation time 30 days, 1,75 % weight loss	(Taghavi *et al.*, 2021)
Contaminated site	*Bacillus subtilis*	-	-	(Matjasic *et al.*, 2020)
-	*Bacillus subtilis*	-	9,26 % weight loss after 30 days	(Zhang *et al.*, 2022)
-	*Bacillus subtilis*	-	22 % weight loss after 1 month	(Zhang *et al.*, 2022)
-	*Bacillus thuringiensis*	-	-	(Jacquim *et al.*, 2019; Nowak et al., 2011)
-	*Bacillus thuringiensis*	-	Incubation time 9 days	(Taghavi *et al.*, 2021)
-	*Brevibaccillus borstelensis*	-	-	(Kale *et al.*, 2015)
Waste Disposal site	*Brevibacillus*	-	40,5 % weight loss after 3 weeks	(Zhang *et al.*, 2022)
-	*Brevibacillus borstelensis*	-	Incubation time- 90 days, 50^{a}C irradiated LDPE, 17 % weight loss	(Ahmed *et al.*, 2018; Bahl *et al.*, 2021; Jacquim *et al.*, 2019; Montazer *et al.*, 2020)
Coastal regions	Brevibacillus borstelensis	-	Incubation time- 30 days, 11,4 % weight reduction	(Ali *et al.*, 2021)
-	*Brevibacillus borstelensis*	-	-	(Iram *et al.*, 2019; Shah *et al.*, 2008)
-	*Brevibacillus borstelensis 707*	-	Incubation time 30 days, 11 % weight loss	(Taghavi *et al.*, 2021)
-	*Brevibacillus parabrevis*	-	-	(Jacquim *et al.*, 2019)

Table A1.1 (continued)

Isolated source	*Bacterium*	Enzymes	Biodegradation conditions	References
Waste disposal site	*Brevibacillus sp.*	-	Incubation time- 3 weeks, Pretreated PE, 37,5 % weight loss	(Montazer *et al.*, 2020)
-	*Brevibacillusborstelensis*	-	-	(Iram *et al.*, 2019)
-	*Brevibacterium sp.*	-	-	(Matjasic *et al.*, 2020)
Wastewater activated sludge soil	*Chryseobacterium gleum*	-	Incubation time- 1 month, UV-radiated LLDPE	(Montazer *et al.*, 2020)
-	*Citrobacter sp.*	-	-	(Matjasic *et al.*, 2020)
-	*Comamonas sp.*	-	-	(Jacquim *et al.*, 2019; Mohanan *et al.*, 2020)
Plastic debris in soil	*Comamonas sp.*	-	Incubation time- 90 days, non-treated LDPE, changing in chemical properties	(Montazer *et al.*, 2020)
Contaminated site	*Comamonas sp.*	-	-	(Matjasic *et al.*, 2020)
Contaminated site	*Comamonas testosteroni*	-	-	(Matjasic *et al.*, 2020)
Plastic debris in soil	*Delftia sp.*	-	Incubation time- 90 days, non-treated LDPE, changing in chemical properties	(Montazer *et al.*, 2020)
-	*Delftia sp.*	-	-	(Jacquim *et al.*, 2019; Mohanan *et al.*, 2020)
Contaminated site	*Delftia sp.*	-	-	(Matjasic *et al.*, 2020)
-	*Diplococcus sp.*	-	-	(Matjasic *et al.*, 2020)
Gut of waxworm	*Enterobacter asburiae YT1*	-	-	(Ru *et al.*, 2020)
-	*Enterobacter asburiae YT1*	-	-	(Jacquim *et al.*, 2019; Mohanan *et al.*, 2020)
-	*Enterobacter sp.*	-	-	(Amobonye *et al.*, 2021; Matjasic *et al.*, 2020)
-	*Enterobacter sp. D1*	-	Change in chemical and surface properties, 14 days incubation	(Zhang *et al.*, 2022)
Pelagic water	*Kocuria palustris M16*	-	Incubation time- 30 days, PE bags, 1 % degradation	(Montazer *et al.*, 2020)
-	*Kocuria palustris M16*	-	-	(Jacquim *et al.*, 2019)
-	*Kosakonia sp.*	-	-	(Matjasic *et al.*, 2020)
-	*Lysinibacillus fusiformis*	-	21,9 % weight loss at 25℃ and pH 3,5	(Ali *et al.*, 2021)

Table A1.1 (continued)

Isolated source	*Bacterium*	Enzymes	Biodegradation conditions	References
-	*Lysinibacillus fusiformis*	-	-	(Amobonye *et al.*, 2021; Matjasic *et al.*, 2020)
-	*Lysinibacillus fusiformis VASB-14/WL*	-	-	(Matjasic *et al.*, 2020)
-	*Lysinibacillus xylanilyticus*	-	-	(Jacquim *et al.*, 2019)
-	*Microbacterium paraoxydans*	-	Incubation time- 2 months, pre-treated LDPE, 61 % weight loss	(Montazer *et al.*, 2020)
-	*Microbacterium paraoxydans*	-	-	(Jaiswal *et al.*, 2020)
-	*Microbacterium paraoxydans*	-	Incubation time 2 months, biodegradation verified by FTIR of 61,0 %	(Kale *et al.*, 2015)
Marine pulp mill wastes, rich in lignin	*Microbulbifer hydrilyticus IRE-31*	-	Incubation time- 30 days, morphological changes on plastic surface, ketone groups formed	(Ali *et al.*, 2021)
-	*Micrococcus luteus*	-	-	(Nowak et al., 2011)
-	*Micrococcus luteus IRN20*	-	-	(Mohanan *et al.*, 2020)
-	*Micrococcus lylae*	-	-	(Nowak et al., 2011)
-	*Micrococcus sp.*	-	-	(Matjasic *et al.*, 2020)
-	*Moraxella sp.*	-	-	(Matjasic *et al.*, 2020)
-	*Nocardia asteroides GK*	-	Surface and structural changes after 6 months	(Zhang *et al.*, 2022)
-	*Nocardia asteroids*	-	-	(Zhang *et al.*, 2022)
-	*Nocardiopsos sp.*	-	-	(Amobonye *et al.*, 2021)
Domestic sewage water	*Oscillatoria subbrevis*	-	30 % of the initial weight of tested PE over a 42-day period	(Ru *et al.*, 2020)
-	*Paenibacillus macerans*	-	-	(Nowak et al., 2011)
Contaminated site	*Paenibacillus woosongensis*	-	-	(Matjasic *et al.*, 2020)
Domestic sewage water	*Phormidium lucidum*	-	30 % of the initial weight of tested PE over a 42-day period	(Ru *et al.*, 2020)
Petroleum contaminated beach soil	*Pseudomonas aeroginosa*	-	Incubation time -80 days, LMWPE, 40,8 % weight loss	(Montazer *et al.*, 2020)
-	*Pseudomonas aeruginosa*	-	80 % weight loss	(Jaiswal *et al.*, 2020)

Table A1.1 (continued)

Isolated source	*Bacterium*	Enzymes	Biodegradation conditions	References
-	*Pseudomonas aeroginosa, Pseudomonas putida, Pseudomonas siringae*	-	Incubation time- 120 days, Untreated PE, degradation 9 %-20 %	(Montazer *et al.*, 2020)
-	*Pseudomonas aeruginosa*	-	Incubation time 120 days, 20 % weight loss	(Taghavi *et al.*, 2021)
-	*Pseudomonas aeruginosa*	-	Incubation time 30 days, 7,3-8,5 % weight loss	(Taghavi *et al.*, 2021)
-	*Pseudomonas aeruginosa*	Alkane hydroxylases		(Mohanan *et al.*, 2020)
-	*Pseudomonas aeruginosa*	-	Incubation time 2 months, biodegradation verified by FTIR of 50,5 %	(Kale *et al.*, 2015)
Contaminated site	*Pseudomonas aeruginosa*	-	-	(Matjasic *et al.*, 2020)
-	*Pseudomonas aeruginosa (ATCC 15692)*	-	-	(Jacquim *et al.*, 2019)
-	*Pseudomonas aeruginosa ATCC*	Alkane hydroxylases	-	(Mohanan *et al.*, 2020)
Contaminated site	*Pseudomonas aeruginosa E7*	-	-	(Matjasic *et al.*, 2020)
-	*Pseudomonas aeruginosa PAO1*	-	-	(Mohanan *et al.*, 2020)
-	*Pseudomonas aeruginosa PAO1 (ATCC 15729)*	-	-	(Jacquim *et al.*, 2019)
Contaminated site	*Pseudomonas alcaligenes*	-	-	(Matjasic *et al.*, 2020)
Municipal landfill	*Pseudomonas citronellolis*	-	Incubation time- 4 days, LDPE, 17,8 % weight loss	(Montazer *et al.*, 2020)
-	*Pseudomonas citronellolis*	-	-	(Jacquim *et al.*, 2019)
-	*Pseudomonas citronellolis*	-	Incubation time 4 days, 17,8 % weight loss	(Taghavi *et al.*, 2021)
-	*Pseudomonas citronellolis*	Alkane hydroxylases	-	(Mohanan *et al.*, 2020)
-	*Pseudomonas fluorescens*	-	-	(Nowak et al., 2011)
-	*Pseudomonas fluorescens*	-	Incubation time 30 days, 7,8-7,9 % weight loss	(Taghavi *et al.*, 2021)
-	*Pseudomonas fluorescens*	Alkane hydroxylases	-	(Mohanan *et al.*, 2020)

Table A1.1 (continued)

Isolated source	*Bacterium*	Enzymes	Biodegradation conditions	References
-	*Pseudomonas oleovarans*	Alkane hydroxylases	-	(Mohanan *et al.*, 2020)
Contaminated site	*Pseudomonas plecoglossicida*	-	-	(Matjasic *et al.*, 2020)
-	*Pseudomonas putida*	-	Incubation time 120 days, 9 % weight loss	(Taghavi *et al.*, 2021)
-	*Pseudomonas putida*	Alkane hydroxylases	-	(Mohanan *et al.*, 2020)
-	*Pseudomonas putida*	-	30 % weight loss after 1 month	(Zhang *et al.*, 2022)
-	*Pseudomonas putida*	Alkane hydroxylases	-	(Mohanan *et al.*, 2020)
-	*Pseudomonas putida IRN22*	-	-	(Mohanan *et al.*, 2020)
-	*Pseudomonas putida KT2440 (ATCC 47054)*	-	-	(Jacquim *et al.*, 2019)
-	*Pseudomonas sp.*	-	Incubation time 30 days, 20,54 % weight loss	(Taghavi *et al.*, 2021)
Mangrove soil	*Pseudomonas sp.*	-	Incubation time- 1 month, PE, 20,54 % weight loss	(Montazer *et al.*, 2020)
Beach soil contaminated with crude oil	*Pseudomonas sp.*	-	Incubation time- 80 days, 37℃ LMWPED, 4,9 %- 28,6 % CO2 production	(Montazer *et al.*, 2020)
Garbage soil	*Pseudomonas sp.*	-	Incubation time- 6 months, PE bags, 37,09 % weight loss	(Montazer *et al.*, 2020)
-	*Pseudomonas sp.*	-	Incubation time- 2 months, Pretreated LDPE 50,5 % weight loss	(Montazer *et al.*, 2020)
Waste disposal site	*Pseudomonas sp.*	-	Incubation time- 3 weeks, Pretreated PE, 40,5 % weight loss	(Montazer *et al.*, 2020)
Contaminated site	*Pseudomonas sp.*	-		(Matjasic *et al.*, 2020)
Mangrove soil	*Pseudomonas sp.*	-	20,54 % weight loss after 1 month	(Zhang *et al.*, 2022)
Waste Disposal site	*Pseudomonas sp.*	-	37,5 % weight loss after 3 weeks	(Zhang *et al.*, 2022)
Garbage soil	*Pseudomonas sp.*	-	37,09 % weight loss after 6 months	(Zhang *et al.*, 2022)
-	*Pseudomonas sp.*	-	Incubation time- 40 days, weight loss- 28,6 % in sterilized compost conditions	(Wilkes *et al.*, 2017)
-	*Pseudomonas sp. AKS2*	Hydrolase	-	(Wilkes *et al.*, 2017)

Table A1.1 (continued)

Isolated source	*Bacterium*	Enzymes	Biodegradation conditions	References
-	*Pseudomonas sp. E4*	Alkene monooxygenase	-	(Amobonye *et al.*, 2021; Wilkes *et al.*, 2017)
-	*Pseudomonas sp. E4*	Alkane hydroxylase	-	(Atanasova, Stoitsova, *et al.*, 2021)
Dumpsites	*Pseudomonas sp. GMB7*	-	Incubation time- 30 days, reduction of 12–15 % in plastic weight	(Ali *et al.*, 2021)
Soil	*Pseudomonas spp.*	-	Incubation time- 180 days, reduction of 24,2 % weight	(Ali *et al.*, 2021)
Water and soil	Pseudomonas spp.	-	Incubation time- 90 days, weight reduction of 35-40 %, production of extracellular lipase observed	(Ali *et al.*, 2021)
-	*Pseudomonas syringae*	-	Incubation time 120 days, 11,3 % weight loss	(Taghavi *et al.*, 2021)
-	*Pseudomonas syringae*	-	-	(Mohanan *et al.*, 2020)
-	*Pseudomonas syringae DC3000 (ATCC 10862)*	-	-	(Jacquim *et al.*, 2019)
Contaminated site	*Pseudomonas thivervalensis*	-	-	(Matjasic *et al.*, 2020)
-	*Rahnella aquatilis*	-	-	(Nowak et al., 2011)
-	*Rhodococcus rhodochrous*	-	Incubation time 240 days	(Taghavi *et al.*, 2021)
-	*Rhodococcus rhodochrous ATCC29672*	-	-	(Kale *et al.*, 2015)
-	*Rhodococcus rhorocuros*	-	Incubation time- 6 months, 27℃ degradable PE, 60 % mineralization	(Montazer *et al.*, 2020)
-	*Rhodococcus rhorocuros*	-	Incubation time - 6 months, PE containing prooxidant additives, different amounts of mineralization	(Montazer *et al.*, 2020)
-	*Rhodococcus rhorocuros*	-	Surface and structural changes after 6 months	(Zhang *et al.*, 2022)
-	*Rhodococcus rubber*	Laccase	Incubation time- 30 days, weight loss- 2,5 %	(Ahmed *et al.*, 2018; Amobonye *et al.*, 2021; Ru et al, 2020)
Treated PE	*Rhodococcus rubber C208*	-	Incubation time 56 days, 7,5 % weight loss	(Taghavi *et al.*, 2021)
PE agricultural waste in soil	*Rhodococcus ruber*	-	Incubation time- 4 weeks, Treated LDPE, 8 % weight loss	(Montazer *et al.*, 2020)
PE agricultural waste in soil	*Rhodococcus ruber*	-	Incubation time- 60 days, LDPE, 0,86 % weight loss/week	(Montazer *et al.*, 2020)

Table A1.1 (continued)

Isolated source	*Bacterium*	Enzymes	Biodegradation conditions	References
PE agricultural waste in soil	*Rhodococcus ruber*	-	Incubation time- 30 days, LDPE, 1,5 %-2,5 % weight loss, 20 % reduction in molecular weight	(Montazer *et al.*, 2020)
-	*Rhodococcus ruber*	-	-	(Bahl *et al.*, 2021; Jacquim *et al.*, 2019; Kale *et al.*, 2015; Shah *et al.*, 2008)
-	*Rhodococcus ruber*	Alkane hydroxylases	-	(Mohanan *et al.*, 2020)
-	*Rhodococcus ruber*	Laccase	-	(Atanasova, Stoitsova, *et al.*, 2021)
-	Rhodococcus ruber strain C208	-	-	(Kale *et al.*, 2015; Matjasic *et al.*, 2020,)
Waste disposal site	*Rhodococcus sp.*	-	Incubation time- 3 weeks, pre-treated PE, 33 % weight loss	(Montazer *et al.*, 2020)
Three forest soil	*Rhodococcus sp.*	-	Incubtation time- 30 days, LDPE coitainting prooxidant additives, adhesion	(Montazer *et al.*, 2020)
-	*Rhodococcus sp. TMP2*	Monoxygenase	-	(Atanasova, Stoitsova, *et al.*, 2021)
Waste Disposal site	*Rhodococcus spp.*		33 % weight loss after 3 weeks	(Zhang *et al.*, 2022)
-	*Rodococcus rubber*	Phenol oxidases	-	(Mohanan *et al.*, 2020)
-	*Sebaldella termitidis*		-	(Matjasic *et al.*, 2020)
Ground soil	*Serratia marcescens*	-	Reached 36 % in an incubation period of 70 days	(Ru *et al.*, 2020)
Soil	*Serratia marcescens*	-	Incubation time- 70 days, 36 % weight loss	(Ali *et al.*, 2021)
-	*Serratia sp.*	-	-	(Zhang *et al.*, 2022)
-	*Staphylococci*	-	-	(Matjasic *et al.*, 2020)
Various soil environment	*Staphylococcus arlettae*	-	Incubation time- 30 days, PE, 13,6 % weight loss	(Montazer *et al.*, 2020)
-	*Staphylococcus arlettae*	-	13,6 % weight loss after 30 days	(Zhang *et al.*, 2022)
-	*Staphylococcus cohnii*	-	-	(Nowak et al., 2011)
-	*Staphylococcus sp.*	-	-	(Matjasic *et al.*, 2020)
-	*Staphylococcus xylosus*	-	-	(Nowak et al., 2011)
Contaminated site	*Stenotrophomonas maltophilia*	-	-	(Matjasic *et al.*, 2020)
-	*Stenotrophomonas pavanii*	-	-	(Amobonye *et al.*, 2021)

Table A1.1 (continued)

Isolated source	*Bacterium*	Enzymes	Biodegradation conditions	References
-	*Stenotrophomonas pavanii*	-	-	(Amobonye *et al.*, 2021)
-	*Stenotrophomonas sp.*	-	-	(Jacquim *et al.*, 2019; Mohanan *et al.*, 2020)
Contaminated site	*Stenotrophomonas sp.*	-	-	(Matjasic *et al.*, 2020)
Solid waste dump site	*Stentrophomonas pavanii*	-	Incubtation time- 56 days, modified LDPE, degradation by FTIR	(Montazer *et al.*, 2020)
Plastic debris in soil	*Stentrophomonas sp.*	-	Incubation time- 90 days, non-treated LDPE, changing in chemical properties	(Montazer *et al.*, 2020)
-	*Streptococcus sp.*	-	-	(Matjasic *et al.*, 2020)
-	*Streptomyces albogriseolus LBX-2*	-	-	(Matjasic *et al.*, 2020)
-	*Streptomyces badius*	-	-	(Zhang *et al.*, 2022)
-	*Streptomyces badius 252*	-	-	(Ali *et al.*, 2021)
-	*Streptomyces setonii*	-	-	(Zhang *et al.*, 2022)
-	*Streptomyces setonii 75Vi2*	-	-	(Ali *et al.*, 2021)
Nile River Delta	*Streptomyces sp.*	-	Incubation time- 1 month, 30℃ heat treated degradabel PE bags, slight weight loss	(Montazer *et al.*, 2020)
-	*Streptomyces sp.*	-	-	(Amobonye *et al.*, 2021; Shah *et al.*, 2008; Zhang *et al.*, 2022)
Soil	*Streptomyces spp.*	-	Incubation time- 180 days, reduction of 46,7 % weight	(Ali *et al.*, 2021)
-	*Streptomyces viridosporus*	-	Weight loss, 4-8 weeks of incubation- heat and UV treted PE	(Zhang *et al.*, 2022)
-	*Streptomyces viridosporus T7A*	-	-	(Ali *et al.*, 2021)
-	*Tremetesversicolor*	Laccase	-	(Iram *et al.*, 2019)

Table A1.2: Bacteria reported as LDPE biodegraders, and information on the isolation source, possible enzymes involved in the biodegradation and the biodegradation conditions

Isolated source	*Bacterium*	Enzymes	Biodegradation conditions	References
-	*Acinetobacter baumannii*	-	-	(Ghatge *et al.*, 2020)
Contaminated site	*Acinetobacter pitti*	-	-	(Matjasic *et al.*, 2020)
-	*Acinetobacter pittii IRN19*	-	-	(Mohanan *et al.*, 2020)
-	*Acinetobacter sp. 351*	Hydrolase	-	(Jaiswal *et al.*, 2020)
Contaminated soil	*Acinetobacter ursingii*	-	-	(Munir *et al.*, 2018)
Mediterranean Sea	*Alcanivorax borkumensis*	-	Incubation time- 7 days, weight loss- 3,5 %	(Ru *et al.*, 2020)
Contaminated site	*Alcanivorax borkumensis*	-	-	(Matjasic *et al.*, 2020)
Sewage treatment plants and waste management landfills	*Aneurinibacillus sp.*	-	-	(Zhang *et al.*, 2022)
-	*Arthrobacter globiformis*	-	-	(Matjasic *et al.*, 2020)
-	*Arthrobacter oxydans*	-	-	(Matjasic *et al.*, 2020)
-	*Arthrobacter paraffineus*	-	-	(Ghatge *et al.*, 2020; Matjasic *et al.*, 2020; Zhang *et al.*, 2022)
-	*Arthrobacter viscosus*	-	-	(Ghatge *et al.*, 2020)
-	*Aspergillus japonicas*	-	-	(Jaiswal *et al.*, 2020)
-	*Aspergillus terreus*	-	-	(Jaiswal *et al.*, 2020)
-	*Bacillus amyloliquefaciens*	-	-	(Ghatge *et al.*, 2020)
Solid waste	*Bacillus amyloliquefaciens BSM-1*	-	11 % weight loss after 60 days	(Zhang *et al.*, 2022)
Solid waste	*Bacillus amyloliquefaciens BSM-2*	-	16 % weight loss after 60 days	(Zhang *et al.*, 2022)
Contaminated site	*Bacillus cereus*	-	-	(Matjasic *et al.*, 2020)
-	*Bacillus cereus*	-	-	(Matjasic *et al.*, 2020; Ghatge *et al.*, 2020; Zhang *et al.*, 2022)

Table A1.2 (continued)

Isolated source	*Bacterium*	Enzymes	Biodegradation conditions	References
Marina water	*Bacillus cereus BF20*	-	-	(Ru *et al.*, 2020)
-	*Bacillus circulans*	-	-	(Ghatge *et al.*, 2020)
-	*Bacillus halodenitrifcans*	-	-	(Ghatge *et al.*, 2020; Zhang *et al.*, 2022)
Solid waste dump site	*Bacillus licheniformis*	-	-	(Zhang *et al.*, 2022)
-	*Bacillus mycoides*	-	-	(Ghatge *et al.*, 2020)
Contaminated site	*Bacillus niacini*	-	-	(Matjasic *et al.*, 2020)
-	*Bacillus pacificus*	-	-	(Zhang *et al.*, 2022)
Contaminated site	*Bacillus pseudomycoides*	-	-	(Matjasic *et al.*, 2020)
-	*Bacillus pumilus*	-	-	(Zhang *et al.*, 2022)
Pelagic waters	*Bacillus pumilus M27*	-	1,5 % weight loss after 30 days	(Zhang *et al.*, 2022)
Contaminated site	*Bacillus safensis*	-	-	(Matjasic *et al.*, 2020)
Contaminated site	*Bacillus sp.*	-	-	(Matjasic *et al.*, 2020)
-	Bacillus sp.	-	Incubation time 60 days, 10,7 % weight loss	(Miri *et al.*, 2022)
-	*Bacillus sp.*	-	Elongation at brake of 98 % in their mechanical properties, incubation time 225 days	(Zhang *et al.*, 2022)
Contaminated site	*Bacillus sp. ISJ55*	-	-	(Matjasic *et al.*, 2020)
Landfill soil	*Bacillus sp. strain SM1*	-	18,9 % weight loss after 180 days	(Zhang *et al.*, 2022)
Gut of waxworm	*Bacillus sp. YP1*	-	Incubation time 60 days, weight loss- 6 %- 11 %	(Ru *et al.*, 2020)
-	*Bacillus sp. YP1*	-	10,7 % weight loss after 60 days	(Zhang *et al.*, 2022)
-	*Bacillus sp. YP2*	-	-	(Matjasic *et al.*, 2020)
-	*Bacillus sphericus*	-	-	(Ghatge *et al.*, 2020; Matjasic *et al.*, 2020)
Shallow waters of ocean	*Bacillus sphericus*	-	19 % weight loss in thermal treated LDPE	(Zhang *et al.*, 2022)
Marina water	*Bacillus sphericus Alt*	-	Incubation time- 180 days, weight loss- 2,5 %-10 %	(Ru *et al.*, 2020)
-	*Bacillus spp.*	-	-	(Matjasic *et al.*, 2020)
Garbage soil	*Bacillus spp.*	-	-	(Munir *et al.*, 2018)

Table A1.2 (continued)

Isolated source	*Bacterium*	Enzymes	Biodegradation conditions	References
Contaminated site	*Bacillus subtilis*	-	-	(Matjasic *et al.*, 2020)
Marina water	*Bacillus subtilis H1584*	-	Incubation time- 30 days, weight loss- 1,75 %	(Ru *et al.*, 2020)
Pelagic waters	*Bacillus subtilis H1584*	-	1,75 % weight loss after 30 days	(Zhang *et al.*, 2022)
-	*Bacillus subtilis MTCC 9447*	-	-	(Matjasic *et al.*, 2020)
-	*Bacillus thuringienesis*	-	-	(Ghatge *et al.*, 2020)
Contaminated site	*Bacillus toyonensis*	-	-	(Matjasic *et al.*, 2020)
Garbage soil	*Bacillus weihenstephanensis*	-	-	(Munir *et al.*, 2018)
-	*Bacilus pumilus*	-	-	(Ghatge *et al.*, 2020)
Soil	*Brevibaccillus borstelensis strain 707*	-	Incubation time 30 days, at 50℃, 30 % molecular weight reduction	(Kale *et al.*, 2015)
Soil	*Brevibaccillus borstelensis strain 707*	-	Gravimetric weight loss 11 %, molecular weight loss 30 % after 30 days, in branched LDPE	(Zhang *et al.*, 2022)
Contaminated site	*Brevibacillus borstelensis*	-	-	(Matjasic *et al.*, 2020)
-	*Brevibacillus borstelensis*	-	-	(Ghatge *et al.*, 2020)
-	*Brevibacillus sp.*	-	-	(Jaiswal *et al.*, 2020)
Sewage treatment plants and waste management landfills	*Brevibacillus sp.*	-	-	(Zhang *et al.*, 2022)
-	*Burkholderia cepacia*	-	-	(Munir *et al.*, 2018)
-	*Cellulosimicrobium funkei*	-	-	(Ali *et al.*, 2021)
Contaminated site	*Cellulosimicrobium funkei*	-	-	(Matjasic *et al.*, 2020)
Wastewater activated sludge soil	*Chryseobacterium gleum EY1*	-	-	(Zhang *et al.*, 2022)
Contaminated site	*Citrobacter amalonaticus*	-	-	(Matjasic *et al.*, 2020)
-	*Comamonas sp*	-	-	(Zhang *et al.*, 2022)

Table A1.2 (continued)

Isolated source	*Bacterium*	Enzymes	Biodegradation conditions	References
The gut of mealworms (Tenebrio molitor)	*Citrobacter sp. and Kosakonia sp.*	-	49,0 ± 1,4 % of the ingested PE was converted to CO2 and 40,1 ± 8,5 % Mn decrease	(Zhang *et al.*, 2022)
-	*Delftia sp.*	-	-	(Zhang *et al.*, 2022)
Contaminated site	*Delftia tsuruhatensis*	-	-	(Matjasic *et al.*, 2020)
Garbage soil	*Diplococcus spp.*	-	-	(Munir *et al.*, 2018)
-	*Enterobacter asburiae*	-	-	(Matjasic *et al.*, 2020)
Gut of waxworm	*Enterobacter asburiae YT1*	-	Incubation time 60 days, weight loss- 6 %- 11 %	(Ru *et al.*, 2020)
-	*Enterobacter asburiae YT1*	-	6,1 % weight loss after 60 days	(Zhang *et al.*, 2022)
-	*Enterobacter cloacae AKS7*	-	-	(Matjasic *et al.*, 2020)
Soil	*Enterobacter sp.*	-	Incubation time- 120 days, reduction of 81 % in weight for LDPE strips and pellets	(Ali *et al.*, 2021)
-	*Enterobacter spp.*	-	-	(Matjasic *et al.*, 2020)
Contaminated site	*Escherichia coli*	-	-	(Matjasic *et al.*, 2020)
-	*Escherichia coli*	-	-	(Munir *et al.*, 2018)
Contaminated site	*Klebsiella sp.*	-	-	(Matjasic *et al.*, 2020)
Pelagic waters	*Kocuria palustris M16*	-	1 % weight loss after 30 days	(Zhang *et al.*, 2022)
The gut of yellow mealworm (Tenebrio molitor)	*Lactobacillus and Mucispirillum*	-	-	(Zhang *et al.*, 2022)
-	*Lysinibacillus macroides*	-	-	(Ali *et al.*, 2021)
Contaminated site	*Lysinibacillus macroides*	-	-	(Matjasic *et al.*, 2020)
Landfill soils	*Lysinibacillus xylanilyticus*	-	29,5 % mineralization for UV-radiated films; 15,8 % mineralization for non-UV-treated films	(Zhang *et al.*, 2022)
-	*Microbacterium paraoxydans*	-	-	(Ghatge *et al.*, 2020; Matjasic *et al.*, 2020)
-	*Microbacterium paraoxydans*	-	61,0 % weight loss after 2 months	(Zhang *et al.*, 2022)

Table A1.2 (continued)

Isolated source	*Bacterium*	Enzymes	Biodegradation conditions	References
Marine pulp mill wastes rich in lignin	*Microbulbifer hydrolyticus IRE*	-	-	(Zhang *et al.*, 2022)
-	*Micrococcus luteous*	-	-	(Ghatge *et al.*, 2020)
Contaminated site	*Micrococcus luteus*	-	-	(Matjasic *et al.*, 2020)
-	*Micrococcus luteus IRN20*	-	-	(Mohanan *et al.*, 2020)
-	*Micrococcus lylae*	-	-	(Ghatge *et al.*, 2020)
Waste dumps and farmlands	*Micrococcus sp.*	-	-	(Zhang *et al.*, 2022)
-	*Moraxella spp*	-	-	(Munir *et al.*, 2018)
-	*Nocardia asteroids*	-	-	(Ghatge *et al.*, 2020)
Contaminated site	*Ochrobactrum intermedium*	-	-	(Matjasic *et al.*, 2020)
Contaminated site	*Ochrobactrum oryzae*	-	-	(Matjasic *et al.*, 2020)
Contaminated site	*Ochrobactrum pseudintermedium*	-	-	(Matjasic *et al.*, 2020)
Domestic sewage water	*Oscillatoria subbrevis*	-	Incubation time- 42 days	(Ru *et al.*, 2020)
Contaminated site	*Oscillatoria subbrevis*	-	-	(Matjasic *et al.*, 2020)
-	*Paenibacillus macerans*	-	-	(Ghatge *et al.*, 2020)
Contaminated site	*Paenibacillus sp.*	-	-	(Matjasic *et al.*, 2020)
-	*Paenibacillus spp.*	-	-	(Matjasic *et al.*, 2020)
Soil	*Pantoea sp.*	-	Incubation time- 120 days, reduction of 38 % in weight for LDPE strips and pellets	(Ali *et al.*, 2021; Jaiswal *et al.*, 2020)
-	*Pantoea spp*	-	-	(Matjasic *et al.*, 2020)
Domestic sewage water	*Phormidium lucidum*	-	Incubation time- 42 days	(Ru *et al.*, 2020)
Contaminated site	*Phormidium lucidum*	-	-	(Matjasic *et al.*, 2020)
-	*Proteus spp.*	-	-	(Matjasic *et al.*, 2020)
-	*Pseudomonas aeroginosa*	-	11 % weight loss after 120 days	(Zhang *et al.*, 2022)
Contaminated site	*Pseudomonas aeruginosa*	-	-	(Matjasic *et al.*, 2020)

Table A1.2 (continued)

Isolated source	*Bacterium*	Enzymes	Biodegradation conditions	References
Contaminated soil	*Pseudomonas aeruginosa*	-	-	(Munir *et al.*, 2018)
-	*Pseudomonas aeruginosa*	-	-	(Ghatge *et al.*, 2020)
-	*Pseudomonas aeruginosa*	-	50,5 % weight loss after 2 months	(Zhang *et al.*, 2022)
Waste dumps and farmlands	*Pseudomonas aeruginosa*	-	-	(Zhang *et al.*, 2022)
-	*Pseudomonas aeruginosa ATCC 15692*	-	-	(Matjasic *et al.*, 2020)
-	*Pseudomonas aeruginosa PAO1*	-	20 % weight loss after 120 days	(Zhang *et al.*, 2022)
-	*Pseudomonas aeruginosa PAO1 ATCC 15729*	-	-	(Matjasic *et al.*, 2020)
Contaminated site	*Pseudomonas aeruginosa SKN1 (ID: 9702593)*	-	-	(Matjasic *et al.*, 2020)
Municipal landfill	*Pseudomonas citronellolis*	-	17,8 % weight loss after 4 days	(Zhang *et al.*, 2022)
Contaminated site	*Pseudomonas citronellolis EMBS027 KF361478*	-	-	(Matjasic *et al.*, 2020)
Contaminated soil	*Pseudomonas fluorescens*	-	-	(Munir *et al.*, 2018)
-	*Pseudomonas fluorescens*	-	-	(Ghatge *et al.*, 2020)
-	*Pseudomonas mucidolens*	-	-	(Zhang *et al.*, 2022)
Contaminated site	*Pseudomonas putida*	-	-	(Matjasic *et al.*, 2020)
-	*Pseudomonas putida*	-	9 % weight loss after 120 days	(Zhang *et al.*, 2022)
-	*Pseudomonas putida IRN22*	-	-	(Mohanan *et al.*, 2020)
-	*Pseudomonas putida KT2440 ATCC 47054*	-	-	(Matjasic *et al.*, 2020)
-	*Pseudomonas putida LS46*	-	-	(Mohanan *et al.*, 2020)
-	*Pseudomonas putida MTCC 2445*	-	-	(Matjasic *et al.*, 2020)
-	*Pseudomonas siringae*	-	11,3 % weight loss after 120 days	(Zhang *et al.*, 2022)

Table A1.2 (continued)

Isolated source	*Bacterium*	Enzymes	Biodegradation conditions	References
Waste dumping soil	*Pseudomonas sp. AKS2*	-	Incubation time- 45 days, weight loss- 5 %	(Ru *et al.*, 2020)
-	*Pseudomonas sp. AKS2*	-	Incubation time- 45 days, degradation 5± 1 %	(Jaiswal *et al.*, 2020)
-	*Pseudomonas sp. AKS2*	-	-	(Ghatge *et al.*, 2020)
-	*Pseudomonas sp. AKS2*	-	1,65 mg/day degradation rate, 12 days incubation time	(Zhang *et al.*, 2022)
-	*Pseudomonas sp. E4*	-	-	(Jaiswal *et al.*, 2020)
Beach soil contaminated with crude oi	*Pseudomonas sp. E4*	-	-	(Zhang *et al.*, 2022)
Contaminated site	*Pseudomonas spp.*	-	-	(Matjasic *et al.*, 2020)
-	*Pseudomonas spp.*	-	-	(Matjasic *et al.*, 2020)
-	*Pseudomonas stutzeri*	-	-	(Jaiswal *et al.*, 2020)
Contaminated site	*Pseudomonas stutzeri*	-	-	(Matjasic *et al.*, 2020)
-	*Pseudomonas stutzeri MTCC 2643*	-	-	(Matjasic *et al.*, 2020)
-	*Pseudomonas syringae DC 3000 ATCC 10862*	-	-	(Matjasic *et al.*, 2020)
-	*Rahnella aquatilis*	-	-	(Ghatge *et al.*, 2020)
Landfill soil	*Ralstonia sp. strain SKM2*	-	18,9 % weight loss after 180 days	(Zhang *et al.*, 2022)
-	*Rhodococcus rhodochrous*	-	-	(Ghatge *et al.*, 2020; Mohanan *et al.*, 2020)
Soil of disposal site	*Rhodococcus ruber C208*	-	Incubation time- 30 days, weight loss- 4 %	(Ru *et al.*, 2020)
-	*Rhodococcus ruber C208*	-	Rate of degradation 0,86 %/week	(Jaiswal *et al.*, 2020)
-	*Rhodococcus ruber C208*	-	-	(Ghatge *et al.*, 2020)
PE agricultural waste in soil	*Rhodococcus ruber C208*	-	8 % weight loss after 30 days incubation, in UV-treated LDPE	(Zhang *et al.*, 2022)
PE agricultural waste in soil	*Rhodococcus ruber C208*	-	0,86 % weight loss per week, for 60 days	(Zhang *et al.*, 2022)
PE agricultural waste in soil	*Rhodococcus ruber C208*	-	1,5-2,5 % weight loss after 30 days, branched LDPE film	(Zhang *et al.*, 2022)

Table A1.2 (continued)

Isolated source	*Bacterium*	Enzymes	Biodegradation conditions	References
Three forest soil Waste	*Rhodococcus sp.*	-	-	(Zhang *et al.*, 2022)
Contaminated site	*Spingobacterium multivorum*	-	-	(Matjasic *et al.*, 2020)
-	*Staphylococcus cohnii*	-	-	(Ghatge *et al.*, 2020)
-	*Staphylococcus epidermidis*	-	-	(Ghatge *et al.*, 2020; Zhang *et al.*, 2022)
Contaminated site	*Staphylococcus sp.*	-	-	(Matjasic *et al.*, 2020)
Garbage soil	*Staphylococcus spp.*	-	-	(Munir *et al.*, 2018)
-	*Staphylococcus xylosus*	-	-	(Ghatge *et al.*, 2020)
Contaminated site	*Stenotrophomonas humi*	-	-	(Matjasic *et al.*, 2020)
Contaminated site	*Stenotrophomonas maltophilia*	-	-	(Matjasic *et al.*, 2020)
Contaminated site	*Stenotrophomonas pavanii CC18*	-	-	(Matjasic *et al.*, 2020)
-	*Stenotrophomonas spp.*	-	-	(Matjasic *et al.*, 2020)
Solid waste dump site	*Stentrophomonas pavanii*	-	-	(Zhang *et al.*, 2022)
Contaminated site	*Streptococcus*	-	-	(Matjasic *et al.*, 2020)
Garbage soil	*Streptococococcus spp.*	-	-	(Munir *et al.*, 2018)
-	*Streptomyces badius*	-	-	(Jaiswal *et al.*, 2020)
-	*Streptomyces viridosporous*	-	-	(Jaiswal *et al.*, 2020)
-	*Streptomyces setnii*	-	-	(Jaiswal *et al.*, 2020)

Table A1.3: Bacteria reported as HDPE biodegraders, and information on the isolation source, possible enzymes involved in the biodegradation and the biodegradation conditions

Isolated source	*Bacterium*	Enzymes	Biodegradation conditions	References
Soil	*Achromobacter xylosoxidans*	-	Incubation time- 150 days, weight loss- 9.38 %	(Ru *et al.*, 2020)
Contaminated site	*Achromobacter xylosoxidans PE-1*	-	-	(Matjasic *et al.*, 2020)

Table A1.3 (continued)

Isolated source	*Bacterium*	Enzymes	Biodegradation conditions	References
Contaminated site	*Acinetobacter sp.*	-	-	(Matjasic *et al.*, 2020)
-	*Aneurinibacillus sp.*	-	-	(Zhang *et al.*, 2022)
-	*Arthrobacter paraffineus*	-	-	(Ghatge *et al.*, 2020)
-	*Arthrobacter sp.*	-	-	(Ghatge *et al.*, 2020; Jaiswal *et al.*, 2020)
-	*Arthrobacter sp.*	-	12 % weight loss after 30 days	(Zhang *et al.*, 2022)
Plastic waste dumpsite	*Arthrobacter sp. GMB5*	-	Incubation time- 30 days, weight loss- 12 % -15 %	(Ru *et al.*, 2020)
Contaminated site	*Arthrobacter sp. GMB5*	-	-	(Matjasic *et al.*, 2020)
-	*Aspergillus flavus*	-	-	(Jaiswal *et al.*, 2020)
Contaminated site	*Bacillus amyloliquefaciens*	-	-	(Matjasic *et al.*, 2020)
Contaminated site	*Bacillus aryabhattai*	-	-	(Matjasic *et al.*, 2020)
Contaminated site	*Bacillus cereus*	-	-	(Matjasic *et al.*, 2020)
Contaminated site	*Bacillus licheniformis*	-	-	(Matjasic *et al.*, 2020)
Contaminated site	*Bacillus pumilus*	-	-	(Matjasic *et al.*, 2020)
-	*Bacillus sp. BCBT21*	-	-	(Jaiswal *et al.*, 2020)
-	*Bacillus sphericus*	-	-	(Ghatge *et al.*, 2020)
Shallow waters of ocean	*Bacillus sphericus*	-	9 % weight loss with thermal treated HDPE	(Zhang *et al.*, 2022)
-	*Bacillus spp.*	-	-	(Matjasic *et al.*, 2020)
Contaminated site	*Bacillus subtilis*	-	-	(Matjasic *et al.*, 2020)
-	*Bravibacillus sphericus*	-	-	(Matjasic *et al.*, 2020)
-	*Brevibacillus borstelensis KY49486*	-	-	(Matjasic *et al.*, 2020)
-	*Brevibacillus sp.*	-	-	(Zhang *et al.*, 2022)
-	*Comamonas acidovorans*	-	-	(Jaiswal *et al.*, 2020)
-	*Klebsiekka pneumonia CH001*	-	-	(Jaiswal *et al.*, 2020)
-	*Klebsiella pneumonia*	-	-	(Ghatge *et al.*, 2020)
Wastewater	*Klebsiella pneumonia CH001*	-	18,4 % weight loss after 60 days	(Zhang *et al.*, 2022)

Table A1.3 (continued)

Isolated source	*Bacterium*	Enzymes	Biodegradation conditions	References
Contaminated site	*Klebsiella pneumoniae CH001*	-	-	(Matjasic *et al.*, 2020)
Contaminated site	*Leucobacter sp.*	-	-	(Matjasic *et al.*, 2020)
Contaminated site	*Micrococcus sp.*	-	-	(Matjasic *et al.*, 2020)
-	*Nocardia asteroids*	-	-	(Ghatge *et al.*, 2020)
-	*Paenibacillus spp*	-	-	(Matjasic *et al.*, 2020)
-	*Penicillium oxalicum NS4*	-	-	(Jaiswal *et al.*, 2020)
-	*Pseudomonas aeruginosa*	-	Incubation time 2 months, weight loss 50.5 % after pre-treatments	(Wilkes *et al.*, 2017)
Contaminated site	*Pseudomonas aeruginosa*	-	-	(Matjasic *et al.*, 2020)
-	*Pseudomonas fluorescen*	-	-	(Matjasic *et al.*, 2020)
-	*Pseudomonas putida S3A*	-	-	(Jaiswal *et al.*, 2020)
-	*Pseudomonas sp.*	-	-	(Ghatge *et al.*, 2020)
-	*Pseudomonas sp.*	-	15 % weight loss after 30 days	(Zhang *et al.*, 2022)
-	*Pseudomonas sp. AKS2*	-	Incubation time- 45 days, weight loss of 5 %	(Wilkes *et al.*, 2017)
Plastic waste dumpsite	*Pseudomonas sp. GMB7*	-	Incubation time- 30 days, weight loss- 12 % -15 %	(Ru *et al.*, 2020)
Contaminated site	*Pseudomonas sp. GMB7*	-	-	(Matjasic *et al.*, 2020)
-	*Pseudomonas spp.*	-	-	(Matjasic *et al.*, 2020)
-	*Rhodococcus rhodochrous*	-	-	(Ghatge *et al.*, 2020)
-	*Rhodococus sp.*	-	-	(Jaiswal *et al.*, 2020)
-	Serratia marcescens	-	-	(Matjasic *et al.*, 2020)
Contaminated site	*Staphylococcus sp.*	-	-	(Matjasic *et al.*, 2020)
-	*Stenotrophomonas spp.*	-	-	(Matjasic *et al.*, 2020)
Soybean	-	Peroxidase	-	(Ru *et al.*, 2020)

Table A1.4: Fungi reported as PE biodegraders, and information on the isolation source, possible enzymes involved in the biodegradation and the biodegradation conditions

Isolated source	*Fungi*	Enzymes	Biodegradation conditions	References
-	*Amycolaptosis sp.*	Manganese peroxidase	-	(Iram *et al.*, 2019)
-	*Aspergillus awamori*	-	-	(Montazer *et al.*, 2020)
-	*Aspergillus clavatus*	-	-	(Amobonye *et al.*, 2021)
-	*Aspergillus flavus*	-	-	(Alshehrei, 2017; Jacquim *et al.*, 2019; Kale *et al.*, 2015; Montazer *et al.*, 2020; Shah et a., 2008; Zhang *et al.*, 2022)
-	*Aspergillus flavus*	Laccase	-	(Amobonye *et al.*, 2021)
-	*Aspergillus flavus*	-	*Incubation time of 28 days, 3,9 % of weight loss*	(Taghavi *et al.*, 2021)
-	*Aspergillus flavus*	-	*Incubation time of 100 days, 5,5 % of weight loss*	(Taghavi *et al.*, 2021)
Plastic buried in soil	*Aspergillus flavus*	-	*Efficiently broke down PE after 2 months*	(Santacruz-ju *et al.*, 2021)
Soil	*Aspergillus flavus and Aspergillus tubingensis*	-	*Incubation time-30 days, biofilm formation, weight loss, and HDPE surface modification*	(Ali *et al.*, 2021)
-	*Aspergillus fumigatus*	-		(Amobonye *et al.*, 2021)
-	*Aspergillus fumigatus*	-	*Incubation time of 30 days, 2,49 % of weight loss*	(Taghavi *et al.*, 2021)
-	*Aspergillus glaucus*	-	-	(Jacquim *et al.*, 2019)
-	*Aspergillus glaucus*	-	*Incubation time of 30 days, 28,8 % of weight loss*	(Taghavi *et al.*, 2021)
Soil	*Aspergillus japonicas*	-	*Incubation time- 30 days36 % loss of LDPE weight*	(Ali *et al.*, 2021)
-	*Aspergillus japonicas*	-	*Incubation time of 30 days, 11,11 % of weight loss*	(Taghavi *et al.*, 2021)
-	*Aspergillus niger*	-	-	(Jacquim *et al.*, 2019)
-	*Aspergillus niger*	-	*Incubation time of 30 days, 17,35 % of weight loss*	(Taghavi *et al.*, 2021)
-	*Aspergillus niger*	-	*Incubation time of 30 days, 4,32 % of weight loss*	(Taghavi *et al.*, 2021)
-	*Aspergillus niger*	-	*Incubation time of 30 days, 5,8 % of weight loss*	(Taghavi *et al.*, 2021)
Plastic buried in soil	*Aspergillus niger*	-	-	(Santacruz-ju *et al.*, 2021)
-	*Aspergillus nomius*	-	-	(Amobonye *et al.*, 2021)
-	*Aspergillus oryzae*	-	-	(Amobonye *et al.*, 2021)
-	*Aspergillus oryzae*	-	*Incubation time 3 months, 47,2 % weight loss*	(Kale *et al.*, 2015)

Table A1.4 (continued)

Isolated source	*Bacterium*	Enzymes	Biodegradation conditions	References
-	*Aspergillus oryzae*	-	*36 % weight reduction*	(Ali *et al.*, 2021)
-	*Aspergillus sp.*	-	-	(Jacquim *et al.*, 2019; Montazer *et al.*, 2020; Sankhla *et al.*, 2020)
-	*Aspergillus sydowii*	-	-	(Amobonye *et al.*, 2021)
-	*Aspergillus sydowii*	-	*Efficient biodegradation after 60 days incubation*	(Santacruz-ju *et al.*, 2021)
-	*Aspergillus sydowii PNPF15/TS*	-	-	(Miri *et al.*, 2022)
-	*Aspergillus terreus*	-	-	(Amobonye *et al.*, 2021)
-	*Aspergillus terreus*	-	*Efficient biodegradation after 60 days incubation*	(Santacruz-ju *et al.*, 2021)
-	*Aspergillus terreus AF5*	-	-	(Shah et a., 2008)
-	*Aspergillus terreus MANGFI/WL*	-	*28,4 % weight loss*	(Miri *et al.*, 2022)
Plastic buried in soil	*Aspergillus versicolor*	-	-	(Santacruz-ju *et al.*, 2021)
-	*Aspergillus versicolos*	-	*Incubation time of 90 days, 40,6 % of weight loss*	(Taghavi *et al.*, 2021)
Plastic buried in soil	*Chaetomium globosum*	-	-	(Santacruz-ju *et al.*, 2021)
-	*Chaetomium globsum*	La and MnP	-	(Kale *et al.*, 2015)
-	*Chaetomium sp.*	-	-	(Jacquim *et al.*, 2019)
Plastic buried in soil	*Chrysonilia setophila*	-	-	(Santacruz-ju *et al.*, 2021)
-	*Cladosporium cladosporioides*	-	-	(Montazer *et al.*, 2020; Zhang *et al.*, 2022)
-	*Cladosporium cladosporoide ATCC 20251*	-	-	(Kale *et al.*, 2015)
-	*Curvularia senegalensis*	-	-	(Sankhla *et al.*, 2020)
Landfill soil	*Fusarium falciforme*	-	-	(Zhang *et al.*, 2022)
Plastic buried in soil	*Fusarium oxysporum*	-	*Efficiently broke down PE after 2 months*	(Santacruz-ju *et al.*, 2021)
Landfill soil	*Fusarium oxysporum*	-	-	(Zhang *et al.*, 2022)
Plastic buried in soil	*Fusarium solani*	-	-	(Santacruz-ju *et al.*, 2021)
-	*Fusarium sp.*	-	-	(Montazer *et al.*, 2020)
Soil	*Fusarium sp.*	-	*Incubation time- 30 days36 % loss of LDPE weight*	(Ali *et al.*, 2021)
-	*Fusarium sp. AF4*	-	-	(Shah et a., 2008)

Table A1.4 (continued)

Isolated source	*Bacterium*	Enzymes	Biodegradation conditions	References
-	*Gliocladium virens*	-	-	(Jacquim *et al.*, 2019; Montazer *et al.*, 2020; Zhang *et al.*, 2022)
-	*Lasiodiplodia theobromae*	-	-	(Jacquim *et al.*, 2019; Sankhla *et al.*, 2020)
-	*Mortierella subtilissima*	-	-	(Montazer *et al.*, 2020)
Plastic buried in soil	*Mucor hiemalis*	-	-	(Santacruz-ju *et al.*, 2021)
-	*Mucor rouxii*	-	-	(Montazer *et al.*, 2020)
-	*Mucor rouxii*	-	*Slight weight reduction*	(Ali *et al.*, 2021)
-	*Mucor rouxii NRRL 1835*	-	-	(Alshehrei, 2017; Kale *et al.*, 2015; Shah et a., 2008)
-	*Nocardia asteroides*	-	-	(Montazer *et al.*, 2020)
-	*Paecilomyces lilacinus*	-	-	(Jacquim *et al.*, 2019; Sankhla *et al.*, 2020)
-	*Penicillium pinophilum*	-	-	(Jacquim *et al.*, 2019)
Treated PE	*Penicillium chrysogenum NS10*	-	*Incubation time of 90 days, 34,3-58,5 % of weight loss*	(Taghavi *et al.*, 2021)
-	*Penicillium frequentans*	-	*Incubation time of 60 days, 0,45 % of weight loss*	(Taghavi *et al.*, 2021)
Soil	*Penicillium oxalicum and Penicillium chrysogenum*	-	*Incubation time- 90 days, morphological damages on PE sheets*	(Ali *et al.*, 2021)
Treated PE	*Penicillium oxalicum NS4*	-	*Incubation time of 90 days, 36,6-55,3 % of weight loss*	(Taghavi *et al.*, 2021)
-	*Penicillium pinophilum*	-	*Incubation time of 942 days*	(Taghavi *et al.*, 2021)
-	*Penicillium pinophilum*	-	-	(Zhang *et al.*, 2022)
Treated PE	*Penicillium simplicissimum*	-	*Incubation time of 90 days, 38 % of weight loss*	(Taghavi *et al.*, 2021)
-	*Penicillium simplicissimum*	-	-	(Jacquim *et al.*, 2019; Montazer *et al.*, 2020; Zhang *et al.*, 2022)
-	*Penicillium simplicissimum*	-	*Incubation time 90 days, molecular weight reduction*	(Ali *et al.*, 2021)
-	*Penicillium simplicissimum YK*	-	-	(Alshehrei, 2017; Kale *et al.*, 2015; Sankhla *et al.*, 2020; Shah et a., 2008)
Plastic buried in soil	*Penicillium sp.*	-	-	(Santacruz-ju *et al.*, 2021)
Soil	*Penicillum simplicissimum YK*	-	-	(Zhang *et al.*, 2022)
-	*Penicillum sp. AF6*	-	-	(Shah et a., 2008)
-	*Phanerochaete chrysosporium*	Manganese peroxidase	-	(Jacquim *et al.*, 2019; Ru *et al.*, 2020)

Table A1.4 (continued)

Isolated source	*Bacterium*	Enzymes	Biodegradation conditions	References
-	*Phanerochaete chrysosporium*	-	-	(Zhang *et al.*, 2022)
Plastic buried in soil	*Phoma spp.*	-	*Efficiently broke down PE after 2 months*	(Santacruz-ju *et al.*, 2021)
-	*Pleurotis ostreatus*	Laccase	-	(Amobonye *et al.*, 2021)
Landill soil	*Purpureocillum lilacinum*	-	-	(Zhang *et al.*, 2022)
-	*Trarnetes versicolor*	Manganese peroxidase	-	(Amobonye *et al.*, 2021)
-	*Trichoderma harzianum*	-	-	(Sankhla *et al.*, 2020)
Soil sample of dumpsite	*Trichoderma harzianum*	-	*Biodegraded UV-treated PE*	(Santacruz-ju *et al.*, 2021)
-	*Zalerion maritimum*	-	-	(Montazer *et al.*, 2020)
Seawater	*Zalerion maritimum*	-	*Incubation time- 28 days, the pellets mass and size were decreased*	(Ali *et al.*, 2021)

Table A1.5: Fungi reported as LDPE biodegraders, and information on the isolation source, possible enzymes involved in the biodegradation and the biodegradation conditions

Isolated source	*Fungi*	Enzymes	Biodegradation conditions	References
Soil	*Acremonium kiliense*	-	-	(Zhang *et al.*, 2022)
Mangrove of Red Sea coast	*Alternaria alternate*	-	*Enzymatic activity observed after 4 weeks*	(Santacruz-ju *et al.*, 2021)
Mangrove of Red Sea coast	*Aspergillus caespitosus*	-	*Enzymatic activity observed after 4 weeks*	(Santacruz-ju *et al.*, 2021)
Film	*Aspergillus flavus*	-	-	(Ghatge *et al.*, 2020)
Garbage soil	*Aspergillus flavus*	-	*16 % weight reduction after 6 months*	(Santacruz-ju *et al.*, 2021)
Polyethylene polluted sites	*Aspergillus flavus*	-	*30 % weight loss after 4 weeks*	(Santacruz-ju *et al.*, 2021)
Aerobic aged municipal landfill	*Aspergillus fumigatus*	-	-	(Santacruz-ju *et al.*, 2021)
Polyethylene polluted sites	*Aspergillus japonicus*	-	*36 % weight loss after 4 weeks*	(Santacruz-ju *et al.*, 2021)
-	*Aspergillus niger*	-	-	(Munir *et al.*, 2018)
Thermal treated LDPE	*Aspergillus niger*	-	-	(Ghatge *et al.*, 2020)
Municipal solid waste	*Aspergillus niger*	-	*High biodegradation efficiency after 90 days*	(Santacruz-ju *et al.*, 2021)
Garbage soil	*Aspergillus niger*	-	*26 % weight reduction after 6 months*	(Santacruz-ju *et al.*, 2021)

Table A1.5 (continued)

Isolated source	*Bacterium*	Enzymes	Biodegradation conditions	References
Polyethylene polluted sites	*Aspergillus niger*	-	*Around 20 % weight loss after 4 weeks*	(Santacruz-ju *et al.*, 2021)
Landfill soils Municipal	*Aspergillus niger*	-	-	(Zhang *et al.*, 2022)
Landfill soil	*Aspergillus niger (a mixed culture with Lysinibacillus xylanilyticus)*	-	*16 % biodegradation for non-treated LDPE after 126 days; 29 % biodegradation for UV-treated LDPE, after 126 days*	(Santacruz-ju *et al.*, 2021)
Landfill soil	*Aspergillus nomius*	-	*Weight loss after 45 days of incubation*	(Santacruz-ju *et al.*, 2021)
-	*Aspergillus oryzae*	-	*Weight reduction after 4 months*	(Santacruz-ju *et al.*, 2021)
-	*Aspergillus sp.*	-	-	(Miri *et al.*, 2022)
Soil buried LDPE films	*Aspergillus sp.*	-	*Weight loss after 60 days*	(Santacruz-ju *et al.*, 2021)
Sea water	*Aspergillus sp.*	-	-	(Santacruz-ju *et al.*, 2021)
	Aspergillus terreus	-	-	(Munir *et al.*, 2018)
Mangrove of Red Sea coast	*Aspergillus terreus*	-	*Enzymatic activity observed after 4 weeks*	(Santacruz-ju *et al.*, 2021)
Aerobic aged municipal landfill	*Aspergillus terreus*	-	-	(Santacruz-ju *et al.*, 2021)
Se water	*Aspergillus versicolor*	-	-	(Santacruz-ju *et al.*, 2021)
Soil	*Aspergillus versicolor*	-	-	(Zhang *et al.*, 2022)
-	*Aureobasidium pullulans*	-	-	(Munir *et al.*, 2018)
Mangrove of Red Sea coast	*Eupenicillium hirayamae*	-	*Enzymatic activity observed after 4 weeks*	(Santacruz-ju *et al.*, 2021)
-	*Fusarium redolens*	-	-	(Ghatge *et al.*, 2020)
Garden soil	*Fusarium redolens*	-	-	(Zhang *et al.*, 2022)
Soil	*Fusarium redolens*	-	-	(Zhang *et al.*, 2022)
Aerobic aged municipal landfill	*Fusarium solani*	-	-	(Santacruz-ju *et al.*, 2021)
Polyethylene polluted sites	*Fusarium sp.*	-	*32 % weight loss after 4 weeks*	(Santacruz-ju *et al.*, 2021)
Soil buried LDPE films	*Fusarium sp.*	-	*Weight loss after 60 days*	(Santacruz-ju *et al.*, 2021)
Thermal treated LDPE	*Glioclodium virens*	-	-	(Ghatge *et al.*, 2020)
Polyethylene polluted sites	*Mucor sp.*	-	*Around 20 % weight loss after 4 weeks*	(Santacruz-ju *et al.*, 2021)

Table A1.5 (continued)

Isolated source	*Bacterium*	Enzymes	Biodegradation conditions	References
-	*Penicillium citrinum*	-	*15,29 % weight loss after 90 days*	(Zhang *et al.*, 2022)
-	*Paecilomyces varioti*	-	-	(Munir *et al.*, 2018)
Mangrove of Red Sea coast	*Paecilomyces varioti*	-	*Enzymatic activity observed after 4 weeks*	(Santacruz-ju *et al.*, 2021)
Soil sample from a plastic dumping	*Penicillium chrysogenum*	-	*Morphological damage after 60 days*	(Santacruz-ju *et al.*, 2021)
-	*Penicillium funiculosum*	-	-	(Munir *et al.*, 2018)
-	*Penicillium ochrochloron*	-	-	(Munir *et al.*, 2018)
Soil sample from a plastic dumping	*Penicillium oxalicum*	-	*Morphological damage after 60 days*	(Santacruz-ju *et al.*, 2021)
Polyethylene polluted sites	*Penicillium sp.*	-	*Around 20 % weight loss after 4 weeks*	(Santacruz-ju *et al.*, 2021)
-	*Penicillum sp.*	-	-	(Miri *et al.*, 2022)
Powder	*Penicillum pinophilum*	-	-	(Ghatge *et al.*, 2020)
-	*Penicillum pinophilum*	-	-	(Zhang *et al.*, 2022)
-	*Phanerochaete chrysosporium*	-	-	(Zhang *et al.*, 2022)
Mangrove of Red Sea coast	*Phialophora alba*	-	*Enzymatic activity observed after 4 weeks*	(Santacruz-ju *et al.*, 2021)
-	*Scopulariopsis brevicaulis*	-	-	(Munir *et al.*, 2018)
-	*Streptomyces sp.*	-	-	(Miri *et al.*, 2022)
-	*Trichoderma viride*	-	-	(Munir *et al.*, 2018)
Landfill soil	*Trichoderma viride*	-	*Weight loss after 45 days of incubation*	(Santacruz-ju *et al.*, 2021)
-	*Verticillium lecanii*	-	-	(Ghatge *et al.*, 2020)
Soil	*Verticillium lecanii*	-	-	(Zhang *et al.*, 2022)
-	*Zalerion maritimum*	-	*Weight loss of 6,5 %*	(Miri *et al.*, 2022)

Table A1.6: Fungi reported as HDPE biodegraders, and information on the isolation source, possible enzymes involved in the biodegradation and the biodegradation conditions

Isolated source	*Fungi*	Enzymes	Biodegradation conditions	References
Film	*Aspergillus flavus*	-	-	(Ghatge *et al.*, 2020)
Guts of wax moth Galleria mellonella	*Aspergillus flavus*	-	-	(Santacruz-ju *et al.*, 2021)
-	*Aspergillus sp.*	-	5.5 % weight loss after 100 days	(Zhang *et al.*, 2022)
Plastic waste dump yard	*Aspergillus terreus*	-	Observable weight loss after 30 days	(Santacruz-ju *et al.*, 2021)
Film	*Cephalosporium sp*	-	Weight decrease of 7.18 % after 20 days incubation	(Santacruz-ju *et al.*, 2021)
Garden soil	*Fusarium redolens*	-	-	(Zhang *et al.*, 2022)
Soil sample from a plastic dumping	*Penicillium chrysogenum*	-	Morphological damage in the film after 60 days	(Santacruz-ju *et al.*, 2021)
Soil sample from a plastic dumping	Penicillium oxalicum	-	Morphological damage in the film after 60 days	(Santacruz-ju *et al.*, 2021)
-	*Penicillium sp.*	-	-	(Zhang *et al.*, 2022)
UV treated	*Penicillum simplicissimum*	-	-	(Ghatge *et al.*, 2020)

Table A1.7: Bacteria reported as PET biodegraders, and information on the isolation source, possible enzymes involved in the biodegradation and the biodegradation conditions

Isolated source	*Bacterium*	Enzymes	Biodegradation conditions	References
-	*Actinomycete sp.*	-	-	(Amobonye *et al.*, 2021)
-	*Alteromonas macleodii*	-	-	(Miri *et al.*, 2022)
-	*Bacillus amyloliquefaciens*	-	-	(Jacquim *et al.*, 2019)
-	*Bacillus borstelensis*	-	-	(Ahmed *et al.*, 2018)
-	*Bacillus cereus*	-	Incubation time 40 days, 6,6 % weight loss	(Taghavi at al., 2021)
-	*Bacillus cereus*	-	-	(Matjasic *et al.*, 2020)
-	*Bacillus gottheilii*	-	Incubation time 40 days, 3 % weight loss	(Taghavi at al., 2021)
-	*Bacillus gottheilii*	-	-	(Matjasic *et al.*, 2020)
-	*Bacillus muralis*	-	-	(Matjasic *et al.*, 2020)
Thermobifida fusca	*Bacillus subtilis*	Cutinase de T.fusca TfCut2	Incubation time- 120h, 70℃, weight loss- 97 %	(Ru *et al.*, 2020)
-	*Bacillus subtilis*	-	Incubation time 24h at 30℃	(Mohanan *et al.*, 2020)
-	*Brevibacterium sp.*	-	-	(Matjasic *et al.*, 2020)

Table A1.7 (continued)

Isolated source	*Bacterium*	Enzymes	Biodegradation conditions	References
-	*Bacillus subtilis UCP 999*	-	Incubation time 60 days, 0,06 % weight loss	(Taghavi at al., 2021)
-	*Burkholderia spp.*	Lipase	-	(Mohanan *et al.*, 2020)
-	*Celeribacter neptunius*	-	-	(Miri *et al.*, 2022)
-	*Humicola insolens*	-	-	(Jacquim *et al.*, 2019)
-	*Ideonella sakaiensis*	PETase and MHETase	Incubation time- 1 day, weight loss 1 %	(Ali *et al.*, 2021)
-	*Ideonella sakaiensis*	PETase	-	(Miri *et al.*, 2022)
-	*Ideonella sakaiensis*	-	-	(Amobonye *et al.*, 2021; Jacquim *et al.*, 2019)
-	*Ideonella sakaiensis 201-F6*	-	-	(Ahmed *et al.*, 2018; Iram *et al.*, 2019; Matjasic *et al.*, 2020)
-	*Ideonella sakaiensis 201-f6*	-	Incubation time 42 days, 58 % weight loss	(Taghavi at al., 2021)
-	*Ideonella sakaiensis 201-F6*	Aromatic polyesterase Esterase	-	(Atanasova, Stoitsova, *et al.*, 2021)
-	*Ideonella sakaiensis 201-F6*	PETase and MHETase, Hydrolases, lipases	Incubation time- 1 days, 30℃, weight loss 1 %	(Jaiswal *et al.*, 2020; Ru *et al.*, 2020)
-	*Nocardia sp.*	-	-	(Jacquim *et al.*, 2019)
-	*Oleispira antarctica*	LipA	-	(Danso *et al.*, 2019)
-	*Oleispira antarctica RB-8*	PET5	-	(Miri *et al.*, 2022)
-	*Polyangium brachysporum*	Triacylglycerol lipase	-	(Danso *et al.*, 2019)
-	*Pseudoalteromonas citrea*	-	-	(Miri *et al.*, 2022)
-	*Pseudomonas aestusnigri*	-	-	(Amobonye *et al.*, 2021)
-	*Pseudomonas aestusnigri*	PETase	-	(Mohanan *et al.*, 2020)
-	*Pseudomonas aestusnigri*	Polyester hydrolase	-	(Maurya *et al.*, 2020)
-	*Pseudomonas fluorescens*	Cutinase	-	(Mohanan *et al.*, 2020)
-	*Pseudomonas litoralis*	Cutinase	-	(Mohanan *et al.*, 2020)
-	*Pseudomonas mendocina*	-	-	(Jacquim *et al.*, 2019)
-	*Pseudomonas mendocina*	PmC	PET surface-modifying enzyme	(Ali *et al.*, 2021)

Table A1.7 (continued)

Isolated source	*Bacterium*	Enzymes	Biodegradation conditions	References
-	*Pseudomonas mendocina*	-	5 % degradation rate of low crystallinity PET, at 50℃	(Maurya *et al.*, 2020)
-	*Pseudomonas pelagia*	PpelaLip	-	(Danso *et al.*, 2019)
-	*Pseudomonas pseudoalcaligenes*	PpCutA	-	(Danso *et al.*, 2019)
-	*Pseudomonas putida*	-	Incubation time 48 h at 30℃	(Mohanan *et al.*, 2020)
-	*Pseudomonas sp.*	Lipase	-	(Iram *et al.*, 2019)
-	*Pseudomonas sp. JG-B*	Cutinase	-	(Mohanan *et al.*, 2020)
-	*Saccharomonospora viridis*	Cutinase	-	(Danso *et al.*, 2019; Mohanan *et al.*, 2020)
-	*Serratia proteamaculans*	-	-	(Matjasic *et al.*, 2020)
-	*Streptomyces scabies*	-	-	(Amobonye *et al.*, 2021)
-	*Streptomyces sp*	-	-	(Amobonye *et al.*, 2021; Matjasic *et al.*, 2020)
-	*Streptomyces sp. SM14*	Esterase	-	(Atanasova, Stoitsova, *et al.*, 2021)
-	*Thermobifida alba*	Cutinase	-	(Maurya *et al.*, 2020; Mohanan *et al.*, 2020)
-	*Thermobifida alba AHK119*	-	Incubation time 14 days at 50℃	(Mohanan *et al.*, 2020)
-	*Thermobifida cellulosilytica*	Cutinase	-	(Maurya *et al.*, 2020; Mohanan *et al.*, 2020)
-	*Thermobifida cellulosilytica*	-	12 % degradation rate of low crystalinity PET and 24 % with semicrystalline PET, at 50℃	(Maurya *et al.*, 2020)
-	*Thermobifida fusca*	Cutinase (TfCut2)	Incubation time- 5 days, 97 % degradation of the tested material	(Ali *et al.*, 2021)
-	*Thermobifida fusca*	Cutinase-like hydrolase	Incubation time- 21 days, 55℃, degradation of 54 % of PET weight	(Ali *et al.*, 2021)
-	*Thermobifida fusca*	Cutinase	-	(Mohanan *et al.*, 2020)
-	*Thermobifida fusca*	TfH	-	(Miri *et al.*, 2022)
-	*Thermobifida fusca*	Hydrolases	-	(Miri *et al.*, 2022)
-	*Thermobifida fusca*	Cutinase	-	(Maurya *et al.*, 2020)
-	*Thermobifida fusca*	Carboxylesterases	-	(Maurya *et al.*, 2020)

Table A1.7 (continued)

Isolated source	*Bacterium*	Enzymes	Biodegradation conditions	References
-	*Thermobifida fusca (DSM 43793)*	Hydrolases	-	(Amobonye *et al.*, 2021; Jacquim *et al.*, 2019)
-	*Thermobifida fusca KW3*	-	25 % degradation rate in 24h, at 55℃-65℃	(Maurya *et al.*, 2020)
-	*Thermobifida halotolerans*	Carboxylesterases and esterase	Incubation time 2h at 50℃	(Mohanan *et al.*, 2020)
-	*Thermobifida halotolerans*	Serine hydrolase	-	(Danso *et al.*, 2019)
-	*Thermomonospora curvata*	-	Incubation time 7 days	(Mohanan *et al.*, 2020)
-	*Thermomonospora curvata*	Tcur0390	-	(Miri *et al.*, 2022)
-	*Thermomonospora curvata*	Polyester hydrolase	-	(Maurya *et al.*, 2020)
-	*Thermomosnospora curvata*	Triacylglycerol lipase	-	(Danso *et al.*, 2019)
Plant compost	*Thermomonospora fusca*	-	Incubation time 14 days at 55℃	(Mohanan *et al.*, 2020)
-	*Vibrio gazogenes*	Lipase	-	(Danso *et al.*, 2019)
-	*Vibrio gazogenes*	PET6	-	(Miri *et al.*, 2022)
Seawater	*Vibrio sp.*	-	Incubation time- 42 days, weight reduction of 35 %	(Ali *et al.*, 2021)
-	*Vibrio sp.*	-	-	(Matjasic *et al.*, 2020)
Saccharomonospora viridis AHK190	-	Cutinase Cut190	Incubation time- 3 days, 63℃, weight loss- 13,5 e 27 %	(Ru *et al.*, 2020)
Thermobifida fusca	-	Cutinase like hydrolase TfH	Incubation time- 21 days, 55℃, weight loss- 54,2 %	(Ru *et al.*, 2020)
Pseudomonas mendocina	-	Cutinase PmC	Incubation time- 96h, 70℃, weight loss- 5 %	(Ru *et al.*, 2020)
Ideonella sakaiensis 201-F6	-	IsPETase	Incubation time- 24 h, a 30℃, weight loss- 1 %	(Ru *et al.*, 2020)
Ideonella sakaiensis 201-F6	-	IsPETase	Weight loss 30 %- 40 %	(Ru *et al.*, 2020)
Compost metagenomic library	-	LC- cutinase	Incubation time- 7 days, 50℃, weight loss- 50 %	(Ru *et al.*, 2020)

Table A1.8: Fungi reported as PET biodegraders, and information on the isolation source, possible enzymes involved in the biodegradation and the biodegradation conditions

Isolated source	*Fungi*	Enzymes	Biodegradation conditions	References
-	*Aspergillus fumigatus*	Cutinase	-	(Maurya *et al.*, 2020)
-	*Aspergillus oryzae*	Cutinase	-	(Mohanan *et al.*, 2020)
Seawater	*Aspergillus sp.*	-	Incubation time- 42 days, weight reduction of 22 %	(Ali *et al.*, 2021)
-	Candida antarctica	Lipase	-	(Mohanan *et al.*, 2020)
-	*Fusarium oxysporum*	-	-	(Iram *et al.*, 2019; Jacquim *et al.*, 2019)
-	*Fusarium oxysporum*	Cutinase	-	(Maurya *et al.*, 2020; Mohanan *et al.*, 2020)
-	*Fusarium solani*	Cutinase PsC	-	(Iram *et al.*, 2019; Jacquim *et al.*, 2019; Ru *et al.*, 2020)
-	*Fusarium solani*	FsC	PET surface-modifying enzyme	(Ali *et al.*, 2021)
-	*Fusarium solani*	Cutinase	-	(Mohanan *et al.*, 2020)
-	*Fusarium solani*	-	5 % degradation rate of low crystalinity PET, at 40℃	(Maurya *et al.*, 2020)
-	*Fusarium solani pisi*	FsC	-	(Miri *et al.*, 2022)
-	*Fusarium solani pisi*	Cutinase	-	(Maurya *et al.*, 2020)
-	*Humicola insolens*	Cutinase	-	(Maurya *et al.*, 2020)
-	*Humicola insolens*	-	97 % degradation rate of low crystallinity PET, at 80℃	(Maurya *et al.*, 2020)
-	*Penicillium citrinum*	-	-	(Jacquim *et al.*, 2019)
-	*Penicillium citrinum*	Cutinase and polyeserase	-	(Ali *et al.*, 2021)
-	*Penicillium citrinum*	Cutinase	-	(Mohanan *et al.*, 2020)
Soil	*Penicillium funiculosum*	-	Incubation time- 84 days, chemical changes in polymeric chain	(Ali *et al.*, 2021)
-	*Penicillium funiculosum*	-	Incubation time 84 days, 0,21 % weight loss	(Taghavi *et al.*, 2021)
Engineered yeast strain	*Pichia pastoris*	-	Incubation time- 18h	(Ali *et al.*, 2021)
-	*Saccharomonospora viridis*	Cutinase 190	Incubation time- 3 days, degradation of 27 % of PET	(Ali *et al.*, 2021)
-	*Saccharomonospora viridis*	Cutinase	-	(Maurya *et al.*, 2020)
-	*Thermomonospora fusca*	-	-	(Jacquim *et al.*, 2019)
-	*Thermomyces insolens*	HiC	PET hydrolase	(Ali *et al.*, 2021)

Table A1.8 (continued)

Isolated source	*Fungi*	Enzymes	Biodegradation conditions	References
-	*Thermomyces insolens (or Humicola insolens)*	Cutinase HiC	-	(Ru *et al.*, 2020)
-	*Thermomyces lanuginosus*	Lipase	-	(Maurya *et al.*, 2020; Mohanan *et al.*, 2020)

Table A1.9: Bacteria reported as PCL biodegraders, and information on the isolation source, possible enzymes involved in the biodegradation and the biodegradation conditions

Isolated source	*Bacterium*	Enzymes	Biodegradation conditions	References
-	*Achromobacter sp.*	-	-	(Ahmed *et al.*, 2018)
-	*Alcaligenes faecalis*	Lipase	-	(Atanasova, Stoitsova, *et al.*, 2021)
-	*Alcaligenes faecalis*	Depolymerase	-	(Karamanlioglu *et al.*, 2017)
Sea water	*Alcanivorax sp.*	-	-	(Emadian et al, 2017)
Soil	*Amycolatopsis sp.*	-	-	(Emadian et al, 2017)
-	*Actinomadura*	-	-	(Tokiwa *et al.*, 2009)
Fresh water	*Bacillus pumilus*	-	-	(Emadian et al, 2017)
-	*Clostridium acetobutylicum*	-	-	(Ahmed *et al.*, 2018; Bahl *et al.*, 2021; Shah *et al.*, 2008)
-	*Clostridium botulinum*	-	-	(Ahmed *et al.*, 2018; Bahl *et al.*, 2021; Shah *et al.*, 2008)
-	*Colonostachys roseas*	-	52,91 % of biodegradation at 28°C, for 30 days	(Iram *et al.*, 2019)
-	*Coprothermobacter*	-	-	(Jin *et al.*, 2022)
-	*Firmicutes sp.*	-	-	(Bhardwaj *et al.*, 2013)
Soil/ Freshwater	*Leptothrix sp.*	-	-	(Emadian et al, 2017)
-	*Methanosaeta sp.*	-	-	(Yagi *et al.*, 2014)
-	*Methanothermobacter*	-	-	(Jin *et al.*, 2022).
-	*Microbisora*	-	-	(Tokiwa *et al.*, 2009)
Sea	*Moritella sp.*	-	-	(Emadian et al, 2017)
Soil	*Paenibacillus amylolyticus*	-	-	(Emadian et al, 2017)
Soil	*Paenibacillus sp.*	-	-	(Emadian et al, 2017)
-	*Protobacteria sp.*	-	-	(Bhardwaj *et al.*, 2013)
Sea water	*Pseudomonas sp.*	-	-	(Emadian et al, 2017)
-	Pseudomonas sp.	-	-	(Matjasic *et al.*, 2020)

Table A1.9 (continued)

Isolated source	*Bacterium*	Enzymes	Biodegradation conditions	References
Sea	*Psychrobacter sp.*	-	-	(Emadian et al, 2017)
-	*Rhizopus arrhizus*	Lipase	-	(Ahmed *et al.*, 2018; Iram *et al.*, 2019)
-	*Rhizopus delemar*	Lipase	-	(Ahmed *et al.*, 2018; Bhardwaj *et al.*, 2013)
-	*Rosleateles depolymerans strain TB-87*	-	-	(Iram *et al.*, 2019)
-	*Saccharomonospora*	-	-	(Tokiwa *et al.*, 2009)
Sea	*Shewanella sp.*	-	-	(Emadian et al, 2017)
Soil	*Streptomyces sp.*	-	-	(Emadian et al, 2017)
River sediment	*Streptomyces sp.*	-	-	(Emadian et al, 2017)
Compost	*Streptomyces thermonitrificans*	-	-	(Emadian et al, 2017)
Soil	*Streptomyces thermovioaceus*	-	-	(Emadian et al, 2017)
Sea water	*Tenacibaculum sp.*	-	-	(Emadian et al, 2017)
-	*Thermoactinomyces*	-	-	(Tokiwa *et al.*, 2009)
-	*Thermomyces lanuginosus*	-	-	(Hosni, 2019)
-	-	Bifunctional lipase-cutinase	-	(Kaushal *et al.*, 2021)
-	-	Esterases	-	(Ahmed *et al.*, 2018)

Table A1.10: Fungi reported as PCL biodegraders, and information on the isolation source, possible enzymes involved in the biodegradation and the biodegradation conditions

Isolated source	*Fungi*	Enzymes	Biodegradation conditions	References
-	*Aspergillus niger*	-	-	(Sankhla *et al.*, 2020)
-	*Achromobacter sp.*	Lipase	-	(Sankhla *et al.*, 2020)
-	*Amycolaptosis sp*	Cutinase	-	(Sankhla *et al.*, 2020)
-	*Aspergillus flavus*	Glycosidase	-	(Ahmed *et al.*, 2018; Iram *et al.*, 2019)
-	*Aspergillus flavus*	Glycosidases, Protease	-	(Bhardwaj *et al.*, 2013)
-	*Aspergillus flavus*	-	Degradation of amorphous region	(Karamanlioglu *et al.*, 2017)
-	*Aspergillus flavus*	Glycosidase	-	(Iram *et al.*, 2019)
-	*Aspergillus fumigatus*	-	-	(Sankhla *et al.*, 2020)
-	*Aspergillus fumigatus strain S45*	-	-	(Sankhla *et al.*, 2020)

Table A1.10 (continued)

Isolated source	*Fungi*	Enzymes	Biodegradation conditions	References
-	*Aspergillus niger*	Catalase protease	-	(Ahmed *et al.*, 2018; Iram *et al.*, 2019)
-	*Aspergillus sp. ST-01*	-	-	(Ahmed *et al.*, 2018; Iram *et al.*, 2019)
-	*Aspergillus ST-01*	-	Incubation- 6 days at 50℃	(Karamanlioglu *et al.*, 2017)
-	*Aureobasidium sp.*	-	-	(Sankhla *et al.*, 2020)
-	*Candida cylindracea*	-	-	(Ahmed *et al.*, 2018)
-	*Candida cylindracea*	Lipase	-	(Sankhla *et al.*, 2020)
-	*Cephalosporium sp. F. solani strain 77-2-3*	-	-	(Iram *et al.*, 2019)
-	*Chaetomium globosum*	-	-	(Sankhla *et al.*, 2020)
Soil	*Cladosporium sp.*	-	-	(Emadian et al, 2017)
-	*Cladosporium sp.*	-	-	(Sankhla *et al.*, 2020)
-	*Clonostachys rosea*	-	-	(Sankhla *et al.*, 2020)
-	*Cryptococcus sp.*	-	-	(Sankhla *et al.*, 2020)
-	*Fusarium moniliforme*	-	-	(Sankhla *et al.*, 2020)
-	*Fusarium solani*	-	-	(Shah *et al.*, 2008)
-	*Fusarium solani ATCC 38136*	-	-	(Sankhla *et al.*, 2020)
-	*Fusarium solani strain 77-2-3*	-	-	(Iram *et al.*, 2019; Sankhla *et al.*, 2020)
-	*Fusarium sp.*	Cutinase	-	(Ahmed *et al.*, 2018; Bhardwaj *et al.*, 2013; Iram *et al.*, 2019)
-	*Fusarium sp.*	Cutinase and lipase	-	(Sankhla *et al.*, 2020)
-	*Paecilomyces lilacinus*	Depolymerase	Incubation time- 10 days, optimum pH of 3,5-4,5 at 30℃, 10 % degradation	(Sankhla *et al.*, 2020)
-	*Penicillium dupontii IFO 31798*	-	-	(Sankhla *et al.*, 2020)
-	*Penicillium oxalicum*	-	-	(Sankhla *et al.*, 2020)
-	*Penicillium sp.*	Lipase	-	(Bhardwaj *et al.*, 2013; Sankhla *et al.*, 2020)
-	*Penicillium strain 26-1*	-	Complete degradation in 12 days	(Karamanlioglu *et al.*, 2017)
-	*Penicullium funiculosum*	-	Degradation of amorphous region	(Karamanlioglu *et al.*, 2017)
-	*Pencillium funiculosum*	-	-	(Sankhla *et al.*, 2020)
-	*Pseudozyma japonica-Y7-09*	Extracellular cutinase	Incubation time- 15 days, 30℃, 93,33 % degradation	(Sankhla *et al.*, 2020)
Soil	*Purpureocillium sp.*	-	-	(Emadian et al, 2017)

Table A1.10 (continued)

Isolated source	*Fungi*	Enzymes	Biodegradation conditions	References
-	*Purpureocillium sp.*	-	-	(Sankhla *et al.*, 2020)
-	*Rhizopus delemar*	Lipase	-	(Sankhla *et al.*, 2020)
-	*Rhizopus. arrizus*	Lipase	-	(Sankhla *et al.*, 2020)
-	*Streptomyces sp.*	-	-	(Bhardwaj *et al.*, 2013)
-	*Thermoascus aurantiacus IFO 31910*	-	-	(Sankhla *et al.*, 2020)
-	*Trichoderma sp.*	-	-	(Sankhla *et al.*, 2020)

Appendix 2- Materials and methods

2.1- VSS determination

Source: APHA / AWWA / WPCF, 1985. "Standard Methods for the examination of water and wastewater". 16th edition. APHA Washington, DC.; 2005

1- Wash a filter of glass fibre with 3 portions of 20 mL of distilled water;
2- Place the filter + porcelain crucible in the muffle (for about 0,5h);
3- Retrieved the crucible and let it cool in a desiccator until constant weight;
4- Weight the crucible + filter (mass a);
5- Place the filter in a filtration system, and filter the sample;
6- Let the crucible + filter with sample to dry in an oven, at 105℃, until constant weight, meaning a variation of less than 4 %;
7- Weight the crucible after it is cooled (mass b);
8- Place the crucible in a muffle, at 550℃ ± 50℃, for 2 hours;
9- Weight the crucible after it is cooled in a desiccator (mass c).

Calculations:

With V being the volume of biomass filtered in step 5; in mL, and the masses in g, the VSS (g/L) can be calculated with the following equations:

Volatile suspended solids: VSS= (b-c) x 1000/V

2.2- Description of the assays from the first anaerobic experiment

Table A2.1: Description of the assays from the first anaerobic experiment, with information on the amount of plastic/substrate added in each one of the vials.

Description	Designation in the vial	Plastic mass (mg)	Growth medium (mL)	Volume of leachate added (mL)
Only leachate	Blank 1	Not added	11	1,5
Only leachate	Blank 2	Not added	11	1,5

Only leachate	Blank 3	Not added	11	1,5
Leachate plus VFA	VFA 1	125uL of the VFA mixture	11	1,5
Leachate plus VFA	VFA 2	125uL of the VFA mixture	11	1,5
Leachate plus polyethylene	PE 1	15,9	11	1,5
Leachate plus polyethylene	PE 2	15,2	11	1,5
Leachate plus polyethylene	PE 3	15,0	11	1,5
Leachate plus polyethylene terephthalate	PET 1	15,5	11	1,5
Leachate plus polyethylene terephthalate	PET 2	15,3	11	1,5
Leachate plus polyethylene terephthalate	PET 3	15,4	11	1,5
Leachate plus polycaprolactone	PCL 1	16,6	11	1,5
Leachate plus polycaprolactone	PCL 2	16,5	11	1,5
Leachate plus polycaprolactone	PCL 3	15,8	11	1,5
Leachate plus Poly(3-hydroxybutyrate-co-3-hydroxyvalerate)	PHB/PBAT 1	15,6	11	1,5
Leachate plus Poly(3-hydroxybutyrate-co-3-hydroxyvalerate)	PHB/PBAT 2	15,4	11	1,5
Leachate plus Poly(3-hydroxybutyrate-co-3-hydroxyvalerate)	PHB/PBAT 3	16,1	11	1,5
Leachate plus cellulose	Cellulose 1	15,4	11	1,5
Leachate plus cellulose	Cellulose 2	15,6	11	1,5
Leachate plus cellulose	Cellulose 3	15,0	11	1,5

2.3- Anaerobic medium preparation

The basic medium was prepared from the following stock solutions, (chemicals given below are concentrations in g/L, in distilled water)

(A) NH_4Cl, 100; NaCl, 10; $MgCl_2 \cdot 6H_2O$, 10; $CaCl_2 \cdot 2H_2O$, 5

(B) $K_2HPO4 \cdot 3H_2O$, 200

(C) Resazurin 0,5

(D) Trace-metal and selenite solution: $FeCl_2 \cdot 4H_2O$, 2; H_3BO_3, 0,05; $ZnCl_2$, 0,05; $CuCl_2.2H_2O$, 0,038; $MnCl_2 \cdot 4H_2O$, 0,05; $(NH_4)_6Mo_7O_{24} \cdot 4H_2O$, 0,05; $AlCl_3$, 0,05; $CoCl_2 \cdot 6H_2O$, 0,05; $NiCl_2 \cdot 6H_2O$, 0,092; ethylenediaminetetraacetate, 0,5; concentrated HCl, 1 ml; $Na_2SeO_3 \cdot 5H_2O$, 0,1;

(E) Vitamin mixture (components are given in mg/L): Biotin, 2; folic acid, 2; pyridoxine acid, 10; ridoflavin, 5; thiamine hydrochloride, 5; cyanocobalamine, 0.1; nicotinic acid, 5; P-aminobenzoic acid, 5; lipoic acid, 5; DL-pantothenic acid.

To 974 ml of distilled water, the following stock solutions were added A, 10 ml; B, 2 ml; C, 1 ml; D, 1 ml and E, 1 ml. The mixture is gassed with 80 % N_2 –20 % CO_2. Cysteine hydrochloride, 0,5 g and $NaHCO_3$, 2,6 g, are added and the medium is dispensed to serum vials and autoclaved if necessary. Before inoculation the vials are reduced with $Na_2S \bullet 9H_2O$ to a final concentration of 0,025 %.

Retrieved from (Stams *et al.*, 1993)

2.5- Description of the second anaerobic experiment and aerobic experiment

Table A2.2: Description of the assays from the second anaerobic experiment, with information on the amount of plastic/substrate added in each one of the vials

Description	Designation in the vial	Plastic mass (mg)	Growth medium (mL)	Volume of leachate added (mL)
Only leachate	Branco 1	Not added	45	1,5
Only leachate	Branco 2	Not added	45	1,5
Only leachate	Branco 3	Not added	45	1,5
Leachate plus polyethylene film	PE 1f	63,5	45	1,5
Leachate plus polyethylene film	PE 2f	64,3	45	1,5
Leachate plus polyethylene film	PE 3f	64,4	45	1,5
Leachate plus polyethylene terephthalate film	PET 1f	62,5	45	1,5
Leachate plus polyethylene terephthalate film	PET 2f	63,7	45	1,5
Leachate plus polyethylene terephthalate film	PET 3f	64,2	45	1,5
Leachate plus polycaprolactone film	PCL 1f	64,1	45	1,5
Leachate plus polycaprolactone film	PCL 2f	61,6	45	1,5
Leachate plus polycaprolactone film	PCL 3f	65,7	45	1,5
Leachate plus cellulose film	Cellu 1f	64,9	45	1,5
Leachate plus polyethylene powder	PE 1p	67,1	45	1,5
Leachate plus polyethylene powder	PE 2p	65,8	45	1,5
Leachate plus polyethylene powder	PE 3p	68,9	45	1,5
Leachate plus polyethylene terephthalate powder	PET 1p	66,0	45	1,5
Leachate plus polyethylene terephthalate powder	PET 2p	66,8	45	1,5
Leachate plus polyethylene terephthalate powder	PET 3p	68,1	45	1,5

Leachate plus polycaprolactone powder	PCL 1p	67,1	45	1,5
Leachate plus polycaprolactone powder	PCL 2p	66,5	45	1,5
Leachate plus polycaprolactone powder	PCL 3p	65,5	45	1,5
Leachate plus cellulose powder	Cellu 1p	67,3	45	1,5
Leachate plus cellulose powder	Cellu 2p	67,4	45	1,5
Leachate plus cellulose powder	Cellu 3p	67,0	45	1,5

Table A2.3: Description of the assays from the aerobic experiment, with information on the amount of plastic/substrate added in each one of the vials

Description	Designation in the vial	Plastic mass (mg)	Growth medium (mL)	Volume of leachate added (mL)
Only leachate	Branco 1	Not added	49	1,5
Only leachate	Branco 2	Not added	49	1,5
Only leachate	Branco 3	Not added	49	1,5
Leachate plus polyethylene film	PE 1f	63,5	49	1,5
Leachate plus polyethylene film	PE 2f	64,3	49	1,5
Leachate plus polyethylene film	PE 3f	64,4	49	1,5
Leachate plus polyethylene terephthalate film	PET 1f	62,5	49	1,5
Leachate plus polyethylene terephthalate film	PET 2f	63,7	49	1,5
Leachate plus polyethylene terephthalate film	PET 3f	64,2	49	1,5
Leachate plus polycaprolactone film	PCL 1f	64,1	49	1,5
Leachate plus polycaprolactone film	PCL 2f	61,6	49	1,5
Leachate plus polycaprolactone film	PCL 3f	65,7	49	1,5
Leachate plus polyethylene powder	PE 1p	67,1	49	1,5
Leachate plus polyethylene powder	PE 2p	65,8	49	1,5
Leachate plus polyethylene powder	PE 3p	68,9	49	1,5
Leachate plus polyethylene terephthalate powder	PET 1p	66,0	49	1,5
Leachate plus polyethylene terephthalate powder	PET 2p	66,8	49	1,5
Leachate plus polyethylene terephthalate powder	PET 3p	68,1	49	1,5
Leachate plus polycaprolactone powder	PCL 1p	67,1	49	1,5
Leachate plus polycaprolactone powder	PCL 2p	66,5	49	1,5

Leachate plus polycaprolactone powder	PCL 3p	65,5	49	1,5
Leachate plus cellulose powder	Cellu 1p	67,3	49	1,5
Leachate plus cellulose powder	Cellu 2p	67,4	49	1,5
Leachate plus cellulose powder	Cellu 3p	67,0	49	1,5

2.6- Theoretical methane production and oxygen consumption calculations

Table A2.4: Determination of the number of moles of methane produced per mol of polymer (PE, PET, PCL, and cellulose)

Polymer	Equation of polymers' conversion to methane	Moles CH_4 produced from 1 mol of polymer
PE	$2C_2H_4 + 2H_2O \rightarrow CO_2 + 3CH_4$	1,5
PET	$C_{10}H_8O_4 + 6H_2O \rightarrow 5CO_2 + 5CH_4$	5
PCL	$4C_6H_{10}O_2 + 10H_2O \rightarrow 9CO_2 + 15CH_4$	3,75
Cellulose	$C_6H_{10}O_5 + 1H_2O \rightarrow 3CO_2 + 3CH_4$	3

Table A2.5: Calculation of the theoretical methane production of each polymer studied-PE, PET, PCL, and cellulose, considering total conversion to methane, calculated as described in section 5.1.4

Polymer	Moles CH_4 produced	Polymer weight (g)	Polymer molar mass (g/mol)	Moles of polymer in the vials (mol)	Theoretical CH4 (mmol)/0,0652g plastic
PE powder	1,5	0,0672	28	0,0024	3,60
PE film	1,5	0,0641	28	0,0023	3,43
PET powder	5	0,067	192	0,0003	1,74
PET film	5	0,0627	192	0,0003	1,63
PCL powder	3,75	0,0678	114	0,0006	2,23
PCL film	3,75	0,0638	114	0,0006	2,10
Cellulose powder	3	0,0672	162,14	0,0004	1,24
Cellulose film	3	0,0649	162,14	0,0004	1,20

Table A2.6: Determination of the number of moles of oxygen consumed per mol of polymer (PE, PET, PCL and cellulose)

Polymer	Equation of polymer consumption of oxygen	Moles of O_2 consumed from 1 mol of polymer
PE	$C_2H_4 + 3O_2 \rightarrow 2CO_2 + 2H_2O$	3
PET	$C_{10}H_8O_4 + 10O_2 \rightarrow 10CO_2 + 4H_2O$	10
PCL	$C_6H_{10}O_2 + 7,5O_2 \rightarrow 6CO_2 + 5H_2O$	7,5
Cellulose	$C_6H_{10}O_5 + 6O_2 \rightarrow 6CO_2 + 5H_2O$	6

Table A2.7: Calculation of the theoretical oxygen consumption of each polymer studied-PE, PET, PCL, and cellulose, considering total consumption of oxygen, calculated as described in section 5.1.4

Polymers	Moles of O_2 consumed	Polymer weight (g)	Polymer molar mass (g/mol)	Moles of plastic in the vials	Theoretical O_2 (mmol)/0,0652g plastic
PE powder	3	0,0673	28	0,0024	7,21
PE film	3	0,0641	28	0,0023	6,87
PET powder	10	0,067	192	0,0003	3,49
PET film	10	0,0635	192	0,0003	3,31
PCL powder	7,5	0,0664	114	0,0006	4,37
PCL film	7,5	0,0638	114	0,0006	4,20
Cellulose	6	0,0672	162,14	0,0004	2,49

Appendix 3- Results of the experiments with leachate as inoculum

3.1- First anaerobic experiment

Table A3.1: Values of the mass of the cleaned muffle filters, after addition of the biomass, after overnight incubation at 105℃, and after incubation at 550℃, and respective standard deviation. Values of the resulting VSS for each sample, the average value for the first anaerobic assay and corresponding standard deviation, the volume necessary to obtain 3g/L VSS and the real value of VSS used in this work

Samples	Filter mass (g)	Mass after incubation at 105℃ (g)	Mass after incubation at 550℃ (g)	VSS (g/L)	Average VSS (g/L)	Volume to 3 g/L VSS (mL)	Real value of VSS in 1,5 mL (g/L)
1	2,59 ± 0,0001	2,59 ± 0,0001	2,59 ± 0,0001	7,20	7,67 ± 0,411	4,9	0,92
2	2,63 ± 0,0001	2,64 ± 0,0001	2,63 ± 0,0001	7,60			
3	2,60 ± 0,0001	2,60 ± 0,0001	2,60 ± 0,0001	8,2			

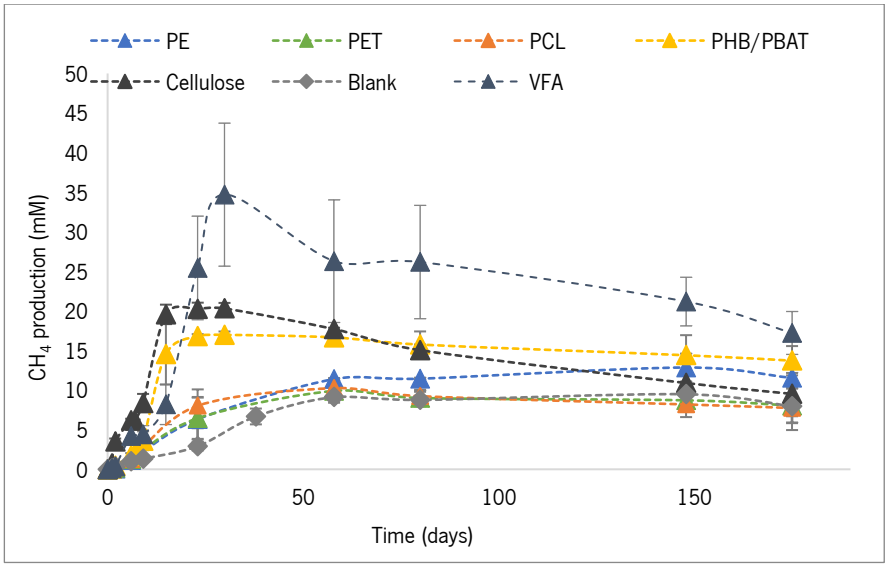

Figure A3.1: Methane production curves of the first anaerobic experiment, for 180 days of incubations. Average values of the PE, PET, PCL, PHB/PBAT; cellulose, VFA and blank assays, and respective standard deviations.

Table A3.2: Wave numbers for the different FTIR peaks observed for PE, respective type of bond and functional group. Adapted from Montazer *et al.* (2020)

Wave number (cm^{-1})	Bond	Functional group
3000-2850	-C-H stretch	Alkanes
2850-2695	H-C= O: C-H stretch	Aldehyde
1710-1665	-C=O stretch	Ketones, aldehyde
1470-1450	-C-H bend	Alkanes
1320-1000	-C-O stretch	Alcohol, carboxylic acid, esters, ethers
1000-650	=C-H bond	Alkenes

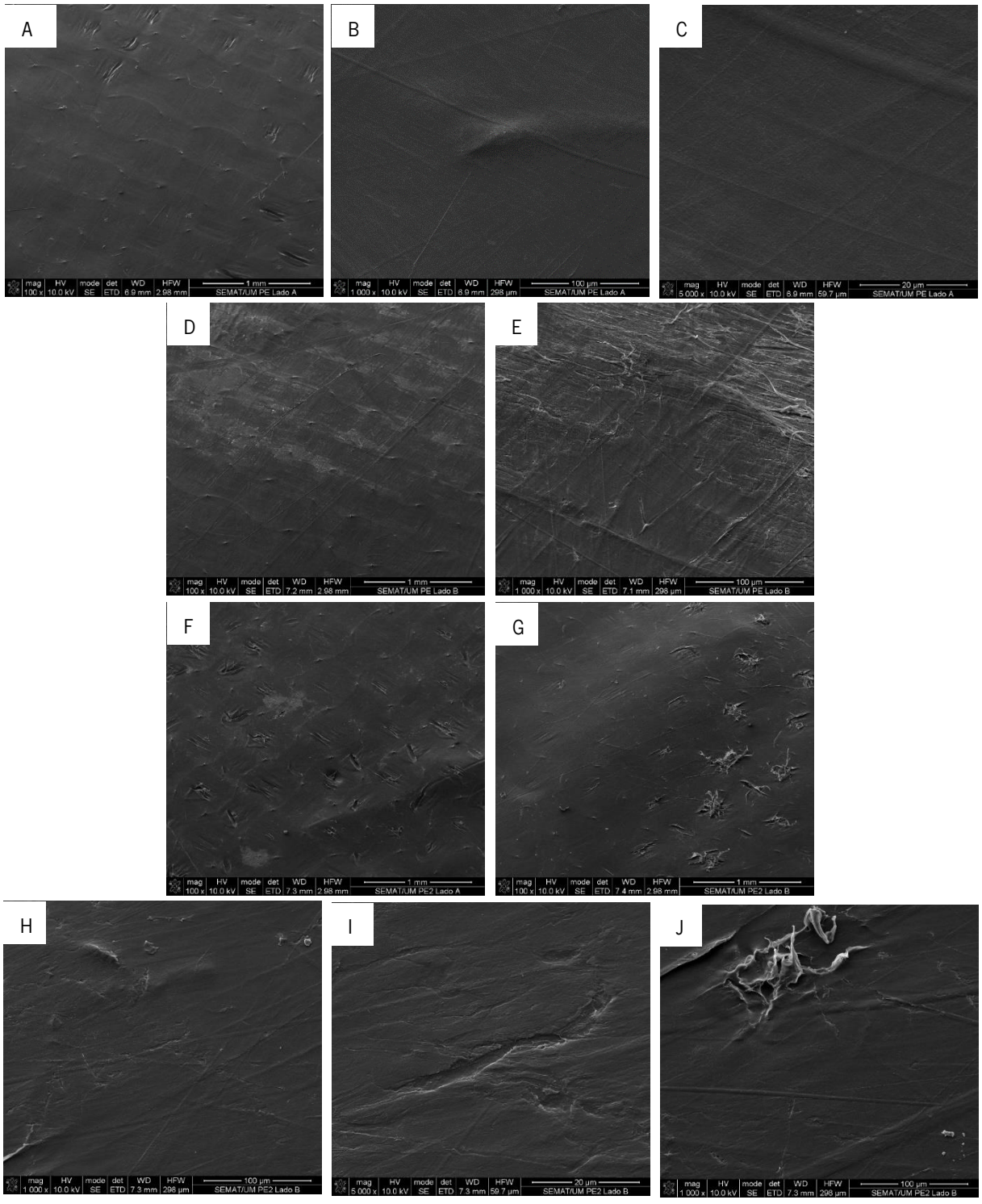

Figure A3.2: SEM images of the PE film that was not subjected to biodegradation (A, B, C, D and E) and that was used in the biodegradability assays (F, G, H, I, J and K) in different magnifications. A) side A of the original film with 100x magnification; B) side A of the original film with 100 x magnification; C) side A of the original film with 5000x magnification; D) side B of the original film with 100x magnification; E) side B of the original film with 1000x magnification; F) side A of the tested film with 100x magnification; G) side B of the tested film with 100x magnification; H) side B of the tested film with 1000x magnification; I) side B of the tested film with 5000x magnification; J) side B of the tested film with 1000x magnification.

3.2- Second anaerobic experiment

Table A3.3: Values of the mass of the cleaned muffle filters, after addition of the biomass, after overnight incubation at 105°C, and after incubation at 550°C, and respective standard deviation. Values of the resulting VSS for each sample, the average value for the first anaerobic assay and corresponding standard deviation, the volume necessary to obtain 3 g/L VSS and the real value of VSS used in this work

Sample	Filter mass (g)	Mass after incubation at 105°C (g)	Mass after incubation at 550°C (g)	VSS (g/L)	Average VSS (g/L)	Volume to 3 g/L VSS (mL)	Real value of VSS in 1,5 mL (g/L)
1	2,56 ± 0,0001	2,59 ± 0,0001	2,57 ± 0,0001	45,00	45,60 ± 0,43	3,23	1,40
2	2,55 ± 0,0001	2,58 ± 0,0001	2,56 ± 0,0001	46,00			
3	2,60 ± 0,0001	2,64 ± 0,0001	2,62 ± 0,0001	45,8			

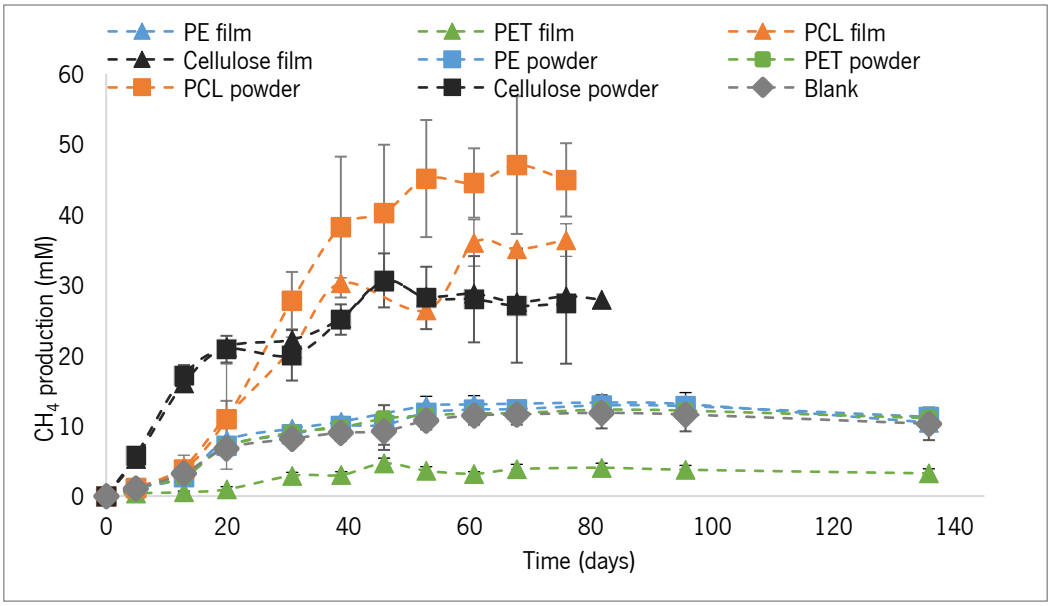

Figure A3.3: Methane production curves from the second anaerobic experiment, for 140 days of incubations. Average values of the PE, PET, PCL, cellulose, and blank assays, in film and powder, and respective standard deviation.

Figure A3.4: PE film observed floating at the surface of the anaerobic growth medium

Figure A3.5: Anaerobic assays with PE (on the left) and PET (on the right) films duplicates

3.3- Aerobic experiment

Table A3.4: Values of the mass of the cleaned muffle filters, after addition of the biomass, after overnight incubation at 105°C, and after incubation at 550°C, and respective standard deviation. Values of the resulting VSS for each sample, the average value for the first anaerobic assay and corresponding standard deviation, the volume necessary to obtain 3 g/L VSS and the real value of VSS used in this work

Samples	Filter mass (g)	Mass after incubation at 105°C (g)	Mass after incubation at 550°C (g)	VSS (g/L)	Average VSS (g/L)	Volume to 3 g/L VSS (mL)	Real value of VSS in 1,5 mL (g/L)
1	2,59 ± 0,0001	2,61 ± 0,0001	2,60 ± 0,0001	30,20	30,20 ± 0,33	4,9	0,92
2	2,59 ± 0,0001	2,61 ± 0,0001	2,60 ± 0,0001	29,80			
3	2,61 ± 0,0001	2,63 ± 0,0001	2,61 ± 0,0001	30,60			

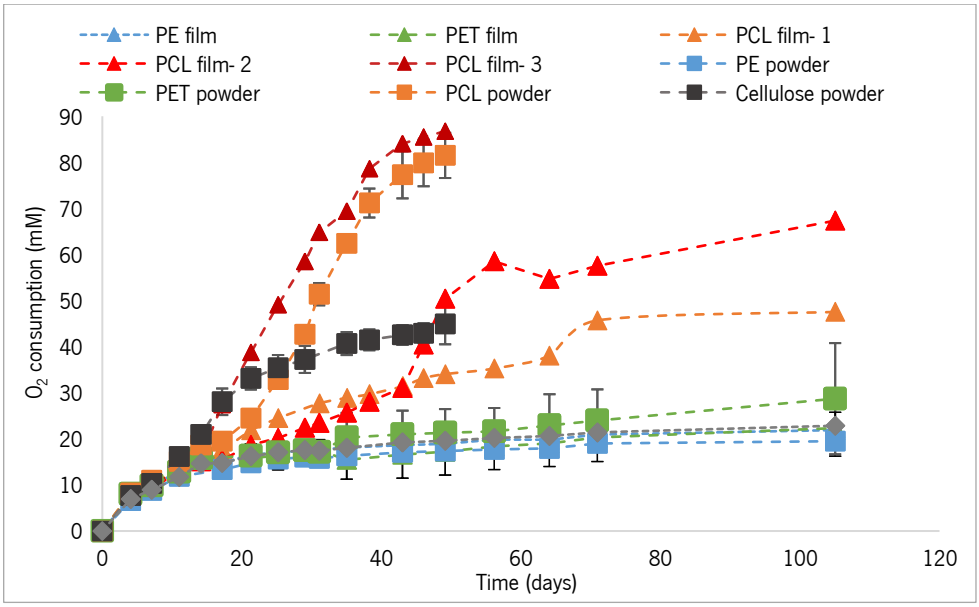

Figure A3.6: Aerobic biodegradability results of the samples with films and powder, for the 120 days of incubation.

Table A3.5: Biodegradation percentages of the three replicas of PCL in film from the aerobic experiment

PCL film replica	Biodegradation (%)
Replica 1	28,8
Replica 2	62,7
Replica 3	111,2

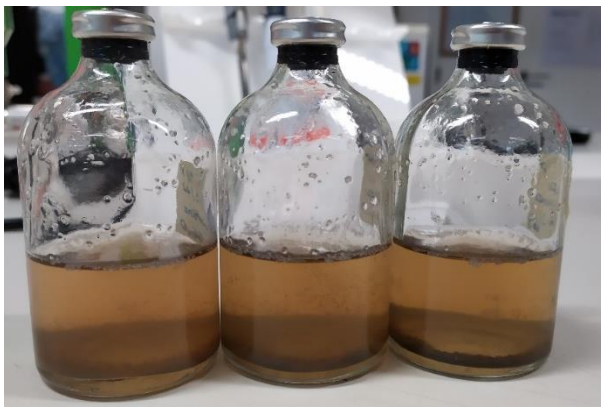

FigureA3.7: Vials with PE powder from the aerobic incubation. Attachment of the powder to the walls, and deposition of the biomass t the bottom of the vials

Figure A3.8: Aerobic assays triplicates with powder: with cellulose (on the left) and with PCL (on the right). Visible darkening of the growth medium.

Appendix 4- Krona plots from the sequencing of the aerobic and anaerobic PCL samples, and leachate inoculum, and table with relative abundance of each microorganism in the three samples

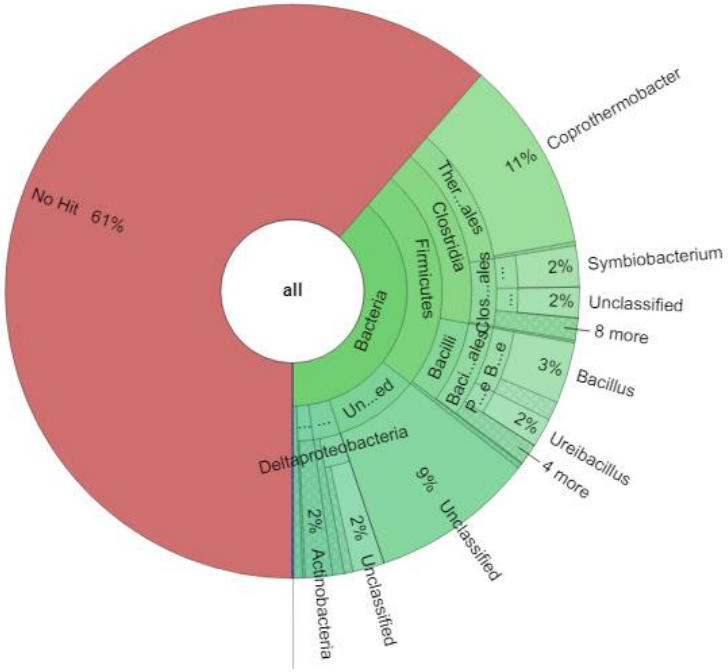

FigureA4.1: Relative abundance of the organisms from the PCL incubation performed under aerobic conditions, represented in a krona plot.

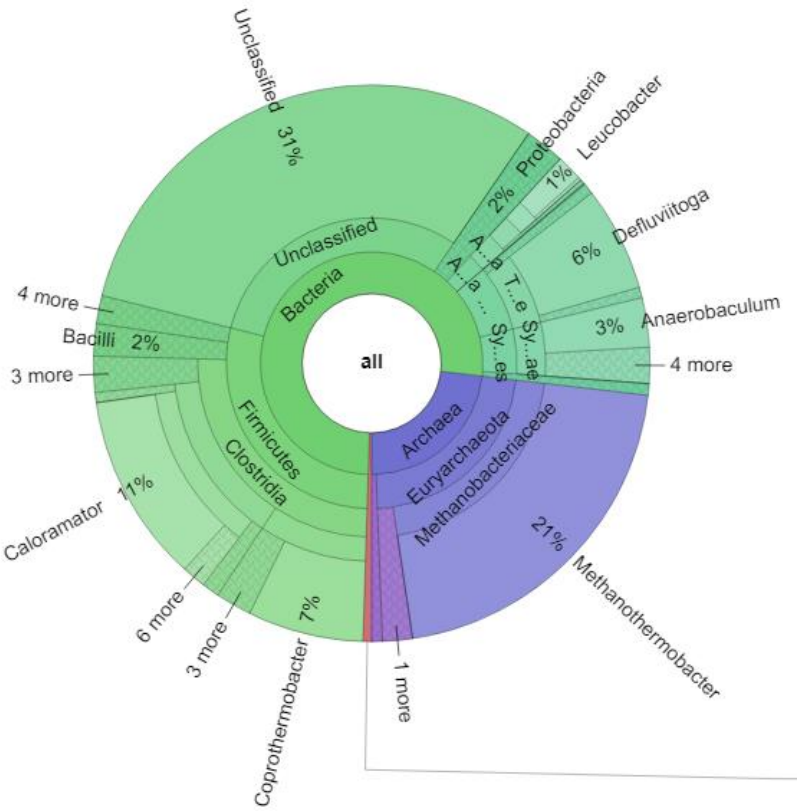

Figure A4.2: Relative abundance of the organisms from the PCL incubation performed under anaerobic conditions, represented in a krona plot.

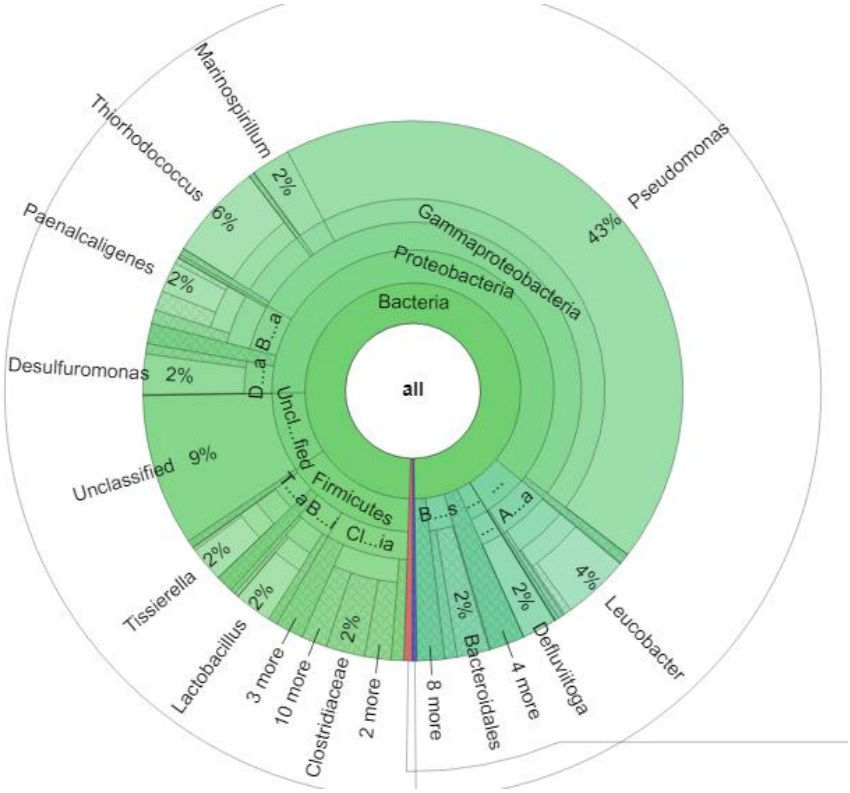

Figure A4.3: Relative abundance of the organisms from the leachate inoculum, represented in a krona plot.

Table A4.1: Relative abundance of identified microorganisms assigned to *Archaea* domain in the PCL powder aerobic and anaerobic sample, as well as and in the inoculum

Kingdom	Genus	Species	Aerobic	Anaerobic	Inoculum
Crenarchaeota	Unclassified	Unclassified	0,0000	0,0029	0,0000
Crenarchaeota	Unclassified	Unclassified	0,0018	0,0043	0,0000
Euryarchaeota	*Methanobacterium*	*Methanobacterium sp.*	0,0029	0,0179	0,0439
Euryarchaeota	*Methanobrevibacter*	*Methanobrevibacter smithii*	0,0000	0,0000	0,0027
Euryarchaeota	*Methanobrevibacter*	*Methanobrevibacter sp.*	0,0000	0,0029	0,0137
Euryarchaeota	*Methanothermobacter*	*Methanothermobacter sp.*	0,0318	20,7941	0,0082
Euryarchaeota	*Methanocorpusculum*	*Methanocorpusculum sinense*	0,0000	0,0000	0,0062
Euryarchaeota	*Methanoculleus*	*Methanoculleus sp.*	0,0253	0,1353	0,0816
Euryarchaeota	*Methanoculleus*	*Methanoculleus thermophilus*	0,0065	0,0437	0,0014
Euryarchaeota	*Methanofollis*	*Methanofollis formosanus*	0,0006	0,0093	0,0110
Euryarchaeota	*Methanosaeta*	*Methanosaeta sp.*	0,0000	1,0857	0,0000
Euryarchaeota	*Methanosarcina*	*Methanosarcina sp.*	0,0000	0,4530	0,0048

Table A4.2: Relative abundance of identified microorganisms assigned to *Bacteria* domain in the PCL powder aerobic and anaerobic sample, as well as and in the inoculum

Kingdom	Genus	Species	Aerobic	Anaerobic	Inoculum
Actinobacteria	*Actinobaculum*	*Actinobaculum sp.*	0,0000	0,0000	0,0027
Actinobacteria	*Actinomadura*	*Actinomadura sp.*	0,0018	0,0000	0,0034
Actinobacteria	*Actinomyces*	*Actinomyces sp.*	0,0000	0,0165	0,0185
Actinobacteria	*Actinopolymorpha*	*Actinopolymorpha sp.*	0,0012	0,0000	0,0027
Actinobacteria	*Aeromicrobium*	*Aeromicrobium sp.*	0,0000	0,0057	0,0199
Actinobacteria	*Agreia*	*Agreia sp.*	0,0000	0,0057	0,0233
Actinobacteria	*Agromyces*	*Agromyces sp.*	0,0000	0,0000	0,0014
Actinobacteria	*Alloscardovia*	*Alloscardovia sp.*	0,0000	0,0021	0,0055
Actinobacteria	*Arthrobacter*	*Arthrobacter sp.*	0,0000	0,0050	0,0164
Actinobacteria	*Bifidobacterium*	*Bifidobacterium adolescentis*	0,0024	0,0100	0,0137
Actinobacteria	*Bifidobacterium*	*Bifidobacterium animalis*	0,0000	0,0014	0,0014
Actinobacteria	*Bifidobacterium*	*Bifidobacterium callitrichos*	0,0000	0,0000	0,0027
Actinobacteria	*Bifidobacterium*	*Bifidobacterium mongoliense*	0,0024	0,0208	0,0089
Actinobacteria	*Bifidobacterium*	*Bifidobacterium pseudolongum*	0,0018	0,0079	0,0021
Actinobacteria	*Brevibacterium*	*Brevibacterium sp.*	0,0000	0,0000	0,0041
Actinobacteria	*Cellulomonas*	*Cellulomonas sp.*	0,0000	0,0136	0,0500

Table A4.2 (continued)

Kingdom	*Genus*	*Species*	Aerobic	Anaerobic	Inoculum
Actinobacteria	*Collinsella*	*Collinsella aerofaciens*	0,0000	0,0000	0,0117
Actinobacteria	*Collinsella*	*Collinsella intestinalis*	0,0000	0,0000	0,0014
Actinobacteria	*Conexibacter*	*Conexibacter sp.*	0,0513	0,0029	0,0144
Actinobacteria	*Corynebacterium*	*Corynebacterium humireducens*	0,0000	0,0086	0,0048
Actinobacteria	*Corynebacterium*	*Corynebacterium sp.*	0,0018	0,0651	0,0432
Actinobacteria	*Dietzia*	*Dietzia maris*	0,0047	0,0179	0,0445
Actinobacteria	*Dietzia*	*Dietzia sp.*	0,0012	0,0064	0,0103
Actinobacteria	*Eggerthella*	*Eggerthella sinensis*	0,0000	0,0021	0,0069
Actinobacteria	*Eggerthella*	*Eggerthella sp.*	0,0000	0,0021	0,0123
Actinobacteria	*Flaviflexus*	*Flaviflexus salsibiostraticola*	0,0000	0,0036	0,0226
Actinobacteria	*Frondihabitans*	*Frondihabitans sp.*	0,0041	0,0544	0,1069
Actinobacteria	*Gulosibacter*	*Gulosibacter chungangensis*	0,0006	0,0057	0,0075
Actinobacteria	*Leifsonia*	*Leifsonia sp.*	0,0000	0,0057	0,0343
Actinobacteria	*Leucobacter*	*Leucobacter aridicollis*	0,0006	0,0279	0,1323
Actinobacteria	*Leucobacter*	*Leucobacter komagatae*	0,0000	0,0093	0,0055
Actinobacteria	*Leucobacter*	*Leucobacter sp.*	0,1132	1,4450	3,8470
Actinobacteria	*Microbacterium*	*Microbacterium sp.*	0,0000	0,0043	0,0055
Actinobacteria	*Microbispora*	*Microbispora sp.*	0,0047	0,0000	0,0000
Actinobacteria	*Mycobacterium*	*Mycobacterium hassiacum*	0,0006	0,0000	0,0027
Actinobacteria	*Mycobacterium*	*Mycobacterium parascrofulaceum*	0,0000	0,0100	0,0096
Actinobacteria	*Mycobacterium*	*Mycobacterium thermoresistibile*	0,0041	0,0129	0,0199
Actinobacteria	*Neoscardovia*	*Neoscardovia arbecensis*	0,0000	0,0014	0,0069
Actinobacteria	*Nocardioides*	*Nocardioides sp.*	0,0000	0,0000	0,0055
Actinobacteria	*Olsenella*	*Olsenella sp.*	0,0000	0,0000	0,0034
Actinobacteria	*Patulibacter*	*Patulibacter minatonensis*	0,0000	0,0007	0,0021
Actinobacteria	*Phycicoccus*	*Phycicoccus dokdonensis*	0,0006	0,0000	0,0014
Actinobacteria	*Pseudoclavibacter*	*Pseudoclavibacter chungangensis*	0,0077	0,1116	0,2508
Actinobacteria	*Pseudoclavibacter*	*Pseudoclavibacter helvolus*	0,0000	0,0072	0,0206
Actinobacteria	*Rhodococcus*	*Rhodococcus sp.*	0,0000	0,0029	0,0000
Actinobacteria	*Rubrobacter*	*Rubrobacter sp.*	0,0000	0,0029	0,0034
Actinobacteria	*Senegalimassilia*	*Senegalimassilia anaerobia*	0,0000	0,0029	0,0007
Actinobacteria	*Solirubrobacter*	*Solirubrobacter sp.*	0,0000	0,0000	0,0014
Actinobacteria	*Sphaerisporangium*	*Sphaerisporangium sp.*	0,0012	0,0000	0,0014
Actinobacteria	*Streptomyces*	*Streptomyces sp.*	0,0047	0,0143	0,0404

Table A4.2 (continued)

Kingdom	*Genus*	*Species*	Aerobic	Anaerobic	Inoculum
Actinobacteria	*Thermobifida*	*Thermobifida fusca*	0,0000	0,0014	0,0021
Actinobacteria	*Timonella*	*Timonella senegalensis*	0,0000	0,0000	0,0343
Actinobacteria	*Tomitella*	*Tomitella biformata*	0,0000	0,0000	0,0034
Actinobacteria	Unclassified	Unclassified	0,0000	0,0050	0,0014
Actinobacteria	Unclassified	Unclassified	1,3766	0,0415	0,0740
Actinobacteria	Unclassified	Unclassified	0,0000	0,0250	0,1302
Actinobacteria	Unclassified	Unclassified	0,0808	0,0000	0,0048
Actinobacteria	Unclassified	Unclassified	0,0000	0,0050	0,0377
Actinobacteria	*Yaniella*	*Yaniella sp.*	0,0006	0,0057	0,0069
Bacteroidetes	*Alkaliflexus*	*Alkaliflexus sp.*	0,0000	0,0000	0,0912
Bacteroidetes	*Alkalitalea*	*Alkalitalea sp.*	0,0000	0,0000	0,0055
Bacteroidetes	*Bacteroides*	*Bacteroides sp.*	0,0000	0,0000	0,0240
Bacteroidetes	*Balneola*	*Balneola sp.*	0,0000	0,0000	0,0027
Bacteroidetes	*Brumimicrobium*	*Brumimicrobium sp.*	0,0000	0,0000	0,0055
Bacteroidetes	*Cytophaga*	*Cytophaga sp.*	0,0000	0,0000	0,2385
Bacteroidetes	*Fermentimonas*	*Fermentimonas caenicola*	0,0000	0,0386	0,1542
Bacteroidetes	*Flavobacterium*	*Flavobacterium sp.*	0,0000	0,0000	0,0021
Bacteroidetes	*Flavobacterium*	*Flavobacterium ummariense*	0,0000	0,0000	0,0062
Bacteroidetes	*Gelidibacter*	*Gelidibacter mesophilus*	0,0000	0,0000	0,0055
Bacteroidetes	*Lutibacter*	*Lutibacter sp.*	0,0000	0,0000	0,0021
Bacteroidetes	*Mariniphaga*	*Mariniphaga anaerophila*	0,0000	0,0029	0,2001
Bacteroidetes	*Marixanthomonas*	*Marixanthomonas sp.*	0,0000	0,0000	0,0027
Bacteroidetes	*Paludibacter*	*Paludibacter sp.*	0,0000	0,0000	0,0267
Bacteroidetes	*Petrimonas*	*Petrimonas sp.*	0,0000	0,1396	0,9534
Bacteroidetes	*Porphyromonas*	*Porphyromonas sp.*	0,0000	0,0072	0,0247
Bacteroidetes	*Prevotella*	*Prevotella paludivivens*	0,0000	0,0000	0,0027
Bacteroidetes	*Proteiniphilum*	*Proteiniphilum sp.*	0,0000	0,0200	0,0404
Bacteroidetes	*Taibaiella*	*Taibaiella sp.*	0,0000	0,0000	0,0096
Bacteroidetes	Unclassified	Unclassified	0,0000	0,0429	0,4071
Bacteroidetes	Unclassified	Unclassified	0,0000	0,0000	0,0768
Bacteroidetes	Unclassified	Unclassified	0,0000	0,0379	0,4852
Candidatus Atribacteria	Unclassified	Unclassified	0,0077	0,0952	0,1282
Chloroflexi	*Bellilinea*	*Bellilinea sp.*	0,0000	0,0265	0,0233
Chloroflexi	*Dehalococcoides*	*Dehalococcoides sp.*	0,0000	0,0072	0,0000
Chloroflexi	*Levilinea*	*Levilinea sp.*	0,1391	0,0000	0,0000
Chloroflexi	*Sphaerobacter*	*Sphaerobacter sp.*	0,0000	0,0021	0,0048

Table A4.2 (continued)

Kingdom	*Genus*	*Species*	Aerobic	Anaerobic	Inoculum
Chloroflexi	*Sphaerobacter*	*Sphaerobacter thermophilus*	0,2246	0,0014	0,0000
Chloroflexi	*Thermomicrobium*	*Thermomicrobium sp.*	0,0000	0,0014	0,0000
Chloroflexi	Unclassified	Unclassified	0,0000	0,0014	0,0021
Chloroflexi	Unclassified	Unclassified	0,0000	0,0000	0,0027
Chloroflexi	Unclassified	Unclassified	0,0000	0,0000	0,0014
Cyanobacteria	*Tychonema*	*Tychonema sp.*	0,0000	0,0000	0,0034
Deferribacteres	*Deferribacter*	*Deferribacter sp.*	0,0000	0,0050	0,0055
Deferribacteres	Unclassified	Unclassified	0,0000	0,0029	0,0000
Deinococcus-Thermus	*Deinococcus*	*Deinococcus sp.*	0,0000	0,0029	0,0439
Deinococcus-Thermus	Unclassified	Unclassified	0,0000	0,0086	0,0247
Elusimicrobia	Unclassified	Unclassified	0,0000	0,0709	0,0000
Fibrobacteres	*Fibrobacter*	*Fibrobacter sp.*	0,0000	0,0000	0,0062
Firmicutes	*Acetivibrio*	*Acetivibrio sp.*	0,0141	0,0909	0,4092
Firmicutes	*Acetobacterium*	*Acetobacterium sp.*	0,0000	0,0000	0,0027
Firmicutes	*Acetobacterium*	*Acetobacterium woodii*	0,0000	0,0036	0,0713
Firmicutes	*Acidaminococcus*	*Acidaminococcus fermentans*	0,0000	0,0021	0,0041
Firmicutes	*Acidaminococcus*	*Acidaminococcus intestini*	0,0000	0,0000	0,0041
Firmicutes	*Acidaminococcus*	*Acidaminococcus sp.*	0,0000	0,0000	0,0164
Firmicutes	*Aeribacillus*	*Aeribacillus pallidus*	0,0637	0,0007	0,0000
Firmicutes	*Alkalibacter*	*Alkalibacter sp.*	0,0000	0,0072	0,0192
Firmicutes	*Alkalibacterium*	*Alkalibacterium putridalgicola*	0,0000	0,0050	0,0055
Firmicutes	*Alkaliphilus*	*Alkaliphilus halophilus*	0,0094	0,0544	0,8787
Firmicutes	*Alkaliphilus*	*Alkaliphilus oremlandii*	0,0041	0,0250	0,0473
Firmicutes	*Alkaliphilus*	*Alkaliphilus sp.*	0,0000	0,0014	0,3859
Firmicutes	*Amphibacillus*	*Amphibacillus sp.*	0,0000	0,0000	0,0411
Firmicutes	*Anaeroarcus*	*Anaeroarcus sp.*	0,0000	0,0000	0,0164
Firmicutes	*Anaerobranca*	*Anaerobranca gottschalkii*	0,0000	0,0000	0,0356
Firmicutes	*Anaerobranca*	*Anaerobranca horikoshii*	0,0012	0,0014	0,0000
Firmicutes	*Anaerofilum*	*Anaerofilum sp.*	0,0000	0,0000	0,0034
Firmicutes	*Anaerofustis*	*Anaerofustis sp.*	0,0000	0,0014	0,0000
Firmicutes	*Anaerosalibacter*	*Anaerosalibacter bizertensis*	0,0047	0,0265	0,0089
Firmicutes	*Anaerovirgula*	*Anaerovirgula sp.*	0,0000	0,0007	0,0048
Firmicutes	*Anaerovorax*	*Anaerovorax sp.*	0,0000	0,0000	0,1892
Firmicutes	*Aneurinibacillus*	*Aneurinibacillus thermoaerophilus*	0,0200	0,0000	0,0000

Table A4.2 (continued)

Kingdom	*Genus*	*Species*	Aerobic	Anaerobic	Inoculum
Firmicutes	*Atopostipes*	*Atopostipes sp.*	0,0000	0,0000	0,0021
Firmicutes	*Bacillus*	*Bacillus horti*	0,0000	0,0036	0,0000
Firmicutes	*Bacillus*	*Bacillus infernus*	0,2965	0,0029	0,0007
Firmicutes	*Bacillus*	*Bacillus jeotgali*	0,1362	0,0014	0,0000
Firmicutes	*Bacillus*	*Bacillus pervagus*	0,0000	0,0029	0,0000
Firmicutes	*Bacillus*	*Bacillus sp.*	3,0072	0,1439	0,2940
Firmicutes	*Bacillus*	*Bacillus subtilis*	0,0012	0,0193	0,0075
Firmicutes	*Bacillus*	*Bacillus thermoamylovorans*	0,0006	0,0029	0,0014
Firmicutes	*Blautia*	*Blautia obeum*	0,0000	0,0000	0,0021
Firmicutes	*Brevibacillus*	*Brevibacillus thermoruber*	0,8814	0,0000	0,0000
Firmicutes	*Butyrivibrio*	*Butyrivibrio sp.*	0,0000	0,0000	0,0027
Firmicutes	*Caldibacillus*	*Caldibacillus debilis*	0,0053	0,0000	0,0000
Firmicutes	*Caldinitratiruptor*	*Caldinitratiruptor microaerophilus*	0,0159	0,0000	0,0000
Firmicutes	*Calditerricola*	*Calditerricola sp.*	0,0024	0,0000	0,0000
Firmicutes	*Caloramator*	*Caloramator sp.*	0,0024	10,9871	0,0000
Firmicutes	*Candidatus Contubernalis*	*Candidatus Contubernalis alkalaceticum*	0,0000	0,0000	0,0021
Firmicutes	*Candidatus Desulforudis*	*Candidatus Desulforudis audaxviator*	0,0059	0,0215	0,0089
Firmicutes	*Candidatus Soleaferrea*	*Candidatus Soleaferrea massiliensis*	0,0000	0,0000	0,0096
Firmicutes	*Carboxydocella*	*Carboxydocella sp.*	0,0000	0,0043	0,0000
Firmicutes	*Catabacter*	*Catabacter hongkongensis*	0,0000	0,0000	0,0021
Firmicutes	*Clostridiisalibacter*	*Clostridiisalibacter sp.*	0,0366	0,0680	0,0267
Firmicutes	*Clostridium*	*Clostridium acetireducens*	0,0035	0,0000	0,0000
Firmicutes	*Clostridium*	*Clostridium botulinum*	0,0035	0,0172	0,0041
Firmicutes	*Clostridium*	*Clostridium halophilum*	0,0896	0,0064	0,0007
Firmicutes	*Clostridium*	*Clostridium novyi*	0,0000	0,0014	0,0000
Firmicutes	*Clostridium*	*Clostridium sp.*	0,2352	1,0320	0,9280
Firmicutes	*Clostridium*	*Clostridium thermopalmarium*	0,0006	0,0050	0,0021
Firmicutes	*Cohnella*	*Cohnella laeviribosi*	0,0908	0,0000	0,0000
Firmicutes	*Cohnella*	*Cohnella sp.*	0,0501	0,0000	0,0000
Firmicutes	*Compostibacillus*	*Compostibacillus humi*	0,0000	0,0072	0,0007
Firmicutes	*Coprothermobacter*	*Coprothermobacter sp.*	10,8179	6,7296	0,0014
Firmicutes	*Cryptanaerobacter*	*Cryptanaerobacter phenolicus*	0,0000	0,0057	0,0096
Firmicutes	*Dehalobacter*	*Dehalobacter sp.*	0,0513	0,0000	0,0836

Table A4.2 (continued)

Kingdom	*Genus*	*Species*	Aerobic	Anaerobic	Inoculum
Firmicutes	*Dehalobacterium*	*Dehalobacterium formicoaceticum*	0,0000	0,0000	0,0048
Firmicutes	*Dehalobacterium*	*Dehalobacterium sp.*	0,0029	0,0208	0,1336
Firmicutes	*Desulfitibacter*	*Desulfitibacter alkalitolerans*	0,0000	0,0000	0,0274
Firmicutes	*Desulfitobacterium*	*Desulfitobacterium dichloroeliminans*	0,0000	0,0014	0,0021
Firmicutes	*Desulfitobacterium*	*Desulfitobacterium sp.*	0,0018	0,0000	0,0000
Firmicutes	*Desulfonispora*	*Desulfonispora sp.*	0,0000	0,0050	0,0555
Firmicutes	*Desulfonispora*	*Desulfonispora thiosulfatigenes*	0,0000	0,0000	0,0432
Firmicutes	*Desulfonispora*	*Desulfonosporus sp.*	0,0000	0,0150	0,0274
Firmicutes	*Desulfosporosinus*	*Desulfosporosinus sp.*	0,0018	0,0021	0,0192
Firmicutes	*Desulfotomaculum*	*Desulfotomaculum defluvii*	0,0000	0,0000	0,0027
Firmicutes	*Desulfotomaculum*	*Desulfotomaculum peckii*	0,0024	0,0036	0,0034
Firmicutes	*Desulfotomaculum*	*Desulfotomaculum sp.*	0,0035	0,0208	0,0082
Firmicutes	*Desulfotomaculum*	*Desulfotomaculum thermobenzoicum*	0,0454	0,0000	0,0000
Firmicutes	*Desulfotomaculum*	*Desulfotomaculum thermocisternum*	0,0024	0,0000	0,0000
Firmicutes	*Dethiobacter*	*Dethiobacter alkaliphilus*	0,0018	0,0079	0,0007
Firmicutes	*Enterococcus*	*Enterococcus casseliflavus*	0,0006	0,0036	0,0014
Firmicutes	*Enterococcus*	*Enterococcus sp.*	0,0012	0,0100	0,1069
Firmicutes	*Ercella*	*Ercella succinigenes*	0,0000	0,0029	0,0473
Firmicutes	*Erysipelothrix*	*Erysipelothrix rhusiopathiae*	0,0000	0,0021	0,0027
Firmicutes	*Erysipelothrix*	*Erysipelothrix sp.*	0,0000	0,0208	0,0144
Firmicutes	*Ethanoligenens*	*Ethanoligenens sp.*	0,0000	0,0000	0,0048
Firmicutes	*Eubacterium*	*Eubacterium coprostanoligenes*	0,0000	0,0000	0,0014
Firmicutes	*Eubacterium*	*Eubacterium sp.*	0,0041	0,0043	0,0713
Firmicutes	*Exiguobacterium*	*Exiguobacterium sp.*	0,0000	0,0000	0,0021
Firmicutes	*Facklamia*	*Facklamia sp.*	0,0000	0,0100	0,0137
Firmicutes	*Garciella*	*Garciella sp.*	0,0018	0,0129	0,0445
Firmicutes	*Gelria*	*Gelria sp.*	0,0071	0,0143	0,0000
Firmicutes	*Geobacillus*	*Geobacillus caldoxylosilyticus*	0,0024	0,0000	0,0000
Firmicutes	*Geobacillus*	*Geobacillus sp.*	0,7870	0,0014	0,0000
Firmicutes	*Geobacillus*	*Geobacillus stearothermophilus*	0,0236	0,0000	0,0000
Firmicutes	*Geobacillus*	*Geobacillus thermodenitrificans*	0,0713	0,0043	0,0034
Firmicutes	*Gracilibacter*	*Gracilibacter sp.*	0,0000	0,0000	0,0014

Table A4.2 (continued)

Kingdom	*Genus*	*Species*	Aerobic	Anaerobic	Inoculum
Firmicutes	*Herbinix*	*Herbinix hemicellulosilytica*	0,0012	0,0007	0,0000
Firmicutes	*Herbinix*	*Herbinix sp.*	0,0012	0,0107	0,0103
Firmicutes	*Hespellia*	*Hespellia porcina*	0,0000	0,0029	0,0007
Firmicutes	*Hespellia*	*Hespellia sp.*	0,0000	0,0036	0,0034
Firmicutes	*Hydrogenibacillus*	*Hydrogenibacillus schlegelii*	0,1002	0,0000	0,0014
Firmicutes	*Keratinibaculum*	*Keratinibaculum paraultunense*	0,0059	0,0372	0,0123
Firmicutes	*Kroppenstedtia*	*Kroppenstedtia eburnea*	0,0000	0,0021	0,0014
Firmicutes	*Lachnoclostridium*	*Clostridium fimetarium*	0,0000	0,0000	0,0021
Firmicutes	*Lachnoclostridium*	*Clostridium saccharolyticum*	0,0000	0,0014	0,0000
Firmicutes	*Lactobacillus*	*Lactobacillus acidipiscis*	0,0012	0,0043	0,0000
Firmicutes	*Lactobacillus*	*Lactobacillus algidus*	0,0000	0,0021	0,0014
Firmicutes	*Lactobacillus*	*Lactobacillus amylotrophicus*	0,0000	0,0029	0,0158
Firmicutes	*Lactobacillus*	*Lactobacillus casei*	0,0000	0,0107	0,0370
Firmicutes	*Lactobacillus*	*Lactobacillus concavus*	0,0000	0,0007	0,0151
Firmicutes	*Lactobacillus*	*Lactobacillus coryniformis*	0,0000	0,0229	0,1234
Firmicutes	*Lactobacillus*	*Lactobacillus harbinensis*	0,0000	0,0064	0,0110
Firmicutes	*Lactobacillus*	*Lactobacillus helveticus*	0,0000	0,0036	0,0048
Firmicutes	*Lactobacillus*	*Lactobacillus insicii*	0,0000	0,0000	0,0027
Firmicutes	*Lactobacillus*	*Lactobacillus kefiri*	0,0000	0,0157	0,0151
Firmicutes	*Lactobacillus*	*Lactobacillus nenjiangensis*	0,0018	0,0043	0,2591
Firmicutes	*Lactobacillus*	*Lactobacillus nodensis*	0,0000	0,0000	0,0493
Firmicutes	*Lactobacillus*	*Lactobacillus parabrevis*	0,0377	1,0971	0,5387
Firmicutes	*Lactobacillus*	*Lactobacillus sakei*	0,0029	0,0351	0,3173
Firmicutes	*Lactobacillus*	*Lactobacillus sanfranciscensis*	0,0000	0,0258	0,2234
Firmicutes	*Lactobacillus*	*Lactobacillus sp.*	0,0000	0,0615	0,6251
Firmicutes	*Lactobacillus*	*Lactobacillus zymae*	0,0006	0,0072	0,0014
Firmicutes	*Lactococcus*	*Lactococcus lactis*	0,0000	0,0000	0,0082
Firmicutes	*Lactococcus*	*Lactococcus sp.*	0,0000	0,0000	0,0151
Firmicutes	*Leuconostoc*	*Leuconostoc fallax*	0,0000	0,0029	0,0000
Firmicutes	*Leuconostoc*	*Leuconostoc kimchii*	0,0000	0,0072	0,0158
Firmicutes	*Leuconostoc*	*Leuconostoc lactis*	0,0047	0,0429	0,0576
Firmicutes	*Lutisp.ora*	*Lutisp.ora sp.*	0,0000	0,0014	0,0315
Firmicutes	*Lutispora*	*Lutispora thermophila*	0,1816	0,1224	0,0014
Firmicutes	*Megasphaera*	*Megasphaera micronuciformis*	0,0000	0,0000	0,0034

Table A4.2 (continued)

Kingdom	*Genus*	*Species*	Aerobic	Anaerobic	Inoculum
Firmicutes	*Megasphaera*	*Megasphaera paucivorans*	0,0000	0,0021	0,0027
Firmicutes	*Megasphaera*	*Megasphaera sp.*	0,0000	0,0000	0,0055
Firmicutes	*Moorella*	*Moorella glycerini*	0,0018	0,0000	0,0007
Firmicutes	*Moorella*	*Moorella sp.*	0,0000	0,0064	0,0000
Firmicutes	*Natronoanaerobium*	*Natronoanaerobium sp.*	0,0707	0,8932	0,1823
Firmicutes	*Oceanobacillus*	*Oceanobacillus luteolus*	0,0000	0,0014	0,0027
Firmicutes	*Oceanobacillus*	*Oceanobacillus polygoni*	0,0000	0,0000	0,0027
Firmicutes	*Oceanobacillus*	*Oceanobacillus sp.*	0,0006	0,0007	0,0021
Firmicutes	*Ornithinibacillus*	*Ornithinibacillus sp.*	0,0018	0,0029	0,0014
Firmicutes	*Oxobacter*	*Oxobacter sp.*	0,0000	0,0000	0,0014
Firmicutes	*Paenibacillus*	*Paenibacillus sp.*	0,0707	0,0279	0,0117
Firmicutes	*Papillibacter*	*Papillibacter sp.*	0,0000	0,0000	0,0110
Firmicutes	*Pediococcus*	*Pediococcus parvulus*	0,0012	0,0029	0,0069
Firmicutes	*Pelospora*	*Pelospora sp.*	0,0000	0,0007	0,0055
Firmicutes	*Planifilum*	*Planifilum fulgidum*	0,0083	0,0136	0,0014
Firmicutes	*Planifilum*	*Planifilum sp.*	0,0024	0,0029	0,0021
Firmicutes	*Planococcus*	*Planococcus sp.*	0,0065	0,0165	0,0123
Firmicutes	*Propionispira*	*Propionispira arcuata*	0,0000	0,0000	0,0096
Firmicutes	*Proteiniborus*	*Proteiniborus sp.*	0,0112	0,3099	0,0062
Firmicutes	*Pseudogracilibacillus*	*Pseudogracilibacillus sp.*	0,0000	0,0000	0,0041
Firmicutes	*Roseburia*	*Roseburia sp.*	0,0000	0,0000	0,0014
Firmicutes	*Ruminiclostridium*	*Clostridium cellulosi*	0,0000	0,0122	0,0034
Firmicutes	*Ruminiclostridium*	*Clostridium hungatei*	0,0006	0,0057	0,0021
Firmicutes	*Ruminiclostridium*	*Clostridium stercorarium*	0,0065	0,0000	0,0069
Firmicutes	*Ruminococcus*	*Ruminococcus bromii*	0,0000	0,0072	0,0027
Firmicutes	*Ruminococcus*	*Ruminococcus flavefaciens*	0,0006	0,0007	0,0007
Firmicutes	*Ruminococcus*	*Ruminococcus sp.*	0,0012	0,0107	0,0027
Firmicutes	*Rummeliibacillus*	*Rummeliibacillus pycnus*	0,0018	0,0007	0,0048
Firmicutes	*Schwartzia*	*Schwartzia sp.*	0,0000	0,0000	0,2145
Firmicutes	*Sedimentibacter*	*Sedimentibacter sp.*	0,0000	0,0000	0,0103
Firmicutes	*Selenomonas*	*Selenomonas sp.*	0,0000	0,0014	0,0391
Firmicutes	*Soehngenia*	*Soehngenia sp.*	0,0000	0,0000	0,1782
Firmicutes	*Sporanaerobacter*	*Sporanaerobacter acetigenes*	0,0041	0,0079	0,0027
Firmicutes	*Sporanaerobacter*	*Sporanaerobacter sp.*	0,0448	0,1861	0,0329
Firmicutes	*Sporobacter*	*Sporobacter termitidis*	0,0047	0,0072	0,0014
Firmicutes	*Sporosarcina*	*Sporosarcina sp.*	0,0000	0,0000	0,0014
Firmicutes	*Staphylococcus*	*Staphylococcus equorum*	0,0006	0,0057	0,0007

Table A4.2 (continued)

Kingdom	*Genus*	*Species*	Aerobic	Anaerobic	Inoculum
Firmicutes	*Streptococcus*	*Streptococcus thermophilus*	0,0000	0,0014	0,0000
Firmicutes	*Symbiobacterium*	*Symbiobacterium sp.*	1,7981	0,5289	0,5764
Firmicutes	*Symbiobacterium*	*Symbiobacterium terraclitae*	0,5141	0,0014	0,0000
Firmicutes	*Syntrophaceticus*	*Syntrophaceticus schinkii*	0,0053	0,0465	0,0658
Firmicutes	*Syntrophaceticus*	*Syntrophaceticus sp.*	0,0595	0,4530	0,3269
Firmicutes	*Syntrophomonas*	*Syntrophomonas bryantii*	0,0053	0,0286	0,0555
Firmicutes	*Syntrophomonas*	*Syntrophomonas sp.*	0,0041	0,0250	0,0240
Firmicutes	*Syntrophomonas*	*Syntrophomonas wolfei*	0,0018	0,0057	0,0014
Firmicutes	*Syntrophomonas*	*Syntrophomonas zehnderi*	0,0041	0,0565	0,0233
Firmicutes	*Syntrophothermus*	*Syntrophothermus lipocalidus*	0,1550	0,0973	0,0000
Firmicutes	*Tepidanaerobacter*	*Tepidanaerobacter acetatoxydans*	0,0136	0,1138	0,0432
Firmicutes	*Tepidanaerobacter*	*Tepidanaerobacter sp.*	0,0106	0,0272	0,0041
Firmicutes	*Tepidimicrobium*	*Tepidimicrobium sp.*	0,0065	0,0909	0,0329
Firmicutes	*Thermacetogenium*	*Thermacetogenium sp.*	0,0867	0,2140	0,2611
Firmicutes	*Thermaerobacter*	*Thermaerobacter sp.*	0,0472	0,0272	0,0295
Firmicutes	*Thermanaeromonas*	*Thermanaeromonas sp.*	0,0000	0,0007	0,0007
Firmicutes	*Thermoactinomyces*	*Thermoactinomyces intermedius*	0,0000	0,0036	0,0021
Firmicutes	*Thermoactinomyces*	*Thermoactinomyces vulgaris*	0,0253	0,0064	0,0027
Firmicutes	*Thermoanaerobacter*	*Thermoanaerobacter kivui*	0,0000	0,0000	0,0055
Firmicutes	*Thermoanaerobacter*	*Thermoanaerobacter thermocopriae*	0,0200	0,0000	0,0000
Firmicutes	*Thermoanaerobacterium*	*Thermoanaerobacterium thermosaccharolyticum*	0,0000	0,0021	0,0000
Firmicutes	*Thermosyntropha*	*Thermosyntropha lipolytica*	0,0000	0,0379	0,0000
Firmicutes	*Tissierella*	*Tissierella creatinini*	0,0000	0,0000	0,0034
Firmicutes	*Tissierella*	*Tissierella creatinophila*	0,0000	0,0000	0,1076
Firmicutes	*Tissierella*	*Tissierella praeacuta*	0,0000	0,0000	0,1241
Firmicutes	*Tissierella*	*Tissierella sp.*	0,0006	0,0236	1,8587
Firmicutes	*Trichococcus*	*Trichococcus sp.*	0,0006	0,0522	0,0295
Firmicutes	*Turicibacter*	*Turicibacter sp.*	0,0000	0,0043	0,0034
Firmicutes	Unclassified	Unclassified	0,0189	0,0179	0,0069
Firmicutes	Unclassified	Unclassified	0,0000	0,0000	0,0014
Firmicutes	Unclassified	Unclassified	0,0088	0,1145	0,2865
Firmicutes	Unclassified	Unclassified	0,0000	0,0179	0,0014
Firmicutes	Unclassified	Unclassified	0,0018	0,0179	0,1426

Table A4.2 (continued)

Kingdom	*Genus*	*Species*	Aerobic	Anaerobic	Inoculum
Firmicutes	Unclassified	Unclassified	0,2995	0,0000	0,0000
Firmicutes	Unclassified	Unclassified	0,0000	0,0000	0,0048
Firmicutes	Unclassified	Unclassified	1,7155	0,1710	0,9904
Firmicutes	Unclassified	Unclassified	0,0000	0,0100	0,0082
Firmicutes	Unclassified	Unclassified	0,0106	1,2202	0,0418
Firmicutes	Unclassified	Unclassified	0,0631	1,1902	1,4742
Firmicutes	Unclassified	Unclassified	0,0000	0,0107	0,0123
Firmicutes	Unclassified	Unclassified	0,0000	0,0057	0,0021
Firmicutes	Unclassified	Unclassified	0,0012	0,0064	0,0014
Firmicutes	Unclassified	Unclassified	0,2299	1,2195	1,0377
Firmicutes	*Ureibacillus*	*Ureibacillus composti*	1,5175	0,0007	0,0007
Firmicutes	*Ureibacillus*	*Ureibacillus sp.*	0,0130	0,0000	0,0000
Firmicutes	*Ureibacillus*	*Ureibacillus thermosphaericus*	0,1161	0,0007	0,0007
Firmicutes	*Veillonella*	*Veillonella sp.*	0,0000	0,0465	0,0994
Firmicutes	*Virgibacillus*	*Virgibacillus sp.*	0,0000	0,0029	0,0089
Firmicutes	*Weissella*	*Weissella confusa*	0,0018	0,0072	0,0075
Lentisphaerae	*Victivallis*	*Victivallis sp.*	0,0000	0,0014	0,0062
Lentisphaerae	*Victivallis*	*Victivallis vadensis*	0,0000	0,0014	0,0007
Nitrospirae	*Nitrospira*	*Nitrospira sp.*	0,0024	0,0057	0,0027
Planctomycetes	*Thermogutta*	*Thermogutta terrifontis*	0,0000	0,0973	0,0000
Planctomycetes	Unclassified	Unclassified	0,0029	0,0036	0,2138
Proteobacteria	*Achromobacter*	*Achromobacter sp.*	0,0000	0,0322	0,0452
Proteobacteria	*Acidovorax*	*Acidovorax sp.*	0,0006	0,0208	0,0336
Proteobacteria	*Acinetobacter*	*Acinetobacter sp.*	0,0000	0,0000	0,0069
Proteobacteria	*Advenella*	*Advenella faeciporci*	0,0000	0,0522	0,3023
Proteobacteria	*Alcaligenes*	*Alcaligenes faecalis*	0,0000	0,0000	0,0103
Proteobacteria	*Alcaligenes*	*Alcaligenes sp.*	0,0000	0,0265	0,0925
Proteobacteria	*Alcanivorax*	*Alcanivorax sp.*	0,0000	0,0000	0,0192
Proteobacteria	*Aliidiomarina*	*Aliidiomarina taiwanensis*	0,0000	0,0000	0,1110
Proteobacteria	*Aquamicrobium*	*Aquamicrobium segne*	0,0000	0,0179	0,0117
Proteobacteria	*Aquamicrobium*	*Aquamicrobium sp.*	0,0000	0,0315	0,0164
Proteobacteria	*Aquamicrobium*	*Defluvibacter sp.*	0,0000	0,0021	0,0007
Proteobacteria	*Arcobacter*	*Arcobacter sp.*	0,0000	0,0000	0,1412
Proteobacteria	*Azoarcus*	*Azoarcus sp.*	0,0000	0,0007	0,0117
Proteobacteria	*Bdellovibrio*	*Bdellovibrio sp.*	0,0366	0,0000	0,0000
Proteobacteria	*Bilophila*	*Bilophila sp.*	0,0000	0,0000	0,0041
Proteobacteria	*Bordetella*	*Bordetella sp.*	0,0000	0,0036	0,0089

Table A4.2 (continued)

Kingdom	*Genus*	*Species*	Aerobic	Anaerobic	Inoculum
Proteobacteria	*Bosea*	*Bosea sp.*	0,0000	0,0021	0,0034
Proteobacteria	*Brachymonas*	*Brachymonas denitrificans*	0,0000	0,0007	0,0021
Proteobacteria	*Bradyrhizobium*	*Bradyrhizobium sp.*	0,0000	0,0029	0,0062
Proteobacteria	*Burkholderia*	*Burkholderia tropica*	0,0000	0,0029	0,0034
Proteobacteria	*Camelimonas*	*Camelimonas lactis*	0,0000	0,0179	0,0363
Proteobacteria	*Candidatus Accumulibacter*	*Candidatus Accumulibacter sp.*	0,0094	0,0057	0,0055
Proteobacteria	*Candidatus Endobugula*	*Candidatus Endobugula glebosa*	0,0000	0,0000	0,0055
Proteobacteria	*Castellaniella*	*Castellaniella defragrans*	0,0000	0,0093	0,0055
Proteobacteria	*Castellaniella*	*Castellaniella denitrificans*	0,0000	0,0150	0,0130
Proteobacteria	*Cellvibrio*	*Cellvibrio sp.*	0,0000	0,0000	0,0096
Proteobacteria	*Chelativorans*	*Chelativorans composti*	0,0000	0,0021	0,0007
Proteobacteria	*Chelatococcus*	*Chelatococcus sp.*	0,5188	0,0036	0,0000
Proteobacteria	*Chromohalobacter*	*Chromohalobacter sp.*	0,0000	0,0000	0,0014
Proteobacteria	*Comamonas*	*Comamonas sp.*	0,0000	0,0136	0,0171
Proteobacteria	*Dechloromonas*	*Dechloromonas sp.*	0,0000	0,0000	0,0027
Proteobacteria	*Desulfobacterium*	*Desulfobacterium sp.*	0,0000	0,0336	0,3914
Proteobacteria	*Desulfobotulus*	*Desulfobotulus sp.*	0,0000	0,0000	0,0363
Proteobacteria	*Desulfobulbus*	*Desulfobulbus sp.*	0,0000	0,0029	0,1672
Proteobacteria	*Desulfomicrobium*	*Desulfomicrobium sp.*	0,0000	0,0014	0,0048
Proteobacteria	*Desulfovibrio*	*Desulfovibrio desulfuricans*	0,0000	0,0000	0,0206
Proteobacteria	*Desulfovibrio*	*Desulfovibrio sp.*	0,0000	0,0007	0,0219
Proteobacteria	*Desulfuromonas*	*Desulfuromonas sp.*	0,0000	0,0694	2,4112
Proteobacteria	*Desulfuromonas*	*Desulfuromonas thiophila*	0,0000	0,0000	0,0048
Proteobacteria	*Devosia*	*Devosia sp.*	0,0000	0,0029	0,0075
Proteobacteria	*Devosia*	*Devosia terrae*	0,0000	0,0079	0,0041
Proteobacteria	*Diaphorobacter*	*Diaphorobacter sp.*	0,0000	0,0172	0,0226
Proteobacteria	*Dyella*	*Dyella sp.*	0,0000	0,0000	0,0041
Proteobacteria	*Ensifer*	*Ensifer adhaerens*	0,0000	0,0007	0,0027
Proteobacteria	*Gemmobacter*	*Gemmobacter intermedius*	0,0000	0,0014	0,0034
Proteobacteria	*Gemmobacter*	*Gemmobacter sp.*	0,0000	0,0057	0,0103
Proteobacteria	*Halochromatium*	*Halochromatium sp.*	0,0000	0,0036	0,0082
Proteobacteria	*Halomonas*	*Halomonas sp.*	0,0000	0,0000	0,0041
Proteobacteria	*Halothiobacillus*	*Halothiobacillus sp.*	0,0000	0,0000	0,0117
Proteobacteria	*Herminiimonas*	*Herminiimonas sp.*	0,0000	0,0050	0,0055
Proteobacteria	*Hydrogenophaga*	*Hydrogenophaga sp.*	0,0000	0,0021	0,0596
Proteobacteria	*Hyphomicrobium*	*Hyphomicrobium sp.*	0,0000	0,0050	0,0137

Table A4.2 (continued)

Kingdom	*Genus*	*Species*	Aerobic	Anaerobic	Inoculum
Proteobacteria	*Ideonella*	*Ideonella sp.*	0,0000	0,0830	0,0994
Proteobacteria	*Idiomarina*	*Idiomarina sp.*	0,0000	0,0000	0,0117
Proteobacteria	*Janthinobacterium*	*Janthinobacterium sp.*	0,0000	0,0000	0,0021
Proteobacteria	*Koukoulia*	*Koukoulia aurantiaca*	0,0000	0,0007	0,0007
Proteobacteria	*Labrenzia*	*Labrenzia sp.*	0,0000	0,0036	0,0027
Proteobacteria	*Luteimonas*	*Luteimonas composti*	0,0000	0,0000	0,0014
Proteobacteria	*Luteimonas*	*Luteimonas sp.*	0,0000	0,0000	0,0034
Proteobacteria	*Marinobacter*	*Marinobacter sp.*	0,0000	0,0000	0,1851
Proteobacteria	*Marinospirillum*	*Marinospirillum minutulum*	0,0000	0,0029	2,3214
Proteobacteria	*Marinospirillum*	*Marinospirillum sp.*	0,0000	0,0000	0,0144
Proteobacteria	*Mesorhizobium*	*Mesorhizobium sp.*	0,0000	0,0236	0,0274
Proteobacteria	*Methylibium*	*Methylibium sp.*	0,0000	0,0007	0,0021
Proteobacteria	*Methylobacillus*	*Methylobacillus sp.*	0,0000	0,0000	0,0164
Proteobacteria	*Methylobacter*	*Methylobacter sp.*	0,0000	0,0014	0,0117
Proteobacteria	*Methylocaldum*	*Methylocaldum sp.*	0,0024	0,0064	0,0199
Proteobacteria	*Methylococcus*	*Methylococcus sp.*	0,0024	0,0029	0,0069
Proteobacteria	*Methylocystis*	*Methylocystis sp.*	0,0083	0,0200	0,0912
Proteobacteria	*Methylophaga*	*Methylophaga sp.*	0,0000	0,0000	0,0096
Proteobacteria	*Methylosinus*	*Methylosinus trichosp.orium*	0,0059	0,0215	0,0761
Proteobacteria	*Nitrosomonas*	*Nitrosomonas stercoris*	0,0000	0,0007	0,0014
Proteobacteria	*Nitrosovibrio*	*Nitrosovibrio sp.*	0,0000	0,0057	0,0014
Proteobacteria	*Ochrobactrum*	*Ochrobactrum sp.*	0,0000	0,0537	0,0322
Proteobacteria	*Octadecabacter*	*Octadecabacter sp.*	0,0000	0,0544	0,1659
Proteobacteria	*Oligella*	*Oligella ureolytica*	0,0000	0,0029	0,0089
Proteobacteria	*Paenalcaligenes*	*Paenalcaligenes hominis*	0,0000	0,1138	1,8272
Proteobacteria	*Paenochrobactrum*	*Paenochrobactrum sp.*	0,0000	0,0129	0,0089
Proteobacteria	*Pandoraea*	*Pandoraea sp.*	0,0000	0,0000	0,0021
Proteobacteria	*Paracoccus*	*Paracoccus sp.*	0,0000	0,1295	0,2995
Proteobacteria	*Pelagibacterium*	*Pelagibacterium sp.*	0,0000	0,0036	0,0034
Proteobacteria	*Pelistega*	*Pelistega europaea*	0,0000	0,0043	0,0062
Proteobacteria	*Ponticoccus*	*Ponticoccus litoralis*	0,0000	0,0064	0,0247
Proteobacteria	*Pseudaminobacter*	*Pseudaminobacter defluvii*	0,0006	0,0165	0,0226
Proteobacteria	*Pseudaminobacter*	*Pseudaminobacter salicylatoxidans*	0,0006	0,1596	0,1796
Proteobacteria	*Pseudochrobactrum*	*Pseudochrobactrum sp.*	0,0000	0,0143	0,0110
Proteobacteria	*Pseudolabrys*	*Pseudolabrys sp.*	0,0000	0,0000	0,0027
Proteobacteria	*Pseudomonas*	*Pseudomonas caeni*	0,0000	0,0043	0,1535

Table A4.2 (continued)

Kingdom	*Genus*	*Species*	Aerobic	Anaerobic	Inoculum
Proteobacteria	*Pseudomonas*	*Pseudomonas sp.*	0,0000	0,5453	42,8896
Proteobacteria	*Pseudorhodobacter*	*Pseudorhodobacter aquimaris*	0,0000	0,0007	0,0021
Proteobacteria	*Pusillimonas*	*Pusillimonas ginsengisoli*	0,0000	0,0014	0,0034
Proteobacteria	*Pusillimonas*	*Pusillimonas sp.*	0,0000	0,2519	0,8999
Proteobacteria	*Rhizobium*	*Rhizobium sp.*	0,0000	0,0250	0,0281
Proteobacteria	*Rhodobacter*	*Rhodobacter sp.*	0,0000	0,0050	0,0069
Proteobacteria	*Roseomonas*	*Roseomonas frigidaquae*	0,0000	0,0021	0,0027
Proteobacteria	*Roseovarius*	*Roseovarius sp.*	0,0000	0,0072	0,0103
Proteobacteria	*Serratia*	*Serratia marcescens*	0,0000	0,0000	0,0014
Proteobacteria	*Sphingopyxis*	*Sphingopyxis ginsengisoli*	0,0000	0,0000	0,0322
Proteobacteria	*Sphingopyxis*	*Sphingopyxis sp.*	0,0000	0,0000	0,0014
Proteobacteria	*Sphingorhabdus*	*Sphingorhabdus litoris*	0,0000	0,0000	0,0082
Proteobacteria	*Stenotrophomonas*	*Stenotrophomonas sp.*	0,0000	0,0000	0,0027
Proteobacteria	*Sulfurimonas*	*Sulfurimonas denitrificans*	0,0000	0,0014	0,0089
Proteobacteria	*Sulfurimonas*	*Sulfurimonas sp.*	0,0000	0,0064	0,3304
Proteobacteria	*Sulfurovum*	*Sulfurovum sp.*	0,0000	0,0050	0,0158
Proteobacteria	*Tepidiphilus*	*Petrobacter sp.*	0,0053	0,0057	0,0075
Proteobacteria	*Thauera*	*Thauera sp.*	0,0000	0,0000	0,0123
Proteobacteria	*Thauera*	*Thauera terpenica*	0,0006	0,0029	0,1412
Proteobacteria	*Thiomicrospira*	*Thiomicrospira arctica*	0,0000	0,0036	0,2269
Proteobacteria	*Thiomicrospira*	*Thiomicrospira chilensis*	0,0000	0,0000	0,0665
Proteobacteria	*Thiomicrospira*	*Thiomicrospira sp.*	0,0000	0,0086	0,0144
Proteobacteria	*Thiorhodococcus*	*Thiorhodococcus sp.*	0,0000	0,0021	5,7956
Proteobacteria	Unclassified	Unclassified	0,0660	0,0043	0,0000
Proteobacteria	Unclassified	Unclassified	0,0000	0,0157	0,0624
Proteobacteria	Unclassified	Unclassified	0,0000	0,0000	0,0014
Proteobacteria	Unclassified	Unclassified	0,0000	0,1732	0,1371
Proteobacteria	Unclassified	Unclassified	0,0259	0,0358	0,5819
Proteobacteria	Unclassified	Unclassified	0,0000	0,0072	0,0164
Proteobacteria	Unclassified	Unclassified	0,0000	0,0000	0,0041
Proteobacteria	Unclassified	Unclassified	0,0000	0,0029	0,0069
Proteobacteria	Unclassified	Unclassified	0,4687	0,0000	0,0000
Proteobacteria	Unclassified	Unclassified	0,0000	0,0000	0,0014
Proteobacteria	Unclassified	Unclassified	1,7792	0,0014	0,0027
Proteobacteria	Unclassified	Unclassified	0,0000	0,0000	0,0699
Proteobacteria	Unclassified	Unclassified	0,0006	0,0050	0,0110
Proteobacteria	Unclassified	Unclassified	0,0000	0,0000	0,0089

Table A4.2 (continued)

Kingdom	*Genus*	*Species*	Aerobic	Anaerobic	Inoculum
Proteobacteria	Unclassified	Unclassified	0,0000	0,0021	0,0466
Proteobacteria	*Wolinella*	*Wolinella sp.*	0,0000	0,0000	0,0082
Spirochaetes	*Leptospira*	*Leptospira sp.*	0,0000	0,0007	0,0041
Spirochaetes	*Spirochaeta*	*Spirochaeta sp.*	0,0000	0,0000	0,0062
Spirochaetes	*Treponema*	*Treponema sp.*	0,0000	0,0243	0,0439
Spirochaetes	*Treponema*	*Treponema zuelzerae*	0,0000	0,0064	0,0158
Spirochaetes	Unclassified	Unclassified	0,0000	0,0000	0,0021
Spirochaetes	Unclassified	Unclassified	0,0000	0,0107	0,0740
Spirochaetes	Unclassified	Unclassified	0,0000	0,0000	0,0062
Synergistetes	*Acetomicrobium*	*Acetomicrobium faecale*	0,0000	0,0036	0,0069
Synergistetes	*Aminobacterium*	*Aminobacterium colombiense*	0,0000	0,5346	0,1583
Synergistetes	*Aminobacterium*	*Aminobacterium sp.*	0,0000	0,4079	0,1864
Synergistetes	*Aminobacterium*	*Aminobacterium thunnarium*	0,0000	0,3228	0,0747
Synergistetes	*Anaerobaculum*	*Anaerobaculum hydrogeniformans*	0,0000	0,5260	0,0219
Synergistetes	*Anaerobaculum*	*Anaerobaculum mobile*	0,0307	0,0115	0,0000
Synergistetes	*Anaerobaculum*	*Anaerobaculum sp.*	0,0183	2,3324	1,0246
Synergistetes	*Dethiosulfovibrio*	*Dethiosulfovibrio russensis*	0,0000	0,0043	0,0014
Synergistetes	*Dethiosulfovibrio*	*Dethiosulfovibrio salsuginis*	0,0000	0,0000	0,0027
Synergistetes	*Synergistes*	*Synergistes sp.*	0,0000	0,8102	0,2570
Synergistetes	Unclassified	Unclassified	0,0000	0,0079	0,0027
Tenericutes	*Acholeplasma*	*Acholeplasma axanthum*	0,0000	0,0000	0,0822
Tenericutes	*Acholeplasma*	*Acholeplasma cavigenitalium*	0,0000	0,0014	0,0034
Tenericutes	*Acholeplasma*	*Acholeplasma sp.*	0,0000	0,0000	0,1309
Tenericutes	*Candidatus Phytoplasma*	*Phytoplasma sp.*	0,0000	0,0014	0,0000
Tenericutes	Unclassified	Unclassified	0,0000	0,0029	0,0679
Tenericutes	Unclassified	Unclassified	0,0000	0,0000	0,0014
Thermotogae	*Defluviitoga*	*Defluviitoga tunisiensis*	0,0094	6,0690	2,0493
Thermotogae	*Mesotoga*	*Mesotoga infera*	0,0000	0,0064	0,0075
Thermotogae	Unclassified	Unclassified	0,0000	0,6098	0,0000
Thermotogae	Unclassified	Unclassified	0,0672	0,6477	0,0288
Unclassified	Unclassified	Unclassified	0,0012	0,0143	0,0027
Unclassified	Unclassified	Unclassified	9,2704	30,6061	9,1155
Verrucomicrobia	*Methylacidimicrobium*	*Methylacidimicrobium fagopyrum*	0,0000	0,0007	0,0082
Verrucomicrobia	Unclassified	Unclassified	0,0000	0,0315	0,2447
Verrucomicrobia	Unclassified	Unclassified	0,0000	0,0086	0,8704
No Hit	*No Hit*	*No Hit*	61,4069	0,5010	0,5408

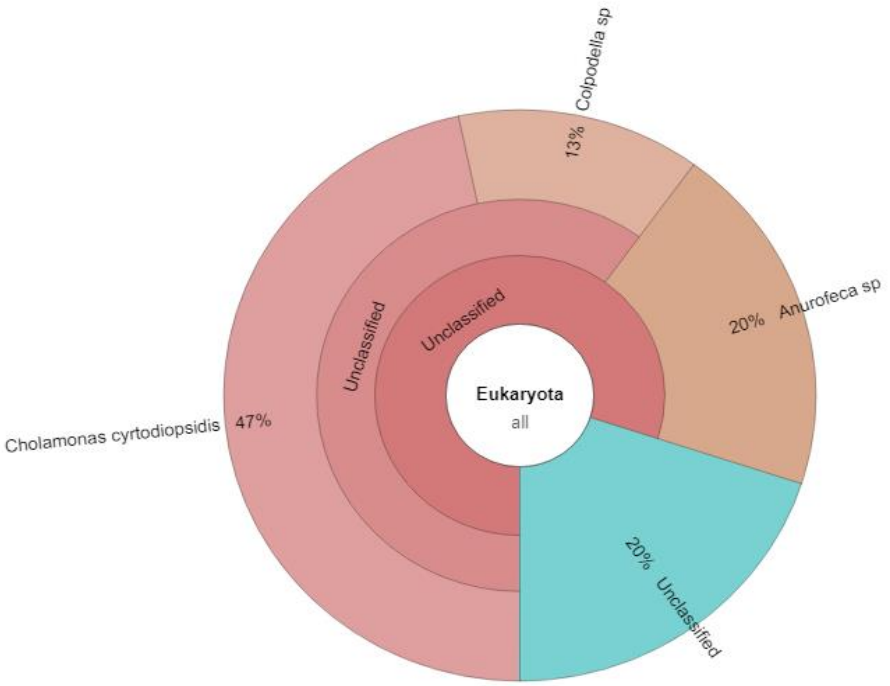

Figure A4.4: Relative abundance of the organisms assigned to *Eukaryota*, represented in a krona plot, given by the 18S amplicon sequencing of the PCL incubation performed under aerobic conditions.

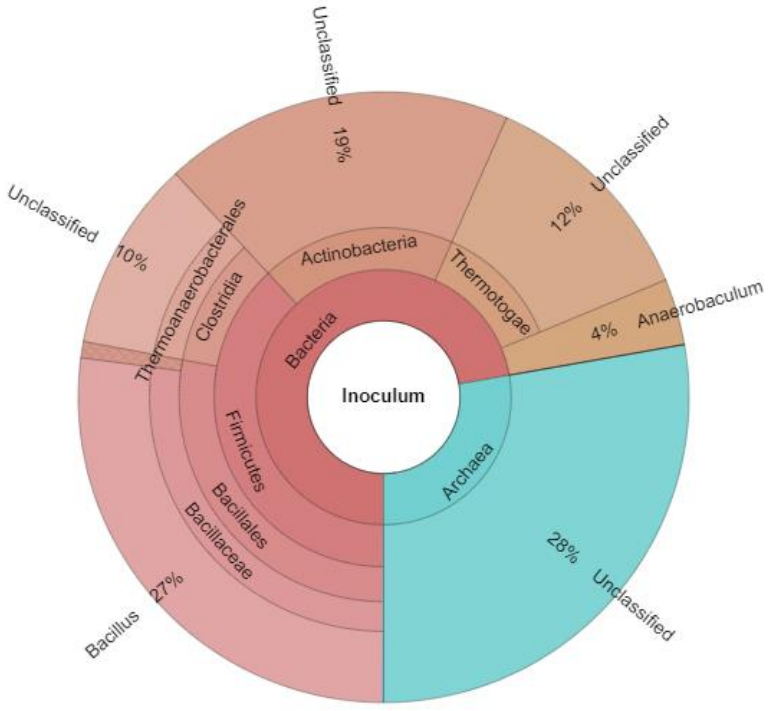

Figure A4.5: Relative abundance of the organisms assigned in the inoculum, represented in a krona plot, after data treatment. Bacteria (in reddish) account for 72 % of the prokaryotes present in the sample, and Archaea account for 28 %.

Appendix 5- Results of the experiments with marine sediment as inoculum

Table A5.1: Values of the mass of the cleaned muffle filters, after addition of the biomass, after overnight incubation at 105°C, and after incubation at 550°C, and respective standard deviation. Values of the resulting VSS for each sample, the average value for the first anaerobic assay and corresponding standard deviation, the quantity of inoculum added to obtain 3 g/L VSS

Samples	Filter mass (g)	Filter mass + biomass(g)	Mass after incubation at 105°C (g)	Mass after incubation at 550°C (g)	VSS (g/L)	Average VSS (g/L)	Quantity of inoculum added to the vials (for 3 g/L VSS) (g)
1	18,33 ± 0,0001	23,76 ± 0,0001	20,31 ± 0,0001	20,10 ± 0,0001	0,038	0,0341 ± 0,0037	4,40
2	19,20 ± 0,0001	22,45 ± 0,0001	20,45 ± 0,0001	20,34 ± 0,0001	0,033		
3	17,81 ± 0,0001	21,00± 0,0001	19,11 ± 0,0001	19,01 ± 0,0001	0,031		

TableA5.2: Values of the mass of the cleaned muffle filters, after addition of the biomass, after overnight incubation at 105°C, and after incubation at 550°C, and respective standard deviation. Values of the resulting VSS for each sample, the average value for the first anaerobic assay and corresponding standard deviation, the quantity of inoculum added to obtain 3 g/L VSS

Samples	Filter mass (g)	Filter mass + biomass(g)	Mass after incubation at 105°C (g)	Mass after incubation at 550°C (g)	VSS (g/L)	Average VSS (g/L)	Quantity of inoculum added to the vials (for 3 g/L VSS) (g)
1	20,30 ± 0,0001	23,60 ± 0,0001	21,64 ± 0,0001	21,53± 0,0001	0,0332	0,0330 ± 0,0015	4,54
2	17,87 ± 0,0001	20,66 ± 0,0001	19,10± 0,0001	19,01± 0,0001	0,0315		
3	19,52 ± 0,0001	23,51 ± 0,0001	21,17± 0,0001	21,03± 0,0001	0,0345		